JUAN A. GALLEGO

STATICALLY BALANCED COMPLIANT MECHANISMS

THEORY AND SYNTHESIS

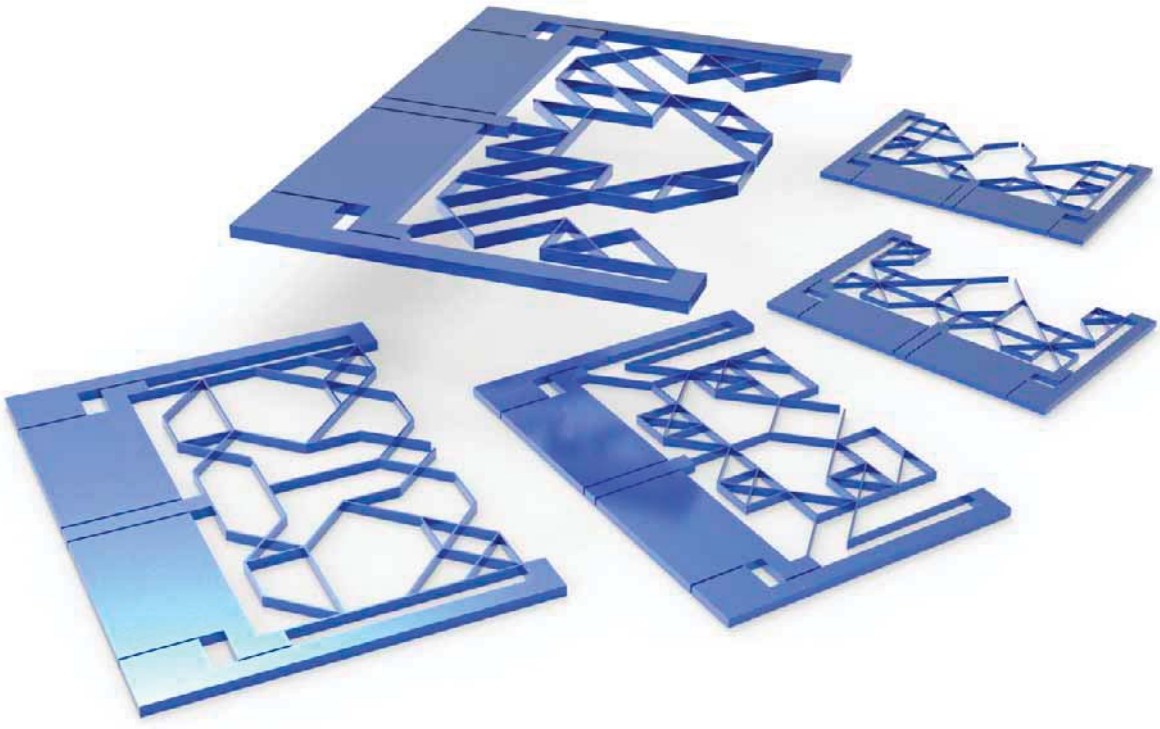

STATICALLY BALANCED COMPLIANT MECHANISMS THEORY AND SYNTHESIS

JUAN A. GALLEGO

Statically Balanced Compliant Mechanisms

Theory and Synthesis

Juan Andrés Gallego Sánchez

Statically Balanced Compliant Mechanisms

Theory and Synthesis

Proefschrift

ter verkrijging van de graad van doctor
aan de Technische Universtiteit Delft,
op gezag van de Rector Magnificus Prof. Ir. K.C.A.M. Luyben,
voorzitter van het College voor Promoties,
in het openbaar te verdedigen op woensdag 9 oktober 2013 om 15:00 uur
door

Juan Andrés GALLEGO SÁNCHEZ

Master of Science in Mechanical Engineering
EAFIT University, Medellín, Colombia
geboren te Medellín, Colombia

Dit proefschrift is goedgekeurd door de promotoren:

Prof.Dr. F.C.T. van der Helm
Prof.Dr.Ir. J.L. Herder

Samenstelling promotiecommissie:

Rector Magnificus,	voorzitter
Prof.Dr. F.C.T. van der Helm,	Technische Universiteit Delft, promotor
Prof.Dr.Ir. J.L. Herder,	Technische Universiteit Delft, promotor
Prof.Dr.Ing. B. Corves,	RWTH Aachen University, Duitsland
Prof.Dr.Ir. A. de Boer,	Universiteit Twente
Prof.Dr.Ir. L.J. Sluys,	Technische Universiteit Delft
Prof.Dr.Ir. A. van Keulen,	Technische Universiteit Delft
Dr. L. Birglen,	École Polytechnique de Montréal, Canada
Prof.Dr.Ir. P. Breedveld,	Technische Universiteit Delft, reservelid

This research was funded by Technology Foundation STW project number NWO-STW 7583

ISBN 978-94-6186-215-0

Keywords: Compliant mechanisms, static balancing, neutral stability, energy-free systems, optimization, stiffness reduction, constant force mechanisms

Printed in the Netherlands

Author email: jgalleg5@eafit.edu.co

Dedicated to

Maria del Carmen,

For being my role model and enlighten my path.
Her determination, perseverance, and love started the journey.

To

Elizabeth, Nicolás and Isabel,

For being the driving force that links my reason and passion into one goal...
keep going!

Contents

Preface

In this book, we address the problem of how to design compliant mechanisms which are statically balanced. This is, how to design mechanisms that work by elastic deformation of their constitutive elements, and require virtually no forces to induce static deflections in them.
Static balancing eliminates the need for actuation forces besides those required to overcome the inertia and friction of the system. Static balancing is an intuitive notion with which we are familiarized. When we think of lifting a heavy weight a common solution is to use a counterweight. When the counterweight makes the lifting of the weight effortless, then we have statically balanced the system. But weights can also be statically balanced by springs and furthermore, springs can be statically balanced by other springs.
This work has its origins in the work of Prof. Just L. Herder. During his work on the static balancing of rigid body mechanisms using precisely "springs", he came with the idea of applying the same design notion on compliant mechanisms since the flexible elements in this type of mechanisms can be considered as springs. If a spring can be used to statically balance other springs, then it should be possible to design compliant mechanisms that statically balance themselves.
These thoughts resonated with the idea that compliant mechanisms are mechanically inefficient due to the storage of the input work as strain energy during actuation. This latter notion that has been considered as a necessary evil could be overthrown through the use static balancing.
Thus, with these issues in mind we embarked on this journey in which we found ourselves plunging into the junction where the classical theory of mechanisms meets structural analysis, design optimization, non-linear theory of elasticity, MEMS, non-linear finite element analysis, and many more fascinating disciplines.
This book covers from the synthesis methods of compliant mechanisms and the theory of static balancing to the introduction of a design methodology for static balancing of compliant mechanisms and the initial results of topology optimization applied into this field.
For those interested in design theories of technical systems and artifacts, the book also presents a brief discussion about the author's view of compliant mechanisms and static balancing under the perspective of technical system representation.
Along four years of work, people come and go, but their contributions stay. I wish to thank to all the persons that contributed to the development of this work with their creativity and sharp

insights. To Nima, Gert, Volkert, Karin, Ditske, Elko, Jet, Mark, Giuseppe, Toon, and Sergio.
To my wife Elizabeth, for her acute observation, her ideas, thoughts and hours of discourse and talks.
To Prof. Dr. G. K. Ananthasuresh, Prof. Dr. A. Saxena and Dr.Ir M. Langelaar for their comments and support, without their help it would not have been possible to develop the analysis tools.
Special gratitude to Prof. Dr. Just L. Herder and Prof. Dr. Frans van der Helm for their guidance and counsel; for the confidence placed in me.
To the Lord for giving me the chance to live a life in which I can wonder why.

1 Introduction

Bend and be straight; The stiff and unbending is the disciple of death. The gentle and yielding is the disciple of life.

Lao Tse

To introduce statically balanced compliant mechanisms, it is desirable to understand individually three basic concepts: “mechanisms”, “compliance” and “static balancing”.
For a comprehensive definition of mechanisms it is useful to observe the relation between mechanisms and machines. Machines are built with an intended use or purpose so they perform some kind of work. As defined by Pahl et al. [94] they are technical systems consisting of assemblies and components whose main flow is energy-based. Using this definition we can say that mechanisms are then assemblies and components used in the machines, and more specific as defined by Howell [40] mechanisms are mechanical devices used to transmit or transform motion, force or energy. But keep in mind that differentiating between mechanisms and machines is not always clear as mentioned by Norton [93] where in some cases their difference is just defined by the magnitude of the transmitted or transformed motions, forces and energies.
Conventionally, mechanisms are collections of rigid body elements connected by overlapping joints, gaining their functionality by the relative motion among these elements. An advantage of rigid-body-based mechanisms is that the overlapping joints —neglecting friction— do not introduce stiffness in the actuation of the mechanisms.
Mechanisms based on rigid bodies can be replaced by compliant mechanisms that achieve to some extent the same function, see Fig. 1.1. Compliant mechanisms are monolithic structures that gain their motion due to deformation of their constitutive elements. If the motion comes only from deformation then it is said that compliant mechanisms are fully compliant, but if motion comes from a combination of deformation and relative motion between elements, then it is said that compliant mechanisms are partially compliant [40]. If we assume a traditional view where structures are designed to withstand forces with a minimum of deflection, then we can say that compliant mechanisms are structures that fail under the action of a load, and they are designed to deflect the most in a desired way with the least force.

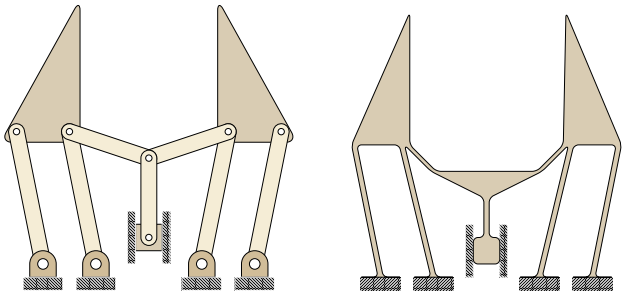

Figure 1.1: A rigid body mechanism can be replaced by its compliant version. (a) A gripper constructed from rigid links. (b) A gripper constructed from as monolithic compliant structure.

Compliant mechanisms rely on the idea of *compliance* which is defined as "the ability of an object to yield elastically when a force is applied" [19]. Compliance can be lumped or distributed depending on how deformation is localized along the deforming elements in compliant mechanisms. Compliance is one of nature's favorite design principles. It can be seen from cells to plants and from the tiniest insects to the biggest mammals. For instance, compliance in trees allows them to move with the breeze to disperse their progeny. It also allow them to resist the weight of the leaves and in some cases as in the willows compliance allows the branches to yield under the weight of the snow to keep the leaves clear during winter [50]. Compliance can be also traced back to earliest human designs. Take for instance bows and arrows. Bows are designed compliant to store the energy provided by the archer as strain energy which is later transferred to the arrow during the release. The arrow itself is compliant to bend and oscillate during flight to correct its trajectory.

Compliant mechanisms are not a recent idea in engineering, they have been used in the design of scientific precision instruments for more than a century. The design of precision instruments makes extensive use of compliant joints and flexures as a way to implement the principles of exact constraint design [14]. The use of compliant mechanisms introduces performance benefits like the absence of sliding friction, wear, noise, vibration and the need for lubrication. Furthermore, backlash is eliminated so positioning error is reduced and precision is increased [4]. However, the monolithic nature of compliant mechanisms brings some drawbacks. Potential energy is stored in the compliant segments as strain energy, introducing stiffness that affects the input-output relationship. In particular the energy efficiency is challenged, see Fig. 1.2a.

It would be desirable to have compliant mechanisms and all their benefits together with the energy efficiency of rigid body mechanisms. However, a question arises: how to overcome the energy inefficiency of compliant mechanisms? An answer is by reintroducing into the energy stream between input and output, the stored strain energy from another source of potential energy, see Fig. 1.2b. This energy compensation to keep the total potential energy constant is referred to

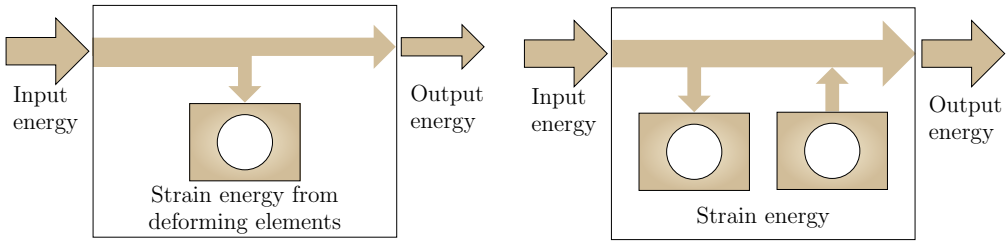

Figure 1.2: Flow of the energy stream during actuation. (a) In compliant mechanisms, some of the actuation energy is stored as strain energy in the deforming elements. The energy efficiency is less than 100%. (b) In statically balanced compliant mechanisms, some energy is still stored as strain energy in some deforming elements while the same amount of energy is released into the energy stream by another source of potential energy. Ideally, the energy efficiency is now equal to 100%.

as static balancing.

Static balancing is a conservative state of motion where all the internal forces are kept in static equilibrium. A mechanism in such a state does not require any force for its actuation besides those to overcome the inertial loads and non-conservative forces such as friction. Static balancing is the working principle of weighing balances and it can be found from bascule bridges to kinetic art. See for instance George Rickey's Breaking Columns [33] and V. van der Wijk's De Acrobaat [140].

Static balancing is a familiar notion used in the solution of problems where heavy masses need to be lifted repeatedly. Think for instance of the two systems shown in Fig. 1.3. In these examples mass m_1 is statically balanced by the mass m_2 and vice versa. The conventional view of these systems is that the moments exerted by both masses at the pivot point o cancel each other, keeping the systems in static equilibrium. But a less intuitive view is that during motion the total potential energy of both systems is kept constant, so the potential energy lost by one mass is gained by the other mass and vice versa. This view is easier to observe in the system shown in Fig. 1.3a.

Static balancing has been used in problems related to gravity compensation, vibration isolation and stiffness reduction. Although there is a body of literature on static balancing applied to the stiffness reduction of compliant mechanisms, there are not many methods for their synthesis and design. Currently, the design of Statically Balanced Compliant Mechanisms (SBCM's) relies greatly on the designer's experience and it is based on modifications of a few typical configurations. In a world with growing demands on miniaturization, design simplification, cost reduction, and energy efficiency among others, the use of SBCM will potentially increase.

The aim of this work is the development of a methodology to provide methods for the design of statically balanced compliant mechanisms. This in order to (i) improve the design quality,

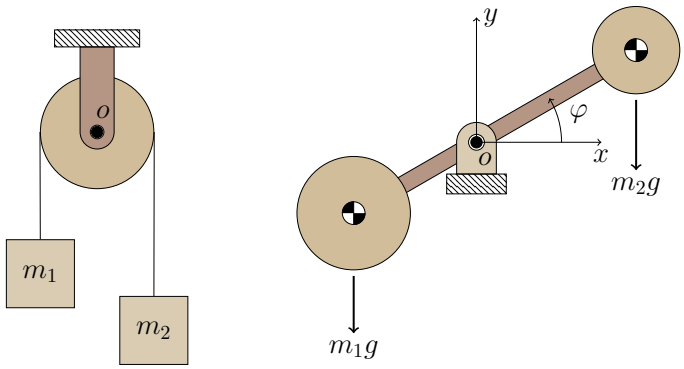

Figure 1.3: In these examples, during motion, the potential energy lost by one mass is gained by the other mass, so one mass statically balance the other mass keeping the total potential energy constant. (a) Two masses connected by a frictionless pulley. (b) Two masses connected by a rod.

(ii) structure the design process, and the most important, (iii) widen the solution space. It is considered that the design quality is improved when the final design reflects the inclusion of more design requirements during the design process and when the marginal values of the design behavior and attributes expressed as requirement metrics are narrowed down. The solution space is considered widen when for the same problem it is possible to obtain different solutions in terms of their topologies, shapes and sizes.

Design methods for any mechanism have to be able to provide solutions inside a prescribed design domain. Such design solutions should be defined in terms of a valid topology, shapes and sizes of the mechanism's constitutive elements. Topology can be thought of as the connectivity between the elements. A topology is considered valid when it guarantees connectivity between the essential ports, typically the input, the output, and the ground port.

To conceive a methodology that is able to provide design methods, we need a methodological framework. In our case, we will use the elements of technical system representation, where mechanisms are viewed as design objects that perform a function on a flow of energy, and their behavior complies with a set of requirements.

To develop structured design methods for SBCM's we need to answer in depth four critical questions:

What is a design method?
How are compliant mechanisms designed?
What are the conditions that characterize a state of static balancing?
How to include a state of static balancing in the design of compliant mechanisms?

Answers to these questions are presented along the chapters of this work. Chapter 2 answers

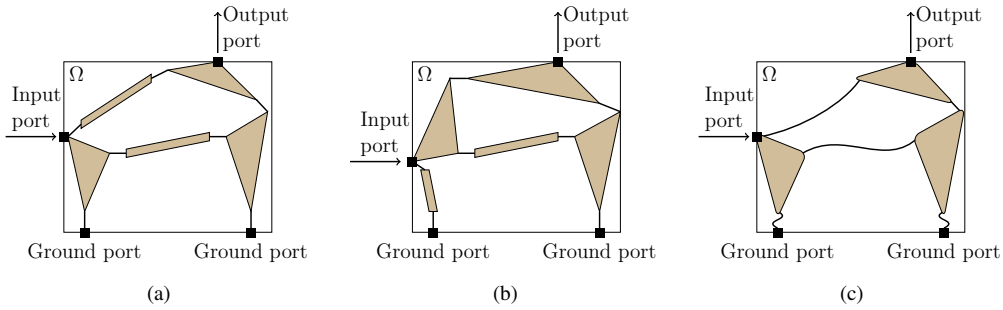

Figure 1.4: The design domain includes the essential ports (input, output, ground). A mechanism is described by its topology, shapes and sizes. (a) and (b) have the same number of elements but their topologies are different. (a) and (c) have the same topology but some of their elements have different shape and size.

the first question by introducing the design framework and the design perspectives on which this work is based. The chapter focuses on mechanisms viewed as design objects and discusses the relations between requirements, characteristics, constraints and design variables as well as the implications of static balancing and compliance in the conceptual and detailed design stage.

Chapter 3 gives answers to the question of how compliant mechanisms are designed. This is done through a literature review on the design methods for compliant mechanisms. The review concentrates on the design methods reported in books, theses, journals, proceedings, and reports using as search keywords combinations of the terms ‘compliant’, ‘mechanisms’, ‘micro-mechanisms’, ‘flexures’, ‘flexible’, ‘hinges’, ’notch hinges’. The body of knowledge gathered from the literature review is organized into a proposed new classification which expands the possibilities for the allocation of new methods and literature. The chapter concentrates on the description of the three main design approaches: (i) the rigid body replacement as a straight forward approach, which takes a conventional rigid body mechanism and replaces the overlapping joints by monolithic flexures, (ii) the building blocks which searches for simple blocks with simple functions and then combine them to create complex functions, and (iii) structural optimization or automation of the design search which poses the design problem as a mathematical function that at its minimum value attains the design solution by setting the design search space as the function’s domain.

To answer the question about the conditions that characterize a state of static balancing, we refer to chapters 4 and 5. These two chapters explore and synthesize the knowledge about static balancing. Chapter 4 presents the results from the study based on virtual experimentation of mathematical models of well-known statically balanced mechanisms. The intention of the chapter is to show static balancing and its properties in the context of a simple mechanism.

Chapter 5 presents initially a review on static balancing. The review reports the literature re-

trieved by combinations of the terms: ‘energy-free’, ‘static balancing’, ‘continuous equilibrium’, ‘zero stiffness’ and ‘force compensation’. This review is also expanded by the relevant articles included in the reference lists. The presentation of the literature follows a proposed classification based on applications and design approaches. The remainder of chapter 5 is devoted to the generalization of the static balancing conditions in a physical and mathematical context. The generalization of the conditions is presented using linear algebra in order to relate static balancing with the conventional description of elastic systems in terms of their stiffness matrices. The generalization explains statically balanced compliant mechanisms as structures described by singular stiffness matrices as well as the relation among null spaces, buckling and vibration modes, eigenvalues and eigenvectors, for these particular systems.

Chapter 6 explains how to include a state of static balancing in the design of compliant mechanisms through the introduction of a novel design methodology for SBCM’s. The design methodology is derived by combining the two bodies of knowledge presented in chapters 3 and 5 — the design methods for compliant mechanisms and the static balancing conditions. From the proposed design methodology several design methods are derived through the development of examples of SBCM’s.

Chapter 7 is fully dedicated to one of the methods derived from chapter 6. This chapter explores the viability of a new design method based on structural optimization, specifically topology optimization. The method tests two different formulations for the solution of two benchmark examples common in literature, (i) the gripper and (ii) the inverter. The chapter introduces a modification of Warshall’s algorithm to identify disconnected nodes and/or elements on structures represented by undirected graphs.

Final discussion and conclusions are presented in chapters 8 and 9, where we address many unresolved issues and open questions as well as the final message of this work which is the view of statically balanced compliant mechanisms as failed structures that do not require any force to fail. This view is based on the fact that statically balanced compliant mechanisms are structures that load themselves to the critical buckling load, with a finite and maximized range of motion where the self-buckling load is kept critical.

2 The design framework

It's not enough that we do our best; sometimes we have to do what's required.

Winston Churchill

To answer the question of what is a design method, first we need to understand what are design requirements and their classification as well as the relation between design requirements and design attributes. Understanding of this relation helps to interpret the attributes of *compliant* and *static balancing* in terms of design requirements. The relation between requirements and attributes is presented as the design problem from the view of technical system representation.
Once we understand design requirements and their relation with the design attributes we introduce design methods as iterative design cycles in which design requirements are translated into design attributes. The presentation of the design process is treated from the teleological perspective of design, that is to say from the end and purpose of the design.

2.1 Technical system representation of the design problem

This section will introduce a view of statically balanced compliant mechanisms through the prism of technical systems. Under this view we give an answer to the questions of why *compliant* and why *static balancing*, what means *compliant* and *static balancing* to mechanisms and what is the relation of *compliant* and *static balancing* with the design requirements. Answering these questions helps the designer to understand when *compliant* and/or *static balancing* is the goal of the design. The view used in this section is constructed on the analysis of a proposed categorization of the design requirements, and tested through the grammatical logic of human language.
Mechanisms as machine components are designed for a purpose, and this purpose defines what is called in representation of technical systems [94], the *main function*. The main function is the fundamental reason for which the mechanism is designed. It is expressed as an action on a flow, and defined in terms of the functional requirements. By flow we refer to any form of matter, energy or information on which the design object acts, and without being part of this, it flows

physically and/or functionally, across the design object.

In a conventional sense, mechanisms are designed to fulfill some functional requirements that normally can be categorized as, (i) path generation, (ii) function generation, or (iii) motion generation. These allows to define the main function in a general way as *transmit power* or more specific as either *transform motion* and/or *transform force*, depending if we give more relevance to the displacement or force component of the power. Here *transmit* or *transform* is the action, and *power*, *motion* or *force* is the flow —an energy flow. Figure 2.1 depicts the black box representation of a mechanism with its main flow and function.

Notice that these two more specific functions —*transform motion* and *transform force*— are the root of the two dimensions of the design of mechanisms, (i) mechanisms as mobile structures and (ii) mechanisms as structures that coup with reaction forces. In the design of conventional mechanisms, the second dimension is subrogated to the assumption of rigid bodies, but this is not the case for compliant mechanisms.

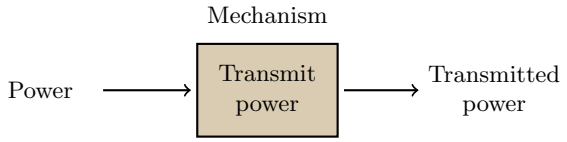

Figure 2.1: Black box representation of a mechanism. Here the design object, the mechanism, applies the function transmit onto a flow of energy, in this case power.

In essence, the functional requirements define the main function, what the mechanism should do, but they are not the only requirements. In the design of mechanisms the non-functional requirements are related to constraints and characteristics [113]. While the constraints are limits to functional requirements and characteristics, the characteristics express what the mechanism and its function should be. Certainly functional characteristics do not define but condition the main function to when, where, or how it is accomplished, while product characteristics condition or qualify the mechanism itself. At the end of the design process, all the requirements (functional and non-functional) should be reflected by the behavior attributes and physical attributes of the real and tangible design object. Figure 2.2 shows how requirements are classified and how they relate to the function and attributes.

When we talk about a compliant mechanism, implicitly we are referring to a design object (here the mechanism), that has been conditioned to bear the attribute *compliant*. If we translate back this attribute into requirements, we find that it does not say anything about what the mechanism does, but how it is. *Compliant* for a mechanism defines product characteristics such as monolithic, predictable, precise, reliable, compact, noiseless, durable, as well as functional characteristics like energetically inefficient and motion limited.

Conditioning the design object to be *compliant* has its advantages and disadvantages, but how to

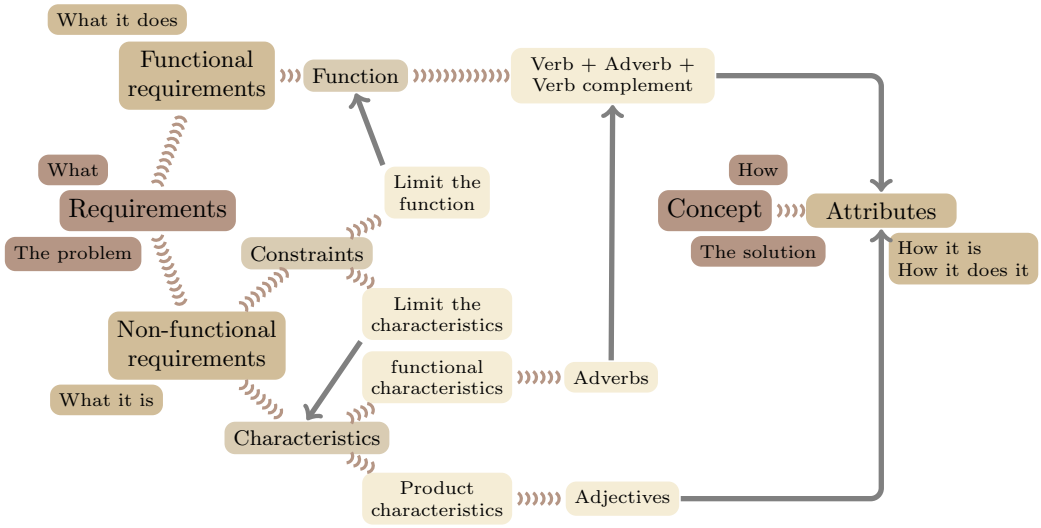

Figure 2.2: Requirements and their relation with the function and attributes.

make use of the advantages while the disadvantages are minimized? Clearly the root of all the characteristics for the attribute *compliant* is the monolithic nature imposed on the design object, which means limited motion and motion implies strain energy storage.

For the limited motion, not too much has been done, but for the energetic inefficiency the immediate answer has been maximize the deflection with the minimum strain energy storage, as proposed in most of the literature on the subject [27]. But there is a problem with this approach, if elements deflect, then the strain energy storage will never be zero, no matter how good the strain energy is minimized.

Here in this work we intend to tackle the energetic inefficiency problem not by minimizing the strain energy storage but making the strain energy constant. This is done by using the concepts of self-principles [128], to reach a state of static balancing on which all the internal elastic forces are balanced during motion, making the operation of the mechanism effortless. The idea is to design a mechanism, that accomplish a function attaining the desirable characteristics related to the attribute of *compliant* and remove the undesired energetic inefficiency using static balancing (one functional characteristic cancels the other).

Static balancing is an attribute that when expressed as a requirement bears the functional characteristic of energetically efficient and the product characteristic of prestressed, overconstrained, and enlarged. Conditioning the design object to be compliant as well as statically balanced has as a consequence the reduction of the search space in the design domain, making their design complex (Fig. 2.3). To design a mechanism that is compliant as well as statically balanced, is to talk about a design approach that is able to combine functional requirements with characteristics

on both, the design object and its function.

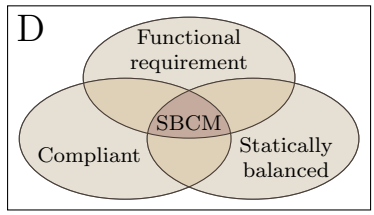

Figure 2.3: Reduction of the search space as a consequence of imposing functional requirements, functional characteristics and design object attributes.

The design of SBCM's could lead to the oversight of the characteristics that the design of such mechanisms convey, this is the case when the designer tends to think in terms of how to do it, instead of what to do. To see the latter, we relate in a grammatical sentence the existing logical relation among the elements used in the representation of technical systems (the design object, its given function and its characteristics) [109], in order to verify the coherence of the design problem formulation (see Fig. 2.4).

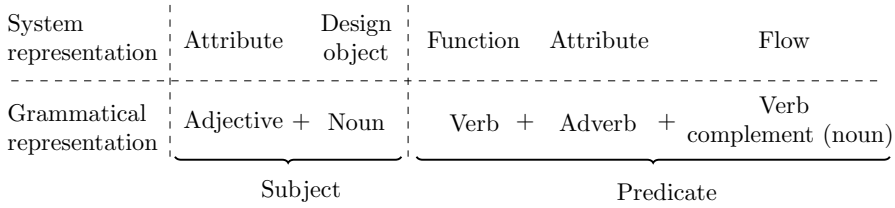

Figure 2.4: The design problem and the equivalence between technical system representation and grammatical representation.

The sentence expressing the design solution in terms of *how to do it*, would be something like:

Statically balanced compliant mechanisms transmit power.

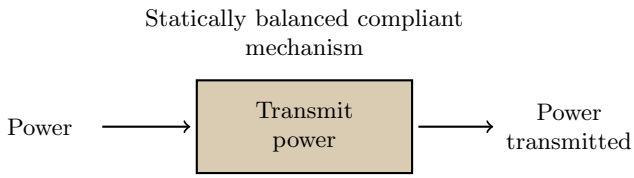

Figure 2.5: Black box representation of the design solution. The design solution expresses how the problem is solved.

We observe a coherent sentence, but requirements have been diluted into the attributes, obscuring the intention of the design. Now the sentence expressing the design problem in terms of *what to do*, would be:

> *The monolithic, predictable, precise, reliable, compact, noiseless and durable mechanisms transmit power efficiently*.

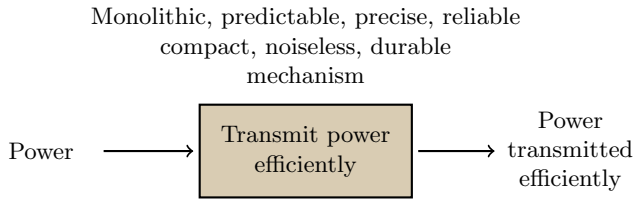

Figure 2.6: Black box representation of the design problem. The design problem expresses what is the problem to be solved.

Certainly, this sentence reflects congruently what the design should do and should be. The design of statically balanced compliant mechanisms then requires from the designer to keep in mind that static balancing and the use of compliance are not the ultimate goals of the design but the means to fulfill the requirements. It is to say that a nice design that is fully compliant and has been statically balanced but which its motion does not satisfy any functional requirement is then useless.
Compliant mechanisms and statically balanced mechanisms should not be designed for the sake of compliance and balancing.

2.2 The design process

The development of a design methodology requires to (i) understand the design process, (ii) understand how the problem is translated into solutions, and (iii) understand the complexities on design derived from the selection of compliance and static balancing as the means to achieve the requirements.
The design of statically balanced compliant mechanisms is certainly more complex with respect to the design of what we call conventional mechanisms, or mechanisms based on rigid bodies. This complexity arises from the association of the design variables with the requirements and attributes, since this association defines the independence between design stages and design steps. To get the idea, first we need to understand the design framework for conventional mechanisms to later discern the design of statically balanced compliant mechanisms.

Design as such is the act of finding useful solutions to a problem that arises from unsatisfied needs. In the case of mechanisms, design arises from the need to transmit power or transform motion and forces between actuating and effecting elements.
In the design of technical systems, such as mechanisms, the needs are translated into requirements which in turn, as explained in the previous section, will define the function, the characteristics and the constraints of the design. But keep in mind that these definitions are intangible abstractions. Therefore, the function, characteristics and constraints are associated to design variables that later will frame the manifest attributes of the real design object. In the case of mechanisms, the most important attributes are those related to topologies, shapes and sizes, since they finally define the mechanism from a technical system view.

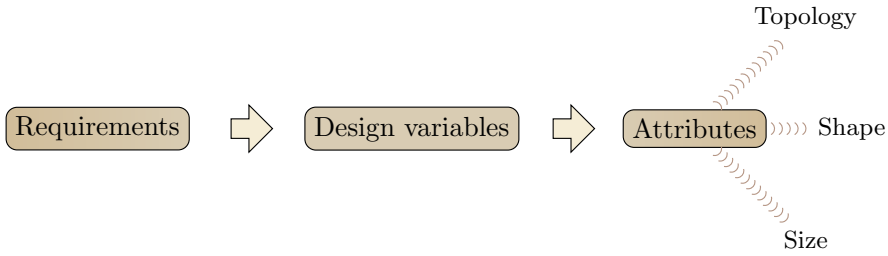

Figure 2.7: Attributes relate to requirements through the design variables.

The design of mechanisms in a broad view can be decomposed in two stages, (i) the conceptual design, and (ii) the detailed design. Within each stage it is possible to identify the iterative design cycle comprising four steps, (i) set requirements, (ii) synthesis, (iii) analysis, and (iv) evaluation (see Fig. 2.8).

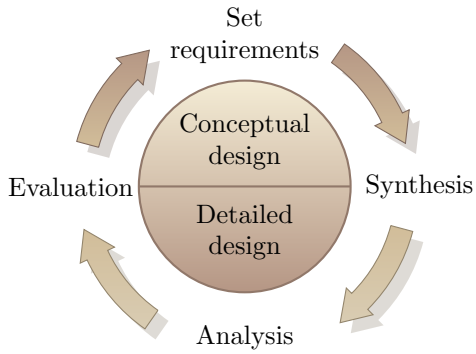

Figure 2.8: Design of mechanisms decomposed in two stages, comprising the four iterative design steps.

In a general way, the design cycle consists of giving values to the design variables —the synthesis

step— to later verify the behavior of the resultant concept —the analysis step— and compare this behavior with the desired behavior expressed by the requirements —the evaluation step— to finally, based on the evaluation, update the requirements if needed —the set requirements step. How these four steps are performed is what gives birth to all sorts of design methods.

At stage level, the conceptual design stage provides solutions —concepts— considering only the functional aspects, while the detailed design stage refines the concepts to comply with requirements that are not function related.

The conceptual design stage and the detailed design stage can or can not be carried out independently. The independence between stages is given by the interrelation degree between requirements and design variables. That is to say if functional requirements, functional characteristics and functional constraints are in function of a set of design variables, and this set of design variables are fully independent from the set from which product characteristics and product constraints are in function, then both design stages are fully independent. But once that both groups of requirements share design variables in their domains, the design stages lose their independence.

An example of independence between design stages is the design of a mechanism with a functional requirement for path generation and the non-functional requirement of lightweight. Assuming a linkage as the solution, then in the conceptual stage it is possible to find a solution to the trajectory by only considering the topological variables and the length of the links, while omitting the remaining variables that fully define the link shapes and their mass. The remaining variables are defined later in the detailed design stage. In this kind of examples the independence among design variables allows to define topologies, shapes and sizes individually.

The design of compliant mechanisms poses the problem of the intricate interrelation between requirements and design variables due to their monolithic nature which intertwines the functional and non-functional requirements. The execution of the design stages rather than being stepwise becomes an evolutionary process. The design variables define the topology, shapes and sizes simultaneously considering the mechanism as a whole. This is why the attribute *compliant* encloses so many different requirements.

On the other hand, the design of statically balanced mechanisms is typically done in two phases, each phase comprising the latter mentioned stages and steps. First the conventional mechanism is designed through the selection of a design principle that introduces the functional characteristic of energetic inefficiency, then the second phase or static balancing phase is defined by the function *balance the mechanism* subject to a functional constraint imposed by the mechanism's kinematics.

The design of statically balanced (rigid body) mechanisms is a relocating and/or additive design process, in which masses, elastic elements, charges, or fields are relocated and/or added to the existing mechanism without modifying its kinematic behavior. Design variables for static balancing are then fully independent from the design variables defining the conventional mechanism.

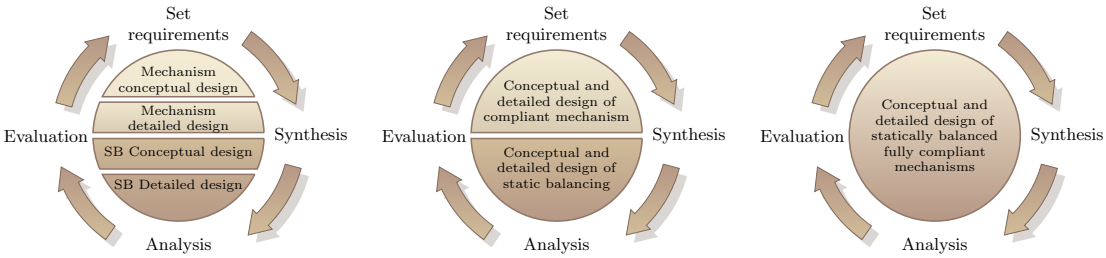

Figure 2.9: Stage independence in the design cycle for (a) statically balanced conventional mechanisms, (b) statically balanced partially compliant mechanisms, and (c) statically balanced fully compliant mechanisms.

They do not belong even to the same design phase, see Fig. 2.9a.

Now, the design of statically balanced *compliant* mechanisms certainly carries all the difficulties of the design of compliant mechanisms, but for static balancing two situations are observed if the design is either (i) partially compliant or (ii) fully compliant.

Partially compliant designs are mechanisms with overlapping elements, where motion is a product of rigid body motion and deformations, while fully compliant designs are monolithic mechanisms where motion is only product of deformations.

If the aim of the design allows the use partially compliant designs then the static balancing phase can be carried out independently (Fig. 2.9b). This is the case when the balancing elements are connected to the unbalanced design through the use of stiffness-free overlapping joints.

If the design must be fully compliant, the addition of the balancing elements is done by the use of compliant joints which are sources of strain energy and stiffness, therefore disrupting the action of the balancing elements and the kinematic behavior of the unbalanced design. The static balancing phase is not independent, making the design of statically balanced fully compliant mechanisms a one stage process (Fig. 2.9c) in which the conceptual and detailed design take place simultaneously, and the definition of the topology, shapes and size are carried out at the same time.

There is an exception to the above reasoning. It occurs when at the kinematic pair connecting the compliant modules, (i) there are no overlapping pre-stressed sources of stiffness and (ii) there is no relative motion between the balancing elements and the unbalanced design. In this case the partially compliant design is transformed into a fully compliant design by replacing the connecting kinematic pair by an inactive compliant joint.

2.3 Summary

Combination of the framework for requirements and attributes illustrated in Fig. 2.2 and the iterative design cycle illustrated in Fig. 2.8 provides the whole framework for the design of mechanisms used in this work. This framework is illustrated in Fig. 2.10. The framework summarizes the classification of the design requirements and their relation with the design attributes through the iterative design cycle. Here, design requirements are divided into functional requirements and non-functional requirements —constraints and characteristics. The framework also summarizes the relation of characteristics with the grammatical representation of technical systems, where functional characteristic are adverbs to the main function and product characteristics are adjectives of the design object.

The iterative design cycle is shown as a process of two design stages —conceptual and detailed design— comprising the four design steps —set requirements, synthesis, analysis, and evaluation— from which the design variables define the design attributes in terms of topologies, shapes and sizes.

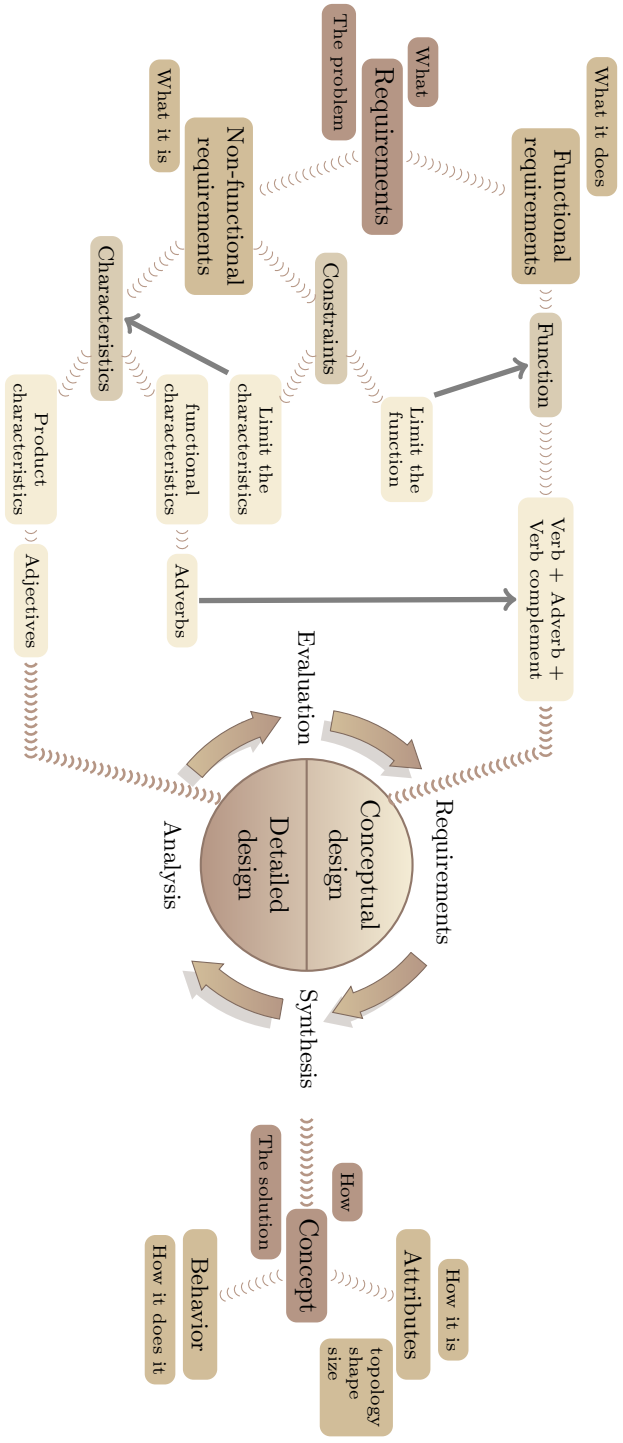

Figure 2.10: Complete design framework.

3 Synthesis of Compliant Mechanisms

Get the habit of analysis - analysis will in time enable synthesis to become your habit of mind.
Frank Lloyd Wright

This chapter provides an answer to the question how compliant mechanisms are designed. The chapter gives a glimpse of the state of the art on the synthesis methods for compliant mechanisms and introduces a classification of the synthesis methods which serves as the structure for the presentation. The main idea behind each synthesis approach is conceptually explained. At the end of the chapter it is presented a final discussion of the main design approaches considering benefits and disadvantages.

3.1 Introduction

Compliant mechanisms are those mechanisms that accomplish their function due to the deformation of one or more slender segments of their members; they do not rely exclusively on the relative motion between joints and the rigid links. From the referenced literature, advantages of compliant mechanisms were collected, which may be summarized as follows.

Due to their monolithic nature compliant mechanisms possess two main benefits over conventional rigid-link mechanisms, namely no relative motion among pieces and no overlapping pieces (see Fig. 3.1a). The absence of relative motion implies the absence of sliding friction, which eliminates wear, noise, vibration and the need for lubrication. Consequently, less maintenance is required. Furthermore, backlash is eliminated, which leads to reduced positioning error and therefore increased precision. The fact that there are no overlapping pieces allows fewer parts and single piece production, which reduces the assembly and weight. Therefore, compactness and miniaturization characteristics are enhanced while production costs are reduced.

All the benefits of compliant mechanisms help to create more innovative designs and actuation arrangements which increase the solution search space. In the case of adaptive structures, compliant mechanisms mean that fewer actuators are required.

Apart from the above advantages, the monolithic nature of compliant mechanisms also gives rise to some drawbacks (see Fig. 3.1b). Due to potential energy storage in the compliant segments, the input-output relationship is affected. In particular, energy efficiency is challenged. As consequence, synthesis and analysis cannot be done by separating kinematics and dynamics. The design process is even more complicated if the compliant segments undergo large deflections, in which case the governing stress and strain equations become non-linear. In the design process of compliant mechanisms the stress and strain relationships must be considered because they determine the deformed shape of the elements and therefore the input-output behavior of the mechanism.
These disadvantages tend to turn the design into a trial and error process highly dependent on the designer's experience [42]. This prevents the wide use of compliant mechanisms and therefore few examples are available to be used as inspiration for new developments [89].

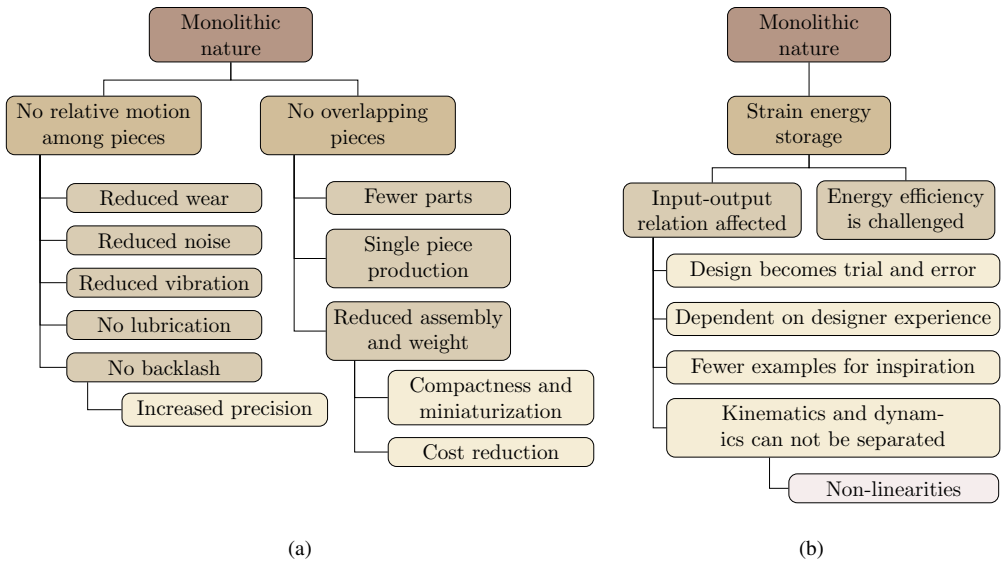

Figure 3.1: Features of compliant mechanisms due to their monolithic nature. (a) Advantages. (b) Disadvantages.

Although compliant mechanisms have been used for more than a century, the last 20 years have shown a proliferation of new methods for analysis and synthesis of such mechanisms.
Despite all the work that has been done in compliant mechanisms, there are only a few introductory documents and books available [12][40][125], but none of them present an accessible and comprehensive introduction to the synthesis methods.
For those with little or no experience in the field of compliant mechanisms this poses a problem, which is finding a starting point from where they can be guided towards the solution of a specific design problem. This problem is also enlarged by the amount of knowledge areas that

converge here: compliant mechanisms involve kinematics of mechanisms, multi-body dynamics, non-linear mechanics of materials, numerical optimization techniques, etc. This chapter aims to present a comprehensive overview of the most common synthesis approaches for compliant mechanisms. The chapter is also intended to provide the reader with a basic understanding of the methods in a way that the reader acquires a sufficiently wide knowledge base to investigate particular methods or to find methods that are suitable for particular application. Three main different design synthesis approaches for compliant mechanisms are distinguished; the kinematics based approaches, the building blocks approaches and the structural optimization based approaches. The organization of the individual methods within these main approaches is represented in Fig. 3.2.

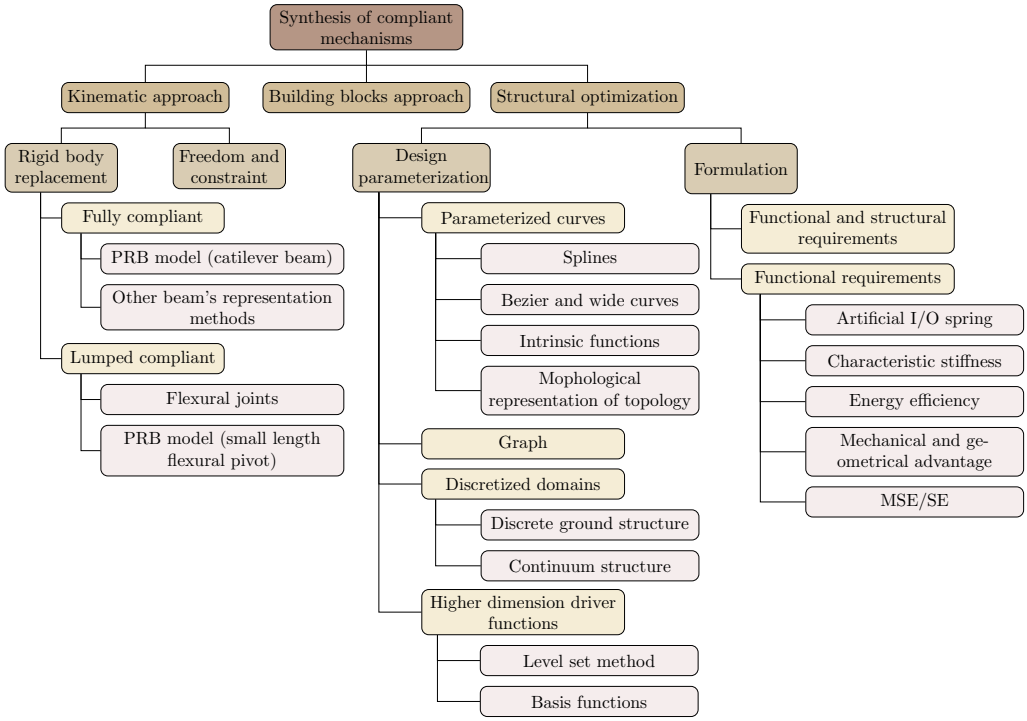

Figure 3.2: Synthesis of compliant mechanisms

In the kinematics based approaches two methods are discussed: the rigid-body-replacement method based on flexure joints and pseudo-rigid-body models, and the freedom and constraints topologies. In the building blocks approaches two methods were identified: the instant center approach and the flexible building blocks. In the topology and shape optimization approach the optimization problem is presented as well as the most common parameterizations and objective formulations found in the literature on the subject.

3.2 Kinematic approaches

Two main methods can be found here; the Freedom and Constraints Topologies (FACT) and the Rigid-Body-Replacement method. As the name suggest these methods aim to obtain designs by focusing on kinematic requirements.

3.2.1 The FACT method

The FACT method [37][38][39] is based on mapping a set of geometric entities in the freedom space onto a set of geometric entities in the constraint space where the topology solutions for the design problem can be found.
Basically the designer translates the required motion of the mechanism into degrees of freedom (DOF) which are used to find the geometric entities that describe the required motion in the freedom space. Knowing these geometric entities, it is possible to find in the constraint space the topologies of the flexure elements that provide the desired motion.
In the FACT method there are twelve sets of geometric entities, but only eight have importance in flexure systems. The other four are still in the process of being correlated with flexure systems.
To give a clear idea of the method a simple example will be given. Imagine that some device is needed having two DOFs; a displacement in the z axis and a rotation about the x axis, Fig. 3.3.

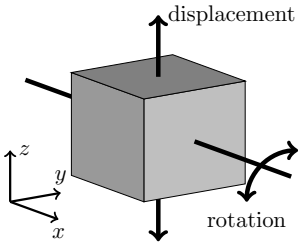

Figure 3.3: Device with two DOFs.

The rotation can be represented by one of the twelve geometrical entities, the P-plane. The P-plane represents a plane containing all co-planar and parallel rotation lines with a specific orientation. In our case the P-plane is parallel to the xy plane, and the lines have the same orientation of the rotation axis, see Fig. 3.4a.
The displacement can be represented by the geometrical entity, the Hoop. This entity represents the displacement as a rotation in the infinite about any axis that lies in the xy plane, Fig. 3.4b.
Now that the DOFs have been translated into a set of two geometrical entities, a Hoop and a P-plane, the mapping from the freedom space to the constraint space can be performed.
According to the FACT method the Hoop and P-plane together in the freedom space are mapped in the constraint space with two other geometrical entities, the Box and the A-plane, see Fig. 3.5.

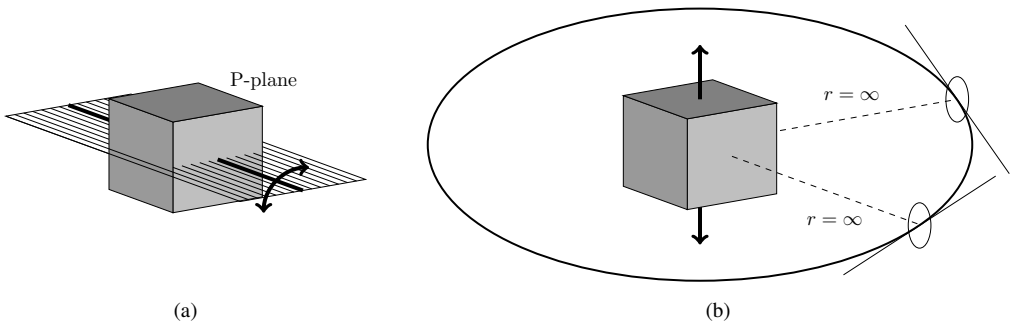

Figure 3.4: Geometrical entities representing the freedom space of the design problem shown in Fig. 3.3. (a) The P-plane entity represents all the coplanar rotation axes with the same orientation. (b) The Hoop entity represents displacements as rotations pivoting at infinity.

From these geometrical entities the constraints will be obtained.
The Box represents the constraint lines inside this box, which are parallel in the direction specified by the P-plane in the freedom space. The A-plane represents any constraint line that lies on this plane, which is parallel or coincident with the lines in the Box.

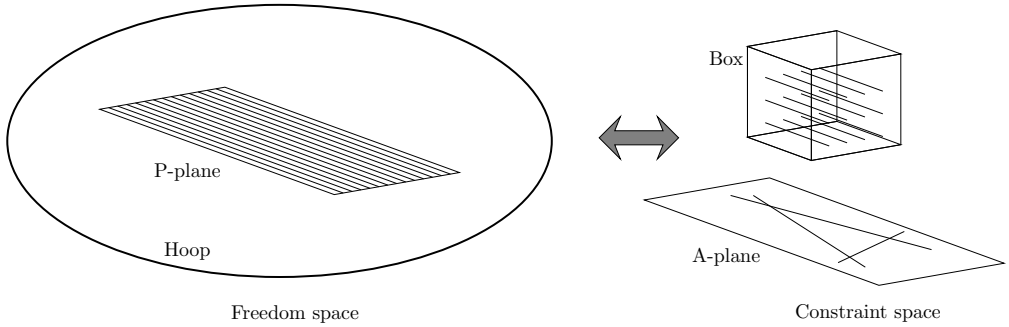

Figure 3.5: Mapping between the freedom space and the constraint space.

Because the problem has two DOF it means that it needs four non-redundant constraints. The constraints can be thought of as truss elements (a bar between ground and the object, connected by spherical joints). A solution to the example can be seen in Fig. 3.6a. Notice that the three lower constraints lie in the A-plane, while the three parallel constraints lie in the Box. Now the constraints are replaced by beam elements designed in such a way that they provide the proper flexibility and stiffness in the required directions to replace the constraints, see Fig. 3.6b.
In the FACT method the mapping is done by searching in a table the case and the type that better suit the concerning problem. In the example, the problem requires four non-redundant constraints which match with Case 4 and the geometrical entities in the freedom space (hoop and P-plane) match with a Type 2 problem.

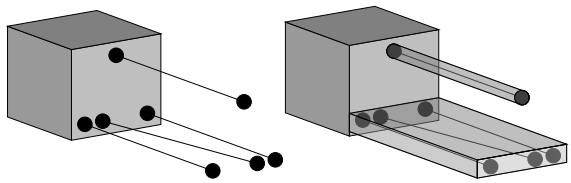

Figure 3.6: Possible solution for the FACT example. (a) Selected constraints, (b) possible solution, here the compliant beam replaces three of the constraints.

The FACT method is a type synthesis method that only provides topologies for the mechanisms. The FACT method requires the use of some complementary dimensional synthesis to complete the design process. The method not only considers the rotational and translational displacements but also the screw movement, which is a coupled rotation and translation movement.

3.2.2 The Rigid-Body-Replacement

The Rigid-Body-Replacement method consists of finding a rigid body mechanism that accomplishes the desired function and then converting it into a compliant version. The conversion is performed by replacing the joints using a Pseudo-Rigid-Body model or beam deflection model, or by simply replacing the conventional joints with flexure joints. The Rigid-Body-Replacement method [12][42] as presented in literature makes extensive use of the Pseudo-Rigid-Body (PRB) model [40] but it is not limited to it.
In the classification of compliant mechanisms two main types of compliance can be distinguished, lumped compliance and distributed compliance. In the case of a lumped compliant mechanism the deformation takes place in a concentrated part of the constitutive elements while in a distributed compliant mechanism the deformation occurs along a broader part on the constitutive elements, Fig. 3.7.

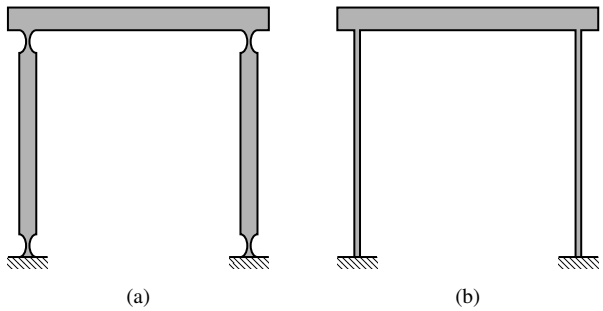

Figure 3.7: (a) Lumped compliance, (b) distributed compliance.

Based on the mentioned distinctions, the synthesis approaches in the rigid-body-replacement can be divided in design based on flexure joints (either with lumped compliance or distributed compliance) and design based on PRB model (either for lumped compliance or distributed compliance).

Flexure joints

A flexure joint is a region which can undergo large deflections relative to stiffer adjacent regions in the same element. Normally these stiffness differences are attained through the geometrical characteristics of the deflection regions. Depending on these characteristics, the flexure joint can show single or multiple deflection axes which can be rotational or translational axes.
Flexure joints can be categorized as primitive and complex flexures [148]. Flexural joints with rotational axes are also known as flexure hinges or flexure pivots.

Flexure joints for lumped compliance Among primitive flexures there are the small length flexures and the notch-type flexure hinges were the notch profile can be a rectangular section, corner filleted, circular, parabolic, hyperbolic, elliptical, inverse parabolic, secant or hybrid sections [69, 70, 71, 149], some of which are shown in Fig. 3.8.

Figure 3.8: Notch-type flexure hinges. (a) Corner filet, (b) circular, (c) parabolic, (d) hybrid.

Flexure joints for lumped compliance have the advantage of a low variation in the locus of the axis of rotation since deflections tend to be localized at the thinnest section of the notch hinge. This advantage have as a consequence high stress concentration that limits the range of motion. Therefore the design of the notch-type flexure hinges is normally confined to small displacements, however they can be designed to undergo large deformations as presented in [85, 52] if stress concentrations are properly handle.

Flexure joints for distributed compliance Flexure joints for distributed compliance can be both primitive and complex flexures. The primitive flexures can be shaped as ellipses, four-bars, chevron, etc. See Fig. 3.9.
Complex flexures are combinations of more simple flexures which can be design to act as revolute joints, prismatic joints or as universal joints [87, 138], Fig. 3.10.

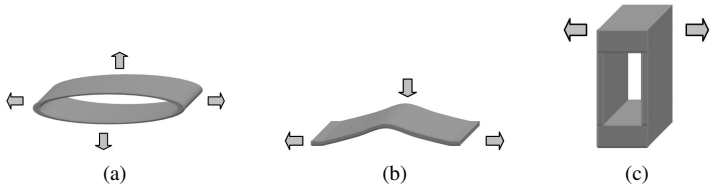

Figure 3.9: Primitive flexures for distributed compliance. (a) ellipse, (b) chevron, (c) four-bar.

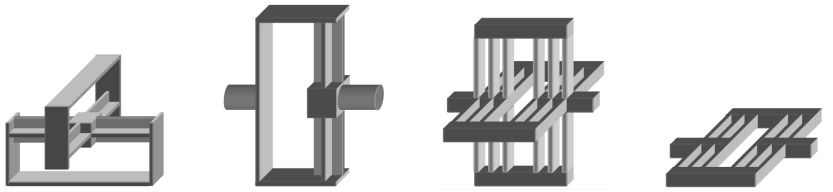

Figure 3.10: Complex flexural joints, reproduced from [138]. (a) universal joint, (b) revolution joint, (c) and (d) prismatic joints.

Complex flexures can be combined to create even more complex elements. Moon and Kota [86] for instance present the design of Compliant Parallel Kinematic Machines (CPKMs) using a set of constraining legs. Their design is based on a set of three complex flexure joints, see Fig. 3.11.

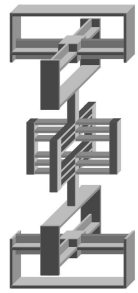

Figure 3.11: Flexural joints for the design of constraining legs for compliant parallel kinematic machines. Reproduced from [86].

Examples of other complex flexures are the Compliant Contact-Aided Revolute (CCAR) joint [16] and the Compliant Rolling-contact Element (CORE) [17], which can act as a combination of bearings and springs, see Fig. 3.12.

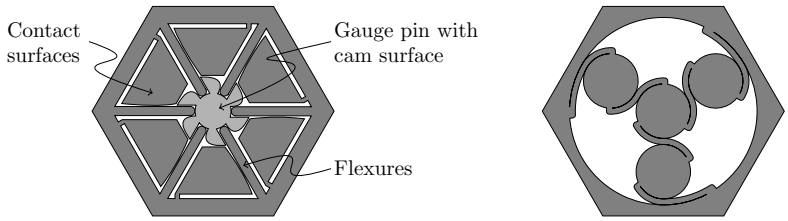

Figure 3.12: Contact-based joints. (a) The CCAR joint [16], (b) The CORE joint [17].

Pseudo-Rigid-Body model (PRB)

The pseudo-rigid-body model is an approach that allows to find a rigid-body mechanism that emulates the behavior of a compliant member that undergoes large, nonlinear deflections. The deflection path is given by the kinematics of the rigid-body mechanism whilst the force-deflection relation is approximated by springs that represent the member's stiffness.
During the design of a compliant mechanism, the pseudo-rigid-body model has its main role in the conceptual design stage in the transition from the type synthesis to the dimensional synthesis. Analyses based on kinematics are simpler, so the use of pseudo-rigid-body model provides with a quick way to test concepts and therefore reduces efforts to obtain final concepts, just before proceeding with the detailed design.
The pseudo-rigid-body models vary depending on the boundary conditions applied at both ends of the beam, these conditions can be fixed-fixed, fixed-pinned and pinned-pinned; they determined how the loads are applied.
When two compliant members interact it is important to determine which condition better suits this interaction.

PRB model for lumped compliance The design of compliant mechanisms with lumped compliance using pseudo-rigid-body models is based on the pseudo-rigid-body model for small-length flexural pivots [42, 40]. Here the compliant member to be designed shows two segments, one large and stiff and the other short and flexible. The short one and flexible is known as the small-length flexural pivot.
The idea is to find the position of the characteristic pivot and the characteristic stiffness for the torsion spring in the pseudo-rigid-body model. Figure 3.13 shows a member with a small-length flexural pivot and its pseudo-rigid-body model.
The pivot is placed in the middle of the short segment and the stiffness constant of the spring is given by

$$K = \frac{(EI)_l}{l} \tag{3.1}$$

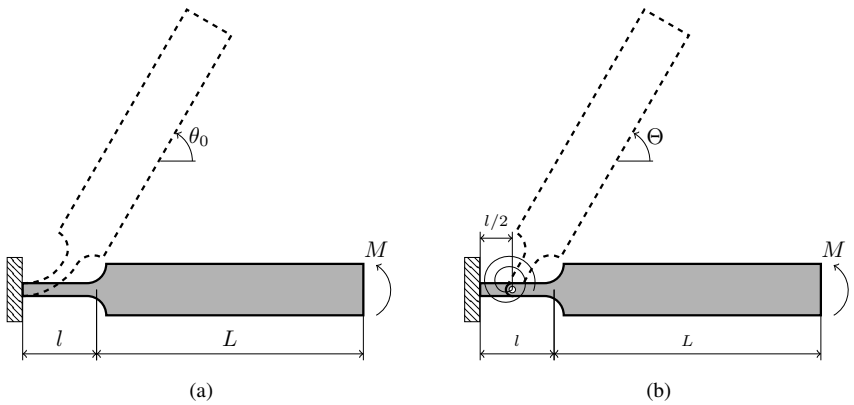

Figure 3.13: pseudo-rigid-body for a beam with small-length flexural pivot, reproduced from [40]. (a) Deflected beam, (b) equivalent pseudo-rigid-body model.

Where l is the length of the small-length flexure pivot, E and I are the Young's modulus and cross-section second moment of inertia respectively for this segment.

An accurate use of the pseudo-rigid-body model requires that: $L \gg l$ (L ten times or more larger then l), and $EI_L \gg EI_l$, also the member must be subjected to pure bending.

PRB model for distributed compliance In this approach the compliant member is assumed to have a constant cross-section.

The most important pseudo-rigid-body model for distributed compliance is the model for a fixed-pinned cantilever beam (no moments at the free end of the beam) with a force acting at the free end [43, 40], see Fig. 3.14.

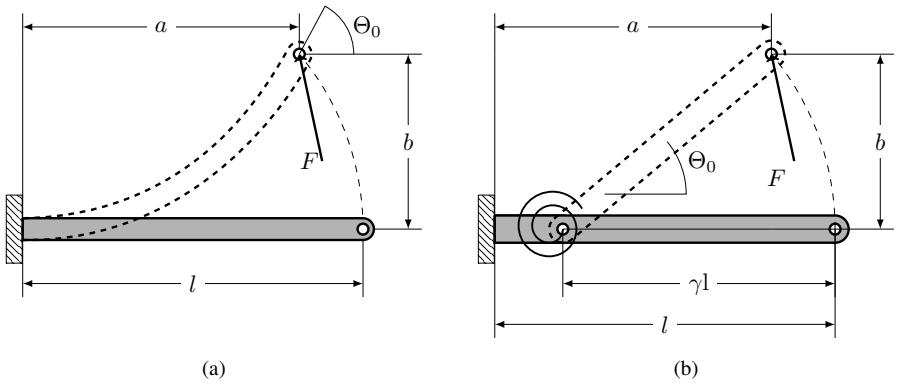

Figure 3.14: Pseudo-rigid-body for a cantilever beam with force at free end, reproduced from [40]. (a) Deflected beam, (b) Equivalent pseudo-rigid-body model

The position of the characteristic pivot is given by the value of characteristic radius γ. The characteristic stiffness for the spring is given by a stiffness coefficient k_θ and γ, see Eq. 3.2.

$$K = \frac{\gamma K_\theta EI}{l} \tag{3.2}$$

Both, k_θ and γ, are function of the *n* parameter which sets the orientation of the applied force at the free end as a proportion of its components, see Fig. 3.15. The equation to compute $\gamma(n)$ can be found in [41, 43, 44, 40]. The equation to compute $k_\theta(n)$ can be found in [41, 44, 40].

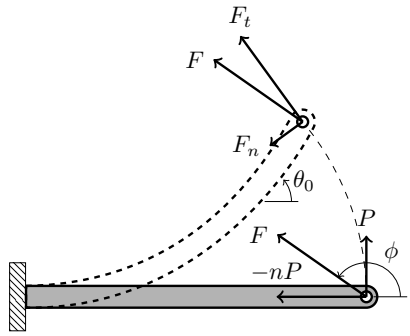

Figure 3.15: Applied force at the free end of the beam.

When the applied force at the free end has an orientation angle ranging $63.4 \leq \phi \leq 135$ or $-0.5 \leq n \leq 1$, a constant value of γ=0.85 and k_θ=2.65 can be assumed for rough calculations, otherwise the equations for $\gamma(n)$ and $k_\theta(n)$ must be used . These values provide an accuracy of 0.5% on the deflection path for deflection angles below 77°.

In literature, there are many other pseudo-rigid-body models for beams with different boundary and load conditions. For instance Saxena and Kramer [118] present a pseudo-rigid-body model for combined end loads with positive end moments, while Edwards at al. [25] present a pseudo-rigid-body model for compliant members that are initially-curved with pinned-pinned boundary condition (no moments at both ends of the beam). Kimball and Tsai [63] present a pseudo-rigid-body model for a cantilever beam with an end moment acting opposite to an end force. Lyon and Howell [80] present a pseudo-rigid-body model for a beam with boundary conditions fixed-fixed, while Su [132] presents a pseudo-rigid-body model for deflection angles larger than 77°. Here the deflection of a cantilever beam is approximated by a pseudo-rigid-body model composed of four rigid segments which are connected by three revolute joints with their respective characteristic springs. This model allows the use of combined force and moment at the free end of the cantilever beam.

3.3 Building block approaches

In the building block approach the idea is to concatenate multiple compliant mechanisms that perform simple functions to create compliant mechanisms that can perform more complex functions. There are two main building block approaches; one based on instant centers and compliance ellipsoids and the other one based on flexible building blocks and optimization.

3.3.1 Building blocks by instant centers

The building block approach based on instant centers [58, 57, 59, 60, 61, 62] is a conceptual design procedure. The idea is to find a mechanism that provides for a given input displacement an output with a desired displacement direction and geometric advantage (GA). The mechanism is found by concatenating two different basic blocks, the *compliant dyad building block* (CDB) illustrated in Fig. 3.16a and the compliant *fourbar building block* (C4B) illustrated in Fig. 3.16b. These two blocks can be used to form combinations, like those presented in Fig. 3.17a and 3.17b

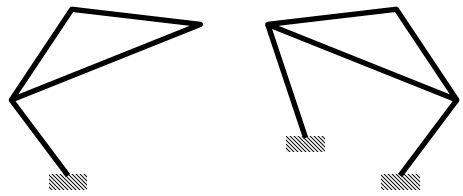

Figure 3.16: Basic compliant building blocks (reproduced from [60]). (a) A compliant dyad building block (CDB). (b) A compliant fourbar building block (C4B).

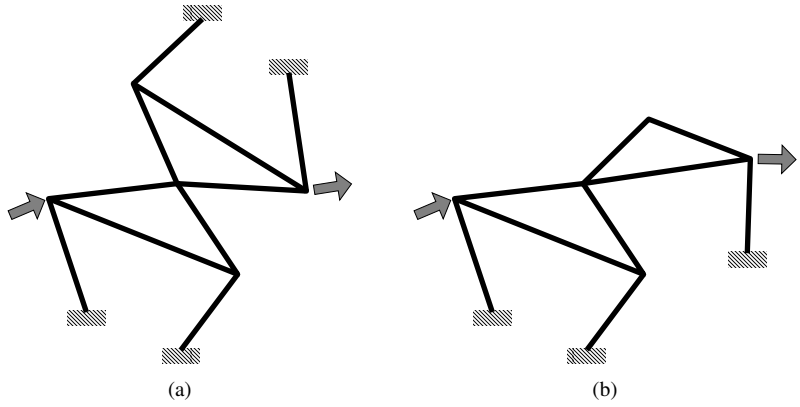

Figure 3.17: Building blocks concatenation (reproduced from [60]). (a) Combination of two C4B. (b) Combination of C4B and CDB.

This synthesis process is called the dual stage synthesis. Before explaining how the dual stage synthesis is used, three concepts are introduced: the principal compliance vector, the instant center and the decomposition point.

The *principal compliance vector* (PCV) is a unit vector that points in the direction of the major compliance at the output port of a mechanism. By intuition it can be seen that a cantilever beam like the one in Fig. 3.18a is more compliant in the vertical direction than in the horizontal one, then the PCV for the tip of the beam points in the vertical direction. Another example is presented on Fig. 3.18b, at the input port the PCV shows that the displacement will be vertical due to the input force, while at the output port the PCV indicates that the mechanism will move in the horizontal direction.

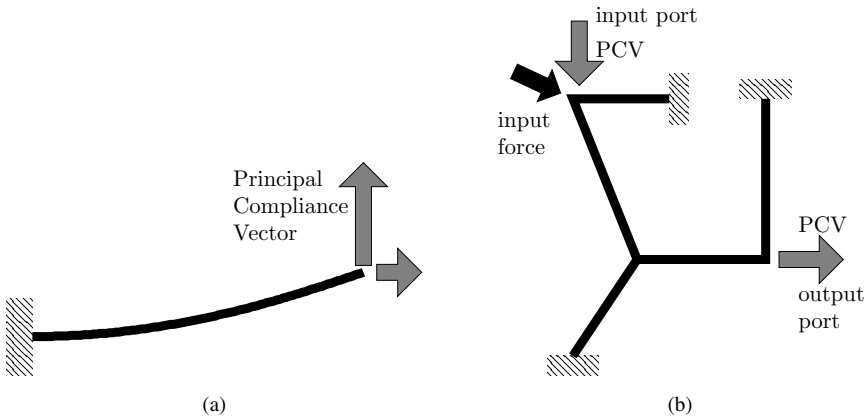

Figure 3.18: Principal compliance vector. (a) PCV of a Cantilever beam, (b) PCV of a compliant mechanism at the input and output port.

The *instant center* is defined as the point around which a rigid body with plane motion seems to rotate in a particular instant. For the case of a C4B the instant center can be identified by projecting the perpendicular lines from the PCV at the input and output port and finding the intersection point of these lines as shown in Fig. 3.19.

The *decomposition point* (DP) is the point inside the design space where two building blocks are concatenated. At this point the output port of the first building block coincides with input port of the second one.

In the dual stage synthesis, two building blocks are concatenated by finding the proper decomposition point, and by finding at this point the direction of the principal compliance vector that ensures the desired GA (Fig. 3.20).

Basically any point in the design space can act as a decomposition point, and for any decomposition point there is a PCV that ensures the geometrical advantage. Now, what distinguishes one decomposition point from another one is the way that the total GA is generated by the two

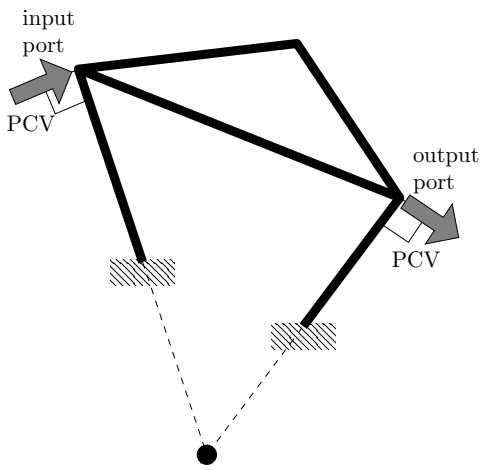

Figure 3.19: Instant center of a C4B is the point at which the rigid body (the coupler link) seems to rotate when at the given configuration the C4B undergo small deflections.

blocks, meaning that one building block could contribute more to the total GA than the other one. This is reflected in the expression for the GA:

$$GA_{total} = GA_1 \cdot GA_2 \tag{3.3}$$

where GA_1 and GA_2 are the geometrical advantages generated by block 1 and block 2 respectively. These geometrical advantages are equal to the ratio of the distance between the output port and the instant center over the distance between the input port and the instant center. The fitness of the decomposition point that provides a proper GA is measured by the *geometric advantage index* (n_{GA}) [60].

$$n_{GA} = \log_{GA_{target}}(GA_2) \tag{3.4}$$

The GA index normalizes the GA for block 2 in the range [0, 1]. Ideally, decomposition points are selected to yield a GA index of 0.5, which means that block 1 and 2 generate equal GA.

Another important issue in the design process is the selection of the position for the moving junctions. Moving junction are the elements that connect the floating links with the ground. A proper selection gives less error between the desired and the real GA. In Fig. 3.21 it can be seen how the same decomposition point and PCV's can have different arrangements for the moving junctions.

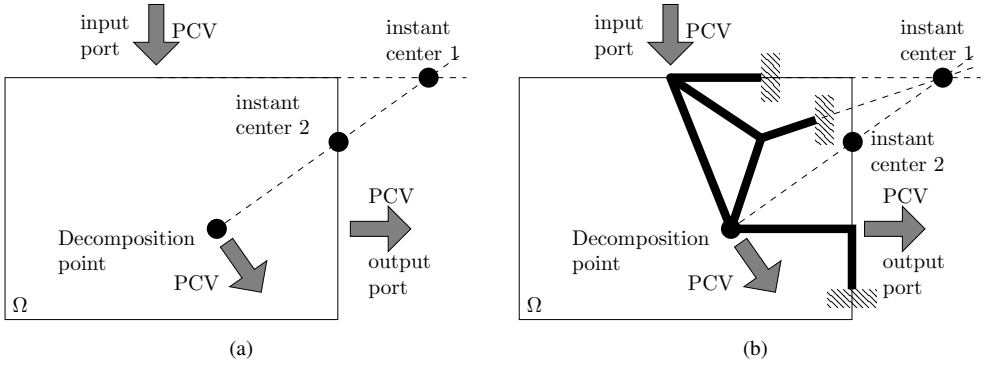

Figure 3.20: Example of the dual stage synthesis using one C4B and one CDB. (a) After setting the PCV at the input and output port, it is searched for the DP and its PCV that provides the desired GA. Then it is possible to find the instant centers. (b) Once the instant centers are known, it is possible to define the moving junctions.

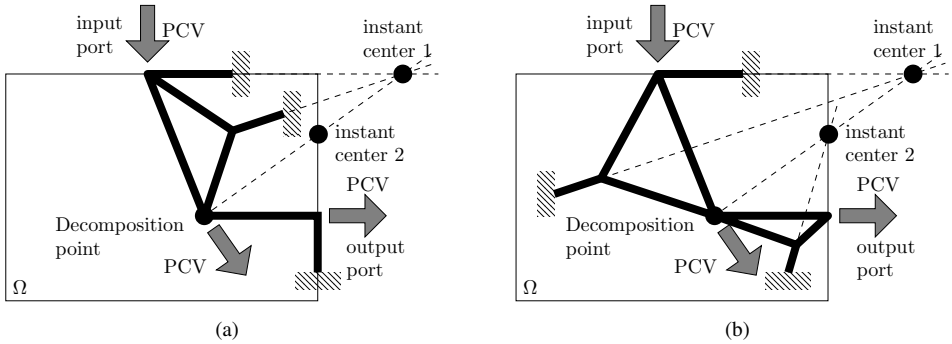

Figure 3.21: Two designs with the same DP, PCV and desired GA but different moving junctions, therefore different GA error between the desired GA and the final GA.

3.3.2 Flexible building blocks and optimization

In this design method, a compliant mechanism is considered as an assembly of multiple flexible building blocks [13]. The idea behind the method consists of searching for an optimal distribution of these flexible building blocks inside a mesh that acts as the design domain. The size of the design domain is defined by the number of building blocks and their size (height and width).
The building blocks are elementary units that are formed by joining two, three or more nodes with beam elements inside a mesh, see Fig. 3.22. Each building block has its own characteristic stiffness matrix which is created by assembling the stiffness matrices of all beam elements that form the building block. The stiffness matrix of the compliant mechanism is calculated by assembling the stiffness matrices of all the building blocks in the design domain.

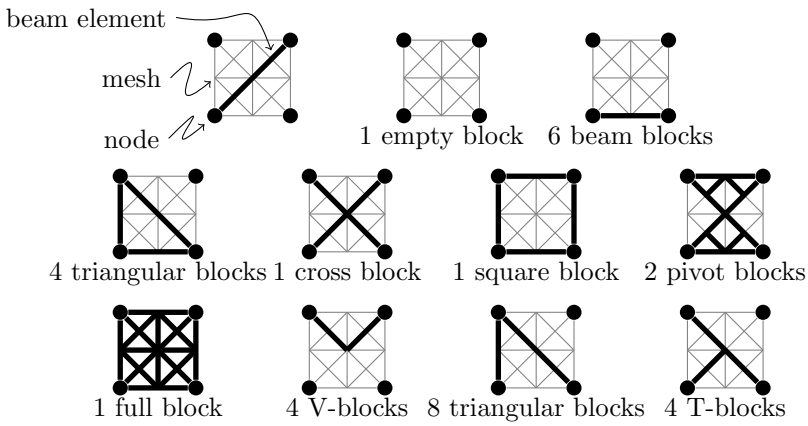

Figure 3.22: Building blocks as elementary units. Reproduce from [13].

After the user manually defines blocks in the design domain as well as inputs, outputs, ground ports, contacts and loading conditions, a multi-objective genetic algorithm generates a set of possible topologies by finding optimal distributions of the building blocks inside the design domain (see Fig. 3.23).
The solutions are found by optimizing the balance between stiffness and compliance, and displacement and force, using different objective formulations, like mutual potential energy, strain energy, geometrical advantage, the mechanical advantage, etc.

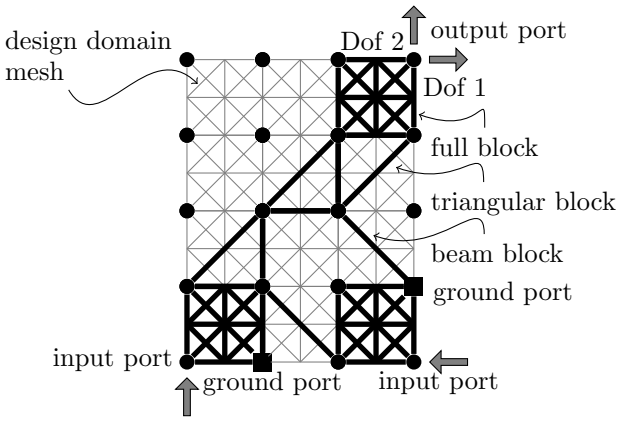

Figure 3.23: Building blocks assembling a two DOF compliant mechanism in the mesh design domain. Reproduce from [13].

Grossard et al. [31] took the approach one step further by adding blocks with integrated piezoelectric actuators. They introduced the finite element formulation for the active building blocks as well as their implementation into the genetic algorithm.

3.4 Structural optimization approaches

Structural optimization as the name suggests is the search for the most favorable (optimum) arrangement of the parts (structure) under specific conditions. The structural optimization approaches are based on the use of optimization and search techniques to obtain the design of a compliant mechanism (its topology, shapes and dimensions) that satisfies an objective function for a set of parameters and constraints.
When a synthesis problem for compliant mechanisms is solved by using either topology, shape or size optimization, three main aspects need to be considered: the objective function formulation, the design parameterization and the solution method. But first it is essential to understand optimization and the concepts behind topology, shape and size optimization. These concepts are treated in section 3.4.1. The objective formulation and the design parametrization are discussed in sections 3.4.2 and 3.4.3, respectively. The solution methods are not discussed, since they are outside the scope of this work.

3.4.1 Optimization

In general, an optimization problem is a procedure to minimize or maximize a function, while a set of constraint functions (equalities and inequalities) are satisfied. Maximizing a function is equal to minimizing its opposite function, for this reason optimization problems are often set as minimization problems.
The function that is being minimized is called the objective function, the variables in the function are called the design variables and the domain of the design variables is called the search space. The formulation of an optimization problem (see Eq. 3.5) contains the objective function $f(\mathbf{x})$, the p equalities h_i, the m inequalities g_j, the n design variables $\mathbf{x}$ and the search space Ω. Normally, the design variables x_1,x_2,...,x_n are clustered into the design vector $\mathbf{x}$.

$$
\begin{aligned}
&\underset{\mathbf{x}\in\Omega}{minimize}\, f(\mathbf{x}) \\
&\textit{subject to} \\
&\quad h_i(\mathbf{x}) = 0 \quad i = 1, 2, ..., p \\
&\quad g_j(\mathbf{x}) \leq 0 \quad j = 1, 2, ..., m \\
&where \\
&\mathbf{x} = \begin{bmatrix} x_1 & x_2 & \dots & x_n \end{bmatrix}
\end{aligned}
\tag{3.5}
$$

Topology, shape and size

In the structural optimization of compliant mechanisms the goal is to obtain three main characteristics: the topology, the shapes and the sizes of the constitutive elements. When the topology, the shapes and the sizes of a structure are defined, then the structure is entirely defined from a

geometrical point of view. If a parallel is done between compliant mechanisms and rigid body mechanisms, finding the topology is equivalent to the number synthesis, while finding the shapes and sizes is equivalent to the dimensional synthesis.

Topology optimization To understand topology optimization, first we need to understand the meaning of the word topology. Topology is a branch of mathematics that studies how the properties of a space are preserved or change when this space is subjected to deformations. If an object is imagined to be composed of small elements connected to their neighbors, then this connectivity is said to define the topology. Deformation does not affect the topology as long as the connections between the elements remain. However if a hole is made, it requires some connections to be broken, in which case the topology is modified.
In the case of mechanisms and structures the topology refers to the connectivity among their constitutive elements, even if they are small discrete elements. Constitutive elements also include the input ports (where input loads and movements are applied), the output ports, ground ports, etc.
Topology optimization then refers to the process of finding the topology (connectivity among constitutive elements) that satisfies in the best way the objective function.

Shape optimization In the shape optimization problem, the word shape refers to the shape of the constitutive elements, if topology forms the skeleton, then the shape is the contour appearance of every bone in the skeleton. Figure 3.24 shows two examples (continuum and discrete representation) , with the same topology but with different shape.
Shape optimization then refers to the process of finding the optimal shape of the contour or surface that satisfies in the best way the objective function in a fixed topology.

Size optimization In the size optimization problem the idea is to find the optimal set of sizing variables that satisfies in the best way the objective function. The design variables are the sizing variables or in other words the variables that define the dimensional properties of a model, i.e., thickness, cross sections, diameters, radii, etc.
In a typical size optimization problem the shape and topology of the model have been already defined, for example think on a plate like the one in Fig. 3.25, where the topology is defined and also the shape of the contours, now the problem is to find the proper dimensions of the two semi-axis (keeping constant their ratio) for the elliptical outer contour and the radius for circular inner contour as well as the thickness of the cross section.
The last example highlights the fact that size variables can define sometimes the shape and even the topology, for example by changing the ratio between the semi-axis, or by making zero the radius of the circular inner contour. Topology optimization using gradient based algorithms typically formulates the problem in this way, using size variables as design variables.

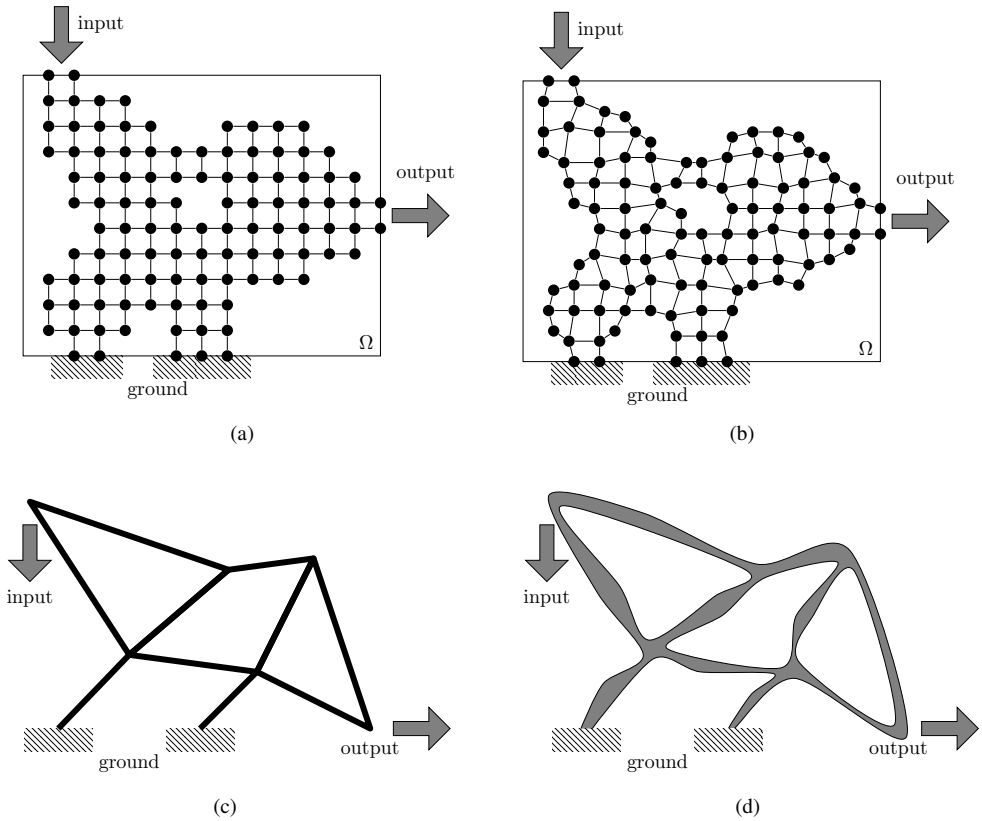

Figure 3.24: Example of same topology, different shape. (a) and (b) continuum structures, (c) and (d) Discrete structures.

3.4.2 The objective function formulation

Deepak et al. [22] present a comparative study about the five dominant objective formulations for the structural optimization of compliant mechanisms that are found in literature. These formulations are:

- Mutual potential energy (MPE) and strain energy (SE)
- Mechanical and geometrical advantage
- Energy efficiency
- Characteristic stiffness
- Artificial I/O spring formulation

Reference [22] provides a thorough overview; therefore they are explained here only briefly.

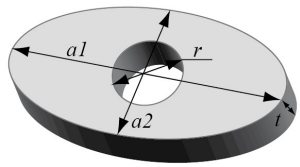

Figure 3.25: Size optimization.

Mutual Potetial Energy (MPE) and Strain Energy (SE)

In this formulation the compliant mechanism is seen as a structure which is stiff enough to resist the applied loads while at the same time it is compliant enough to allow the desired deflection. The Mutual Potential Energy and Strain Energy formulation seeks to conciliate these two requirements.

The Mutual Potential Energy or MPE accounts for the deflection requirements, while the Strain Energy or SE ensures the structural requirements. From this premise Ananthasuresh [3] presents an objective function based on a weighted linear combination of these two parameters.

$$minimize : -wMPE + (1 - w)SE, 0 \leq w \leq 1 \tag{3.6}$$

Where w, which is problem dependent, is the control variable for the relation compliance-stiffness. Frecker et al. [27], present an objective formulation that overcomes this dependency, namely the ratio between these two quantities.s

$$minimize : -(MPE/SE) \tag{3.7}$$

Saxena and Ananthasuresh [115, 116] present a generalization of this objective formulation as a power ratio of MPE and SE.

Frecker et al. [30] present the use of ratio between MPE and SE for the design of compliant mechanisms with multiple outputs.

Observation of the MPE as a form of the reciprocal theorem [135] tell us that maximization of MPE ensures the maximization of compliance as long as the actuation force is constant and the dummy displacement at the output is not predefined. The latter means, in the context of finite elements analysis, that the solution must be found by using load control. The use of displacement control during maximization of the MPE could lead to maximization of stiffness instead of maximization of the compliance.

Mechanical Advantage (MA), Geometrical Advantage (GA) and Mechanical Efficiency (ME)

These formulations are related to the functional specifications of the compliant mechanism rather than their structural requirements as in MPE and SE formulations. In other words, these formulations are more focused on "what" the mechanism should do than "how" it should do it.
The idea in these objective formulations is to maximize the ratio of a parameter between the output and the input port. Table 3.1 shows the maximized ratio (Mechanical Advantage, Geometrical Advantage and Mechanical Efficiency) depending on which parameter is considered between the input and output port.

Table 3.1: Objective formulation depending the parameter at I\O port

I\O Parameter	Maximized Ratio	Expression
Force	MA	f_o/f_i
Displacement	GA	Δ_o/Δ_i
Work	ME	$f_o\Delta_o/f_i\Delta_i$

Normally, the output force is modeled as the force f_o at the output port exerted by a virtual spring whose stiffness k_s is the stiffness of the workpiece and undergoes a deflection equal to the output port deflection Δ_o.

$$f_o = k_s\Delta_o \tag{3.8}$$

Sigmund [126] presents an objective function for the maximization of the mechanism's MA considering an initial gap between the mechanism and the workpiece.

$$minimize : -\frac{\mathbf{R}(\rho)}{\mathbf{f}_{in}} \tag{3.9}$$

$\mathbf{R}(\rho)$ is the reaction force at the output port, ρ is the vector containing the design variables and $\mathbf{f_{in}}$ is the force at the input port.
Canfield and Frecker [15] compare the GA and the ME through the design of an amplifier for piezoelectric actuators. Frecker and Bharti [28] present a similar work using GA for a given force and stroke in the actuator.
Lau et al. [68] compile the objective formulations for MA, GA and ME and show the result of two examples using the three formulations.
Pedersen et al. [97] propose an objective formulation based on [126] for large-displacements mechanisms by maximizing the work of a virtual spring (a spring that simulates the workpiece's stiffness) at the output port, which allows to emphasize on force generation or displacement generation.
Jung and Gea [55] present an objective formulation based on GA for non-linear materials.

Characteristic stiffness

Chen and Wang [18] propose an objective formulation that combines strength and functional requirements.

$$minimize : -e^{-(GA-GA^*)}k_{in}k_{out} \tag{3.10}$$

The term $e^{-(GA-GA^*)}$ accounts for the functional requirements by specifying a desired GA^*. The term k_{in} and k_{out} account for the strength requirements and represent the characteristic stiffness at the input and output port, respectively.
The characteristic stiffness can be thought of as the stiffness k_p of an equivalent spring that allows the same deflection Δ_p of a cantilever beam when force f is applied at point p, see Fig. 3.26.

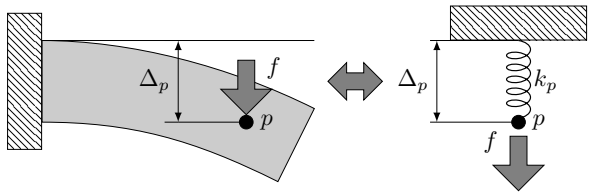

Figure 3.26: Characteristic stiffness of a point p on a cantilever beam.

Error formulations

Objective functions based on error calculation are commonly used for designs where path, function or motion generation is required. Error formulation are normaly found on the design of compliant mechanisms undergoing large deflections.
The main idea is that the behavior of the mechanism during the optimization is fitted to a prescribed behavior. This is done by minimizing the difference between the actual behavior and the prescribed one. The difference between behaviors is calculated by using some form of error function, such as least squares error (LSE).
An example of the aforementioned can be found in Larsen et al. [67] where they present an objective formulation to achieve a desired mechanical advantage combined with a desired geometrical advantage using the error calculation shown in Eq. 3.11.

$$minimize : \frac{(MA - MA^*)^2}{(MA^*)^2} + \frac{(GA - GA^*)^2}{(GA^*)^2} \tag{3.11}$$

More examples developed by using error formulations can be found in [74, 73, 97, 72, 114, 117].

3.4.3 The design parameterization

The design parameterization refers to the model that is used to represent the topology, the shape or the size in order to create a proper set of design variables.

In the case of topology some common design parameterization are the representation of the connectivity by using finite elements like discrete ground structures or by means of graph theory like the load-path and spanning tree representations.

In shape optimization the design parameterization uses two main approaches [7]: The shape optimization based on finite element (FE) models, and the shape optimization based on geometry models. In the shape optimization based on FE, the design variables are the coordinates of the nodes on the contours and surfaces on 2D and 3D models respectively. In the shape optimization based on geometry models, the geometry of the model is described in terms of geometrical parameters which are used as the design variables. For instance, the shape could be given by the values of the parameters r and s that represent the radius of curvature and the arc length of consecutive contour segments or by the coordinates of a set of control points defining a parameterized curve or surface.

In the following sections, the synthesis approaches based on parameterized curves, graphs, discretized domains and higher dimension driver functions (level sets) are discussed.

Parameterized curves

Parameterized curves are those curves that outline a given path by defining the position of every point of the curve as a function of one or more variables called parameters.

Spline Parkinson et al. [96] present a design strategy in which they combine optimization and analysis tools. Their method starts by creating from the design requirements an initial design, which comprises two parametric models; a model for optimization and a model for analysis.

The parameterization means that the mechanism is defined by using parameters like width, thickness, material properties or even the position of control points, in cases when shape is given by spline curves, Bezier, etc.

After the two models are created, an iterative solution process is followed. First an optimization over the optimization model is performed and the new parameters values feed the analysis model which is used in a finite element analysis. If the finite element analysis shows that the design behavior is the desired one, the process ends, otherwise, a new design is selected and the new optimization model is optimized and so on until the desired behavior is achieved.

In [96] the authors develop two examples, one for a constant force mechanism and another for a path generation mechanism by using as the objective function an error formulation between the desired and the actual design.

Vehar-Jutte and Kota [141][56] propose a method based on optimization that provides the topology, shape and size of springs that can achieve a desired nonlinear load-displacement function. The method uses a parametric model that represents the spring as a planar fractal-like network of splines. This design parameterization makes use of cubic B-splines of five control points. The nonlinear behavior is achieved by incorporating geometric nonlinearities while material is considered linear elastic.

The objective function is to minimize the error relative to a prescribed curve at a number of target points (see Fig. 3.27) while displacement and buckling penalties are taken into account. The search for the optimum is performed using genetic algorithms.

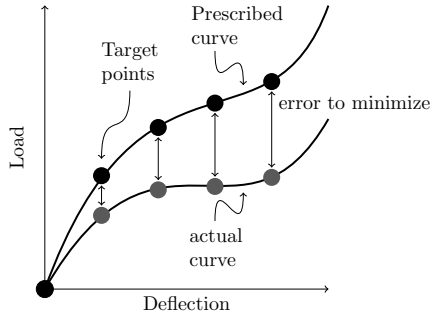

Figure 3.27: Relative error to the prescribed load-displacement curve.

The splines form a ground topology created by three branches joined at the input port. Each branch is formed by one primary spline and two secondary splines (see Fig. 3.28a). All the ends points are ground ports (the input port is also the output port and is called the applied input).

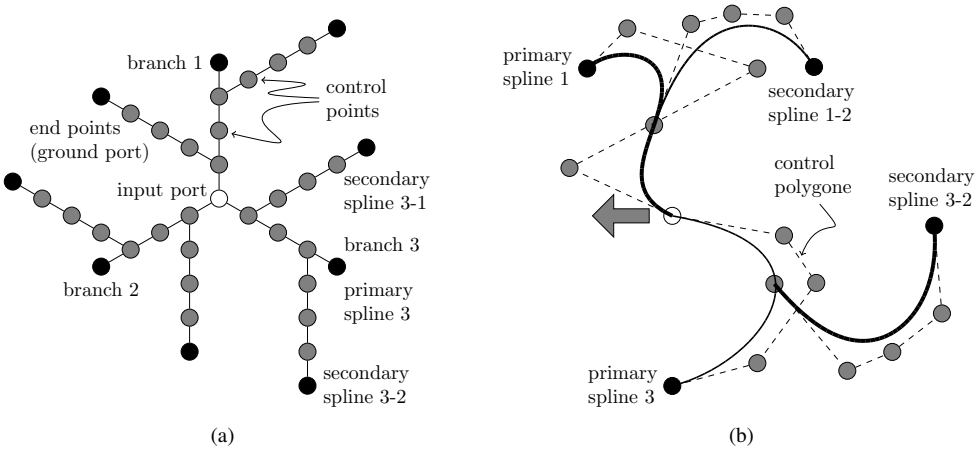

Figure 3.28: (a) Ground topology for the plane-fractal-like network of splines, (b) Pictorial representation of a result using splines in [141][56].

The set of design variables is formed by topology variables, shape variables and size variables. Topology variables are the variables defining the existence or not of a spline, the connection points between primary and secondary splines and the boundary conditions at the end points. The shape variables are the position of all the control points. Finally, size variables are the in-plane height of each spline bounded between a lower and upper limit.
Figure 3.28b presents an example of a possible result after the optimization. In this example, the second branch has been completely removed as well as one of the secondary splines in branch one and three, also the out-of-plane height and the position of the control points and ground ports have been changed.

Bezier Xu and Ananthasuresh proposed a method for shape optimization where the parameterization is based on cubic Bezier curves to represent the compliant segments in a given topology [147]. The design variables in the optimization process are the coordinates of the Bezier's control points, while the points of the Bezier curve are used as nodes in the finite element beam model. This simplifies the re-meshing process after every iteration during the optimization.

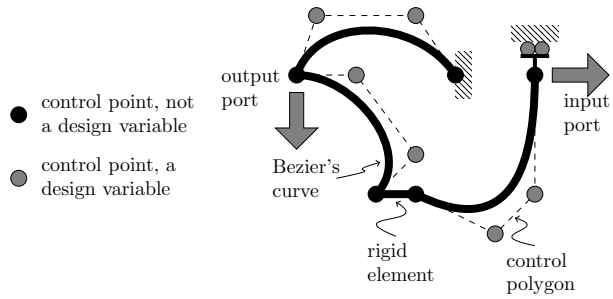

Figure 3.29: Example of design parameterization of a compliant mechanism with Bezier curves.

Figure 3.29 shows a design parameterization example, where the mechanism is composed of one rigid element and three compliant segments which have been parameterized with cubic Bezier curves where only the coordinates of the two middle control points are used as design variables.

Wide curves Zhou and Ting present a design approach where in a given topology the shape and size of the compliant segments are optimized by parameterizing these segments using wide Bezier curves [152][153]. A wide curve is a curve that possesses a variable width or cross section, see Fig. 3.30a. The resulting curve can be thought of as the contour that is left by a moving circle of variable radius.
A wide Bezier curve is then a Bezier curve where its width can vary; to do this the control points are replaced by control circles where the centers of these circles define the control polygon and their radii define the variation of the width along the curve, see Fig. 3.30b. The design variables are the radii and the center positions of the control circles.

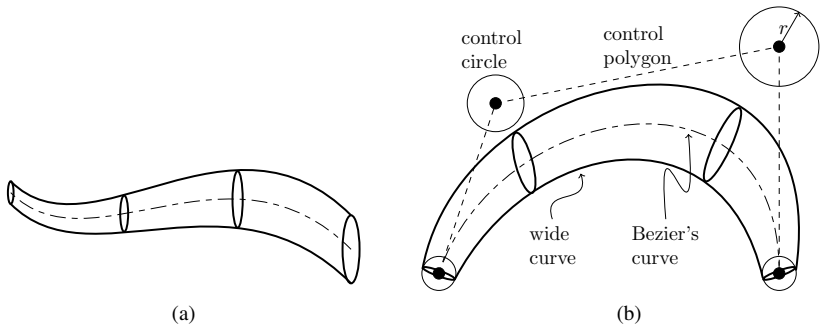

Figure 3.30: (a) Wide curve, (b) Wide Bezier curve.

Morphological representation of topology Tai and Chee [133, 1, 134] present an approach where the topology and shape of a compliant mechanism are optimized by using a parameterization that is inspired by the morphology of vertebrate creatures.
A valid structure for a mechanism is the one that presents a connection among the input, output and ground ports. These connections are made by Bezier curves, which are used to define the structure's skeleton.
The structure of the mechanism is formed by a skeleton which is surrounded or covered by flesh. The skeleton is formed by the elements in the design domain that follow the contour of the Bezier's curves as shown in Fig. 3.31a.
The amount of flesh that is added to the skeleton defines the shape, as well as potentially the topology. This amount of flesh or thickness is added considering each skeleton element and is not constant; it can vary along the curve's segments. The segments are defined every two control points, so if the curve has four control points, it is divided in three segments.
In Fig. 3.31b, 3.31c and 3.31d three examples are shown in which different topologies can be created with the same skeleton by changing the surrounding flesh.
In this example the parameterization variables are the position of the control points of the Bezier curve and the segment's thicknesses along the curves. The optimization procedure is based on a genetic algorithm.

Intrinsic functions Lan and Cheng [65] introduce a parameterization for the shape optimization of a compliant link using intrinsic functions. Intrinsic function parameterization means that the parameterization is made by using essential functions, for instance trigonometric functions.
In this parameterization the shape of a single compliant link is given by an angle function $\eta(u)$ and the lateral thickness function $w(u)$, where $u \in [0\ 1]$ is the non-dimensional length of the link along the neutral axis (see Fig. 3.32); the link is assumed to have constant out-of-plane thickness. Both intrinsic functions are represented as polynomials (Eq. 3.12) and their coefficients are the

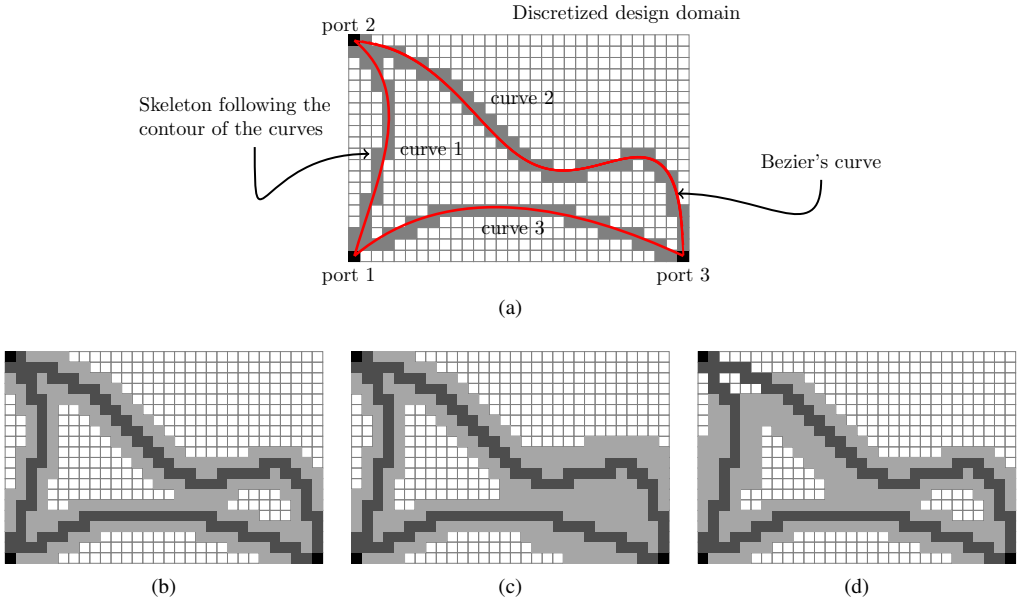

Figure 3.31: Different topologies by adding flesh to the same skeleton structure. (a) Skeleton following the contour of the Bezier's curves. (b) Topology with two holes created by thickness equal to one along all segments at the three curves. (c) Topology with one hole created by thickness equal to two at the final segments on curves 2 and 3. (d) Topology with three holes created by thickness equal to two and zero at the initial and final segments on curve 1 and at the middle and initial segments of curve 2.

design variables for the optimization procedure.

$$\begin{aligned} \eta(u) &= \sum_{i=0}^{m} c_i u^i \\ w(u) &= \sum_{j=0}^{k} d_j u^j \end{aligned} \tag{3.12}$$

In their work, the authors present the equations necessary for the calculation of the Cartesian coordinates for the points on the neutral axis and lateral surfaces as well as the constraints that are required for a correct formulation and to avoid for example self-intersections or loops in the compliant link.

Graph based parameterizations

Load-path representation and the spanning tree based topologies are methods based on graph theory to represent the topology of a mechanism, but they differ on how topologies are obtained during the optimization procedure.

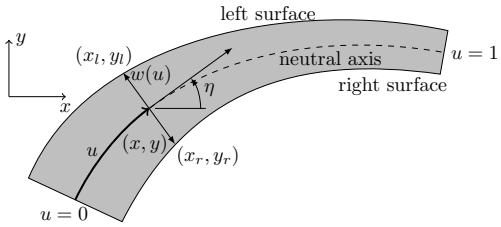

Figure 3.32: Compliant link representation using intrinsic functions (reproduced from [65]).

Load-path representation The load-path representation [64, 74, 75, 76, 77, 84] is a design method that integrates topology, size and geometry synthesis by implementing a design-space parameterization that solves some of the ambiguities in the topology, i.e., gray areas or disconnected structures.

The method treats the mechanism's topology as a graph, where vertices in the graph represent rigid connections with no degrees of freedom and the edges represent the beams where the degrees of freedom occur.

The basic requirement of a valid compliant mechanism is that there must be a physical connection between the input port, output port and the ground port; in other words, there must be a path in the graph connecting every pair of these ports. Those vertices that are not input, output or ground ports are called intermediate connection ports.

The design variables in the load-path representation method are grouped in four sets: variables for the path sequence, variables for the presence of a path, variables for the cross-section dimension of the segments and variables for the location of the intermediate connection ports. The first two sets define the topology, the third set defines the size and the fourth defines the shape.

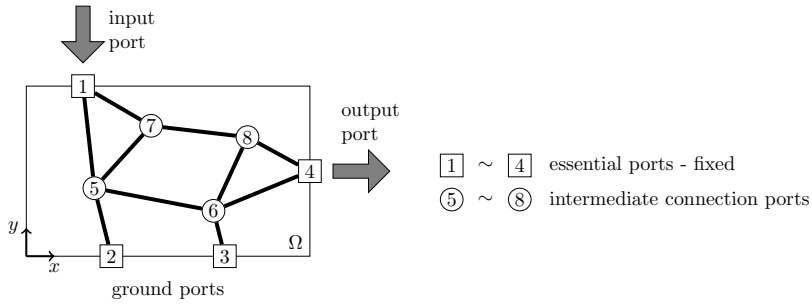

Figure 3.33: Load-path representation.

The optimization is performed by a genetic algorithm, so during the procedure the variables for path sequence and the variables for presence of a path are modified, creating different graphs which mean different topologies.

Spanning tree based topologies In the spanning tree based topologies [150][151], the optimization is performed by a genetic algorithm using as design variables the position of the intermediate nodes and the segment's cross-section dimensions.

The final topology is not defined exclusively by the design variables. The optimum topology is the optimum candidate provided by the optimization algorithm under the condition that it is also a spanning tree from the structural universal. A structural universal can be thought of as a ground structure containing all possible connections among vertices. The edges represent segments (Fig. 3.34).

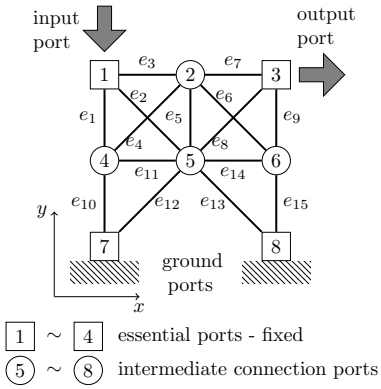

Figure 3.34: Structural universal, reproduced from [151].

The presence or absence of a segment is given by the segments' cross-sectional design variables. A zero value means absence of the segment. When the optimization algorithm finds a candidate topology inside the structural universal, it must be checked for being a spanning tree.

A spanning tree is a tree on a graph that connects all vertices without creating cycles or loops. A spanning tree guaranties the connection among all vertices with a minimum number of edges.

If the candidate topology is a spanning tree, it is a valid topology. Figure 3.35 shows two examples of spanning trees from the structural universal shown in Fig. 3.34

So in other words, every time that the optimization algorithm proposes a new set of design variables, this new set creates a new candidate topology from the structural universal which must be evaluated to be a valid topology using the spanning tree criterion.

Discretized domains

Parameterizations based on discreatized domains refer to design domains where the design variables define the structure in terms of discrete elements. This means that the details of the solution in terms of the topology, shapes and sizes are limited by the resolution of the discrete elements.

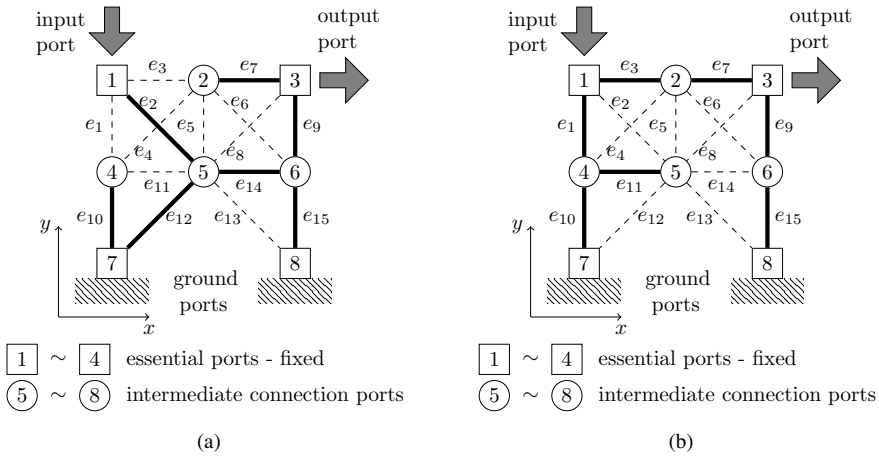

Figure 3.35: Two different spanning trees from the same structural universal. Reproduced from [151].

Unit truss cell The unit truss cell method is a design approach for cellular structures presented by Wang and Rosen [142][143]. A unit truss is a central node surrounded by n half-struts. A common strut connects neighboring unit truss cells.

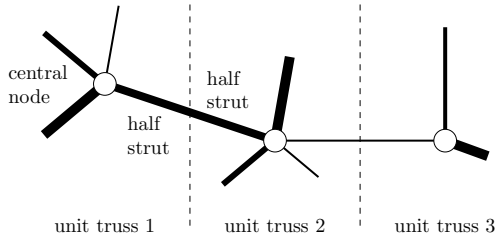

Figure 3.36: Neighboring unit truss cells.

The idea is to create a starting structure topology of unit truss cells and modify the strut diameters by optimization. When a diameter becomes zero, that strut is removed.

The design variables are the struts' diameters. From this point of view, the parameterization works in a similar way as a ground truss structure but according to the authors their method presents the advantage of better accuracy due to the simultaneous analysis of multiple-degree-of-freedom deformations and by considering non-linearities.

The mathematical formulation for the constitutive equations of a unit truss cell, is derived from beam theory.

Discrete structure - Truss, frame, beam ground structures A ground structure is said to be discrete when the design domain has been discretized using common one-dimensional finite elements (elements where one of whose dimensions is larger than the other two) like truss or frames. This implies that not the entire design domain space is represented or mapped by structural finite elements.

The discrete ground structures can be divided in full ground structures and partial or modular ground structures. Hetrick and Kota present in [35] a comparison between the full ground structure and the modular ground structure by developing the design of a compliant gripper and a compliant wrench using both parameterizations. In addition they present a more extensive discussion about both ground structures and their advantages and disadvantages.

When discrete structures are used, the design variables for the optimization procedure are normally variables that describe the geometric characteristics of the finite elements like cross sectional areas, node positions or elements lengths, out-of-plane thickness, in-plane widths, slopes, etc.

The discrete ground structure can be modeled by using truss or frame elements. Examples using frame elements can be found in [15, 28, 29, 104, 103, 117]; examples using truss elements can be found in [27] and [29].

Joo et al. [54] and Joo and Kota [53] present specifically the development of discrete ground structures using linear and nonlinear beam elements, respectively, while Ramrkahyani et al. [105] introduce a model for a hinged beam element that can have a pin connection on one or both ends in contrast to a conventional beam element where both ends are clamped.

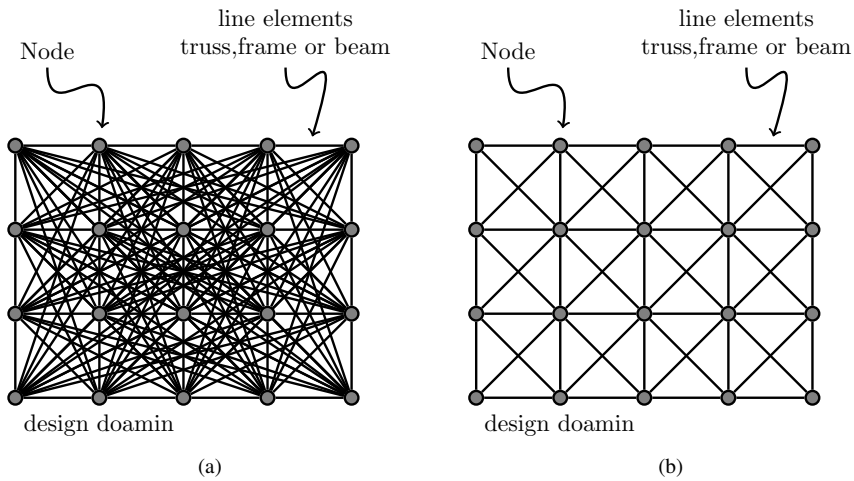

Figure 3.37: Discrete ground structure using one-dimensional finite elements. (a) Full ground structure. (b) Partial ground structure.

Full ground structure In a full ground structure, each node in the design domain is connected with all the other nodes through one-dimensional finite elements as shown in Fig. 3.37a.
The number of elements e in a full ground structure is given by the expression,

$$e = \frac{n\,(n-1)}{2} \tag{3.13}$$

where n is the number of nodes in the mesh.
Dziedzic and Frecker [24] present two design examples of a scissor-grasper mechanism by using three-dimensional full ground structures. Frecker et al. [27] in the presentation of the multi-criteria objective function make use of a two-dimensional full ground structure of truss elements for the design of a compliant gripper.

Partial or modular ground structure It is said that a ground structure is modular when the nodes are connected to neighboring nodes rather than to all the nodes in the design domain. An example of this can be seen in Fig. 3.37b.
The number of elements e in a rectangular partial ground structure is given by the expression,

$$e = 4n_x n_y - 3n_x - 3n_y + 2 \tag{3.14}$$

where n_x and n_y are the respective number of nodes in the horizontal and vertical direction in the mesh.
Frecker and Bharti [28] and Mankame and Ananthasuresh [82] make use of the modular ground structure in the development of their examples.

Continuum structure A ground structure is said to be a continuum structure when the entire design domain has been discretized and every discrete sub-domain is modeled by some mathematical representation of the macro-microstructure, see Fig. 3.38. Consequently, the entire design domain is mapped to some structural model representation.
The basic idea behind the use of continuum structures is to start with a design domain which is full of elements while gradually, during the optimization, those elements that are not effectively used are removed, so that at the end, only the essential elements remain to achieve the design requirements.
The Evolutionary Structural Optimization or ESO also known as Sequential Element Rejections and Admissions or SERA method [110] is representative of this approach. Other approaches can remove or add elements during the optimization like the BESO (Bidirectional ESO) method.
Ansola et al. [5] show an additive version of the ESO method applied to compliant mechanisms. In this method the ground structure is a fully compliant structure which is an empty design domain and gradually, during the optimization, the elements are added where required, instead of being removed.

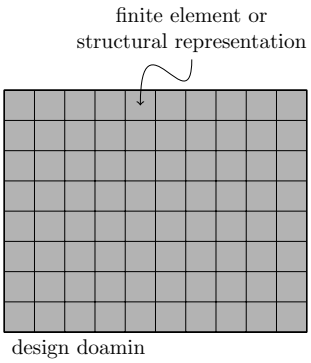

Figure 3.38: Continuum structure.

When continuum structures are used in the design of compliant mechanisms, two parameterization models are highlighted: the SIMP method and artificial density, and the homogenization method or hole-in-cell.

SIMP method and artificial density Normally when a topology optimization is performed, it is desired that the design variables express the existence or inexistence of an element in the design domain. This is done by assuming a value of either 1, the element exists, or 0, the element is removed from the domain.

In the optimization algorithms based on gradients whose variables can range in the [0, 1] interval, a problem arises, namely that the algorithm can not deal with Boolean variables. The SIMP (Solid Isotropic Material Penalization) method helps to overcome this problem by penalizing the design variables, so intermediate values can be assumed as 0 or 1.

When SIMP is used, the design variables are the density of the elements. Here density can be thought as the material density or as some kind of artificial density or cost variable. Sigmund [126] presents an optimization procedure for maximizing the mechanical advantage in compliant mechanisms using artificial density by modifying the Young's modulus for every element in a continuum structure.

$$E^e = (x^e)^\eta \, E^0, \qquad e = 1, \ldots, N \tag{3.15}$$

Here E^0 is the Young's modulus of solid material, E^e is the Young's modulus of a single element,η is a penalty factor and x^e is the design variable for a single element.

When the optimization procedure ends, the design variables modify the Young's modulus in all the elements inside the design domain. If x^e is close to zero (not zero to avoid singularities on the stiffness matrix) it means a low Young's modulus E^e thus low stiffness and therefore the element is removed. Contrarily, values close to one mean that Young's modulus is equal to the modulus

of solid material E^0 thus high stiffness and therefore the element remains.
For a more extensive description of the SIMP method see [110][11]. Examples applied to the design of compliant mechanisms can be found in [67] and [97].

Honeycomb representation Checkerboard patterns are a common problem found in topology optimization due to the use of squared elements for the structural representation of the design domain. These patterns consist of a sequence of void elements and solid elements where the solid elements are joined by their nodes instead of their edges (see Fig. 3.39a), therefore creating areas of zero stiffness.

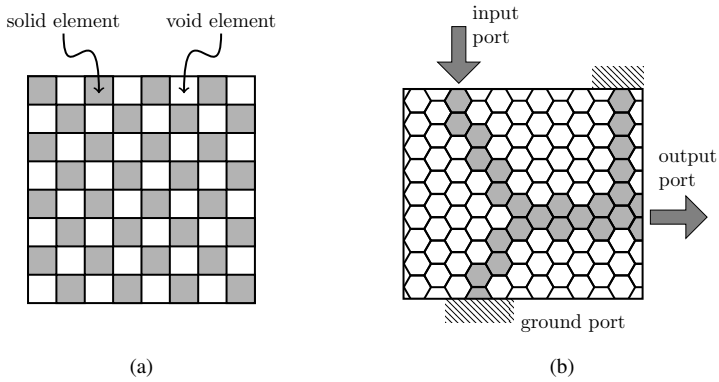

Figure 3.39: A solution to the problem of checkerboard pattern is the use of parameterization using honeycomb patterns. (a) checkerboard pattern. (b) Honeycomb parameterization.

To overcome this problem R.Saxena and A.Saxena [119] and Mankame and A.Saxena [83] present a parameterization using hexagonal elements which discretize the design domain into a honeycomb pattern, see Fig. 3.39b.
This type of discretization avoids the zero stiffness areas by ensuring edge-to-edge contact among the elements. The stiffness matrix for a hexagonal element is derived by considering it as the junction of two four-node finite elements as shown in Fig. 3.40.

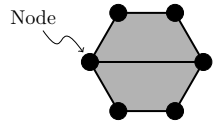

Figure 3.40: Hexagonal cell represented as two four-nodes finite element.

The design variables in this approach can be the artificial densities used in the SIMP method. For each hexagonal element, there is one design variable meaning that the two four-node elements share the design variable to define their material properties.

Homogenization method (Hole-in-cell) The homogenization method allows to obtain a relation between stiffness and density by representing the microstructure as a unit cell where the amount of material can change by modifying the geometry of a hole that is inside the unit cell. The unit cell is defined by the height a and width b of the inner hole and the rotation of the cell θ, see Fig. 3.41. Depending on the values for these variables the unit cell can be completely void (a=b=1) which means no material, completely full (a=b=0) which means solid structure; or something in between.

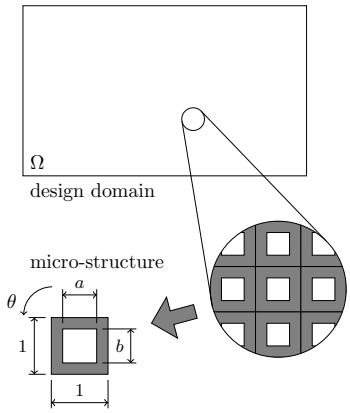

Figure 3.41: Representation of the microstructure by homogenization.

The variables from all the unit cells in the design domain are the design variables. When their optimal values are found, they define the material distribution along the entire design domain. More about the fundamentals of the homogenization method can be found in [10] [9] and [11]. Frecker et al. [27] and Nishiwaki et al.[92] apply the homogenization method to the design of compliant mechanisms.

Control meshes and subdivision In the parameterization based on control meshes and subdivision [45][46], the design variables are the existence state of the control meshes. A single control mesh is a squared subregion in the design domain defined by four control points. This mesh must not be confused with a mesh for an analysis with finite elements. The control mesh is just a geometrical division of the design domain.
During the optimization process, which is performed by a genetic algorithm, the state of the control mesh assumes values of 0 or 1 (existence or inexistence of the control mesh). After the algorithm proposes a new arrangement for the control meshes, a subdivision process is performed.
The subdivision provides a more detailed and smooth design which is used for the meshing in the FEA and then for the evaluation of the objective function. An example of subdivision can be seen in Fig. 3.42.

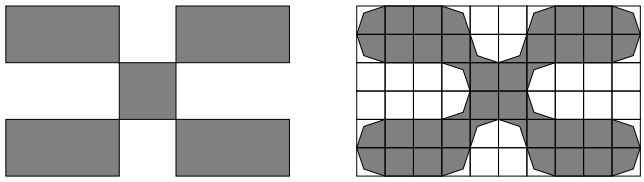

Figure 3.42: Subdivision process. (a) Initial control meshes and control points, (b) Refined geometry after subdivision.

Subdivision is a process that creates more control points from the initial control points that define the control meshes. In this way the optimization variables are fewer, because they do not describe the entire detail of the mechanism's shape and topology but they can be used to recreate them. An important feature of subdivision is the reduction in the formation of lumped compliance. Subdivision relies on the fact that there is a unique mapping from the initial model with few control points to the denser final model.

Figure 3.43, shows three steps during the optimization procedure: the initial control meshes, a proposed control meshes arrangement after some iterations and the arrangement just after subdivision and before meshing for FEA. Notice that using a few design variables it is possible to obtain a more complex geometry by subdivision.

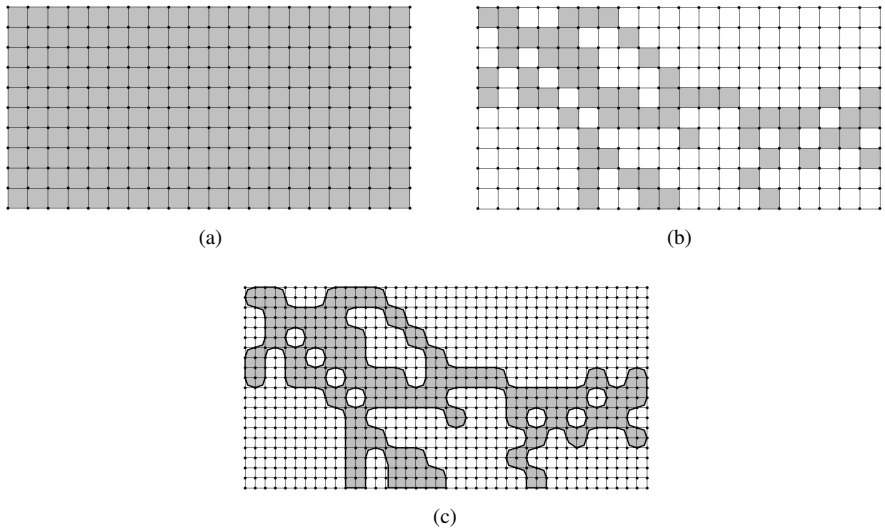

Figure 3.43: Three steps during optimization, reproduced from [45]. (a) Initial control meshes. (b) Proposed control meshes arrangement. (c) Proposed arrangement after subdivision.

Higher dimension driver functions (Level sets)

In this approach the shape and topology of the compliant mechanism is embedded as a level set of a higher-dimension scalar function Φ, called the level set function.
A level set of a function is defined as the set of points where the function has a constant value.

$$\{(x_1 \dots x_n) \,|\Phi\,(x_1 \dots x_n) = c\} \quad c = constant \tag{3.16}$$

If the function domain is defined in $\mathbb{R}^2$, the level sets represent level curves (Fig. 3.44) for domains in $\mathbb{R}^3$ and higher, the level sets represent level surfaces and level hyper-planes respectively.

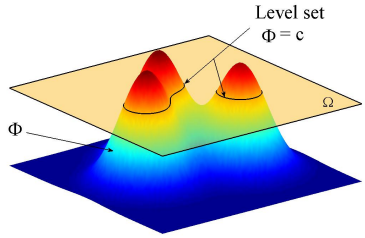

Figure 3.44: Higher dimension function φ and its level set at value c

The idea behind level sets is to modify the shape and topology of the design region Ω by modifying the function Φ. During the optimization procedure the design variables do not control directly the topology and shape of the design, instead they outline the function Φ which in turn defines the design's topology and shape through its level sets. The level set defines the boundary $\partial\Omega$ of the design region Ω, thus bounding the void and material regions.
The formulation of an optimization based on a level set parameterization is written as the problem of finding the function Φ where one of its level sets defines the shape and topology that minimizes the objective function f. For simplicity the most common value used for the level sets is the zero level set ($\Phi = 0$).
Most of the design approaches based on level sets can be categorized in two main methods, (i) *The level set method* and moving interfaces, and (ii) level set using basis functions.

Level set method and moving interfaces Sethian and Osher are among the first to propose a method for tracking moving interfaces based on level sets.
In the level set method the function Φ is defined initially as a signed distance function [120]. It means that $\Phi(\mathbf{x})$ is the distance between a point $\mathbf{x}$ and the closest point on the design region's boundary $\partial\Omega$, with the sign of Φ depending of $\mathbf{x}$ being inside or outside of the region Ω, see Fig. 3.45.

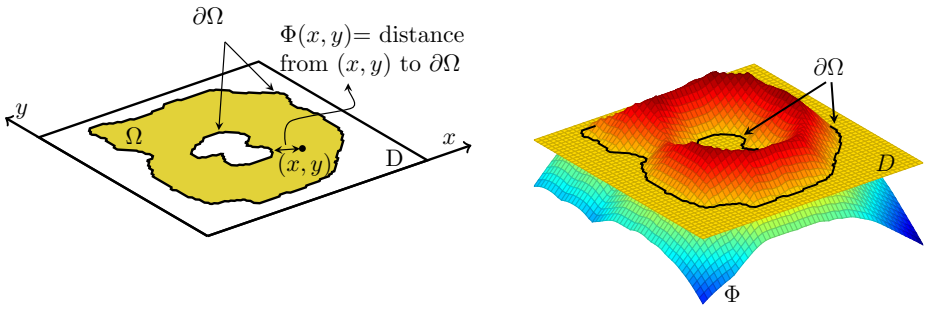

(a) (b)

Figure 3.45: (a) The distance function Φ in this example is the euclidean norm between points in the domain D and the boundary $\partial\Omega$. (b) The higher dimension scalar function Φ where $\Phi > 0$ is the material region Ω, $\Phi < 0$ is void and $\Phi = 0$ is the boundary of the material region $\partial\Omega$

.

The boundary $\partial\Omega$ which is also called the moving interface will always be the zero level set of the function Φ, this is why a distance function is used to define the function Φ (the zero level set has distance value of zero).
The zero level set equation for a function $\Phi(\mathbf{x}, t)$, with $\mathbf{x} \in \mathbb{R}^n$ is expressed as

$$\Phi(\mathbf{x}, t) = 0 \tag{3.17}$$

To see the evolution in time of the zero level set, the chain rule for differentiation is applied to Eq. 3.17

$$\frac{d\Phi}{dt} + \frac{\partial\Phi}{\partial x_i}\frac{dx_i}{dt} = 0 \quad i = 1 \ldots n$$

simplifying

$$\frac{d\Phi}{dt} + \mathbf{F} \cdot \nabla\Phi = 0 \tag{3.18}$$

Here F is what is called the velocity field, which is given by the kind of problem with moving interfaces that is being analyzed, e.g., a shockwave propagation or a moving flame.
From the optimization point of view the velocity field gives the optimization conditions, this is what drives the moving interface. For example Sethian and Wiegmann in [122] used as the velocity field what they called the removal rate, which is a percentage of the maximal stress in the design region. In other words the evolution of the boundary $\partial\Omega$ was determined by some value of the stress distribution.
When the velocity field is assumed to be normal to the level sets for every point in the design domain D, then Eq. 3.18 simplifies into what is known as the level set equation

$$\frac{d\Phi}{dt} + F\left|\nabla\Phi\right| = 0 \tag{3.19}$$

This is an initial value Partial Differential Equation (PDE), where the initial value is the distance function mentioned before ($\Phi(\mathbf{x}, t)$ when $t = 0$). The evolution of the zero level set or moving interface is then driven by the velocity field F and given by the solution to this PDE.

level set using basis functions Here the level set function Φ is defined as the superposition of basis functions φ_i (Eq.3.20) which can be parameterized by a few set of variables, Fig. 3.46.

$$\Phi = \sum_i \varphi_i\left(\mathbf{x}\right) \tag{3.20}$$

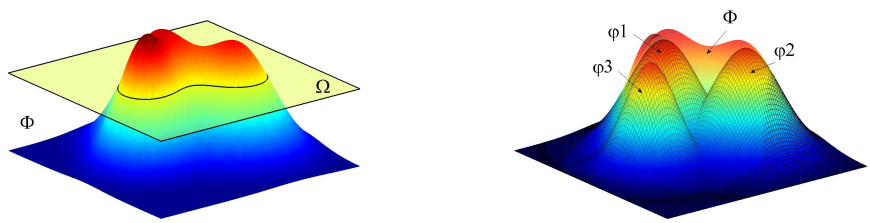

(a) (b)

Figure 3.46: (a) Higher dimension scalar function Φ. (b) Constitutive basis functions φ_i

De Ruiter and Van Keulen present in [112] an approach called Topology Description Functions or TDF's. In this approach the basis functions are 2D Gaussian distributions, where every base function is parameterized by its center position, height and width which is defined similar to the standard deviation in the Gaussian probability distribution. This transforms the shape and topology optimization problem into a size optimization problem, where the design variables are the parameters defining all the TDF's. In some cases the value of the level set is not confined to be the zero level set, this value can be also used as a design variable.
Luo and Tong [78] present the use of Radial Basis Functions (RBF's) for the interpolation of the level set function which in this case include a time dependent term $\alpha_i(t)$.

$$\Phi = \sum_i \varphi_i\left(\mathbf{x}\right)\alpha_i\left(t\right) \tag{3.21}$$

Here the function Φ evolves by reformulating the level set equation, replacing the distance function from the level set method with the interpolated function with radial basis functions. This

implies a separation between the space and time in the Hamilton-Jacobi PDE allowing to transform the problem into an ordinary differential equation.
The problem is not anymore to find a function $\Phi(\mathbf{x}, t)$ that solves the Hamilton-Jacobi PDE but to find the function $\alpha(t)$ that solves an Ordinary Differential Equation (ODE) [146]. Basically the level set function still acts like a moving interface driven by a velocity field, where the vector of design variables is formed by the set of $\alpha_i(t)$.

3.5 Discussion

It can be observed that most of the design methods rely on one or more of the following three basic ideas:

- Design of compliant mechanisms can be done using the well known kinematics of Rigid-Body mechanisms. The conventional joints obtained in this way are replaced by compliant joints to obtain a compliant mechanism.

- Design of compliant mechanisms can be done under the premise "divide and conquer", where the design problem is divided in smaller subproblems and where the final design is obtained by composing the solutions to the subproblems into a complete design. The subsolutions can be obtained either by some automate process or using the well known kinematics from Rigid-Body mechanisms.

- Design of compliant mechanisms can be done by automating the search of a solution that fulfills a desired function and constraints. It is required an appropriate way to describe the topology, shape and size (parameterization), as well as the criteria which define a design as optimal (objective function).

Most of the methods were developed for the synthesis of planar compliant mechanisms based on structural requirements rather than functional requirements like path, function or motion generation. In structural optimization, the majority of the design methods are tested through the design of the one DOF benchmark examples: the motion inverter and the gripper. Very few examples with more than one DOF can be found, and those with more than one DOF, fulfill their functional requirements without coupling their DOF's.
Analysis methods for compliant mechanisms is still an area open to study. Basically, analysis is confined to the use of finite elements or Pseudo-Rigid-Body models and simplified beam models. Their convenience as tools for control is still unexplored, just a few examples in this direction exists, like Arango et al. [6].
Compliant spatial joints, underactuated grippers, compliant differentials, statically balanced compliant mechanisms, compliant robotic manipulators and compliant embedded actuation; just to mention a few, are potential applications still to be developed.

3.5.1 Kinematic approaches

The FACT approach is a rule-based method for type synthesis of spatial or planar compliant mechanisms comprising multiple DOFs. The approach is a fast synthesis method based on the kinematic principles of exact constraining and suited for designs where the ranges of motion are small. It can provide with concepts that are out of the experience of the designer, e.g., over-constrained mechanisms, and at the same time allows incorporating this experience into more complex designs.

The rigid-body-replacement method has the advantage of being a rule-based method that exploits the knowledge on rigid body kinematics and the designer's experience to obtain feasible designs. It is a simple approach that allows to easily obtain the dynamics by modeling the elastic features with simple springs using either PRBM or standard flexure joints, avoiding the solution of complex elasticity equations. The design based on rigid-body-replacement is an iterative process dependent on the initially chosen rigid-body mechanism, making the approach suited for optimization procedures, but as such the design procedure could require multiple initial rigid-body guesses for a proper design, making it a time-consuming approach. The method is not useful to find designs outside the designer's experience and final compliant results will resemble the rigid-body mechanism as long as the compliance tends to be lumped.

The Pseudo-Rigid-Body models are suited for modeling large deflections of large beams with constant cross-section by simplifying calculations. It is a tool that can be used for both analysis and dimensional synthesis. There are several PRBM's, some can be use to model initially straight beams or initially curved beams, single load or combined end forces and moments, one DOF PRBM for end tip rotations below 77° or 3 DOF SRBM allowing 360° rotations. As more features are added to the PRBM, its use and calculation become more complex. The PRBM's not only do not consider cases with changing loads but also do not consider neither the bending on short beams nor the shearing and bending effects due to axial loads. PRBM are mostly limited to planar compliant mechanisms, some exceptions are Jagirdar et al. [48] and Rasmussen et al. [106].

Flexure joints are the conventional way to design compliant mechanisms. Trease et al. [138] propose a set of criteria to evaluate flexure joints, the range of motion, the amount of axis drift, the ratio of off-axis stiffness to axial stiffness, and the stress concentration effects.

Notch-type flexure joints promote lumped compliance and they are the most commonly used variety, for which ample knowledge and experience is available. They are widely used in industrial and precision engineering applications where small displacements are the rule. They are rarely of constant cross-section and therefore highly sensitive to temperature and geometrical changes. The main drawback is the deviation of pure rotation when deflection is increased, due to out-of-plane and axial deflections which shift the rotation axis and introduce shearing, torsion and bending effects in undesired motion planes complicating the kinematic analysis.

Table 3.2: characteristics summary of kinematic based approaches, (+)yes (0)neutral (-)not

		rule based	use designer's experience	Simplicity	Fast	large deflection	distributed compliance	dimensional synthesis
	FACT method	+	0	+	+	0	0	-
Rigid body replacement	PRBM	+	+	+	0	+	+	+
	Notch-type flexures	+	+	0	0	-	-	+
	Complex flexures	-	0	-	-	+	+	0
Building block by instant centers		+	+	+	0	+	+	0

Complex flexures tend to improve the performance of flexure joints. Their complexity allows to constrain motion into the desired directions, but also increase their size and complicate their analysis and manufacturing.

3.5.2 Building blocks

Building blocks is a useful approach for the conceptual synthesis of Single-Input-Single-Output (SISO), Dual-Input-Single-Output (DISO) and Single-Input-Multiple-Output (SIMO) compliant mechanisms. It provides the topology and dimensioning in a systematic way while allowing a role for the intuition of the designer to drive the design process. This approach is suited for the design of realistic planar compliant mechanisms with small displacements in a linear regime. Blocks can be made of different materials. The use of optimization procedures is reserved for dimensioning and combinatorial exploration of blocks which in some sense is a topology optimization.

The building block approach based on instant centers is focused on fulfilling kinematic requirements by characterizing the kinematics through the use of compliance ellipsoids. Multiple solutions can be obtained by changing the orientation and shape of these compliance ellipsoids, thus providing a tool for kinematic inversions. Multiple building blocks with linear input-output relations can be combined to create mechanisms with highly nonlinear input-output relations as a solution for complex problems, but combining blocks transforms the search for solutions in an iterative procedure. Another drawback is the shift in position of the instant center during the operation which for precision applications requires the use of size and shape optimization procedures to correct the behavior. There is a point where the design of flexure joints and building blocks merge together, namely when building blocks are used to accomplish simple function like allowing planar rotation or displacement, acting like kinematic pairs. While this approach is mainly used for planar designs, there is no objection for it to be extended to spatial designs.

The above discussion is summarized in Table 3.2. Due to the fact that building blocks based on instant centers can be also considered as a kinematic approach, it is included in this comparison table. Precision is not considered as a criterion because some methods allow dimensioning while others are just conceptual approaches.

3.5.3 Structural optimization

Performing a structural optimization incorporates the appropriate selection of an objective function, constraints, a parameterization, and a solution method.

Objective function

There is no consensus about which objective function is most suited for the design of compliant mechanisms. There are two kinds of requirements to be fulfilled by any kind of objective function. One is kinematic and the other structural. Kinematic requirements are related with the functional requirements of the mechanisms. When only kinematic requirements are considered, most likely a least square error function would be the objective function. Structural requirements are related with the ability of the mechanisms to withstand the reaction forces. Objective functions considering structural requirements make use of concepts like mean compliance and mutual compliance. Design of compliant mechanisms by structural optimization has two unresolved issues which are the creation of low stiffness areas or lumped compliance and the need for a spring or load at the output port [22]. The latter unresolved issue is a result from the structural requirements.

Constraints

Normally two constraints are considered, stress constraints and deflection constraints. Stress constraints can not be included directly in the formulation, hence they are controlled by deflection constraints. Depending on the parameterization some other constraints need to be considered like volume, shape or connectivity in domain discretization, parameterized curves and graph parameterization, respectively.

Parameterization

All the design domain parameterizations described in this work can be classified in four groups, based on (i) parameterized curves, (ii) graphs (graph theory), (iii) design domain discretization, and (iv) higher dimension driving functions.

Parameterized curves The use of parameterized curves has the advantage of providing valid topologies connecting all the ports in the design domain. It is required to use additional constraints (shape constraints) to avoid cusps and intersecting loops [65]. The use of large deflection and nonlinear analysis is almost a necessity. The design variables are not directly related with the analysis variables. This kind of parameterization is suited for the design of compliant mechanisms with predefined force-deflection relations at the output port (stiffness functions) and can

be easily extended to the design of spatial compliant mechanisms given the proper spatial parameterized curve.

Graphs based The use of parameterizations based on graphs makes use of the idea that a correct topology is the one where any two ports in the design domain are connected at least through one *path* (sequence of alternating vertices and edges, where all vertices and edges are distinct). Therefore design results from this kind of parameterization tend to be realistic and feasible since invalid topologies are discarded. Due to its network nature this parameterization is susceptible to be combined with parameterizations based on trusses, frames and beams like parameterized curves or ground structures. Unless combined with other parameterizations, the solution method for the graph parameterization is likely to be a search algorithm due to the discrete nature of the resulting design variables.

Domain discretization Structural optimization using domain discretization is inherently a material distribution problem. It involves the removal or addition of material for every element in the discretized domain by transforming the topology optimization problem into a size optimization problem. This implies that the design variables can take intermediate values, which can lead to unfeasible designs and requires an interpretation of the final result.
Most of the methods keep a relation one-to-one between the elements in the domain, design variables and the elements in the finite element mesh, but this is not always the case. For instance, in homogenization every element in the domain has three variables whilst in the subdivision method, the number of elements in the domain is less than the number of elements in the finite element mesh. When the elements in domain discretization are also used as the finite element mesh, this may lead to the creation of flexural pivots (local stress concentration and low stiffness areas) or checkboard patterns (areas with high artificial stiffness).
The large number of design variables involved in optimization using domain discretization suggests that emphasis must be placed on calculating the sensitivities to achieve efficiency. Domain discretization approaches are not limited to the design of planar mechanisms, but their use in spatial synthesis of mechanisms due to the large number of design variables and complexity of the finite element models, currently is prohibited from computational cost point of view.
Smooth designs depend on the resolution of the domain discretization, increased resolution and more design variables tend to yield smoother results, however a fine mesh does not implies the same topology result as with a coarse mesh, or in other words the optimal solution depends on the initial discretization resolution [74].

Higher dimension driving functions The use of higher dimension driving function decouples the design variables from the analysis variables. As a consequence, topology can easily evolve to include or remove material, like the creation of new holes, since the topology is not defined

by finite elements and their connectivity. The decoupling between design and analysis variables also makes this kind of approaches suitable for the spatial synthesis of compliant mechanisms.

At the start of an optimization procedure, the initial design is not necessarily empty or full of material, it could be a design with some intermediate material distribution.

Two major approaches can be distinguished, the level set method with moving boundaries and level sets using basis functions.

From an optimization point of view, the numerical implementation of the level set method with moving boundaries is difficult and its efficiency is low (the level set PDE is solved in every iteration during optimization) but gives high accuracy and a smooth evolution of the interface. The fact that the implementation is normally based on the use of upwind schemes and higher efficiency algorithms limits the solution of the level set equation to the region close to the zero level set, this is known as the narrow band level set method [121]. One of the drawbacks in the numerical implementation of the level set method is the need for re-initialization which is the re-calculation of the level set function to keep function Φ as a distance function —distance between a point $\mathbf{x}$ and the closest design region's boundary— since the solution to the PDE drifts away [79].

Some other solution approaches to the level equation commute smoothness for accuracy and speed which are the requirements for an optimization scheme. In general the use of the level set method and moving boundaries poses as negative factors the high dependency between the final design and the initial guess, this tends to drive the optimization to local minimums.

Level sets methods using basis function like the Topology Description Functions or TDF's approach have the advantage that the global character of the function Φ is modified by the local character of the basis function, giving more insight in the local changes [111]. The use of basis functions in the definition by interpolation of the function Φ to transform the problem from a Hamilton-Jacobi PDE into ODE, avoids the numerical difficulties related with the level set method like the re-initialization procedure and the velocity extension algorithm and reduce the result's dependency on the initial guess.

Solution method

No study on the solution methods for structural optimization of compliant mechanisms was found. Basically the use of solution method goes in two directions depending on the nature of the design variables, namely search algorithms for discrete variables and mathematical programming for continuum variables.

The nature of the design variables depends on the kind of parameterization being used but some discrete problems can be relaxed into continuum problems.

Search algorithms in optimization of compliant mechanisms are basically confined to evolutionary structural optimization (ESO and BESO), genetic algorithms, particle swarm, simulated

annealing and tabu search. They are mainly used with parameterized curves and graphs and in some cases with domain discretization.
Typical mathematical programming algorithms in optimization of compliant mechanisms are sequential linear programming (SLP), sequential quadratic programming (SQP), simplex method, quasi-Newton, optimal criteria and moving asymptotes (GMMA) among others. They are mainly used in domain discretization, parameterized curves and level sets using basis functions.

3.6 Summary

The chapter presents an introduction to some of the methods for the design and synthesis of compliant mechanisms. The methods are presented from a conceptual perspective, pointing the reader to the references for detailed information. The idea of the chapter is to serve as a starting reference point for the inexperience designer and help him to make his way in the field. Therefore the presentation of the methods follows a proposed classification of the synthesis methods.
Advantages and disadvantages of compliance mechanisms have their root in the monolithic nature of such mechanisms. Since compliant mechanisms are monolithic, they exhibit three main features from which all the characteristics can be derived: (i) no relative motion among pieces, (ii) no overlapping pieces, and (iii) strain energy storage.
The design methods presented in this work can be categorized in three main groups:

- Kinematic approaches: design of compliant mechanisms is based on known kinematics of Rigid-Body mechanisms. Use what is already known and get rid of the joints.

- Building blocks: design of compliant mechanisms is based on division and simplification of the problem. ”divide and conquer”, find simpler solutions, then combine them.

- Structural optimization: design of compliant mechanisms is based on automation of the search for solutions. Use proper functions to define the problem (the objective function) and use proper variables to describe the solution (the parameterization).

In the kinematic approaches we find two synthesis methods: (i) the FACT method, and (ii) the Rigid-Body-Replacement method. The FACT method is based on the principles of exact constraining while the RBR method relies on the ability of model the elastic deflection of flexible elements as the deflection of rigid bodies connected by kinematic pairs. These pseudo-rigid-body models are classified as models for lumped or distributed compliance. Typical pseudo-rigid-body models are those modeling the behavior of notch-hinges and slender beams with different initial shape and under different load cases and boundary conditions.
In the building block approaches we find two synthesis methods: (i) building blocks by instant centers, and (ii) flexible building blocks and optimization.

In the synthesis of compliant mechanisms based on structural optimization three elements need to be considered: (i) the objective function, (ii) the parameterization, and (iii) the solution algorithm. The objective function answers to design requirements which are either kinematic or structural. Objective functions toward kinematic design requirements are based on some form of error minimization while five major objective functions considering structural design requirements can be found: (i) functions based on combinations of the mutual potential and strain energy, (ii) functions based on mechanical and geometrical advantage, (iii) functions based on mechanical efficiency, (iv) the characteristic stiffness, and (v) the artificial input/output spring formulation. Most of the parameterizations can be classified into four groups: (i) parameterized curves, (ii) structures as graphs or networks, (iii) discretized design domains, and (iv) parameterization based on higher dimension driving functions.

4 The spring-to-spring basic balancer

Nothing has such power to broaden the mind as the ability to investigate systematically and truly all that comes under thy observation in life.

Marcus Aurelius

Static balancing so far has been defined as a conservative state of motion where all the internal forces are kept in static equilibrium. However, this definition is not enough from a design point of view. It is desired to know what are the conditions that characterize a state of static balancing. The importance of identifying such conditions lies on the fact that these conditions later will become the design criteria that will ensure a state of static balancing.

We propose to derive the characteristics and properties of statically balanced mechanisms by experimenting with actual and well known statically balanced mechanisms. The idea is to obtain from these mechanisms general mathematical expressions for a set of statical, kinematical and dynamical functions, such as the potential energy, the reaction force, the stiffness, the stability, the internal work, the speed, the natural frequency and the virtual work. Once these general mathematical expressions are obtained, the condition for static balancing is applied into these expressions and then we observe the resultant behavior of such functions in a state of static balancing.

We also explore the existing relation between the variables chosen to describe the deflection of the strain energy sources (the deflection space) and the variables chosen to describe the real physical statically balanced motion (the workspace).

The aforementioned setup was applied into three well known statically balanced mechanisms, the spring-to-spring balancer, the gravity balancer and the sliding balancer [33], see Fig. 4.1. Here in this chapter we only present the development and results applied to the spring-to-spring basic balancer. The results for the other two balancers were conceptually equal to those presented in the following.

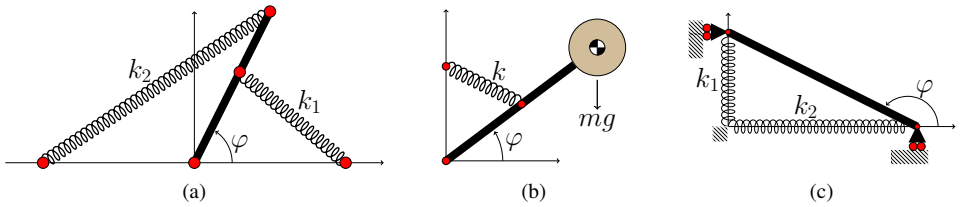

Figure 4.1: Three well known statically balanced mechanisms. (a) The spring-to-spring balancer. (b) The gravity balancer. (c) The sliding balancer

The spring-to-spring zero stiffness balancer is a 1-DOF linkage composed of one rigid link hinged at one end, with two springs attached along its other end. In this configuration it is required collinearity among the three grounded ends as well as collinearity between the springs' moving ends and the grounded end of the link, see Fig. 4.2. The springs used in the balancer are zero-free-length springs, meaning that their elongations are equal to their lengths, see Fig. 4.3.

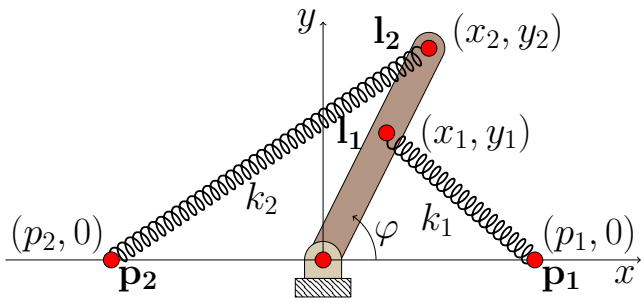

Figure 4.2: Depiction of the spring-to-spring basic balancer.

A state of static balancing on this linkage is guaranteed when the following condition is satisfied,

$$k_1 l_1 p_1 = -k_2 l_2 p_2 \tag{4.1}$$

In the following sections we present the development and results of applying the spring-to-spring balancer's static balancing condition into the general mathematical expressions for the potential energy, reaction force, stiffness, stability, internal work, speed, natural frequency and virtual work.

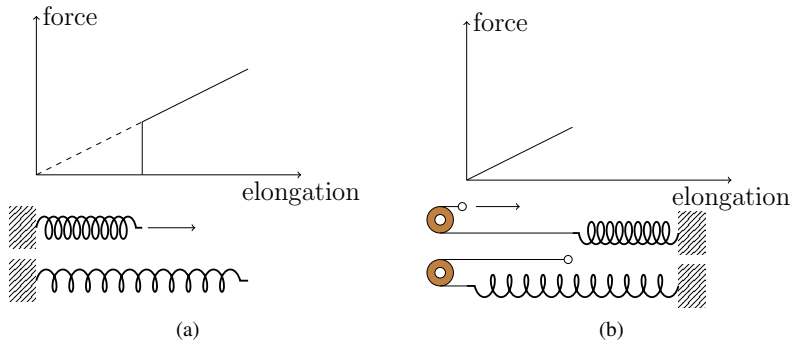

(a) (b)

Figure 4.3: A zero-free-length spring is a spring that exerts zero force when the length between its end points is zero. (a) Physically coil springs do not have a zero-free-length, but they can be built such at their initial length they exert a force equal to the initial length times the spring rate. (b) A spring with a pulley can act as a zero-free-length spring.

4.1 The potential energy

The total elastic potential energy u stored by spring 1 and 2 in the mechanism is given by

$$u = \frac{1}{2}k_1(\mathbf{l}_1 - \mathbf{p}_1)^2 + \frac{1}{2}k_2(\mathbf{l}_2 - \mathbf{p}_2)^2 \tag{4.2}$$

Replacing vectors $\mathbf{l}$ and $\mathbf{p}$ by their coordinates in terms of the rotation angle φ, yields

$$u = \frac{1}{2}k_1\left(l_1^2 - 2l_1p_1\cos\varphi + p_1^2\right) + \frac{1}{2}k_2\left(l_2^2 - 2l_2p_2\cos\varphi + p_2^2\right) \tag{4.3}$$

If we apply to this expression the condition for static balancing (Eq. 4.1) with k_1 as the dependent variable, we get

$$u = \frac{1}{2}k_1\left(l_1^2 - 2l_1p_1\cos\varphi + p_1^2\right) - \frac{1}{2}\frac{k_1l_1p_1}{l_2p_2}\left(l_2^2 - 2l_2p_2\cos\varphi + p_2^2\right) \tag{4.4}$$

Collecting terms yields

$$u = \frac{1}{2}k_1\left(l_1^2 + p_1^2 - \frac{l_1l_2p_1}{p_2} - \frac{l_1p_1p_2}{l_2}\right) \tag{4.5}$$

This result evidences that the total potential energy is constant, and it does not depend on the link's orientation angle φ.

4.2 The force

Now, let's compute the derivative of Eq. 4.3 with respect to φ. This derivative represents the external moment required to keep the link in static equilibrium.

$$f_\varphi = \frac{du}{d\varphi} = k_1 l_1 p_1 \sin\varphi + k_2 l_2 p_2 \sin\varphi \tag{4.6}$$

After applying the condition for static balancing (Eq. 4.1) we get

$$f_\varphi = \frac{du}{d\varphi} = k_1 l_1 p_1 \sin\varphi - k_1 l_1 p_1 \sin\varphi = 0 \tag{4.7}$$

This shows that no external force is required to keep the mechanism in static equilibrium at any point in its range of motion. Because the potential energy is constant along the entire range of motion, the internal forces are continuously kept in static equilibrium.

4.3 The stiffness

To evaluate the stiffness of the system we compute the second derivative of Eq. 4.3 with respect to φ

$$k = \frac{d^2u}{d\varphi^2} = k_1 l_1 p_1 \cos\varphi + k_2 l_2 p_2 \cos\varphi \tag{4.8}$$

Once again by applying the condition for static balancing we get

$$k = \frac{d^2u}{d\varphi^2} = k_1 l_1 p_1 \cos\varphi - k_1 l_1 p_1 \cos\varphi = 0 \tag{4.9}$$

The stiffness of the mechanism becomes zero. Notice that under the same condition the mechanism is also in static equilibrium, Eq. 4.7, then the mechanism has not only zero stiffness but it is also neutrally stable.

4.4 Buckling at critical load

So far, we have seen the expected results from having a constant potential energy, but let's move further and decompose the force of one spring into two forces using the parallelogram law. Here, one component is always parallel to the link, while the other is kept horizontal.

The magnitudes of the two force components as function of the spring's stiffness are given by

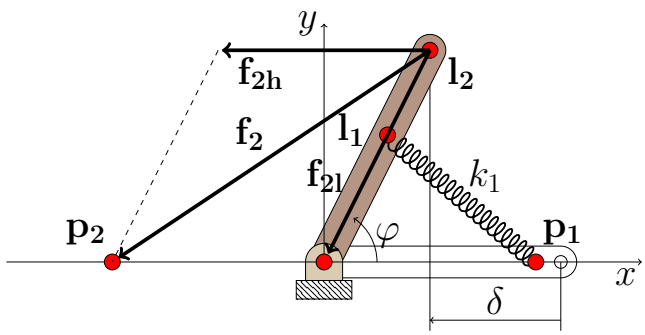

Figure 4.4: Decomposition of the force exerted by spring 2. The decomposition follows the parallelogram method on which one component is always parallel to the link and the other is always horizontal

$$f_{2h} = k_2 p_2 \tag{4.10}$$

$$f_{2l} = k_2 l_2 \tag{4.11}$$

Notice that $\mathbf{f_{2h}}$ is a constant force in both magnitude and direction. Now let's remove one spring, let's say k_2. The remaining spring k_1 will exert a restoring force moving the link to a stable equilibrium point around $\varphi = 0$. If a horizontal force is applied at point l_2 on the link, see Fig. 4.5, then there is a value of f_c at which the stability of the link-spring system around $\varphi = 0$ is lost. To find such critical value, we use equilibrium of moments at the pivot point of the link.

$$f_c l_2 \sin\varphi = -k_1 p_1 l_1 \sin\varphi \tag{4.12}$$

$$f_c = -\frac{k_1 l_1 p_1}{l_2} \tag{4.13}$$

by combining Eq. 4.1 and 4.13, we see that

$$f_c = k_2 p_2 \tag{4.14}$$

which is equal to Eq. 4.10. This means that when the mechanism is in a state of static balancing, the constant horizontal component of one spring is the buckling critical load of the other spring at which stability is lost for the whole range of motion $[-\infty < \varphi < \infty]$. In other words if the mechanism is in a state of static balancing, then the mechanism is in a state of self-buckling at critical load.

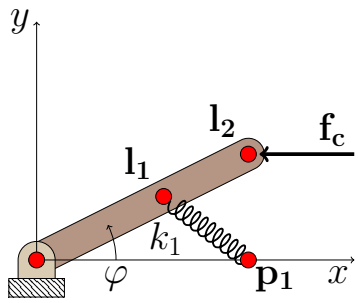

Figure 4.5: The restoring moment at the pivot point exerted by spring k_1 is balanced by the moment exerted by force f_c. In this case the stability of the equilibrium point at $\varphi = 0$ that was previously induced by spring k_1 is lost.

4.5 Linear behavior of internal energies

The elastic energies from the springs u_1 and u_2 are square function of the springs' elongations, and these elongations are coupled by the link's rotation angle φ.

$$u_1 = \frac{1}{2}k_1\left(l_1^2 - 2l_1p_1\cos\varphi + p_1^2\right) \tag{4.15}$$

$$u_2 = \frac{1}{2}k_2\left(l_2^2 - 2l_2p_2\cos\varphi + p_2^2\right) \tag{4.16}$$

$$u = u_1 + u_2 \tag{4.17}$$

If we plot the springs' energies (see Fig. 4.6a) assuming a state of static balancing, we see the cosine behavior of each spring energy with respect to the rotation angle φ, together with the constant behavior of the total potential energy.

But let's return to Fig. 4.4. We can see that the work done by the force component f_{2l} acting along the link is zero and the work done by the horizontal component f_{2h} (the constant force) is

$$w_{2h} = f_{2h}\delta \tag{4.18}$$

where δ is the horizontal displacement of the force application point l_2 on the link. The work done by force f_{2h} is equal to the energy stored by spring 1, while the link is rotating under the action of this force. It is evident that the work is a linear function of the deflection δ, therefore the energy function of the spring is also a linear function of the deflection δ. To see this, let's express δ as a function of the angle φ,

$$\delta = l_2 - l_2\cos\varphi \tag{4.19}$$

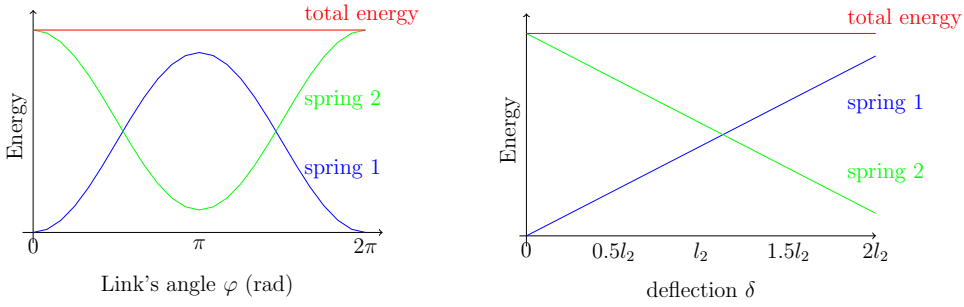

Figure 4.6: The behavior of the springs' energy functions vary with respect to the generalized coordinate that is used. (a) Springs' energies show cosine behavior when they are function of the link's rotation angle φ. (b) Springs' energies show linear behavior when they are function of the link's deflection δ.

Replacing Eq. 4.19 into Eq. 4.16 we get,

$$u_2 = \frac{1}{2}k_2(l_2 - p_2)^2 + k_2 p_2 \delta \tag{4.20}$$

which is clearly a linear function of δ. Figure 4.6b shows the energy functions of the combined and individual springs as function of the deflection δ.

4.6 The speed

Now let's obtain the equation of motion for the linkage by using the LaGrange's equation in the following form,

$$\frac{d}{dt}\left(\frac{\partial T}{\partial \dot{q}_i}\right) - \frac{\partial T}{\partial q_i} + \frac{\partial U}{\partial q_i} = f_i \tag{4.21}$$

To use LaGrange's equation we need to set the kinetic and potential energy functions.

$$T = \frac{1}{2}I\dot{\varphi}^2 \tag{4.22}$$

$$U = \frac{1}{2}k_1\left(l_1^2 - 2l_1 p_1 \cos\varphi + p_1^2\right) + \frac{1}{2}k_2\left(l_2^2 - 2l_2 p_2 \cos\varphi + p_2^2\right) \tag{4.23}$$

$$\tag{4.24}$$

Here I is the mass moment of inertia of the link with respect to the pivot point. Computing each term of Eq. 4.21 we get

$$\frac{d}{dt}\left(\frac{\partial T}{\partial \dot{\varphi}_i}\right) = I\ddot{\varphi} \tag{4.25}$$

$$\frac{\partial T}{\partial \varphi_i} = 0 \tag{4.26}$$

$$\frac{\partial U}{\partial \varphi_i} = (k_1 l_1 p_1 + k_2 l_2 p_2)\sin\varphi \tag{4.27}$$

$$f_i = 0 \tag{4.28}$$

$$\tag{4.29}$$

Replacing the terms into Eq. 4.21, we get the equation of motion

$$I\ddot{\varphi} + (k_1 l_1 p_1 + k_2 l_2 p_2)\sin\varphi = 0 \tag{4.30}$$

Applying the condition for static balancing $k_1 l_1 p_1 = -k_2 l_2 p_2$ to the above equation yields,

$$I\ddot{\varphi} = 0 \tag{4.31}$$

Now, let's solve this equation for velocity,

$$I\frac{d\dot{\varphi}}{dt} = 0 \tag{4.32}$$

$$I\int_{\dot{\varphi}_0}^{\dot{\varphi}_t} d\dot{\varphi} = \int_{t_0}^{t} 0dt \tag{4.33}$$

$$I\left(\dot{\varphi}_t - \dot{\varphi}_0\right) = 0\left(t - t_0\right) \tag{4.34}$$

$$\dot{\varphi}_t = \dot{\varphi}_0 \tag{4.35}$$

Equation 4.35 express that the speed at any time is equal to the initial speed of the mechanism, or in other words, the speed of the mechanism in a state of static balancing is constant. The motion of the link is driven only by its inertial properties.

4.7 The frequency

Let's compute the natural frequency of the system. Assuming that the system is in equilibrium at $\varphi(t) = \varphi_0$, the equation of motion for small disturbances $\Delta\varphi$ around φ_0 is,

$$\begin{aligned} \varphi(t) &= \varphi_0 + \tfrac{d\varphi}{dt}\Delta t \\ \varphi(t) &= \varphi_0 + \Delta\varphi(t) \end{aligned} \tag{4.36}$$

The time dependent term $\Delta\varphi(t)$ is the solution of the linear differential equation,

$$I\Delta\ddot{\varphi} + k\Delta\varphi = 0 \tag{4.37}$$

Where I is the link's moment of inertia with respect to its pivot point and k is the system's stiffness given by Eq. 4.8. Solution to Eq. 4.37 can be found by using an assumed solution,

$$\Delta\varphi(t) = \Delta\varphi_0 e^{\lambda t} \tag{4.38}$$

Taking the second derivative of the assumed solution yields,

$$\Delta\ddot{\varphi}(t) = \Delta\varphi_0 \lambda^2 e^{\lambda t} \tag{4.39}$$

where $\Delta\varphi_0$ is the initial amplitude of the equilibrium disturbance. To find the value of λ we replace Eq. 4.38 and 4.39 into Eq. 4.37,

$$\left(I\lambda^2 + k\right)\Delta\varphi_0 e^{\lambda t} = 0 \tag{4.40}$$

Here, the exponential term is never zero and by ignoring the trivial solution $\Delta\varphi_0 = 0$ we are left with,

$$I\lambda^2 + k = 0 \tag{4.41}$$

Re-arranging the terms we find,

$$\lambda = \pm\sqrt{\frac{k}{I}}i = \pm\omega_0 i \tag{4.42}$$

Here, ω_0 is the harmonic natural frequency for small deflections around the equilibrium point φ_0. Replacing the mechanism's stiffness given by Eq. 4.8 into Eq. 4.42, we get the harmonic natural frequency of the basic balancer,

$$\omega_0 = \sqrt{\frac{k_1 l_1 p_1 \cos\varphi + k_2 l_2 p_2 \cos\varphi}{I}} \tag{4.43}$$

By applying the condition for static balancing $k_1 l_1 p_1 = -k_2 l_2 p_2$ to this equation, we see that the harmonic natural frequency is zero,

$$\omega_0 = \sqrt{\frac{k_1 l_1 p_1 \cos\varphi - k_2 l_2 p_2 \cos\varphi}{I}} = 0 \tag{4.44}$$

It was assumed that the perturbation was taking place around the equilibrium point φ_0, but for the balancer on a state of static balancing all the points $\varphi(t)$ are equilibrium points. Therefore, at any point the basic balancer on a state of static balancing exhibits zero natural frequency.

So far we have assumed small perturbations around an equilibrium point in order to set the problem as a linear differential equation, but it is also possible to prove from the nonlinear problem that the natural frequency of the basic balancer in a state of static balancing is zero.

Simpson [127], Neto [91] and Belendez et al. [8] developed the solution for a nonlinear pendulum in the form,

$$\ddot{\varphi} + {\omega_0}^2 \sin\varphi = 0 \tag{4.45}$$

They showed for the nonlinear pendulum that the natural frequency ω is a function of the harmonic natural frequency ω_0 and the initial conditions φ_0 and $\dot{\varphi}_0$.

$$\omega = \frac{\pi\omega_0}{2K(m)} \tag{4.46}$$

Where $K(m)$ is the complete elliptical integral of the first kind, and m is equal to,

$$m = \sin\left(\frac{\arccos\left(\cos\varphi_0 - \frac{1}{2}\dot{\varphi}_0^2\right)}{2}\right) \tag{4.47}$$

The complete elliptical integral of the first kind expanded into an infinite series is,

$$K(m) = \sum_{n=0}^{\infty}\left(\frac{(2n)!}{2^{2n}{(n!)}^2}m^{2n}\right) \tag{4.48}$$

Then, replacing Eq. 4.47 and Eq. 4.48 into Eq. 4.46, we get the expression for the natural frequency,

$$\omega(\varphi_0,\dot{\varphi}_0) = \frac{\omega_0}{\sum\limits_{n=0}^{\infty}\left(\frac{(2n)!}{2^{2n}{(n!)}^2}\sin^{2n}\left(\frac{\arccos\left(\cos\varphi_0 - \frac{1}{2}\dot{\varphi}_0^2\right)}{2}\right)\right)} \tag{4.49}$$

We can apply this result for the basic balancer by noticing that the equation of motion, Eq. 4.30, has the same form of Eq. 4.45,

$$\ddot{\varphi} + \frac{k_1 l_1 p_1 + k_2 l_2 p_2}{I}\sin\varphi = 0 \tag{4.50}$$

where the harmonic natural frequency ω_0 is the same as in Eq. 4.43. Then is clear from Eq. 4.49 that when the harmonic natural frequency ω_0 is zero, the natural frequency for large deflections is also zero, regardless of the initial conditions φ_0 and $\dot{\varphi}_0$.

4.8 The virtual work

Let's compute the virtual work of the basic balancer. To do so, first we compute the virtual displacements of the springs' anchor points on the link, l_1 and l_2. To do this, first we compute the position of the point and then we compute the position differential as a function of the generalized DOF.
The position vector of point l_1 is,

$$\mathbf{l}_1 = l_1 \cos(\varphi)\,\hat{\mathbf{i}} + l_1 \sin(\varphi)\,\hat{\mathbf{j}} \tag{4.51}$$

Differentiating this expression we get,

$$\delta\mathbf{l}_1 = -l_1 \sin(\varphi)\,\delta\varphi\hat{\mathbf{i}} + l_1 \cos(\varphi)\,\delta\varphi\hat{\mathbf{j}} \tag{4.52}$$

The position vector of point l_2 is,

$$\mathbf{l}_2 = l_2 \cos(\varphi)\,\hat{\mathbf{i}} + l_2 \sin(\varphi)\,\hat{\mathbf{j}} \tag{4.53}$$

Differentiating we get,

$$\delta\mathbf{l}_2 = -l_2 \sin(\varphi)\,\delta\varphi\hat{\mathbf{i}} + l_2 \cos(\varphi)\,\delta\varphi\hat{\mathbf{j}} \tag{4.54}$$

Now we calculate the forces exerted by the springs at points l_1 and l_2. The force exerted by spring 1 is,

$$\mathbf{f}_1 = -k_1\,(\mathbf{l}_1 - \mathbf{p}_1) \tag{4.55}$$

Replacing terms and developing the expression we get,

$$\mathbf{f}_1 = (k_1 p_1 - k_1 l_1 \cos(\varphi))\,\hat{\mathbf{i}} - k_1 l_1 \sin(\varphi)\,\hat{\mathbf{j}} \tag{4.56}$$

The force exerted by spring 2 is,

$$\mathbf{f}_2 = -k_2\,(\mathbf{l}_2 - \mathbf{p}_2) \tag{4.57}$$

Again, replacing terms and developing the expression we get,

$$\mathbf{f}_2 = (k_2 p_2 - k_2 l_2 \cos(\varphi))\,\hat{\mathbf{i}} - k_2 l_2 \sin(\varphi)\,\hat{\mathbf{j}} \tag{4.58}$$

The virtual work of each spring is the dot product between the force from the spring and the virtual displacement of its application point. For the first spring we have,

$$\delta w_1 = \mathbf{f}_1 \cdot \delta \mathbf{l}_1 \tag{4.59}$$

Replacing Eq. 4.52 and Eq. 4.56 into Eq. 4.59 we get,

$$\delta w_1 = \left(\left(k_1 p_1 - k_1 l_1 \cos\left(\varphi\right) \right) \hat{\mathbf{i}} - k_1 l_1 \sin\left(\varphi\right) \hat{\mathbf{j}} \right) \cdot \left(-l_1 \sin\left(\varphi\right) \delta\varphi \hat{\mathbf{i}} + l_1 \cos\left(\varphi\right) \delta\varphi \hat{\mathbf{j}} \right) \tag{4.60}$$

Collecting terms we have,

$$\delta w_1 = -k_1 p_1 l_1 \sin\left(\varphi\right) \delta\varphi \tag{4.61}$$

The virtual work of spring 2 is,

$$\delta w_2 = \mathbf{f}_2 \cdot \delta \mathbf{l}_2 \tag{4.62}$$

Replacing Eq. 4.54 and Eq. 4.58 into Eq. 4.60 we get,

$$\delta w_2 = \left(\left(k_2 p_2 - k_2 l_2 \cos\left(\varphi\right) \right) \hat{\mathbf{i}} - k_2 l_2 \sin\left(\varphi\right) \hat{\mathbf{j}} \right) \cdot \left(-l_2 \sin\left(\varphi\right) \delta\varphi \hat{\mathbf{i}} + l_2 \cos\left(\varphi\right) \delta\varphi \hat{\mathbf{j}} \right) \tag{4.63}$$

Collecting terms we have,

$$\delta w_2 = -k_2 p_2 l_2 \sin\left(\varphi\right) \delta\varphi \tag{4.64}$$

The total virtual work of the basic balancer is the addition of the individual virtual works of the two springs,

$$\delta w = \delta w_1 + \delta w_2 \tag{4.65}$$

Replacing Eq. 4.61 and Eq. 4.64 into Eq. 4.65 and collecting terms we get,

$$\delta w = -\left(k_1 p_1 l_1 + k_2 p_2 l_2 \right) \sin\left(\varphi\right) \delta\varphi \tag{4.66}$$

For a system that is in static equilibrium the virtual work must be zero,

$$0 = \left(k_1 p_1 l_1 + k_2 p_2 l_2 \right) \sin\left(\varphi\right) \tag{4.67}$$

This expression provides the orientation at which the mechanism is in equilibrium for a given set of values of k_1, p_1, l_1, k_2, p_2 and l_2. But also notice that if we apply the condition for static balancing $k_1 l_1 p_1 = -k_2 l_2 p_2$, the expression is equal to zero regardless the orientation angle φ of the link. The basic balancer on a state of static balancing must exhibit a virtual work equal

to zero for any orientation angle φ. This result once again indicates that the basic balancer is in static equilibrium for all the points of its range of motion.

4.9 The workspace and deflection space

Let's assume for the moment a synthesis perspective rather than an analysis perspective. We want to find the way to configure two zero-free-length springs, so they can create a statically balanced system.

Taking away the link as shown in Fig. 4.7, we get a system of two springs, where the springs' configuration is given by the deflection vector $\mathbf{q}$,

$$\mathbf{q} = \begin{bmatrix} x_1 & y_1 & x_2 & y_2 \end{bmatrix}^T \tag{4.68}$$

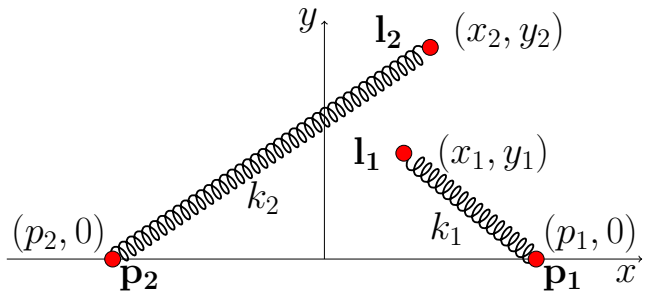

Figure 4.7

The total strain energy of the system as a function of the four deflection variables is,

$$\begin{aligned} u(\mathbf{q}) &= u_1(\mathbf{q}) + u_2(\mathbf{q}) \\ u(\mathbf{q}) &= \tfrac{1}{2}k_1\left(x_1^2 - 2p_1x_1 + p_1^2 + y_1^2\right) + \tfrac{1}{2}k_2\left(x_2^2 - 2p_2x_2 + p_2^2 + y_2^2\right) \end{aligned} \tag{4.69}$$

To obtain the external reaction force vector in this four-dimensional deflection space we compute the partial derivatives of Eq. 4.69 with respect to the deflection variables,

$$\mathbf{f}(\mathbf{q}) = \begin{bmatrix} k_1x_1 - k_1p_1 \\ k_1y_1 \\ k_2x_2 - k_2p_2 \\ k_2y_2 \end{bmatrix} \tag{4.70}$$

The system's stiffness in the deflection space is the Hessian of the total strain energy,

$$\mathbf{K}(\mathbf{q}) = \begin{bmatrix} k_1 & 0 & 0 & 0 \\ 0 & k_1 & 0 & 0 \\ 0 & 0 & k_2 & 0 \\ 0 & 0 & 0 & k_2 \end{bmatrix} \tag{4.71}$$

If we try to find the way to configure these two springs in order to get a system with zero force and zero stiffness, we find that (i) the force is zero only if there is no deflection, $\mathbf{q} = \mathbf{0}$, and (ii) the change in force is zero ($\Delta\mathbf{f} = \mathbf{0}$) only if there is no change in deflection $\Delta\mathbf{q} = \mathbf{0}$, hence no zero stiffness. The latter comes from the fact that the stiffness matrix expressed in the deflection space is always positive definite, so the only solution for Eq. 4.72 is $\Delta\mathbf{q} = \mathbf{0}$.

$$\mathbf{K}\Delta\mathbf{q} = \mathbf{0} \tag{4.72}$$

We already know that these two springs can be configured in a way that they create a statically balanced system with zero force and zero stiffness motion, so let's define in the four dimensional deflection space a position vector $\mathbf{r}$, and let's express this vector as a function of a parameter, in this case a rotation angle φ,

$$\begin{aligned} \mathbf{r}(\varphi) &= x_1\hat{\mathbf{e}}_1 + y_1\hat{\mathbf{e}}_2 + x_2\hat{\mathbf{e}}_3 + y_2\hat{\mathbf{e}}_4 \\ \mathbf{r}(\varphi) &= l_1\cos\varphi\hat{\mathbf{e}}_1 + l_1\sin\varphi\hat{\mathbf{e}}_2 + l_2\cos\varphi\hat{\mathbf{e}}_3 + l_2\sin\varphi\hat{\mathbf{e}}_4 \end{aligned} \tag{4.73}$$

Notice that vector $\mathbf{r}$ is imposing a deflection constraint between the deflection variables, thus mapping the deflection space into what we call the workspace. The workspace is the real physical space in which the mechanism acts. In this case is a one dimensional space defined in terms of the variable φ.

Now, if we compute again the external reaction force of the system but this time taking derivatives with respect to variable φ (this is the external force required to keep a state of static equilibrium along the workspace), we get

$$\mathbf{f}(\varphi) = \mathbf{f}(\mathbf{q}) \cdot \mathbf{r}' \tag{4.74}$$

Where $\mathbf{r}'$ is the derivative of vector $\mathbf{r}$ with respect to φ,

$$\mathbf{r}'(\varphi) = -l_1\sin\varphi\hat{\mathbf{e}}_1 + l_1\cos\varphi\hat{\mathbf{e}}_2 - l_2\sin\varphi\hat{\mathbf{e}}_3 + l_2\cos\varphi\hat{\mathbf{e}}_4 \tag{4.75}$$

Replacing Eq. 4.70 and 4.75 into Eq. 4.74, and collecting terms we get,

$$\mathbf{f}\,(\varphi) = (k_1 p_1 l_1 + k_2 p_2 l_2)\sin\varphi \tag{4.76}$$

Now, if we compute again the stiffness of the system as a function of the variable φ we get,

$$k(\varphi) = \mathbf{r}'^{T}\mathbf{K}(\mathbf{q})\mathbf{r}' + \mathbf{f}(\mathbf{q}) \cdot \mathbf{r}'' \tag{4.77}$$

Where $\mathbf{r}''$ is the second derivative of vector $\mathbf{r}$ with respect to φ,

$$\mathbf{r}''(\varphi) = -l_1 \cos\varphi\hat{\mathbf{e}}_1 - l_1 \sin\varphi\hat{\mathbf{e}}_2 - l_2 \cos\varphi\hat{\mathbf{e}}_3 - l_2 \sin\varphi\hat{\mathbf{e}}_4 \tag{4.78}$$

Replacing Eq. 4.70, 4.71, 4.75 and 4.78 into Eq. 4.77, and collecting terms we get,

$$k\left(\varphi\right) = \left(k_1 p_1 l_1 + k_2 p_2 l_2\right)\cos\varphi \tag{4.79}$$

Notice that both, Eq. 4.76 and Eq. 4.79 are exactly the same expressions obtained in sections 4.2 and 4.3. Remember that if we apply the condition for static balancing (Eq. 4.1) into these two expressions we get the zero force and zero stiffness.

The interesting result from this exercise is to notice that when the system is constrained to move in the workspace defined by vector $\mathbf{r}$, in fact the system is being constrained to move along subset of configurations in the deflection space. But once the system is statically balanced, this subset of configurations corresponds to a level set of the potential energy function in the deflection space. The level set of a function is the set of points where the function has a constant value. Certainly a level set of the potential energy function is a set of points with constant potential energy. A statically balanced mechanism is then a system that has been constrained to move along a level set of the potential energy function in the deflection space. This constrained motion along a level set is reflected as a statically balanced state of motion in the real physical workspace of the system.

The aforementioned in the context of design means that the deflection of a system defined in terms of a set of variables $\mathbf{q}$ may not reflect the possibility to statically balance the system, but this apparent reflection does not mean that the system can not be statically balanced.

4.10 Discussion

The spring-to-spring zero stiffness balancer although mechanically simple exhibits quite elegantly all the characteristics and properties of statically balanced systems. We can observe for instance that the balancer has two springs which can be defined as two clearly distinct elements storing potential energy. This is a common feature in statically balanced systems required to keep the potential energy constant during motion. There must be at least one potential energy storing element losing energy during motion, while at least another storing element is gaining this lost energy.

The classical view of static balancing describes such systems in terms of their constant potential energy, continuous zero force, continuous zero stiffness and neutral stability. Experimentation

with the spring-to-spring balancer allowed the observation of new features that helps to create a more complete view of statically balanced systems.
From a dynamic point of view the spring-to-spring balancer allow to observe that motion in statically balanced systems is driven by the system's inertia so in the absence of external disturbances and non-conservative forces the speed across the workspace is constant. The latter imply that statically balanced systems do not oscillate, so both natural frequency and harmonic natural frequency are zero. The absence of external disturbances and restoring forces implies that statically balanced systems exhibit continuous zero virtual work for all the points along their workspace.
From a stability point of view the spring-to-spring balancer allows to observe that statically balanced systems are pre-stressed systems —potential energy is pre-stored in the elastic elements— on which the pre-stressed areas induce a loss of structural stability so the systems are in a state of self-buckling at critical load, with the addition that if the buckling critical load is constant then statically balanced systems exhibit linear behavior on their internal energies. This view of statically balanced systems gets relevance when self-buckling is viewed as a conceptual design approach towards static balancing.
The spring-to-spring balancer helps to observe in context how statically balanced systems are systems where their workspace is a projection of a level set of the potential energy function which is defined in the deflection space of the systems.

4.11 Summary

The chapter presents the spring-to-spring balancer as an object of study for the observation of the properties in statically balanced systems. We describe the static balancing properties of the spring-to-spring balancer in terms of the potential energy, the force, the stiffness, the stability, the natural frequency. We also introduce four novel descriptions, (i) the spring-to-spring balancer as a self-buckled system at critical load, (ii) the spring-to-spring balancer as a system moving at constant speed and driven by its inertial properties, (iii) the spring-to-spring balancer as a system with continuous zero virtual work along its workspace and (iv) the spring-to-spring balancer as a system that projects a level set of the its potential energy into its workspace.

5 Static Balancing

It is not knowledge, but the act of learning, ... which grants the greatest enjoyment. When I have clarified and exhausted a subject, then I turn away from it, in order to go into darkness again,

Johann Carl Friedrich Gauss

This chapter introduces the theory and foundations for the static balancing of mechanisms. Here, the design criteria that can be used to define and identify a state of static balancing are derived from the concepts of stability and equilibrium on which the theory of static balancing is based.

Identification and understanding of static balancing criteria serves as the angular stone for the development of a synthesis method on a framework that should allow the generation of design concepts.

Literature on the theoretical aspects of equilibrium and stability is focused on how to identify unstable behavior in a structure and how to avoid it in order to ensure a stable state of equilibrium. But static balancing is a special case of equilibrium called neutrally stable equilibrium, for which not too much literature is devoted, therefore here it is attempted to compile most of the ideas about static balancing, in order to provide with a consistent mathematical framework and elucidate the implications of this singular state of equilibrium. The presentation of most of the ideas is done from the perspective of linear algebra, to keep in mind their implementation by numerical schemes towards the analysis of compliant mechanisms.

The theory presented here, although is a general perspective exhibited from several angles, is far from exhaustive and complete.

The chapter presents at the introduction a literature review organized in a proposed classification based on applications and design approaches. Then in the following section the static balancing criteria are developed and explained. The final section presents the mathematical generalization of static balancing problem. The generalization explains static balancing as a transformation problem in which the statically balanced workspace of the compliant mechanisms is a projection of a level set of the potential energy function.

5.1 Introduction

Statically balanced mechanisms (SBM's), also known as energy-free systems, are those mechanisms where the acting forces are balanced or in a state of static equilibrium for all the points of a given range of motion, thus making the quasistatic operation of the mechanisms effortless. Typical applications of static balancing are gravity compensation of mechanisms, vibration isolation and stiffness reduction in compliant mechanisms.

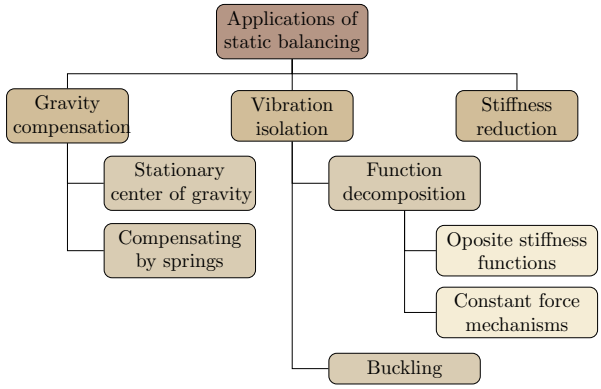

Figure 5.1: Typical applications of static balancing and their design methods

5.1.1 Gravity compensation

The use of static balancing for gravity compensation can be found in applications such as balancing of linkages and parallel manipulators. Typically, the idea is to compensate the weight of a mechanism in order to achieve an effortless actuation when no payload is present.
Design methods for gravity compensation are based on the use of springs and/or stationary centers of gravity. On the use of springs, it can be found the work of Streit and Shin [131], where they present a design method for gravity compensation of planar linkages by extending the methods proposed by Nathan et al. [90] and Pracht et al. [101] where prismatic and revolute joints are included and applied to both, open and close loop linkages. The idea behind the method is the use of two basic 2DOF's linkages —the vertical link system and the parallel link system— which are able to generate a vertical constant force to compensate the weight of every link in the linkage to be balanced.
Further on the use of springs is the work of Herder [33][32], who introduces a design method for static balancing of mechanisms dealing with gravity potentials and elastic potentials from zero-free-length springs. Here, a basic statically balanced mechanism is modified following a set of seven modification rules to obtain new designs. These rules modify the type, shape and topology of the mechanism while the statically balanced state of the mechanism is kept.

Among methods based on stationary centers of gravity is the work of Jean and Gosselin [49], who proposed a method for gravity compensation of one, two and three DOF's planar linkages. They demonstrated that it is possible to find a vertically stationary center of gravity for all the linkage configurations by properly locating the individual link's center of mass. This idea is later extended by Wang and Gosselin to spatial parallel mechanisms of three and four DOF's [144][145] in which the stationary centers of gravity are combined with the use of springs based on the method proposed by Streit and Shin.

5.1.2 Vibration isolation

Another application of static balancing is vibration isolation. Theoretically speaking, statically balanced mechanisms have a natural frequency equal to zero, meaning that when they are perturbed they do not oscillate, thus, making them ideal for passive systems in vibration isolation. The design of vibration isolators is mainly based on two ideas, building blocks and buckling. Both design approaches rely on frequency reduction by reducing the stiffness of the system.
In the building blocks, stiffness reduction is achieved in two ways. The first way is combining two blocks with opposite stiffness functions, one positive and the other negative. Alabuzhev et al. [2] provide with a collection of designs for vibration isolation using this idea, while Park and Luu [95] present the analysis of four different types of isolators based on building blocks in order to identify those that can provide with perfect zero natural frequency.
The second way is using constant force mechanisms. A system which exerts a force of constant value along a range of motion is used, therefore exhibiting zero stiffness. Rivin [107] shows a few designs based in this idea. It should be noted that constant force mechanisms are not statically balance mechanisms but they serve as designing building blocks as it will be shown in chapter 6.
In the buckling approach stiffness reduction is obtained by designing the isolation mounts in a way that when loaded, the load is close to the critical load. Freakley [26] shows the design of rubber mounts for vibration isolation based on buckling, while Rivin [108] describes buckling as a form of vibration isolation and shows the operation of Platus' design [99]. The basic operation of Platus' design can be found in [98] where Platus explains a vibration isolation system for six degrees of freedom using buckling.

5.1.3 Stiffness reduction

There are situations where it is desirable a reduction in the operational stiffness of compliant mechanisms, like increasing energy efficiency or the ability to keep the force feedback between the input and output of a compliant tool.
Imagine a mechanism where its actuator can not exert high forces, in this case it is desired that all the energy from the actuator goes to the payload and it is not wasted deforming the mechanism just to achieve motion. Or imagine a situation where a set of compliant pliers are used and what

is felt at the handle is the reaction force coming from the deformed tool plus the reaction from the workpiece, how can you tell if the applied force is causing damage to the workpiece or is enough to hold it.
Work in these directions were taken by Herder and Van den Berg [34] who presented the static balancing of a compliant surgical forceps by using a rolling mechanism with coil springs. Although the final design was not a fully compliant design, it showed the possibility to statically balance compliant mechanisms. Later Stapel and Herder [129] published a feasibility study for a fully compliant statically balanced mechanism, from where Lange et al. [66], Hoetmer et al. [36], Powell and Frecker [100] and Tolou and Herder [137] presented designs of a grasper by compensating the gripper positive stiffness with a negative stiffness compliant balancer. The first two approaches were fully compliant designs based on topology optimization and building blocks respectively, while the remaining two designs were partially compliant, based on size optimization.
Dede and Trease [21] showed the design of a statically balance gravity compensator by using torsion springs. The balancer consisted of a partially compliant fourbar linkage where two of its joints were replaced by compliant cross-section revolute joints. Radaelli et al. [102] proposed a method for the search of the conditions that guarantees a statically balanced configuration. Here the search space is formed by the energy function of the system. The approach can only be used in the design of compliant mechanisms with flexures or that can be modeled using the Pseudo Rigid Body Model (PRBM).
Tolou et al. [136] introduced two designs of statically balance fully compliant mechanisms with direct application in micro-mechanisms while Morsch and Herder [88] presented the design of a statically balanced fully compliant joint based on a cross-axis flexural pivot [51].

5.2 Theory on static balance

The theory presented in the following sections is defined in the context of isolated and conservative mechanical systems. In the subsequent, references to external forces does not mean that the isolation condition is violated, but that the system is composed at least of two subsystems where one of the subsystems has no more functionality than exert forces onto the main subsystem.
We present for the first time static balancing as a state of motion in the context of compliant mechanisms. The presentation includes three main criteria based on potential energy, force, and stability, as well as a novel criteria based on virtual work, speed, natural frequency, and buckling.

5.2.1 The potential energy

Potential energy can be defined as the capacity of a mechanical system to do a work in virtue of its position or configuration. In the case of a system form by deformable bodies the potential

energy due to the deformed configuration is referred as the strain energy.
Statically balanced mechanisms were previously defined as those mechanical systems where no effort is required for their operation, meaning that the required actuation force is zero. This implies that no acceleration is present and that the motion is driven by the inertial properties of the system or in other words the system's speed is constant.
For isolated and conservative mechanical systems, the law of conservation of energy states that the sum of the potential and kinetic energy is a constant, meaning that no energy is entering or leaving the system.

$$E_{mech} = T + U = constant \tag{5.1}$$

Where T and U are the kinetic and potential energy respectively and E_{mech} the total mechanical energy. During motion these energies can transform from one form of energy into the other one. The foregoing implies that if the potential energy increases then the kinetic energy decreases as well as the speed and vice versa, but when the speed of the system is constant along a motion described by DOF's q_i, no change occur in the kinetic energy and therefore the system's potential energy is constant. This mechanical state is here referred to as statically balanced.

$$U(\mathbf{q}) = \mathbf{constant} \tag{5.2}$$

Definition 5.1. *A mechanical system with constant potential energy along a certain range of motion is a statically balanced system along such of range of motion.*

The constant potential energy criterion is a necessary and sufficient condition to guarantee a state of static balance.
Notice that definition 5.1 states that in statically balanced system there is no change in the potential energy, but it does not mention if the potential energy can be zero or some other value. In the case of deformable structures, if the zero reference level for the strain energy is chosen at undeformed and unstressed configurations, then it is clear that for a structure undergoing motion the strain energy can not be zero (the structure is deforming).

Proposition 5.1. *Deformable structures undergoing motion in a statically balanced state are prestressed structures.*

5.2.2 The force equilibrium

It is said that a mechanical system is in static equilibrium, if the resultant of the internal and external forces in the isolated system are zero. From the mechanics of conservative systems, it is known that the infinitesimal change in the potential energy dU is equal to minus the work done by the mechanical system along a differential of trajectory ds

$$dU = -\mathbf{f} \cdot d\mathbf{s} \tag{5.3}$$

From equation 5.2 it is clear that dU is equal to zero (potential energy is constant then no change), so Eq. 5.3 becomes

$$0 = -\mathbf{f} \cdot d\mathbf{s} \tag{5.4}$$

One could be tempted to integrate along the trajectory s to get

$$0 = -\int_s \mathbf{f} \cdot d\mathbf{s} \tag{5.5}$$

But that would be wrong, Eq. 5.5 is a necessary but not sufficient condition to guarantee static balancing along a trajectory. Observe that if we apply the *fundamental theorem for line integrals* [130], Eq. 5.5 can be written as

$$0 = U_b - U_a = -\int_{s_a}^{s_b} \mathbf{f} \cdot d\mathbf{s} \tag{5.6}$$

which is saying that Eq. 5.5 holds for systems with equal potential energy at the limits of the line integral. A typical example of such situation can be seen in Fig. 5.2.

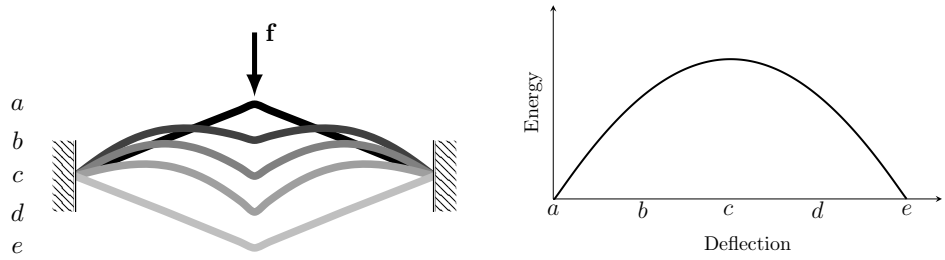

(a) (b)

Figure 5.2: When the truss is deflected from point a to e, the force along the deflection is not zero but clearly there is no change in the potential energy between points a and e. (a) Bistable truss structure. (b) Energy function of the bistable structure while it moves from point a to e.

To integrate Eq. 5.4 we need to ensure that each $(\mathbf{f} \cdot \mathbf{ds})$ along the line integral is in fact zero, and also we need to guarantee that the system is moving along the trajectory.

$$0 = -\int_s |\mathbf{f} \cdot d\mathbf{s}| \quad \text{where} \quad \int_s d\mathbf{s} > 0 \tag{5.7}$$

Equation 5.7 is a necessary and sufficient condition to guarantee motion without change in the potential energy. Notice that the dot product in Eq. 5.7 indicates that only the force components tangent to the trajectory are the ones that contribute to the change in potential energy. If the trajectory s is a function $\mathbf{r}$ of the DOF's q_i that define the trajectory

$$s = \mathbf{r}\left(\mathbf{q}\right) \quad \text{and} \quad ds = \frac{\partial \mathbf{r}}{\partial q_i} dq_i \tag{5.8}$$

and by only taken the force components f_i tangent to the trajectory, equation 5.7, dropping the minus sign, can be written as

$$0 = \int_s \left| f_i \frac{\partial \mathbf{r}}{\partial q_i} dq_i \right| \quad \text{where} \quad \int_s \frac{\partial \mathbf{r}}{\partial q_i} dq_i > 0 \tag{5.9}$$

Equation 5.9 is expressing that the force components f_i tangent to the trajectory are zero,

$$0 = f_i = -\frac{\partial U}{\partial q_i} \tag{5.10}$$

The latter implies that for a statically balanced system in a given range of motion, all the derivatives of the potential energy with respect to the DOF's defining this motion must be zero.

Definition 5.2. *A mechanical system with no tangential forces along a trajectory is a statically balanced system along such trajectory.*

Statically balanced systems are in a continuous state of static equilibrium along a trajectory, rather than in punctual configurations. Continuous equilibrium is a necessary and sufficient condition to guarantee a state of static balancing.
Equation 5.9 shows that in statically balanced systems, the tangential forces to the motion must be zero, but this does not imply that all the forces are zero. In fact equation 5.3 states that normal forces to the trajectory are not necessarily zero. Therefore, if the prestressing of the structure (according to proposition 5.1) is achieved using preloading forces, then, two conclusions arise: Preloading forces must be normal to the motion of their application points (if they move) or preloading forces have any orientation but their application points do not move.

Proposition 5.2. *In deformable structures undergoing motion in a statically balanced state, either the points where prestressing forces are applied do not move or move normal to their respective presstresing forces.*

5.2.3 Virtual work

The principle of virtual work states that a conservative system is in static equilibrium, if the virtual work in such configuration is zero.

$$0 = \mathbf{f} \cdot \delta\mathbf{s} \tag{5.11}$$

Observe that Eq. 5.11 is the same Eq. 5.4, in terms of virtual displacements rather than infinitesimal displacements. Then, by replacing the infinitesimal displacements on Eq. 5.7 for virtual displacements we obtain

$$0 = \int_s |\mathbf{f} \cdot \delta\mathbf{s}| \tag{5.12}$$

This equation in fact states that the virtual work of a statically balanced system evaluated at any point of the trajectory must be zero.

Definition 5.3. *A mechanical system in which the virtual work of the system is always zero, regardless the value of the DOF's q_i defining the motion, is said to be in a state of static balance along such of motion.*

Although Eq. 5.12 is similar to Eq. 5.7, they imply different things from a design perspective. For instance, Eq. 5.7 is telling us that the conditions for a statically balanced behavior can be found by obtaining the force expression of the system under design and then searching for the conditions for which forces are zero along some range of motion, but Eq. 5.12 is telling us that the same can be accomplished by obtaining the virtual work expression and then searching for the condition where the DOF's variables vanish.

5.2.4 Stability

To define stability in a simple way to our purpose, let's imagine a mechanical system that remains in a state of static equilibrium for a given configuration, and apply a small disturbance to the system. If the system after the disturbance returns to its original equilibrium configuration, it is said that the equilibrium configuration is stable and it implies the presence of a restoring force. But if the systems moves away, then the equilibrium configuration is referred as unstable, in which case the force points away from the equilibrium configuration. Now, there is a third possibility. If the disturbance takes the system into a new equilibrium configuration next to the previous one then the original equilibrium configurations is defined as neutrally stable and clearly there is no change in the force.
Now, definition 5.2 states that tangential forces along a statically balanced trajectory are zero and consequently there are no changes in these forces, then is clear that statically balanced trajectories are neutrally stable.

Definition 5.4. *A mechanical system with neutral stability for all the points in a range of motion is a statically balanced system along such of range of motion.*

For systems where the potential energy comes from elastic deformations, the differentiation of the force with respect to a set of DOF's (or second derivative of the potential energy), represents the stiffness of the system, therefore is the stiffness function who provides the information about the stability behavior of an elastic structure.

Here the second differentiation is performed on the external force and not in the system's internal force (Eq. 5.10). In this way we assumed the existence of an equilibrating external force that could or could not be zero, covering in this way both possibilities, balancing due to external forces or self-balancing of the internal forces.

$$\frac{\partial^2 U}{\partial q_j \partial q_i} = \frac{\partial \mathbf{f}}{\partial \mathbf{q}} = \mathbf{K} \tag{5.13}$$

The stability of a system at a given equilibrium point can be evaluated by analyzing the changes in the external force due to changes in a given parameter, which in our case would be the changes in the DOF's defining a trajectory.

$$\Delta \mathbf{f} = \frac{\partial \mathbf{f}}{\partial \mathbf{q}} \Delta \mathbf{q} \tag{5.14}$$

Replacing Eq. 5.13 into Eq. 5.14 it is obtained an equation that resembles the equilibrium equation for a finite element analysis, where $\Delta \mathbf{f}$ is the external force balancing the internal reactions.

$$\Delta \mathbf{f} = \mathbf{K} \Delta \mathbf{q} \tag{5.15}$$

To analyze the stability properties of the stiffness matrix, we multiply Eq. 5.15 by $\frac{1}{2}\Delta \mathbf{q}^T$

$$\tfrac{1}{2}\Delta \mathbf{q}^T \Delta \mathbf{f} = \tfrac{1}{2}\left(\Delta \mathbf{q}^{\mathbf{T}} \mathbf{K} \boldsymbol{\Delta} \mathbf{q}\right) \tag{5.16}$$

Notice that the left hand term is the work done by the change in the external force acting from equilibrium and that the right hand term on parenthesis is the expression to define the definiteness of the stiffness matrix. If $\mathbf{K}$ is positive definite, the entire term on the right must always be positive no matter the motion around the equilibrium point, which implies that the external force is doing a positive work. This means that the internal force oppose to the displacement, so it is a restoring force and therefore the system is stable. On the other hand, if $\mathbf{K}$ is negative definite, the term on the left side by definition is always negative, so the external force is doing negative work which means that the internal force push away the system from the equilibrium point, therefore the system is unstable.

Now, let's return to Eq. 5.15 and rewrite it assuming that there is no change in force (this is for statically balanced systems and constant force systems).

$$\mathbf{K}\Delta\mathbf{q} = \mathbf{0} \tag{5.17}$$

This equation has two solutions, (i) the trivial solution $\Delta\mathbf{q} = \mathbf{0}$ in which we are not interested, because it is expressing that no motion is occurring, and (ii) $\Delta\mathbf{q} \neq \mathbf{0}$ in which we assume motion. This solution requires $\mathbf{K}$ to be singular with a null space composed not only by vector $\mathbf{0}$. If Eq. 5.17 is multiplied by $\Delta\mathbf{q}^T$, then it is obtained an equation that express that matrix $\mathbf{K}$ is semi-definite or semi-indefinite matrix.

$$\Delta\mathbf{q}^T\mathbf{K}\Delta\mathbf{q} = \mathbf{0} \tag{5.18}$$

Still it can not be said anything about statically balanced systems. In order to resolve this, let's express the left hand term of Eq. 5.16 as the work w done by the change in the external force

$$w = \tfrac{1}{2}\Delta\mathbf{q}^T\Delta\mathbf{f} \tag{5.19}$$

and then eigen-decompose the stiffness matrix (notice that w is not the work done by the external force but by its change).

$$w = \tfrac{1}{2}\left(\Delta\mathbf{q}^\mathbf{T}\mathbf{Q}\mathbf{\Lambda}\mathbf{Q}^\mathbf{T}\Delta\mathbf{q}\right) \tag{5.20}$$

Here Λ is the diagonal matrix of n eigenvalues and $\mathbf{Q}$ is the matrix of n linear independent eigenvectors. Notice that the product $\mathbf{Q}^\mathbf{T}\Delta\mathbf{q}$ represents a rotation of the displacement vector into a new displacement vector $\Delta\tilde{\mathbf{q}}$ expressed in the vector space spanned by the eigenvectors.

$$\mathbf{Q}^\mathbf{T}\Delta\mathbf{q} = \Delta\tilde{\mathbf{q}}$$

Then, by rewriting Eq. 5.20 it is possible to observe that the eigenvalues determine the local curvature of the energy function due to the changes in the force.

$$w = \tfrac{1}{2}\left(\Delta\tilde{\mathbf{q}}^\mathbf{T}\mathbf{\Lambda}\Delta\tilde{\mathbf{q}}\right) = \tfrac{1}{2}\lambda_i\Delta\tilde{q}_i^2 \tag{5.21}$$

This equation expresses that motion in the direction of zero curvature $\lambda_i = 0$ (zero eigenvalue) conveys no change in energy w and from Eq. 5.19, w is zero only if the change in force is zero ($\Delta\mathbf{f} = 0$). In other words, zero eigenvalues means zero change in force.
To illustrate the idea of eigenvalues as the curvature on the work function due to changes in force, assume that the stiffness matrix is of size 2x2, then Eq. 5.21 takes the form

$$w = \tfrac{1}{2}\lambda_1\Delta\tilde{q}_1^2 + \tfrac{1}{2}\lambda_2\Delta\tilde{q}_2^2$$

If this function is plotted, there is the possibility for the eigenvalues to be positive, negative or

Table 5.1: Relation between eigenvalues, energy function's curvature and stability

$\lambda 1$	$\lambda 2$	Energy function shape	Stability in $\lambda 1$ direction	Stability in $\lambda 2$ direction	Definiteness of the stiffness matrix
positive	positive	paraboloid open upwards	stable	stable	positive definite
negative	negative	paraboloid open downwards	unstable	unstable	negative definite
positive	negative	hyperbolic paraboloid	unstable	stable	indefinite
zero	positive	parabolic cylinder open upwards	neutrally stable	stable	positive semi-definite
zero	negative	parabolic cylinder open downwards	neutrally stable	unstable	negative semi-definite

zero. All the possible results are listed in Tab. 5.1 and depicted in Fig. 5.3.

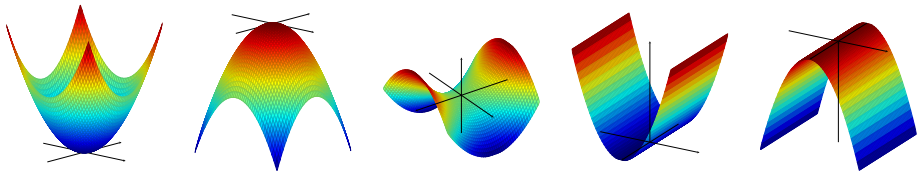

Figure 5.3: Local curvature of the energy function is given by the eigenvalues of the stiffness matrix. x and y axes point in the direction of the eigenvectors. (a) Positive eigenvalues. (b) Negative eigenvalues. (c) Positive and negative eigenvalues. (d) Positive and zero eigenvalues. (e) Negative and zero eigenvalues.

The analysis of the eigenvalues provides another perspective for the observance of stability with respect to the behavior of the energy function due to changes in force. Clearly, motion in the direction of the eigenvector with positive eigenvalues is stable, motion in the direction of the eigenvectors with negative eigenvalues is unstable and motion in the direction of the eigenvectors with zero eigenvalues is neutrally stable.

For a statically balanced system that is discretized and described in terms of its stiffness matrix, is clear that this matrix must be (i) singular and (ii) semi-definite or semi-indefinite for which its null space elements besides the $\mathbf{0}$ vector, describe the statically balanced trajectory of the system. The difference between the positive and negative semi-definiteness and semi-indefiniteness, is that systems with positive semi-definite stiffness matrices are self-constrained to move only along the statically balance trajectory, while negative semi-definite stiffness matrices or semi-indefinite must be constrained in order to avoid motion on the unstable directions.

Proposition 5.3. *A mechanical system moving along a trajectory in a state of self-constraint static balancing, must exhibit at all points a singular positive semi-definite $n \times n$ stiffness matrix*

with n linear independent eigenvectors. The system's change in configuration at each point of the trajectory is defined by the eigenvectors that form the stiffness matrix's null space.

At this point it is necessary to remark that the linear independence of the eigenvectors is conventionally assumed if all eigenvalues are different, but it does not mean that for repeated eigenvalues, necessarily the eigenvectors are not linear independent. In this work it is assume the latter possibility, which means that linear independence of all the eigenvectors must be guaranteed in another way.
To illustrate the former in our context, take for example the case of a system for which the statically balanced motion is a surface rather than a line. In this case the 2-D surface is generated by two independent eigenvectors from the $\mathbf{K}$ matrix, with respective zero eigenvalues.
Now returning to the stability analysis of the stiffness matrix, let's diagonalize the stiffness matrix $\mathbf{K}$ in the form

$$\mathbf{\Lambda} = \mathbf{Q}^T \mathbf{K} \mathbf{Q} \tag{5.22}$$

what we see in this equation, is that matrix $\mathbf{\Lambda}$ is a diagonal matrix for which its values are the eigenvalues of matrix $\mathbf{K}$, but these diagonal values also represent the stiffness values of the system in the space spanned by the eigenvectors. In other words, this is expressing the expected result: the system will exhibit zero stiffness in the direction of neutral stability behavior or zero eigenvalues.

Definition 5.5. *A mechanical system that is a statically balanced for all the points in a range of motion, exhibits zero stiffness along such of range of motion*

An interesting result from proposition 5.3 and definition 5.5, is that if the mechanical system is an elastic system, then the linear independent eigenvectors associated with zero eigenvalues from a singular positive-semidefinite stiffness matrix, (i) span the null space of the matrix that defines the statically balanced motion space and (ii) they are in fact the buckling modes of the elastic system.

Proposition 5.4. *An elastic mechanical system that is statically balanced for all the points in a range of motion is in fact a self-buckled elastic system at exactly the critical buckling load along the range of motion.*

At this point it is important to address an important issue in the definitions regarding zero stiffness and neutral stability as conditions in static balancing. The difference between both definitions is subtle but quite meaningful. Zero stiffness is a necessary but not sufficient condition to guarantee a state of static balancing, since zero stiffness is also a necessary condition for systems with constant force. Zero stiffness does not imply that a system is in equilibrium. On the other hand neutral stability is a necessary and sufficient condition to guarantee a state of static balancing. Neutral stability imply zero stiffness and equilibrium, which is a condition expressed in def. 5.2.

Since constant force systems exhibit zero stiffness, they can be used in the modular design of statically balanced systems. The constant force of one system is compensated by the opposite constant force from another system. An example of this is the spring-to-spring balancer shown in chapter 4, where in section 4.4 is shown that in fact this balancer is a composition of two constant force mechanisms balancing each other. The use of constant force systems as a strategy for the design of statically balanced compliant mechanisms is shown in sections 6.2.3 and 6.2.3.

In the case of statically balanced systems as compositions of constant force systems, it is possible to find a generalized coordinated where the two sources of potential energy exhibit linear behavior. The observation of this energy linearization, specifically in balancers built with zero-free-length springs, in combination with proposition 5.4 has led to the following proposition:

Proposition 5.5. *A 1DOF statically balanced systems where it is possible to find a generalized coordinate in which the constant potential energy can be seen as the superposition of two opposed linear potential energy functions, is a system where the self-buckling critical load is constant along the entire range of motion.*

This proposition relates to the idea of using buckling as a design strategy for statically balanced compliant mechanisms.

5.2.5 The equation of motion

To this point, the characteristics for statically balanced mechanisms related to energy, force and stability have been address. Now, it would be interesting to observe the behavior of these systems from the perspective of their equation of motion.

In order to do so, the system's motion function $\mathbf{q}(t)$ is linearized by assuming small disturbances in the vicinity of point $\mathbf{q_0}$, and expanded in Taylor series

$$\mathbf{q}(t) = \mathbf{q}_0 + \frac{d\mathbf{q}}{dt}\Delta t \tag{5.23}$$

$$= \mathbf{q}_0 + \Delta\mathbf{q}(t) \tag{5.24}$$

Here the time dependent term $\Delta\mathbf{q}(\mathbf{t})$ is the solution of the linear equation of motion

$$\mathbf{M}\Delta\ddot{\mathbf{q}}(t) + \mathbf{K}\Delta\mathbf{q}(t) = \mathbf{0} \tag{5.25}$$

where $\mathbf{M}$ and $\mathbf{K}$ are the mass and stiffness matrices respectively. For this second order homogeneous equation, it is assumed a solution of the form

$$\Delta\mathbf{q}\,(t) = \Delta\mathbf{q}_0 e^{\omega t} \tag{5.26}$$

$$\Delta\dot{\mathbf{q}}\,(t) = \omega\Delta\mathbf{q}_0 e^{\omega t} \tag{5.27}$$

$$\Delta\ddot{\mathbf{q}}\,(t) = \omega^2\Delta\mathbf{q}_0 e^{\omega t} \tag{5.28}$$

By replacing this solution into Eq. 5.25, it is obtained the following expression

$$\left(\omega^2\mathbf{M} + \mathbf{K}\right)\Delta\mathbf{q}_0 e^{\omega t} = \mathbf{0}$$

in which the exponential term is never zero. If the trivial solution $\Delta\mathbf{q_0} = \mathbf{0}$ is not considered, then we end with a generalized eigenvalue problem of the form

$$\left(\omega^2\mathbf{M} + \mathbf{K}\right)\Delta\mathbf{q}_0 = \mathbf{0} \tag{5.29}$$

This generalized problem can be transformed into a standard eigenvalue problem, assuming that both matrices are constant at point $\mathbf{q_0}$, and matrix $\mathbf{M}$ is symmetric positive definite. Then, it is possible to factorize matrix $\mathbf{M}$ using Cholesky decomposition [47],

$$\mathbf{M} = \mathbf{L}\mathbf{L}^T$$

where $\mathbf{L}$ is a lower triangular matrix. Now, by premultiplying Eq. 5.29 by $\mathbf{L^{-1}}$ and applying a transformation on vector $\Delta\mathbf{q}_0$ of the form

$$\Delta\mathbf{q_0} = \left(\mathbf{L^T}\right)^{-\mathbf{1}}\tilde{\mathbf{u}} \tag{5.30}$$

it is obtained a standard eigenvalue problem, which is simpler to solve and from which it is possible to obtain some useful insights

$$\begin{aligned}
\mathbf{L^{-1}}\left(\omega^{\mathbf{2}}\mathbf{M} + \mathbf{K}\right)\left(\mathbf{L^T}\right)^{-\mathbf{1}}\tilde{\mathbf{u}} &= \mathbf{0} \\
\left(\omega^2\mathbf{L^{-1}}\mathbf{M}\left(\mathbf{L^T}\right)^{-\mathbf{1}} + \mathbf{L^{-1}}\mathbf{K}\left(\mathbf{L^T}\right)^{-\mathbf{1}}\right)\tilde{\mathbf{u}} &= \mathbf{0} \\
\left(\left(-\tilde{\mathbf{K}}\right) - \tilde{\lambda}\mathbf{I}\right)\tilde{\mathbf{u}} &= \mathbf{0}
\end{aligned}$$

In this equation, the mass normalized stiffness matrix $\tilde{\mathbf{K}}$ is

$$\tilde{\mathbf{K}} = \mathbf{L}^{-1}\mathbf{K}\left(\mathbf{L}^T\right)^{-1} \tag{5.31}$$

and the system's natural frequencies ω_i are given by the square root of the eigenvalues $\tilde{\lambda}_i$ of matrix $\tilde{\mathbf{K}}$.

$$\omega_i^2 = \tilde{\lambda}_i$$

The system's vibration modes $\Delta\mathbf{q_0}$ around point $\mathbf{q_0}$ correspond to the transformation of the eigenvectors $\tilde{\mathbf{u}}$ through Eq. 5.30.
If the stiffness matrix $\mathbf{K}$ is singular as defined in Eq. 5.17, then matrix $\tilde{\mathbf{K}}$ is also singular. This is proven by realizing that, as previously mention, matrix $\mathbf{M}$ is assumed symmetric positive definite. Then it is possible to take any vector $\Delta\mathbf{q}$ in the null space of $\mathbf{K}$ expressed as a linear combination of the eigenvectors $\mathbf{u_{0_i}}$ with zero eigenvalues that span this null space

$$\Delta\mathbf{q} = a_i\mathbf{u_{0_i}} \tag{5.32}$$

and apply a transformation of this vector by matrix $\mathbf{L^T}$ (same transformation used in Eq. 5.30),

$$\Delta\tilde{\mathbf{q}} = \mathbf{L^T}\Delta\mathbf{q} \tag{5.33}$$
$$= \mathbf{L^T}\left(a_i\mathbf{u_{0_i}}\right) \tag{5.34}$$

if Eq. 5.31 is multiplied by vector $\Delta\tilde{\mathbf{q}}$, then it yields

$$\begin{aligned}\tilde{\mathbf{K}}\Delta\tilde{\mathbf{q}} &= \mathbf{L^{-1}K}\left(\mathbf{L^T}\right)^{-1}\Delta\tilde{\mathbf{q}}\\ &= \mathbf{L^{-1}K}\left(\mathbf{L^T}\right)^{-1}\mathbf{L^T}\Delta\mathbf{q}\\ &= \mathbf{L^{-1}K}\Delta\mathbf{q}\\ &= \mathbf{0}\end{aligned}$$

Clearly, vector $\Delta\tilde{\mathbf{q}}$ is in the null space of $\tilde{\mathbf{K}}$ and $\Delta\tilde{\mathbf{q}} \neq \mathbf{0}$, since $\mathbf{L^T}$ is not singular (see Eq. 5.33). Even more, the size of the null space of $\tilde{\mathbf{K}}$ is equal to the size of the null space of $\mathbf{K}$, which can be evidenced by multiplying Eq. 5.31 by Eq. 5.34, rather than Eq. 5.33.
All these considerations imply that the system's motion described by matrix $\tilde{\mathbf{K}}$ has as many zero natural frequencies as matrix $\mathbf{K}$ has zero eigenvalues, which allows to define statically balance mechanisms from the perspective of their natural frequencies.

Definition 5.6. *A mechanical system exhibiting zero natural frequency at all the points in a range of motion is a statically balanced system along such range of motion.*

Definition 5.6 is just expressing the expected result for a system with zero stiffness, An even more if the natural frequency on a statically balanced system is zero, then by replacing $\omega = 0$ into Eq. 5.27 it is found that the change in speed of the system is zero.

Definition 5.7. *A mechanical system moving along a statically balanced trajectory, exhibits constant speed along such trajectory in the absence of external forces.*

Once again, definition 5.7 is the expected result from a system where all the forces are in equilibrium along a trajectory.
Now notice that vector $\Delta\tilde{\mathbf{q}}$ is a linear combination of the eigenvectors $\tilde{\mathbf{u}}_{\mathbf{0}}$ with zero eigenvalues

$$\Delta\tilde{\mathbf{q}} = b_i\tilde{\mathbf{u}}_{\mathbf{0_i}} \tag{5.35}$$

if Eq. 5.35 is replaced into Eq. 5.34 it is possible to obtain the relation between the null spaces of $\tilde{\mathbf{K}}$ and $\mathbf{K}$ respectively.

$$b_i\tilde{\mathbf{u}}_{\mathbf{0_i}} = \mathbf{L^T}\left(a_i\mathbf{u}_{\mathbf{0_i}}\right) \tag{5.36}$$

If we try to recover the system's vibration mode related with zero frequency by applying the transformation in Eq. 5.30 to Eq. 5.36

$$b_i\mathbf{L^T}\Delta\mathbf{q_0} = a_i\mathbf{L^T}\mathbf{u}_{\mathbf{0_i}} \tag{5.37}$$

and noting that coefficients a_i and b_i are just random scaling values for the eigenvectors, we see that the vibration modes with zero frequency are the same eigenvectors of matrix $\mathbf{K}$ with zero eigenvalues.

$$\Delta\mathbf{q_0} = \mathbf{u}_{\mathbf{0_i}} \tag{5.38}$$

These results at first seems not to be relevant but as it will be shown later, the eigenvectors with zero eigenvalues from matrix $\mathbf{K}$ are the linearized buckling modes of the mechanism.

Proposition 5.6. *Vibration modes related with zero frequencies on statically balanced mechanisms are equal to the stiffness matrix's eigenvectors with zero eigenvalues.*

5.3 Theory generalization

In the preceding section some features from statically balanced mechanisms were identified from the energy, force, stability and motion perspectives, which allowed the derivation of some definitions which later will serve to set the design criteria.
The configurations of these statically balanced mechanisms were described in terms of a set of q_i variables that represent not only the kinematic degrees of freedom, but also geometric and mechanical variables defining the system. In this section a mathematical generalization of the static balancing problem is developed. The system defined in terms of the q_i variables is re-expressed in terms of a set of t_i variables defining its workspace as a statically balanced system.

In order to make things easier, a generalization for systems on which their statically balanced workspace is represented by curves is developed. Once concepts are more clear and understandable, a more complete generalization including complex workspaces is presented.

5.3.1 Workspace as a curve

Think on a system in which its potential energy is a function of its deformed configuration and this configuration is determined by a set of variables $\mathbf{q}$. It is desired to know the potential energy function, force and stiffness of this system when it is moving along a curve, which is a function of a parameter t. But by curve, we do not necessarily refer to a curve in the three dimensional space. It could be a curve or linear trajectory in the vector space of the $\mathbf{q}$ variables. For instance, the $\mathbf{q}$ variables could represent the nodal degrees of freedom (DOF's) on a structure in which case the trajectory is the set of all the values taken by the DOF's defining the motion of the structure while the parameter t, could be a displacement condition at a given node.
Recalling from the previous sections, the potential energy in terms of the $\mathbf{q}$ variables is

$$U\left(\mathbf{q}\right) \tag{5.39}$$

the external force is the gradient of the potential energy with respect to this set of variables $\mathbf{q}$

$$\mathbf{f}\left(\mathbf{q}\right) = \frac{\partial U}{\partial q_i} \tag{5.40}$$

And the stiffness of the system is then the Hessian of the potential energy

$$\mathbf{K}\left(\mathbf{q}\right) = \frac{\partial^2 U}{\partial q_j \partial q_i} \tag{5.41}$$

Now, consider a statically balanced mechanism in motion describing a curve in some vectorial space and let vector $\mathbf{q}$ to represent the configuration of the mechanism at any given point during motion in this vectorial space. If the motion is function of the parameter t, and assuming that it is possible to express each variable q_i in terms of the parameter t

$$q_i = f_i\left(t\right) \tag{5.42}$$

then it is possible to describe the motion of the system by the parametric function $\mathbf{r}\left(t\right)$.

$$\mathbf{r}\left(t\right) = q_i\left(t\right)\hat{\mathbf{e}}_i \tag{5.43}$$

Here, vector $\mathbf{r}\left(t\right)$ is a parametric curve in the space $\hat{\mathbf{e}}_i$ of the q_i variables describing the motion of the system. Calculating the derivative of this trajectory with respect to the parameter t we obtain,

$$\mathbf{r}'(t) = \frac{dq_i}{dt} = \mathbf{J} \tag{5.44}$$

remember that the function $\mathbf{r}'(t)$ is a tangent vector to the parametric curve $\mathbf{r}(t)$, and notice that this derivative is also the Jacobian $\mathbf{J}$ of the systems of equations given in Eq. 5.42.

Now let's say the potential energy of the system can be also expressed in terms of the parameter t and knowing that for statically balanced systems this should be a constant (see def. 5.1) we got

$$U(t) = constant$$

If the external force of the system is calculated in terms of the parameter t, we have

$$\mathbf{f}(t) = 0 = \frac{\partial U}{\partial q_i}\frac{dq_i}{dt} = \mathbf{f}(q_i) \cdot \mathbf{r}'(t) \tag{5.45}$$

Notice that we have found a similar result to the one shown in sec 5.2.2, where it was stated that for statically balanced systems, the forces along the trajectory must by zero.

Now, calculating the stiffness of the system in terms of parameter t yields

$$\begin{aligned} k(t) = 0 &= \frac{d}{dt}\left(\frac{\partial U}{\partial q_i}\frac{dq_i}{dt}\right) \\ &= \frac{d}{dt}\left(\frac{\partial U}{\partial q_i}\right)\frac{dq_i}{dt} + \frac{\partial U}{\partial q_i}\frac{d^2 q_i}{dt^2} \\ &= \left(\frac{\partial^2 U}{\partial q_j \partial q_i}\frac{dq_j}{dt}\right)\frac{dq_i}{dt} + \frac{\partial U}{\partial q_i}\frac{d^2 q_i}{dt^2} \end{aligned}$$

or in matrix notation

$$k(t) = 0 = \mathbf{r}'^T(t)\,\mathbf{K}(q_i)\,\mathbf{r}'(t) + \mathbf{f}(q_i) \cdot \mathbf{r}''(t) \tag{5.46}$$

$$= \mathbf{J}^T \mathbf{K}(q_i)\,\mathbf{J} + \mathbf{f}(q_i)\frac{d\mathbf{J}}{dt} \tag{5.47}$$

In a general form, equation 5.46 allows to observe the stiffness behavior of a system on a given trajectory or workspace. But when the expression is equated to zero it becomes an interesting equation relating the stiffness and force properties of a system with a given trajectory in which the system has zero stiffness and constant potential. In other words, the equation relates the system's stiffness and force properties to the level sets of its potential energy function.

A detail look at Eq.5.46 shows several ways on how stiffness on a trajectory can vanish. Each way provides, from a synthesis perspective, with an insight on how a system can be statically balanced or, from an analysis perspective, with the differences in the characteristics of the level

sets.
Before going further, it is necessary to understand Eq.5.46. Clearly, it is composed of two terms, where their physical meaning can be interpreted as follows:

- The first term is the projection of the stiffness at the given point on the trajectory, indicating the change in the force on the tangential direction expressed by $\mathbf{r}'$.
- The second term is the change of the force $\mathbf{f}(q_i)$ due to the change in the trajectory direction expressed by $\mathbf{r}''$.

Equation.5.46 indicates that to express the stiffness of a system on a new set of variables describing the workspace, we need to not only transform the stiffness in term of the new set variables (first term in the equation) but also we need to take into account the variations of the new set of variables with respect to the old set of variables (second term in the equation)
Now it is possible to analyze the different ways on how stiffness on a trajectory can vanish.

Compensation by trajectory changes

Equation 5.46 is equal to zero when both terms in the equation are equal, with opposite signs and different from zero.

$$\mathbf{r}'^{T}\mathbf{K}\mathbf{r}' = -\mathbf{f}\cdot\mathbf{r}'' \tag{5.48}$$

It means that the change in force, along the tangent direction $\mathbf{r}'$ due to stiffness $\mathbf{K}$, is compensated by changes in the force $\mathbf{f}$ due to changes in the trajectory direction $\mathbf{r}''$.
The use of this approach to design a statically balanced mechanism means that the mechanism must be constrained somehow to follow the trajectory which corresponds to an equipotential line in the potential energy function.
To understand this idea, remember that in section 5.2.2 it was said that a statically balanced system is in equilibrium at any point of the trajectory and notice that the stiffness matrix in this case is not semi-definite, (terms in Eq. 5.48 are different from zero) which implies that if the mechanism is in equilibrium at a given point, this equilibrium will be either stable and/or unstable but not neutrally stable, or in other words the system at the given equilibrium point in a naturally way either will not move or it will move away from the equilibrium point. Therefore it must be constrained or forced to follow the equipotential trajectory in order to be in a neutrally stable state. We can call this approach as a form of forced static balancing.
See for example the system depicted in Fig. 5.4a in its unstressed configuration. This system has two stable equilibrium configurations at p_1 and p_3 and one unstable equilibrium configuration at p_2. Now assume that the system is taken into a new equilibrium point p_4 by a force $\mathbf{f}$ (Fig. 5.4b). Here the whole system (springs plus force $\mathbf{f}$) at p_4 exhibits and indefinite stiffness matrix and

by simple observation it can be realized that the system is stable in the x-direction and unstable in the y-direction. But if the force is removed and replaced by the contact force resulting of constraining the system to follow the level set at p_4 as shown in Fig. 5.4c, then the whole system behaves as neutrally stable.

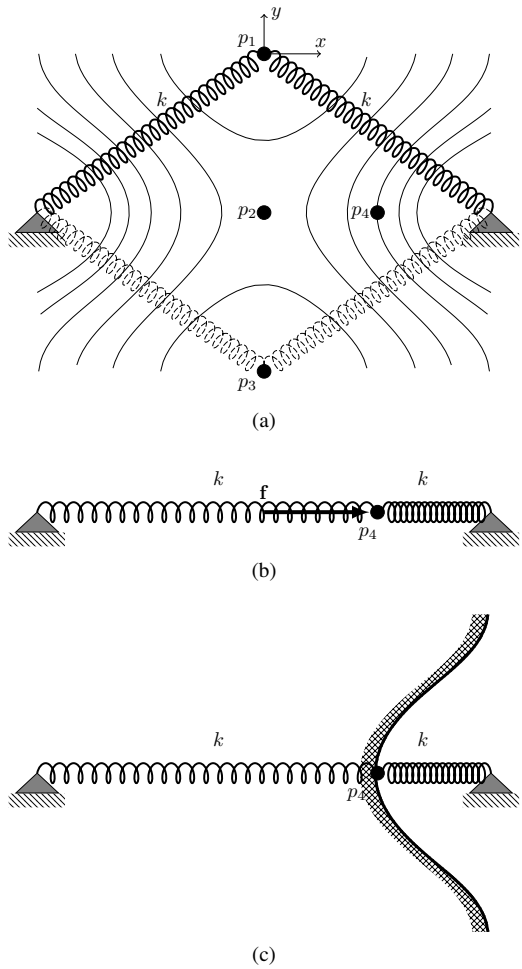

Figure 5.4: (a) Two springs snapping-through with their level sets, (b) the system is stable in x-direction and unstable in y-direction for the equilibrium configuration at p_4, (c) The system has been constrained to follow an equipotential line in which it behaves neutrally stable.

Another way to see this concept is to assume for a moment that the vector $\mathbf{r}'$ has a constant magnitude, then dividing Eq. 5.48 by $|\mathbf{r}'|^2$ allows to re-express this equation as

$$\hat{\mathbf{t}}^T \mathbf{K} \hat{\mathbf{t}} = -\frac{\kappa}{|\mathbf{r}'|} \mathbf{f} \cdot \hat{\mathbf{n}} \tag{5.49}$$

where $\hat{\mathbf{t}}$ and $\hat{\mathbf{n}}$ are the unitary tangent vector and unitary normal vector to the trajectory $\mathbf{r}$, respectively, and κ its curvature. Now the term on the left is expressing the work done by the change in force along a unitary displacement in the tangent direction (Fig. 5.5a). We know that a statically balanced system can not do work, then this work is compensated by the work done by the actual force along a displacement in the normal direction and magnitude $\frac{\kappa}{|\mathbf{r}'|}$ (Fig. 5.5b).

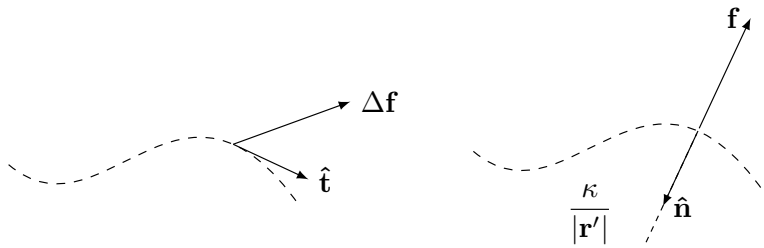

Figure 5.5: (a) Positive work done by the change in force $\Delta\mathbf{f}$ along the tangent direction, (b) Negative work done by the actual force $\mathbf{f}$ in the normal direction.

Singularity and zero force

Another way in which Eq. 5.46 is equal to zero is when both terms in the equation are zero. For both terms, this can occur in different ways.

$$\mathbf{r}'^{T}\mathbf{K}\mathbf{r}' = \mathbf{f} \cdot \mathbf{r}'' = 0 \tag{5.50}$$

For instance, the right term can be zero in three situations, (i) the force $\mathbf{f}$ is normal to vector $\mathbf{r}''$, (ii) the vector $\mathbf{r}''$ is equal to zero or, (iii) the force $\mathbf{f}$ is equal to zero. The left term, can be zero as well in three situations, (i) vector $\mathbf{r}'$ is equal to zero, (ii) matrix $\mathbf{K}$ transforms vector $\mathbf{r}'$ into an orthogonal vector with respect to itself, or (iii) vector $\mathbf{r}'$ is in the null space of $\mathbf{K}$.

This preceding gives another nine different ways in which a system can be statically balanced, but some of these are impractical like $\mathbf{r}' = 0$, because it means that the system is not moving or that the trajectory is not a function of the t parameter, while some others imply that the system, like in section 5.3.1, must be constrained to follow a level set, e.g., $\mathbf{r}'' = 0$ which means that the system moves in a straight trajectory.

But when the force $\mathbf{f}$ is zero, this is interesting, because it means that the system could not require any motion constraining, if it is a stable system.

There are three interpretations for $\mathbf{f} = 0$, (i) the system is moving in a potential energy function that is constant in all direction of the vector space of variables q_i, (ii) the system is already constrained to follow an equipotential line as explained in section 5.3.1, or (iii) the system is at a

stationary point of the potential energy function in all the orthogonal directions to the trajectory. The first interpretation is saying that the statically balanced trajectory is in fact a subspace of higher dimensional statically balanced workspace, which from a synthesis view it is not providing any insights. The second interpretation as well does not provide with new insights besides those given in section 5.3.1. Now the third interpretation is important, because combined with situation (iii) in which the left term in Eq. 5.50 can be zero, saying that matrix $\mathbf{K}$ is singular and $\mathbf{r}'$ is in its null space. It takes back to the results about stability presented in section 5.2.4, where it was shown that matrix $\mathbf{K}$ ideally should be a positive semi-definite matrix.
Notice that in this case vector $\mathbf{r}'$ is related with $\Delta\mathbf{q}$ by

$$\Delta\mathbf{q} = \Delta\mathbf{r} = \mathbf{r}'\Delta t \tag{5.51}$$

5.3.2 Multidimensional workspace

In the previous section it was presented the workspace of the statically balanced system as a parametric curve in t. Here, the same concepts are extended to workspaces as parametric functions of more than one parameter, and basically the same conclusions are drawn.
Consider again the potential energy function, the force and the stiffness as functions of the $\mathbf{q}$ variables

$$U(\mathbf{q}) \tag{5.39}$$

$$\mathbf{f}(\mathbf{q}) = \frac{\partial U}{\partial q_i} \tag{5.40}$$

$$\mathbf{K}(\mathbf{q}) = \frac{\partial^2 U}{\partial q_j \partial q_i} \tag{5.41}$$

If the set of $\mathbf{q}$ variables can be expressed as functions of the parameters $\mathbf{t}$, then we will have a system of equations in the form

$$q_i = f_i(\mathbf{t}) \tag{5.52}$$

and the workspace $\mathbf{r}$ in terms of the $\mathbf{t}$ parameters expressed as

$$\mathbf{r}(\mathbf{t}) = q_i(\mathbf{t})\,\hat{\mathbf{e}}_i \tag{5.53}$$

Clearly, the Jacobian of the system of equations is

$$J_{ik} = \frac{\partial q_i}{\partial t_k} \tag{5.54}$$

Now, assuming that the potential energy function of a statically balanced system in its workspace is constant

$$U(\mathbf{t}) = constant \tag{5.55}$$

Then, the force in the workspace as a function of the parameters $\mathbf{t}$ is

$$\mathbf{f}(\mathbf{t}) = 0 = \frac{\partial U}{\partial t_k} = \frac{\partial U}{\partial q_i}\frac{\partial q_i}{\partial t_k} = \mathbf{f}(q_i)^T \mathbf{J} \tag{5.56}$$

and the stiffness

$$\begin{aligned}\mathbf{K}(\mathbf{t}) = 0 &= \frac{\partial}{\partial t_l}\left(\frac{\partial U}{\partial q_i}\frac{\partial q_i}{\partial t_k}\right) \\ &= \frac{\partial}{\partial t_l}\left(\frac{\partial U}{\partial q_i}\right)\frac{\partial q_i}{\partial t_k} + \frac{\partial U}{\partial q_i}\frac{\partial}{\partial t_l}\left(\frac{\partial q_i}{\partial t_k}\right) \\ &= \left(\frac{\partial^2 U}{\partial q_j \partial q_i}\frac{\partial q_j}{\partial t_l}\right)\frac{\partial q_i}{\partial t_k} + \frac{\partial U}{\partial q_i}\frac{\partial}{\partial t_l}\left(\frac{\partial q_i}{\partial t_k}\right)\end{aligned}$$

Or in matrix notation

$$\mathbf{K}(\mathbf{t}) = 0 = \mathbf{J}^T \mathbf{K}(q_i)\mathbf{J} + \mathbf{f}(q_i)^T \frac{\partial \mathbf{J}}{\partial t_l} \tag{5.57}$$

Notice the similitude between Eq. 5.46 and Eq. 5.57. Basically, they are the same. Equation 5.46 is just a simplification to a one-dimensional workspace of Eq. 5.57. The important issue is to understand the relation of the Jacobian and its rate of change, into the context of trajectories as workspaces, which is more simple and easy to visualize.

Figure 5.6, express the idea behind the theory generalization for static balancing in a graphical way.

$$\begin{array}{ccccc} U(q_i) & \rightarrow & q_i = f_i(t_k) & \rightarrow & U(t_k) = constant \\ \downarrow & & \downarrow & & \downarrow \\ \frac{\partial^2 U}{\partial q_j \partial q_i} & & \mathbf{J} = \frac{\partial q_i}{\partial t_k} & & \frac{\partial^2 U}{\partial t_l \partial t_k} \\ \downarrow & & & & \downarrow \\ \mathbf{K} & & & & \mathbf{0} = \mathbf{J}^T\mathbf{K}\mathbf{J} + \mathbf{f} \cdot \frac{\partial \mathbf{J}}{\partial t_l} \end{array}$$

Figure 5.6: Generalization for static balancing in a graphical way

5.4 Summary

A short literature review was presented at the beginning of the chapter in order to provide a view on the field of applications of static balancing. Gravity compensation, vibration isolation, and stiffness reduction were identified as their main application.
The chapter introduced the definitions of static balancing from different perspectives, aiming on their application into discretized structures being described in terms of multiple degrees of freedom.
Figure 5.7 shows in a graphical way the definitions for static balancing and their interrelations.

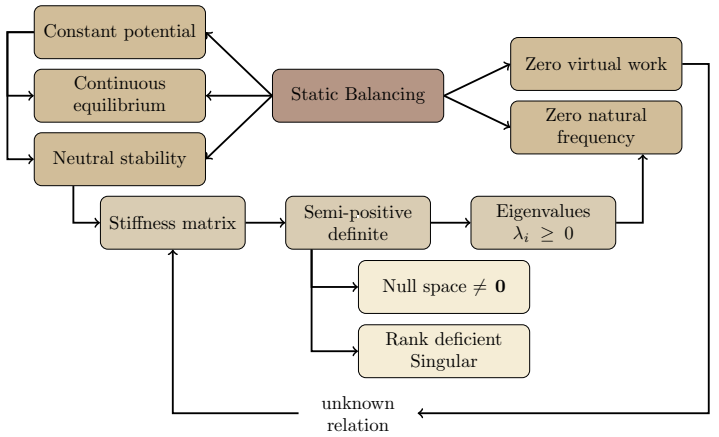

Figure 5.7: Static balancing definitions and their interrelations

All the definitions for static balancing were generalized through a coordinate transformation, in which the multiple degrees of freedom describing the system deflection were projected into the workspace in which the system exhibits a behavior of static balancing.
Definitions for static balancing were developed in a way that they could be applied to discretized systems described in terms of multiple degrees of freedom. In simple systems, most of the time it is possible to obtain analytical expressions describing the behavior of their potential energy, force or stiffness. However for complex systems, obtaining such expressions is not easy, if not impossible. Description of complex systems is better approached by approximated models which are constructed from discrete elements that result in mathematical descriptions in terms of stiffness matrices. The stiffness matrix holds in its structure all the system's size, shape, and topology properties. That is where the static balancing generalization gains relevance, since it is expressed in terms of the stiffness matrix of statically balanced systems.
In section 5.2.1, proposition 5.1, stated that statically balanced systems are in essence prestressed structures, and more specific, prestress inducing high densities of strain energy per unit of deflection. Expanding the implications of this proposition in terms of the definitions for static

balancing, we have that

- The potential energy must have an initial value different from zero, if we assume zero potential at the stress-free configuration.
- Pre-stressing can be achieved in many ways. If force is used, it means preloading.
- From a stability perspective the system should exhibit somewhere in its internal structure, regions subjected to instability exhibiting negative stiffness behavior.
- From a motion perspective, prestressing promotes reduction of the overall stiffness in the system's workspace which means in turn reduced natural frequency and speed variations during motion.

Systems in a state of static balancing are systems with singular configurations, this is why they were explained from the energy, force, stability, virtual work and motion perspectives, intending that each angle could provide with a different insight on this singular state.

6 Design of statically balanced compliant mechanisms

If I have a thousand ideas and only one turns out to be good, I am satisfied.

Alfred Nobel

The idea behind the design of Statically Balanced Compliant Mechanisms (SBCM's) is to design mechanisms that perform their intended function through the use of compliance, thus preserving all the benefits that this conveys while removing the energetic inefficiencies by using static balancing.

In chapter 3, we discussed the most common synthesis methods for compliant mechanisms. The overview included the most characteristic features of each approach and their fundamental principles. Among all the methods presented, three were considered the most relevant, namely, the Rigid-Body-Replacement (RBR), the building blocks (BB), and the structural optimization (SO).

Similarly, chapter 5 presented different definitions of static balancing from the standpoint of potential energy, force, stability, virtual work and motion.

In this chapter, we will explore the combinations between design methods for compliant mechanisms with static balancing criteria towards the definition of a design methodology for statically balanced compliant mechanisms.

Along section 5.2, five definitions about what static balancing is were developed. Now, we want to use those definitions as design criteria to identify a state of static balancing during the synthesis steps. Table 6.1 presents these definitions mathematically, in which $\mathbf{r}\,(\mathbf{t})$ represents the statically balanced workspace.

Table 6.1: Definitions of static balancing as design criteria

Definitions	Criteria	Mathematical expression
Definition 5.1	Energy criterion	$\forall \mathbf{q} \in \mathbf{r}(\mathbf{t}) : U(\mathbf{q}) = constant$
Definition 5.2	Force criterion	$\forall \mathbf{q} \in \mathbf{r}(\mathbf{t}) : \mathbf{f}(\mathbf{q}) = \mathbf{0}$
Definition 5.5	Stiffness criterion	$\forall \mathbf{q} \in \mathbf{r}(\mathbf{t}) : \mathbf{K}(\mathbf{q}) \Delta \mathbf{q} = \mathbf{0}$
Definition 5.3	Work criterion	$\forall \mathbf{q} \in \mathbf{r}(\mathbf{t}) : w(\mathbf{q}) = 0$
Definition 5.6	Frequency criterion	$\forall \mathbf{q} \in \mathbf{r}(\mathbf{t}) : \omega(\mathbf{q}) = 0$

6.1 The design methodology

The construction of the design methodology is done by identifying and interrelating what we will call the *recurrent elements*. Recurrent elements refer to specific features that appear repeatedly in the context of SBCM's and influence the design outcome. Recurrent elements can be identified by analyzing, for instance, the classifications of design requirements, design attributes, design approaches, etc.

Inside the context of SBCM's we can identify seven main recurrent elements: (i) compliancy type, (ii) classification of the functional requirements, (iii) modularity of the mechanism, (iv) static balancing strategy, (v) modularity of the design process, (vi)design methods for compliant mechanisms, and (vii) static balancing criteria.

Compliancy type is a recurrent element indicating that a mechanism achieves its mobility due to either lumped compliance or distributed compliance in the deforming elements. The compliancy type is an imposition of the design requirements but driven by the particularities of the design methods for compliant mechanisms.

In the case of structural optimization, the compliancy type is influenced by the chosen parameterization. For instance, a continuum ground structure is more prone to lumped compliance while a parameterization based on parametric curves is more inclined towards distributed compliance.

For the Rigid-Body-Replacement method, the compliancy is determined by the replacement method. For instance, replacing revolute joints by flexure notch hinges clearly results in lumped compliance while the use Pseudo-Rigid-Body models can result in distributed compliance.

The building block method as presented in literature is intended to promote distributed compliance, but the method can be applied in the design of building blocks promoting lumped compliance if we combine the concepts of instant center of rotation and compliance ellipsoids with the Rigid-Body-Replacement method based on flexure notch hinges.

Classification of the functional requirements relates to the idea that the main function of a mechanism can be classified as either function generation, path generation, or motion generation (see chapter 2.1).

Modularity of the mechanism relates to the possibility of the mechanism to be fully compliant or partially compliant. Remember that fully compliant mechanisms are monolithic structures

in which motion comes entirely from deformation of the constitutive members, while partially compliant mechanisms are modular designs connected through kinematic pairs where motion results from the combination of elastic deformations and relative rigid body motion between modules.

Static balancing strategy refers to the way in which the static balancing problem is addressed. These are the strategies focused on how to statically balance previously existing unbalanced mechanisms. These strategies are used effectively in the context of modular design processes. Chapter 5.1 mentioned some strategies towards static balancing such as stationary centers of gravity, compensation by springs, function decomposition, buckling, etc.

Modularity of the design process relates to the idea of performing the two design phases — design of the mechanism and static balancing of the mechanism— in one or two design stages. In a *modular design process* the functional requirements and the static balancing characteristics are done in independent design stages. In an *integral design process* all the requirements (functional requirements and static balancing characteristics) are completed in one stage (see chapter 2.2).

A modular design process can be used in the design of either partially or fully SBCM's. In the case of fully compliant designs, it is required to remove any relative motion between the connected modules, so that the kinematic pair connecting the modules is in fact a rigid joint.

An integral design process can be used as well in the design of fully and partially SBCM's. The design process is only limited by the selection of the design method for compliant mechanisms. For instance, the use of building blocks does not allow for the inclusion of pre-stressing effects, rendering it ineffective to be used in an integral design process. Another example is the use of structural optimization based on FEA in the design of partially compliant mechanisms. The inclusion of revolute and/or prismatic joints, while not impossible, increases the complexity to a level that makes impractical the use of an integral design process.

Design methods for compliant mechanisms and static balancing criteria are closely related, so the use of one design method limits the use of the static balancing criteria and vice versa. Therefore, we need to explore the feasibility between combinations of these two design features. To do so, we organize the three synthesis methods for compliant mechanisms with the five design criteria for static balancing into a screening matrix (see Fig. 6.1).

Feasibility comes as a result from the possibility of a design method to include pre-stressing effects so it can deal with the static balancing characteristics.

The building block methods (as presented in literature) are based on linear and infinitesimal deflections which do not account for pre-stressing effects, thus making them useful in the design of compliant mechanisms with functional requirements but without static balancing characteristics. Consequently, any direct combination between building blocks and the design criteria for static balancing is considered not feasible.

In the case of the RBR method, the possibility to include pre-stressing effects comes from the inclusion of torsion springs at the revolute joints (using either Psuedo-Rigid-Body model or notch

	Potential energy	Force	Stiffness	Virtual work	Frequency
Structural optimization	✓	✓	✓	×	✓
Rigid body replacement	✓	✓	✓	✓	×
Building blocks	×	×	×	×	×

Figure 6.1: Feasibility of the combinations between the static balancing criteria and the design methods for compliant mechanisms.

hinges), which account for the bending stiffness of its equivalent compliant joint. The inclusion of torsion springs allows to obtain analytical expressions for all the static balancing design criteria, except for the frequency criterion. Analytical expressions for frequency in nonlinear systems are difficult to obtain, therefore the combination RBR-Frequency is considered not feasible due to impracticability.

In the case of structural optimization, the analysis method employed in the design process determines the feasibility in the use of a specific static balancing criterion. Here it is assumed that the evaluation of the objective function at the analysis step is performed with the aid of some numerical approach such as finite elements, in which case estimating the virtual work does not make a new contribution with respect to the use of criteria like potential energy, work or stiffness, and its computation could be rather cumbersome. As a result, the combination between virtual work and structural optimization is regarded as not feasible.

So far we have identified the recurrent elements in the design of SBCM's. Now based in the aforementioned considerations we construct the design methodology for statically balanced compliant mechanisms by coherently interrelating the recurrent elements. In this work we propose the methodology that is depicted in Fig. 6.2. In this methodology each possible path across Fig. 6.2 is a method for the design of statically balanced compliant mechanisms.

To extract a design method from the methodology, first in *diagram A* we select whether the design method will provide fully or partially compliant designs. Then we select the modularity of the design process taking into account the constraints for a specific combination. The next level indicates which design method for compliant mechanisms can be used to comply with the functional requirements (function, path or motion generation) and to comply with the static balancing characteristic.

In the specific case of a design method using a modular design process, the static balancing problem can be conceptualized based on a design strategy to later design the balancer using a specific design method for compliant mechanisms with pre-stressing capabilities (so far only structural optimization and rigid-body-replacement have this capability).

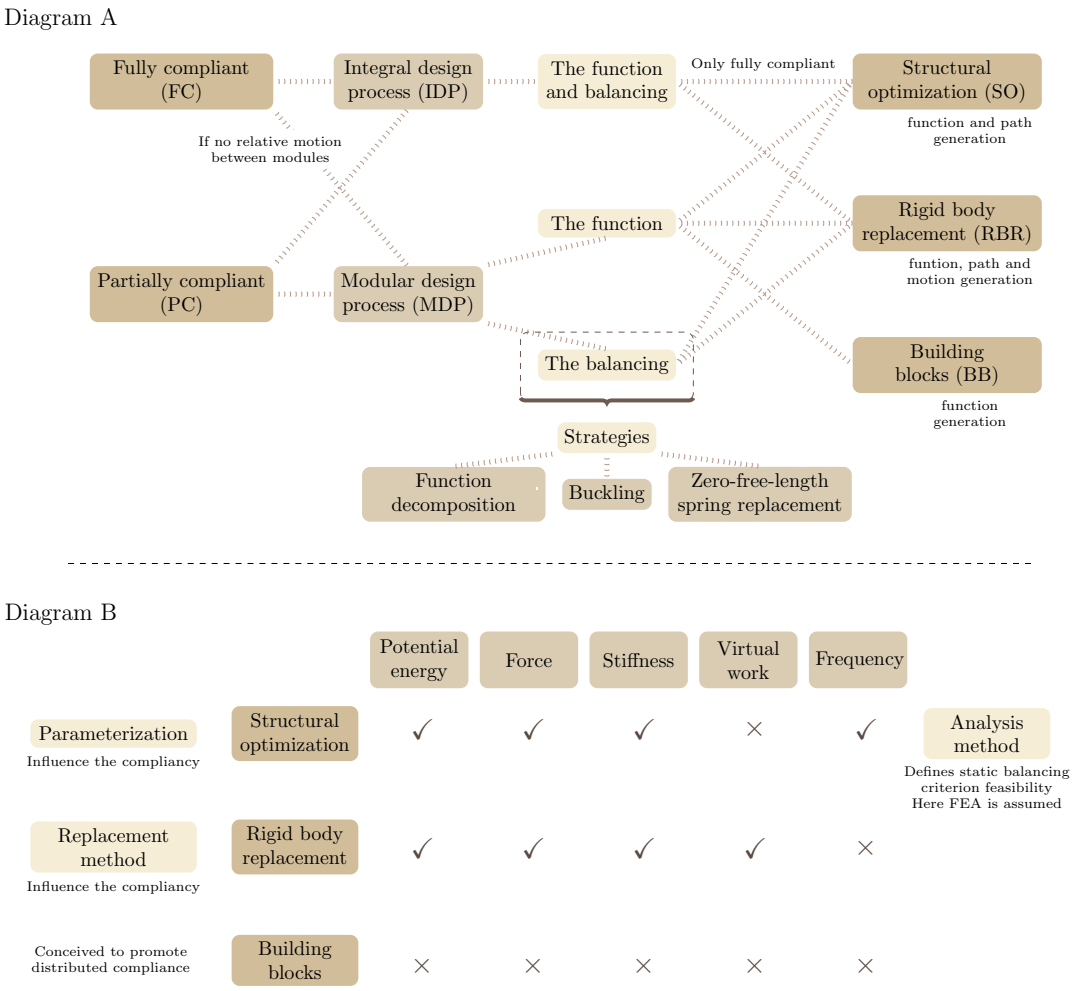

Figure 6.2: Methodology for the design of statically balanced compliant mechanisms. The methodology originates from the interrelation of the recurrent elements in the design of statically balanced mechanisms and the design of compliant mechanisms.

Once the design method for compliant mechanisms that will account for the static balancing characteristic has been selected we proceed to *diagram B* to select the static balancing criterion that will be used to guarantee a static balancing state. Diagram B helps to determine as well the type of compliancy based on the chosen method for the design of compliant mechanisms. For instance in structural optimization the compliancy type is determined mainly by the parameterization while in the rigid-body-replacement method the compliancy is determined by the replacement model, building blocks are conceived to promote distributed compliance.

Figure 6.3 presents an example of a design method for SBCM extracted from the methodology in

Fig. 6.2. The design method is used to obtain partially compliant mechanisms using a modular design process. The functional module is designed through the use of building blocks, while the balancer is conceptualized by the use of zero-free-length springs and designed with the rigid-body-replacement method based on the pseudo-rigid-body model for distributed compliance. The static balancing characteristic is incorporated by using the continuous force criterion.

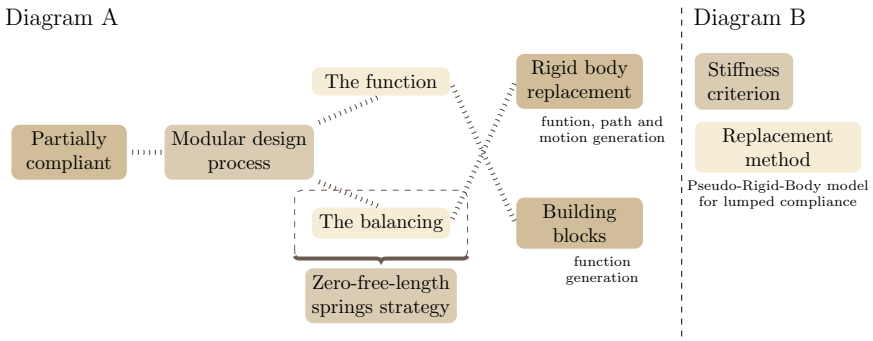

Figure 6.3: One of many possible methods for the design of statically balanced compliant mechanisms derived from the methodology in Fig. 6.2.

6.2 Design methods

In this section we introduce four of the possible design methods that can be derived from the design methodology shown in Fig. 6.2. Each design method is presented through an example comprising the design of a statically balanced compliant mechanism. The design methods presented in the following were chosen to illustrate the concepts and procedures mentioned in previous sections and their use in the design of statically balanced compliant mechanisms.

6.2.1 Integral design method for fully compliant mechanisms using structural optimization

Due to the extension of this particular method, it is presented as an independent chapter. The method is explained in more detail in chapter 7 where it is presented as an integral design method for statically balanced fully compliant mechanisms (see Fig. 6.4).
In this chapter the structural optimization as a design method for compliant mechanisms is set as a binary topology optimization problem of a partial ground structure, solved through the use of genetic algorithms.
To test the design method, two design problems are set: (i) the inverter, and (ii) the gripper. In both design problems, the static balancing characteristic is included as a constraint through the use of the continuous equilibrium criterion and the neutral stability criterion.

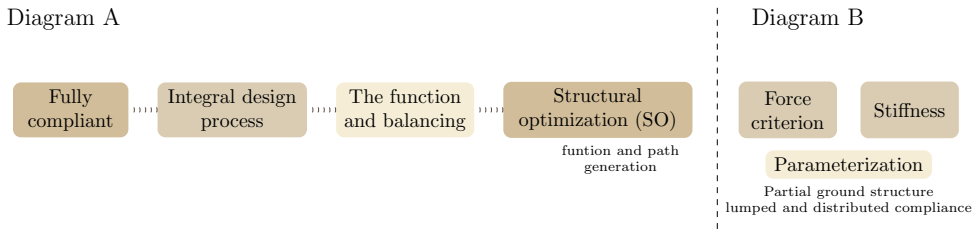

Figure 6.4: Diagram of an integral design method for statically balanced fully compliant mechanisms using structural optimization methods.

6.2.2 Integral design method for fully compliant mechanisms using Rigid-Body-Replacement

In this section we examine an integral design method for fully compliant mechanisms based on the Rigid-Body-Replacement (RBR) method. The idea behind the use of an integral design method is to design a statically balanced compliant mechanism in one single design phase. Figure 6.5 shows the structure of the design method.

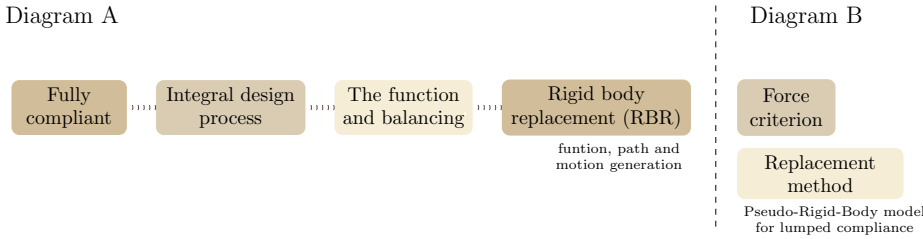

Figure 6.5: Diagram of an integral design method for fully compliant mechanisms using rigid-body-replacement method.

The objective is to induce the static balancing state during the transformation process from a rigid body mechanism to a compliant mechanism in the RBR method by adjusting the values of the stiffness and pre-loading angles at the linkage's joints. Remember that during the transformation process from rigid to compliant, the RBR method uses a model of the deflection of the compliant members as pin jointed rigid links with torsion springs accounting for the stiffness properties of the compliant members. The stiffness and pre-loading angles correspond to parameters of the torsion springs used in the replacement model.

An interesting advantage of using linkages based on rigid bodies is that the angle of rotation between links does not depend on the actual length of the links but on their relative lengths. Therefore, the strain energy of torsion spring at the linkage's joints is not affected by the scaling of the linkage. Also notice that to guarantee a state of static balancing we need to have a constant

strain energy value different from zero, and this constant value is not specific. Therefore, for a given rotation and pre-loading angle of the torsion springs, the static balancing state depends on their stiffness's relative proportions. These two characteristics allow to design a statically balanced rigid-body mechanism in terms of proportions which are later transformed into a statically balanced compliant mechanism during the dimensioning of the compliant joints.

To test this design method, we will design a statically balanced compliant linkage which is to generate a straight line path. The design is based on the Watt's four-bar linkage depicted in Fig. 6.6a, where the middle point of the coupler link is the point of interest tracing a straight line path with a linear correlation coefficient of $r = 0.9995$ for an input link rotation of [-0.7,0.2]rad. Figure 6.6b depicts the replacement model that will be used by the RBR method.

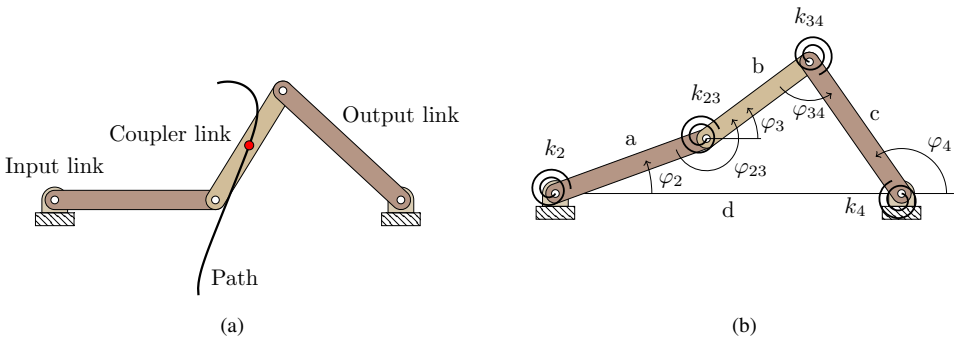

Figure 6.6: The design problem is the design of a statically balanced compliant version of a Watt's four-bar linkage. (a) Watt's four-bar linkage tracing a straight line path at the coupler's middle point. (b) Replacement model of the Watt's four-bar linkage used in its transformation into a compliant mechanism.

Table 6.2 provides the proportions between the lengths of the links on the Watt's linkage.

Table 6.2: Proportions between lengths of a Watt's linkage for straight line path generation

Link		Proportional length
Input link	a	1
Coupler link	b	0.8
Output link	c	1
Ground link	d	2.154

To find the value of the pre-loading angles and proportional stiffness of the torsion springs, we need to express analytically the total strain energy of the linkage with torsion springs. The total strain energy is simply the sum of the strain energy of each torsion spring,

$$U = U_2 + U_{23} + U_{34} + U_4 \tag{6.1}$$

The expression for the expansion of the energy in terms of the stiffness k, the link's relative rotation angle φ and the pre-loading or initial angles φ^0 yields,

$$U = \tfrac{1}{2}k_2\left(\varphi_2 - \varphi_2^0\right) + \tfrac{1}{2}k_{23}\left(\varphi_{23} - \varphi_{23}^0\right) + \tfrac{1}{2}k_{34}\left(\varphi_{34} - \varphi_{34}^0\right) + \tfrac{1}{2}k_4\left(\varphi_4 - \varphi_4^0\right) \tag{6.2}$$

The rotation angle φ_{23} for a linkage in a open configuration is given by

$$\varphi_{23} = \pi - \varphi_2 + \varphi_3 \tag{6.3}$$

while the rotation angle φ_{34} is given by

$$\varphi_{34} = \varphi_4 - \varphi_3 \tag{6.4}$$

Keep in mind that even if the linkage goes into the cross configuration, the measurement of the rotation angles is relative to the linkage's open configuration.
Watt's linkage is a 1 DOF linkage, therefore it is possible to express the rotation angles φ_3 and φ_4 in terms of φ_2. General analytical expressions for these two angles can be found by using vector loop equation 6.5.

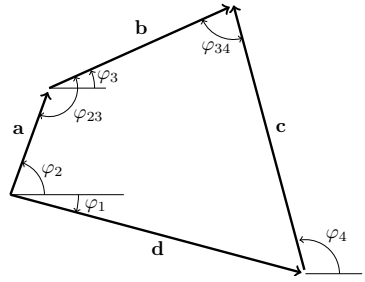

Figure 6.7: Vector loop equation for a fourbar linkage with given ground link orientation φ_1.

$$\mathbf{a} + \mathbf{b} - \mathbf{d} - \mathbf{c} = \mathbf{0} \tag{6.5}$$

Solution to the vector loop equation is provided with Eq. 6.6 and 6.7,

$$\varphi_3 = 2\arctan\left(\frac{-E - \sqrt{E^2 - 4DF}}{2D}\right) \tag{6.6}$$

$$\varphi_4 = 2\arctan\left(\frac{-B - \sqrt{B^2 - 4AC}}{2A}\right) \tag{6.7}$$

where

$$A = \cos\varphi_2 - K_1\cos\varphi_1 + K_3 - K_2\cos(\varphi_2 - \varphi_1) \tag{6.8}$$

$$B = E = -2\sin\varphi_2 + 2K_1\sin\varphi_1 \tag{6.9}$$

$$C = K_1\cos\varphi_1 - \cos\varphi_2 + K_3 - K_2\cos(\varphi_2 - \varphi_1) \tag{6.10}$$

$$D = \cos\varphi_2 - K_1\cos\varphi_1 + K_5 + K_4\cos(\varphi_2 - \varphi_1) \tag{6.11}$$

$$F = K_1\cos\varphi_1 - \cos\varphi_2 + K_5 + K_4\cos(\varphi_2 - \varphi_1) \tag{6.12}$$

$$K_1 = \frac{d}{a} \tag{6.13}$$

$$K_2 = \frac{d}{c} \tag{6.14}$$

$$K_3 = \frac{a^2 - b^2 + c^2 + d^2}{2ac} \tag{6.15}$$

$$K_4 = \frac{d}{b} \tag{6.16}$$

$$K_5 = \frac{c^2 - a^2 - b^2 - d^2}{2ab} \tag{6.17}$$

Substituting Eq. 6.3 to Eq. 6.17 into Eq. 6.2 together with the link lengths in Tab. 6.2, and assuming a horizontal ground link ($\varphi 1 = 0$), we get the total strain energy of the Watt's linkage with torsion springs in terms of the input angle φ_2, the springs' stiffness, and the springs' pre-loading angles.

Differentiation of the total strain energy with respect to the input angle φ_2 gives an analytical expression for the linkage's resultant moment at joint 2 while differentiation of the resultant moment with respect to φ_2 provides the linkage's resultant stiffness at the same joint,

$$f = \frac{dU}{d\varphi_2} \tag{6.18}$$

$$k = \frac{d^2U}{d\varphi_2^2} \tag{6.19}$$

To find the springs' stiffnesses and pre-loading angles that statically balance the linkage along the range of motion defined by φ_2, we solve the constrained nonlinear optimization given by Eq. 6.20,

$$\begin{aligned} \min_{\mathbf{x}} \quad & \mathbf{f}_{rms} \\ s.t.: \quad & \mathbf{x}_{\min} \leq \mathbf{x} \leq \mathbf{x}_{\max} \end{aligned} \tag{6.20}$$

where the design vector $\mathbf{x}$ is formed the by springs' stiffnesses and pre-loading angles,

$$\mathbf{x} = \begin{bmatrix} k_2 & k_{23} & k_{34} & k_4 & \varphi_2^0 & \varphi_{23}^0 & \varphi_{34}^0 & \varphi_4^0 \end{bmatrix} \tag{6.21}$$

and the objective function $\mathbf{f_{rms}}$ is the root mean square (RMS) of the force vector $\mathbf{f}$, see Eq. 6.22. The force vector is formed by the values of the linkage's moment at joint 2 calculated at 10 evenly spaced points in the range of motion φ_2=[-0.7;0.2]rad.

$$\mathbf{f}_{rms} = \sqrt{\frac{1}{10}\sum_{i=1}^{10} f_i^2} \quad where \quad f_i = f\left(\mathbf{x}, \varphi_{2_i}\right) \quad and \quad \varphi_{2_i} = -0.8 + (0.1)\, i \tag{6.22}$$

The constraints are formed by the boundaries of the design variables,

$$\mathbf{x}_{\min} = \begin{bmatrix} 1 & 1 & 1 & 1 & -0.9 & 3.5 & 1.2 & 2 \end{bmatrix} \tag{6.23}$$

$$\mathbf{x}_{\max} = \begin{bmatrix} 10 & 10 & 10 & 10 & 0.4 & 5.2 & 2.4 & 3.4 \end{bmatrix} \tag{6.24}$$

Take into account that the lower limit for the stiffness can not be set to zero. If zero is allowed as the lower limit, the optimization algorithm will give as a solution that all the four stiffness are zero, which in other words means that the optimization will find that the best statically balanced solution is a linkage with no springs.

For the pre-loading angles, the limits are set in a way that the range of allowable values is as large as possible but without violating the rotation limit of 1.344 rad (77°) for the entire joint rotation (rotation during actuation plus pre-loading rotation). The rotation limit is given by the pseudo-rigid-body model for distributed compliance [40], but here it is used as well as the limit for the lumped compliance model.

The optimization problem is solved by sequential quadratic programming (SQP). The initial point for the optimization (found by a trial and error search) is at,

$$\mathbf{x} = \begin{bmatrix} 5 & 5 & 5 & 5 & -0.2 & 4.3 & 1.8 & 2.7 \end{bmatrix} \tag{6.25}$$

A minimum with a force RMS value of 0.012 was found at the point,

$$\mathbf{x} = \begin{bmatrix} 1.0577 & 1.005 & 1 & 1.906 & 0.4 & 3.5 & 2.4 & 3.4 \end{bmatrix} \tag{6.26}$$

Figure 6.8 shows the behavior of the Watt's linkage when the results of the optimization are substituted into Eq. 6.2, Eq. 6.18, and Eq. 6.19

Notice that while the strain energy is nearly constant and the force is close to zero along the range of motion, the stiffness deviates considerably from zero. This result, in theory, can be improved by using as objective function the RMS values of the stiffness instead of the force RMS value, but

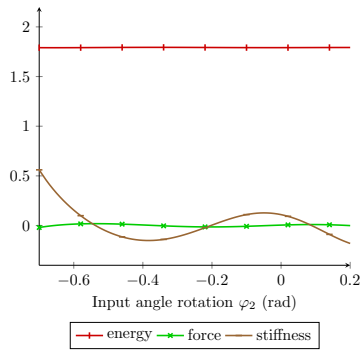

Figure 6.8: Strain energy, force and stiffness for the Watt's linkage along the range of motion φ_2=[-0.7;0.2]rad using the values found by nonlinear optimization of the springs' stiffness and pre-loading angles.

the problem with this is that the optimization leads more naturally to a constant force mechanism than to a statically balanced one. Table 6.3 summarizes the results of the optimization for the statically balanced pseudo-rigid-body model (SB-PRBM) of the Watt's linkage, while Fig. 6.9 depicts the linkage in its unstressed configuration.

Table 6.3: Values for a statically balanced pseudo-ridig-body model of the Watt's linkage

Links' Proportional lengths			springs' stiffness		springs' pre-loading angles	
Input link	a	1	k_2	1.0577	φ_2^0	0.4rad
Coupler link	b	0.8	k_{23}	1.005	φ_{23}^0	3.5rad
Output link	c	1	k_{34}	1	φ_{34}^0	2.4rad
Ground link	d	2.154	k_4	1.906	φ_4^0	3.4rad

Now the design of the statically balanced compliant Watt's linkage is about the design of the compliant flexures that will replace the revolute joints in the pseudo-rigid-body model. The idea is to select the geometry of the flexure that will replace the joint with the highest stiffness, in this case stiffness k_4. Once the geometry is selected, the flexure stiffness is computed and used as the baseline to scale the remaining flexure stiffness and then reverse the calculations to find the remaining flexures' geometry. Choosing the highest stiffness as the stiffness baseline helps to guarantee that the remaining flexures will not violate the yield strength limit.

Assuming a constant rectangular cross section of the flexure beams and a given out-of-plane thickness t, we proceed to find the length l and the in-plane width w of the flexure that will replace the joint with highest stiffness. The geometry of the flexure beam should allow deflections below the yield strength limit.

Remembering from mechanics of materials, the maximum stress of a rectangular constant cross section beam subjected to a moment M at the end tip is given by,

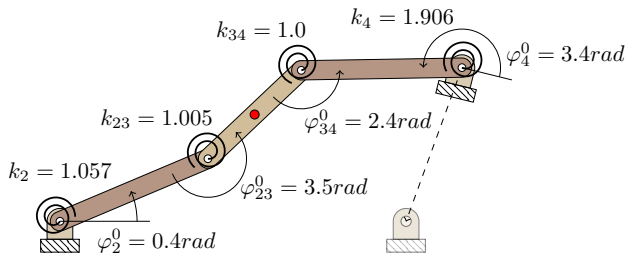

Figure 6.9: Pseudo-rigid-body model of the statically balanced Watt's linkage in the unstressed configuration.

$$\sigma_{\max} = \frac{Mw}{2I} \tag{6.27}$$

Where I is the cross section second moment of inertia. Assuming that the flexures will be subjected mainly to bending stresses, the solution for large deflections of the Bernoulli-Euler equation for beams under pure bending is,

$$\theta = \frac{Ml}{EI} \tag{6.28}$$

Here E is the Young's modulus and θ is the end tip rotation as a result of the applied moment M. Substituting Eq. 6.28 into Eq. 6.27 yields,

$$\sigma_{\max} = \frac{Ew}{2l}\theta \tag{6.29}$$

This expression can be used to find the length l and the in-plane width w of the flexure if we assume a value for the maximum allowable deflection θ of the flexure's end tip, and set $\sigma_{\max}$ as the yield strength limit. The stiffness of the flexure beam is derived by transposing the moment and deflection terms from Eq. 6.28 and by observing Hooke's law for torsion springs,

$$k = \frac{EI}{l} \tag{6.30}$$

Figure 6.10a shows Eq. 6.29 plotted for the assumed values in Tab. 6.4. The colored area $\sigma_{max} \leq \sigma_y$ is the design space for the flexure's geometry, in which the flexure can undergo a 1rad deflection without exceeding the yield strength limit. Remember that pure bending is assumed, so we select a conservative geometry of $l = 16mm$ and $w = 1mm$. Figure 6.10b shows a contour plot of Eq. 6.30 in which we can observe the resultant baseline stiffness $k_b = 52.08N/mm$ for the selected geometry.

Now we compute the vector of the flexures' stiffness $\mathbf{k}$ by scaling the proportional stiffness $\mathbf{k_p}$ (the ones given by the optimization of the PRBM) with respect to the baseline stiffness k_b.

Table 6.4: Initial values assumed for the compliant Watt's linkage

Property	Value
Young's modulus E (N/mm^2)	2000
out-of-plane thickness t (mm)	5
Yield strength σ_y (N/mm^2)	75

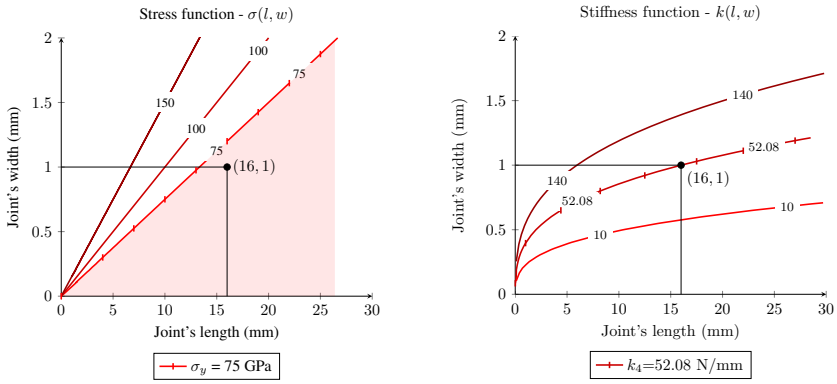

Figure 6.10: Using Eq. 6.29, we select the length and in-plane width of the flexure beam k_4 to establish the baseline stiffness without violating the yield strength limit. It is assumed that $\theta = 1rad$, and $E = 2000$. (a) Contour plot of the stress as a function of length and width (the red area is the feasible design domain). (b) Contour plot of the stiffness as a function of length and width.

$$\mathbf{k} = \frac{k_b}{\max(\mathbf{k}_p)}\mathbf{k}_p \tag{6.31}$$

Replacing the stiffness values from Tab 6.3 into Eq. 6.31 we get

$$\mathbf{k} = \begin{bmatrix} 28.90 & 27.46 & 27.33 & 52.08 \end{bmatrix} \tag{6.32}$$

Once we have the stiffness of the four flexures we need to go backwards to find their geometry. Let's expand Eq. 6.30 for a flexure beam with constant rectangular cross section,

$$k = \frac{Etw^3}{12l} \tag{6.33}$$

Combining Eq. 6.33 and Eq. 6.29 by substitution of either the length l or the in-plane width w yields an expression for the stiffness in function of the stress and either the in-plane or the length respectively.

$$k = \frac{2tl^2\sigma^3}{3E^2\theta^3} \tag{6.34}$$

$$k = \frac{\sigma t w^2}{6\theta} \tag{6.35}$$

With these two expressions we can track the contour level that matches the desired stiffness and then find either the length or the in-plane width of a rectangular cross section flexure beam that does not exceed the yield strength limit.

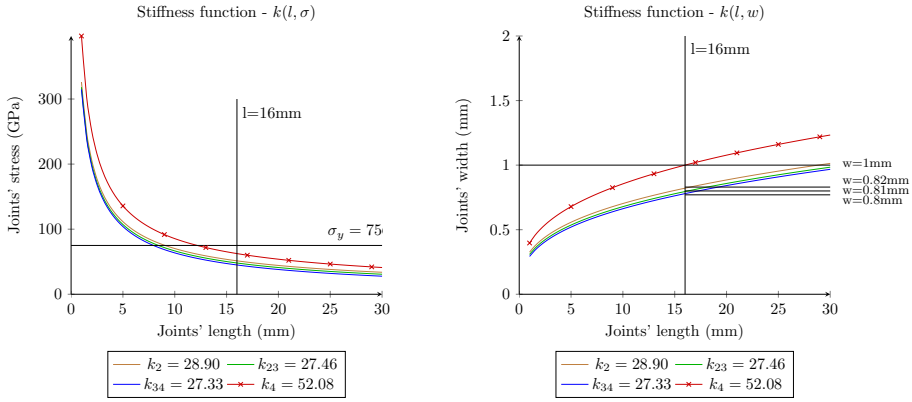

Figure 6.11: These plots are used to select the flexures' geometry for a given stiffness assuming a deflection, material and out-of-plane thickness. (a) Contour plot of the stiffness as a function of the length and stress. (b) Contour plot of the stiffness as a function of the length and width.

Figure 6.11 shows the contour levels of Eq. 6.34 and Eq. 6.33 for the four flexures' stiffness in Eq. 6.32. For example, we chose from Fig. 6.11a the same length of $l = 16mm$ for the four flexures and it is clear that none of the flexures exceed the yield limit for this length. From Fig. 6.11b we determined the in-plane width given by the selected length.

Table 6.5: Stiffness and geometry of the flexure beams of the compliant Watt's linkage

Flexure beam	stiffness (N/mm)	length (mm)	in-plane width (mm)
Flexure 2	28.90	16	0.8218
Flexure 23	27.46	16	0.8079
Flexure 34	27.33	16	0.8065
Flexure 4	52.08	16	1

Once the geometry of the flexure beams is known, we can proceed to dimension the compliant Watt's linkage. First we need to define the length of the rigid portion of the input and output links

with respect to the flexible portion. The theory of the PRBM for lumped compliance recommends a relation of 1:10 between the flexure beam and its rigid section, but due to space constraints we use a proportion of 1:5.25, As a result for a 16mm flexure we get an 84mm rigid section. These dimensions imply that the linkage is scaled by a factor of 100 with respect to the length values in Tab. 6.3.

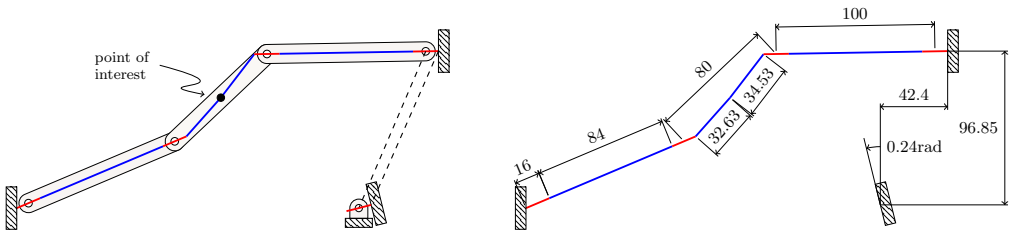

Figure 6.12: Dimensioning process to convert the rigid-body linkage into its monolithic compliant version. (a) Flexures and rigid-body links have the same orientation and the flexures' pseudo pivot coincides in location with the pin joints. (b) Final dimensions of the compliant Watt's linkage.

The final dimensions of the compliant mechanism are obtained by superimposing the flexure beams on the scaled rigid-body linkage while coinciding the flexures' middle point with the revolute joints as shown in Fig. 6.12a. After superimposing the flexures, these are connected by rigid segments such that the point of interest is on one of the rigid segments.

Figure 6.12a also shows how to calculate the required deflection to take the compliant Watt's linkage from the initial unstressed configuration, Fig. 6.13a, into the intermediate pre-stressed configuration prior to actuation, Fig. 6.13b.

With the final dimensioning of the statically balanced compliant mechanism, we proceed to the analysis using finite elements (FEA) based on nonlinear frame elements. The solution is found by displacement control in two time-steps (pre-stressing and actuation). Actuation is performed by displacement control since the actuation force is unknown and we want to find how close it is to zero. The actuation is applied as a vertical deflection of -80mm at the point of interest. Figure 6.13 depicts the deflection results from the FEA for the three configurations of the statically balanced compliant Watt's linkage.

In order to calculate the strain energy reduction required for the actuation of the statically balanced compliant Watt's linkage and its functional performance, we compare the statically balanced design with its non-statically balanced version. To do so, we design a compliant Watt's linkage from the same values found in Tab. 6.4 and 6.5 as an unprestressed structure at the intermediate configuration.

Figures 6.14 and 6.15 show the comparison of both, the statically balanced and unbalanced com-

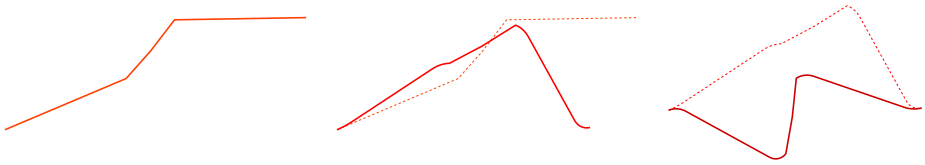

(a) (b) (c)

Figure 6.13: Set of configurations of the SB compliant Watt's linkage. (a) Initial configuration before pre-stressing. (b) Intermediate configuration after pre-stressing and before actuation. (c) Final configuration after actuation is applied as -80mm of vertical deflection at the point of interest.

pliant Watt's linkage, in their force-deflection behavior and straight line path generation, respectively.

The statically balanced design exhibits a strain energy reduction in actuation of 93.98%. The strain energies are estimated as the areas under the curves using the trapezoidal method. From the force point of view, the force reduction is about 94.03%. This index is obtained by estimating the root mean square of the force data in both designs.

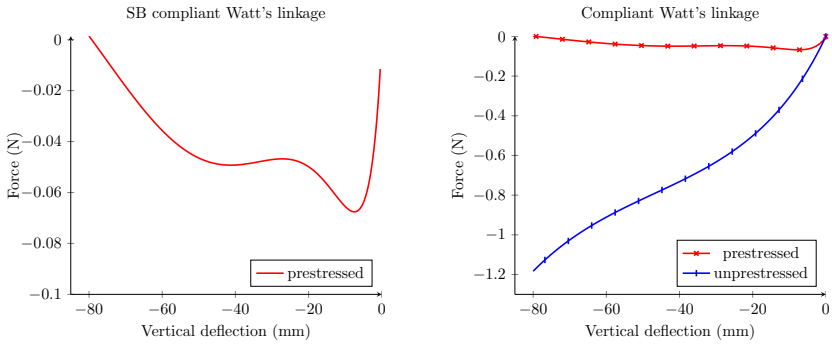

(a) (b)

Figure 6.14: Force - displacement behavior at the point of interest. (a) Amplified view of the behavior during actuation after pre-loading for the statically balanced compliant Watt's linkage . (b) Comparative view of the behavior for the statically balanced and unbalanced compliant Watt's linkage.

In the case of the functional performance, which is the generation of a straight path by the point of interest, the results from the FEA show that in the unbalanced design, the path matches a straight line with a linear correlation coefficient of $r = 0.9994$, while in the statically balanced design the linear correlation coefficient for its path is 0.9718. If the linear correlation coefficient is estimated after a vertical deflection of -10.8mm at the point of interest, the correlation coefficient increases to $r = 0.997$. This value corresponds to 87.5% of the total deflection path.

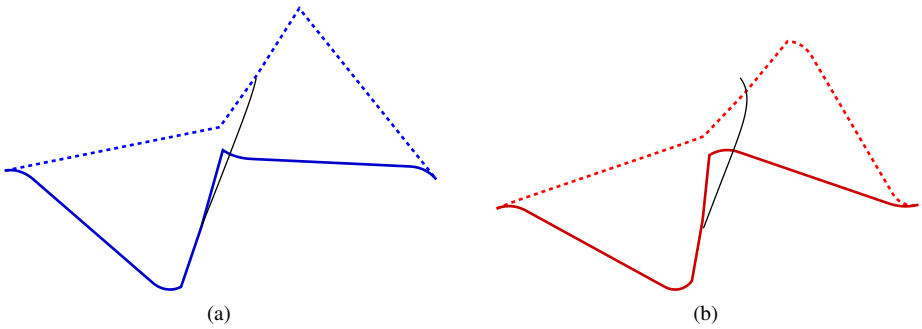

(a) (b)

Figure 6.15: Deflection path traced by the point of interest as predicted by the FEA. (a) Path for the unbalanced compliant Watt's linkage. (b) Path for the statically balanced compliant Watt's linkage.

The maximum stress distribution for the unbalanced design, according to the FEA, stays below the assumed yield strength limit, while the statically balanced design is exactly at the limit (see Fig. 6.16). Clearly, the dimensions for the flexure beams summarized in Tab. 6.5 must be recalculated in order to keep the stresses within a safe range for the statically balanced design. It is also true that the proposed model for the dimensioning of the flexure beams, as depicted in Fig. 6.10, is a good tool for the initial dimensional estimation for designs based on lumped compliance.

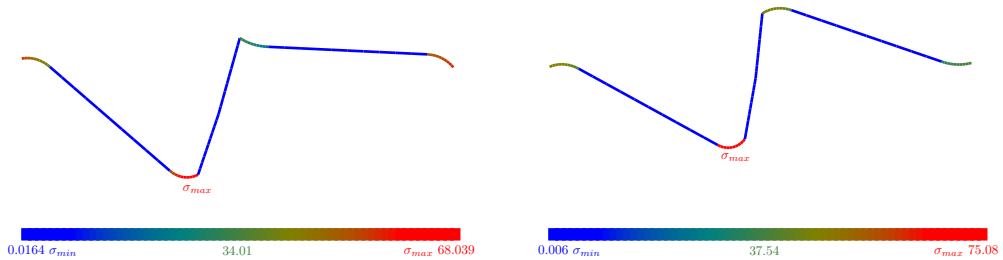

(a) (b)

Figure 6.16: Stress distribution at the deflection with the highest stress value (axial stress + maximum bending stress). (a) Stress distribution for the unbalanced Watt's compliant mechanism. (b) Stress distribution for the statically balanced Watt's compliant mechanism.

6.2.3 Modular design method for fully compliant mechanisms using function decomposition

In this section we take a look at the modular design method for the static balancing of fully compliant mechanisms using function decomposition.

We define function decomposition as the idea of creating a desired function as the combination of two or more functions. The functional module and the balancer are designed in such a way that they exhibit behaviors characterized by two different mathematical functions. When these two modules are combined, so are their functions, resulting in a third mathematical function that represents the final desired behavior of the combined modules. In our case, the desired behavior is either constant potential energy, or continuous zero force and stiffness. Function decomposition is a recursive procedure that can be applied as well in the design of the functional module and/or the balancer as compositions of sub-modules.

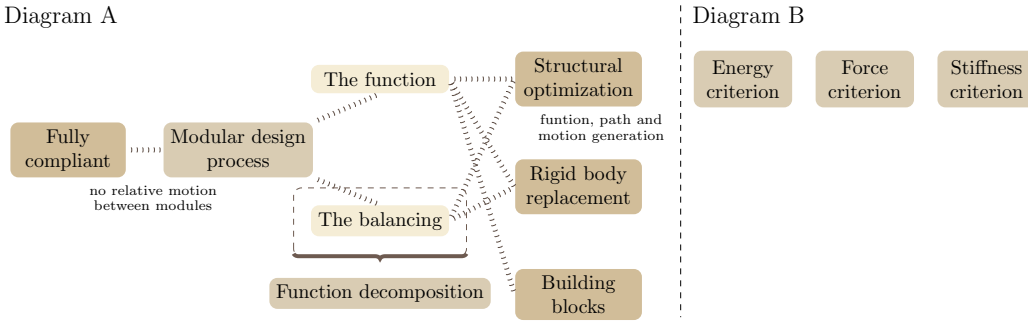

Figure 6.17: Diagram of a modular design method for fully compliant mechanisms using function decomposition

The use of function decomposition for planar fully compliant designs —no pin joint connections— requires that all the functions' domains must lie on the same axis or line of motion without relative motion among the modules at the overlapping point. The condition of no relative motion among the modules at the connection points comes from the monolithic nature of the composed design. This is that at the connection points there is stiffness and as a consequence any relative motion at this points is an unaccounted source of strain energy during the function decomposition.

In the case of statically balanced compliant mechanisms we have the advantage that the decomposed function describing a statically balanced behavior is a zero degree polynomial or constant value. The value of the constant is zero when we observe the force or the stiffness, and is non-zero when we observe the potential energy.

A zero degree polynomial can be constructed as the addition of two opposite or additive inverse functions, in which one of the functions is shifted depending on whether the decomposed function is a zero or a non-zero value, see Fig. 6.18.

The design problem based on this view is simply to design the balancer as the additive inverse of the functional module. Finding the additive inverse for any behavior of structures undergoing large elastic deformations is difficult, so the trick is to design both, the functional module and the balancer, in a way that their behaviors in energy, force or stiffness approximate simple functions.

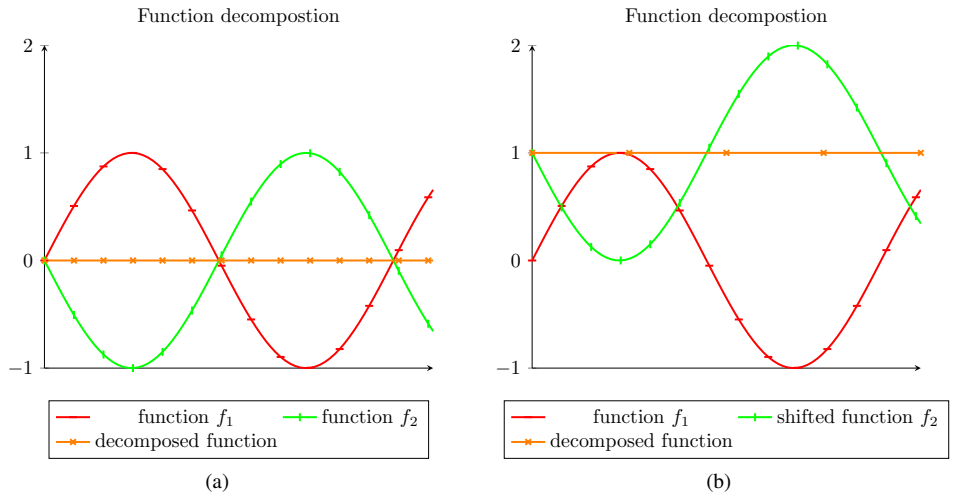

Figure 6.18: A zero degree polynomial can be decomposed as the summation of a function and its additive inverse. (a) Summation of a function and its opposite function creates a zero constant value. (b) Summation of a function and its shifted opposite function creates a non-zero constant value.

In some cases, designing a structure with such simple behavior is not possible, but if we observe that many complex behavior functions can be broken down into portions which individually are simple functions, then the problem becomes to find the module where only a portion of its behavior function is the additive inverse of the other module.

Many structures exhibiting complex behavior functions, once they are broken down, their individual portions can be approximated by polynomials of, as a maximum, second degree. Within this perspective, function decomposition towards static balancing of compliant mechanisms becomes a matter of arranging polynomials of second and first degree to create a zero degree polynomial, as shown in Fig. 6.19.

To test this approach we will proceed to the design of three statically balanced compliant suspensions for linear motion. For this purpose, we will make use of two simple structures, (i) the folded-beam suspension and, (ii) the double arch suspension.

The folded-beam suspension is a structure used to generate linear motion. It is formed by two opposite compliant fourbar linkages, where one linkage is grounded at the other's coupler link, see Fig. 6.20a. When the structure is actuated at the floating coupler link, the upward deflection of the floating coupler link is compensated by the downward deflection of the remaining coupler link, so the net result is a horizontal linear motion of the floating coupler link.

The characteristics of the deflection path on a folded-beam suspension are relatively simple. The force-displacement behavior, even for large deflections is nearly linear. Consequently, the

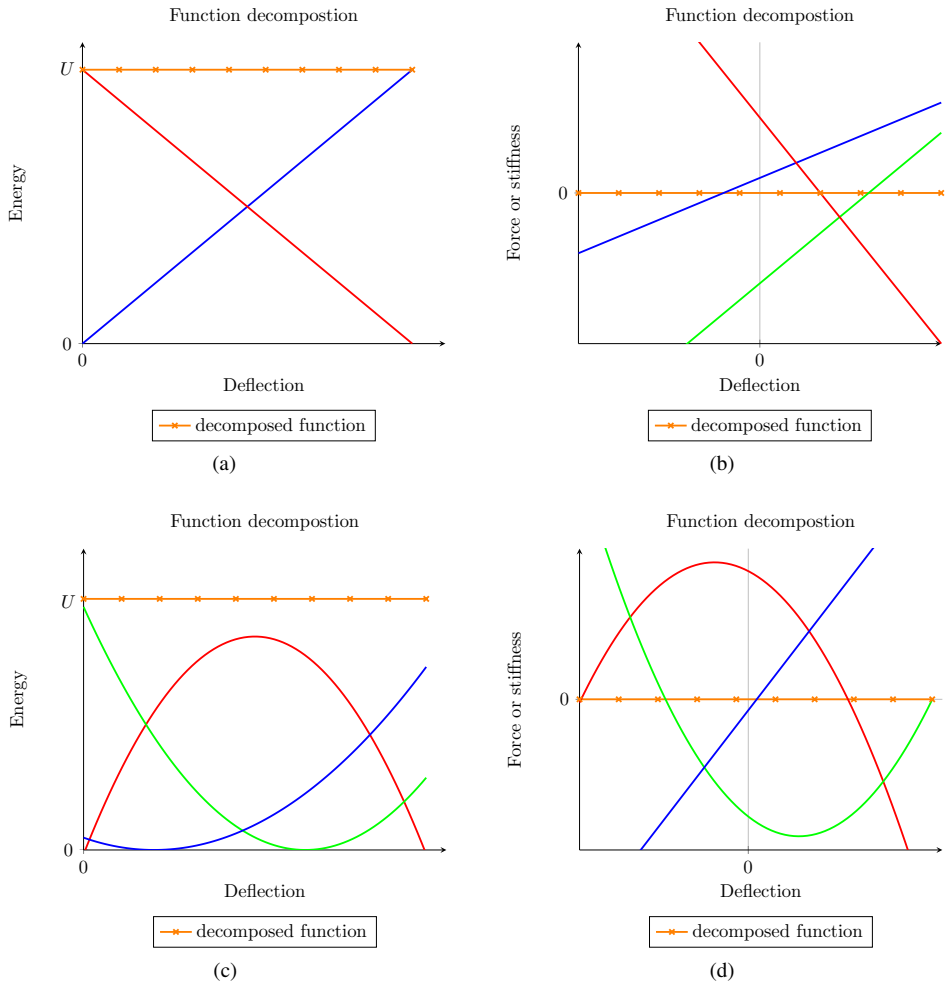

Figure 6.19: First and second degree polynomials can be combined to create a zero degree polynomial. The zero degree polynomial or constant function could represent either the energy or force and stiffness behavior of statically balanced compliant mechanisms.

stiffness is nearly constant and varies proportionally with the beams' in-plane thickness and inversely proportional to the suspension's height. Figure 6.21a shows the variation of the force-deflection due to the variation of the suspension's height.

The double-arch suspension is a structure used to generate a force-deflection function rather than a specific type of motion. The force-deflection function of the suspension is referenced to the connection point of the two arches. With this type of suspension it is possible to generate force-deflection functions with path sections exhibiting zero stiffness and/or variable positive and negative stiffness. It is even possible to create structures with unstable equilibrium points and/or

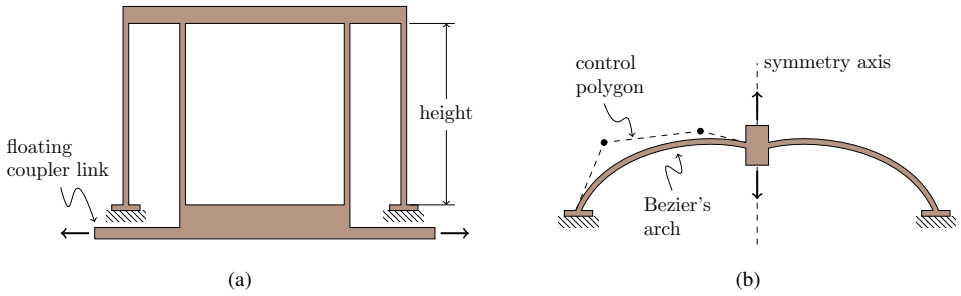

Figure 6.20: These two suspensions are representative examples of individual modules that can be used in the construction of statically balanced compliant mechanisms. (a) The folded-beam suspension. (b) The double-arch suspension.

two stable equilibrium points (bi-stable structures).

In this section, we make use of a symmetric suspension where the geometry of the arches is described by cubic Bezier's curves. The control polygon of the Bezier's curve is defined by two fixed control points —the initial and final— and two moving control points. The use of Bezier's curves allows to control the behavior of the force-deflection path in terms of the position of the two moving control points. Figure 6.21b shows examples of force-deflection paths for the symmetric Bezier's double-arch suspension.

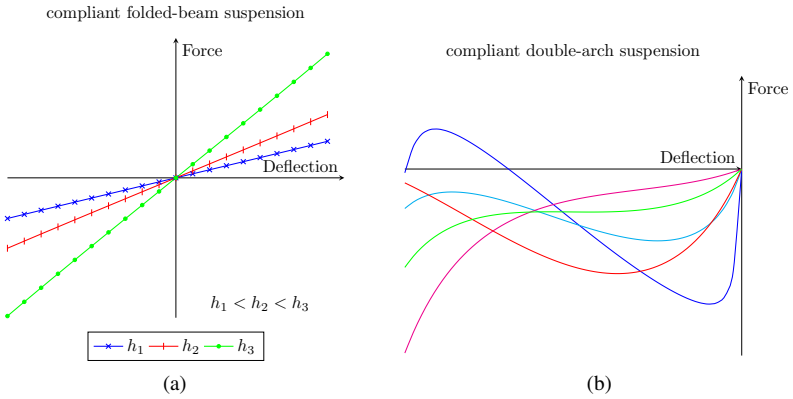

Figure 6.21: Typical force-displacement behavior of a folded-beam suspension and a double-arch suspension. (a) The folded-beam suspension exhibits a linear force-deflection behavior, where the stiffness is inversely proportional to the suspension's height. (b) The double-arch suspension exhibits many different behaviors which can include positive, zero and negative stiffness.

Design of statically balanced compliant suspension - concept 1

The first concept for the design of a statically balanced compliant suspension is composed of two compliant double-arch suspensions. One double-arch suspension acts as the functional module while the second suspension acts as the balancer.
Using the continuous equilibrium as the criterion for static balancing, we see that the force function to be decomposed is a zero degree polynomial with a constant value equal to zero,

$$f(t) = 0 \qquad t_{\min} < t < t_{\max} \tag{6.36}$$

where $f(t)$ represents the force as a function of the deflection t. Remember that t is the parameter defining the statically balanced trajectory $\mathbf{r}(t)$. Decomposed in the most simple way, this function is the sum of a constant c_1 and its additive inverse $-c_1$.

$$f(t) = 0 = c + (-c) \tag{6.37}$$

The constant value c represents a constant force mechanism, while the value $-c$ represents the mirror mechanism of same constant force mechanism. Figure 6.22 depicts the conceptual idea on how the force function is decomposed.

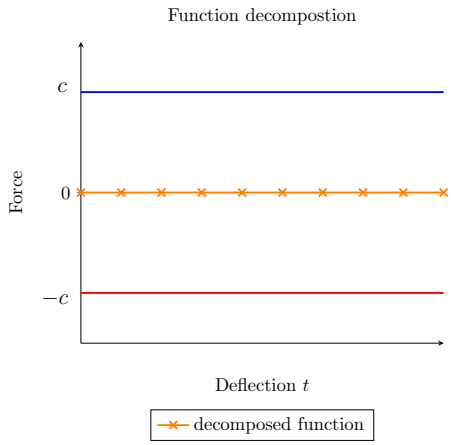

Figure 6.22: Decomposition of a continuous equilibrium function into two constant values.

Now we need to find the proper shape of a double-arch suspension that exhibits, along a portion of its force-deflection path, a constant force. The geometry of the arches is found by shape optimization of the suspension. Because the two arches in the suspension are symmetric, we only need to find the shape of one of the arches. So we set as the design variables the location of the two moving control points of the Bezier's control polygon, while keeping the remaining two control points as the fixed end tips of the arch. The objective function is set as the standard

deviation σ of the suspension force with respect to a given reference force f_{ref}. The standard deviation is only computed along an interval of the deflection path, see Fig. 6.23.

$$\begin{aligned} \min_{\mathbf{x}} \quad & \sigma(\mathbf{x}, f_{ref}) \\ s.t.: \quad & \mathbf{Ku} - \mathbf{f} = 0 \\ & \mathbf{x}_{\min} \leq \mathbf{x} \leq \mathbf{x}_{\max} \end{aligned} \tag{6.38}$$

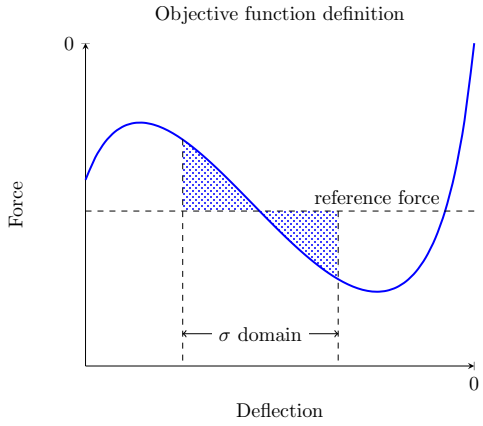

Figure 6.23: The objective function of the shape optimization is taken as the standard deviation σ of the force with respect to a reference force, along an interval in the deflection path.

The optimization problem is solved using genetic algorithms. The objective function is computed from the results of nonlinear finite element analysis solved through displacement control. The structure is modeled using nonlinear frame elements for large deflection, small strains.
By using the values in Tab. 6.6, the result of the optimization is the geometry depicted in Fig. 6.24a. The force-deflection behavior for this structure is shown in Fig. 6.24b, In this figure we observe a nearly constant force behavior for a vertical deflection of around 20mm.

Table 6.6: Values used for the shape optimization of the SBC suspension - concept 1

Property	Value
Young's modulus E (N/mm^2)	2000
out-of-plane thickness t (mm)	5
Yield strength σ_y (N/mm^2)	75
Double-arch suspension span l (mm)	100

Now we mirror the double-arch suspension in order to get the additive inverse to the constant force function, as shown in Fig. 6.25a. Both suspensions are joined using a rigid beam so there is no relative motion between points b_u and b_l.
Let's take any point along the rigid beam that joins the two suspensions and call it *the point of*

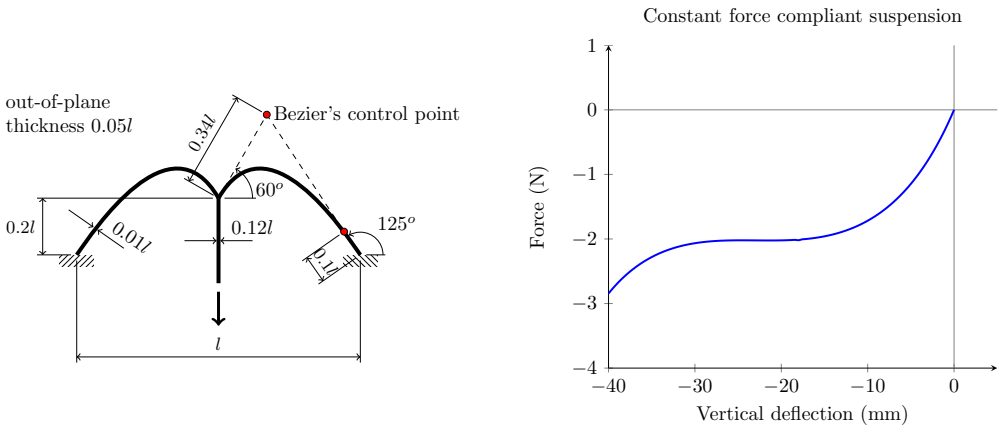

(a) (b)

Figure 6.24: The result of the shape optimization is a nearly constant force compliant mechanism in a deflection range of 15% of the suspension span. (a) Dimensions of the double-arch suspension after shape optimization. (b) Force-deflection behavior of the double-arch suspension after shape optimization

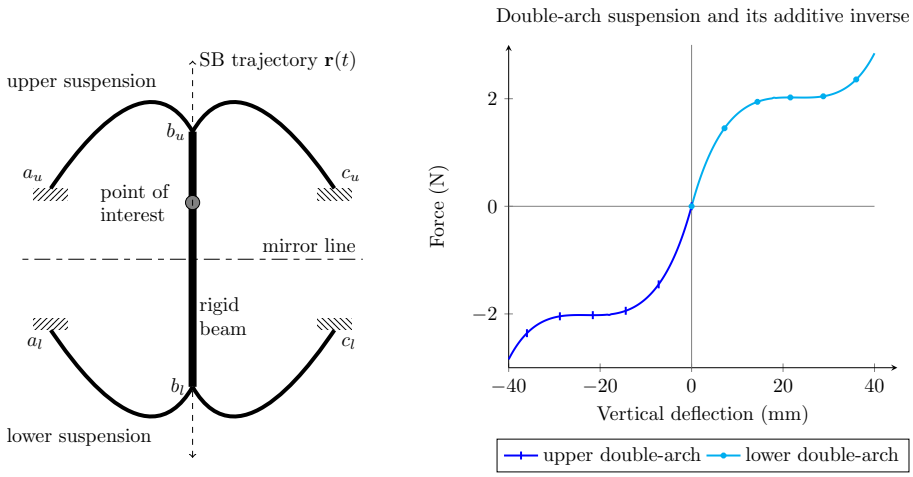

(a) (b)

Figure 6.25: Construction of the statically balanced suspension. (a) The double-arch suspension is mirrored. Both suspensions are connected avoiding relative motion at the connection point. (b) Both suspensions exhibit opposite constant force function but they do not overlap, so they do not cancel each other.

interest. If we observe the force-deflection function of each suspension at the point of interest we notice that these two functions do not overlap, so the two constant forces do not cancel each

other (Fig 6.25b). But if we displace the ground points of the two suspensions (points a_u, c_u, a_l, c_l) relative to the point of interest as shown in Fig. 6.26a and then we actuate the system as shown in Fig. 6.26b, we get the two force-deflection functions to overlap so the two constant forces cancel each other, see Fig. 6.27.

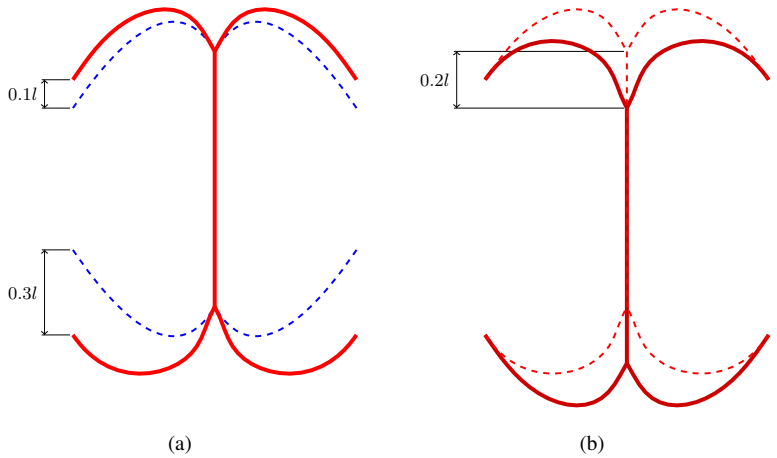

Figure 6.26: Prestressing and actuation of the compliant suspension. (a) The ground ports of the double arch suspension are displaced in order to prestress the structure. (b) The prestressed structure is actuated in a state near to static balancing.

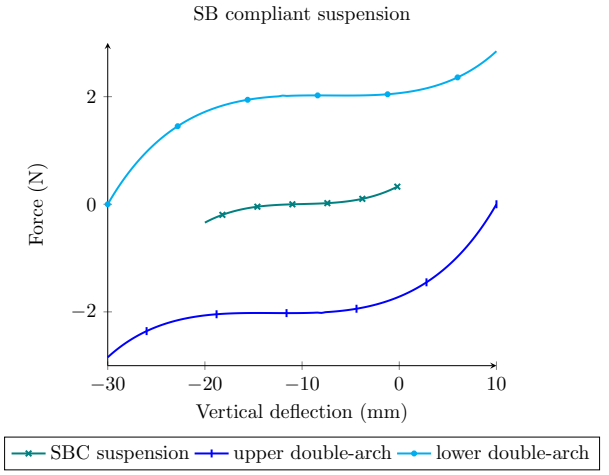

Figure 6.27: Force-deflection path of the individual modules and their combination.

From the potential energy perspective, displacing the ground points of the suspensions relative to the rigid beam corresponds to the pre-stressing of the structure. Notice from the stress distribu-

tion, how during pre-stressing most of the strain energy is concentrated at the lower suspension and after the actuation the strain energy flows to the upper suspension, see Fig. 6.28.

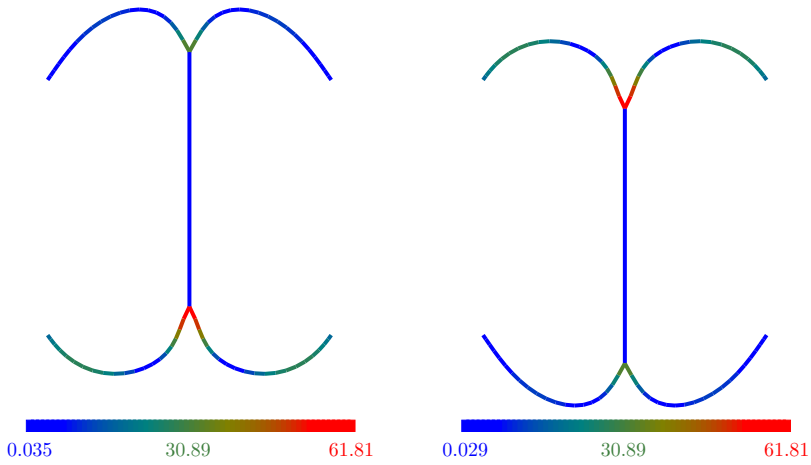

Figure 6.28: Maximum stress distribution of the compliant suspension (axial stress+maximum bending stress) in N/mm^2. (a) Stress distribution after pre-stressing and before actuation. (b) Stress distribution after actuation.

The statically balanced compliant suspension exhibits a standard deviation of 0.137 with respect to a zero force along 20mm of deflection. A comparison along the same 20mm of deflection between the statically balanced compliant suspension and one single double-arch suspension shows a reduction of 95.12% in the energy required for the actuation and a 93.12% reduction in the force RMS value.

Design of statically balanced compliant suspension - concept 2

The design of a statically balanced compliant suspension using only double-arch suspensions like the one shown in section 6.2.3 exhibits a low stiffness perpendicular to the actuation line. This means that while the suspension is actuated effortlessly, it could also move sideways. There are cases when this is an undesired effect so we need to constrain the suspension to restrict sideways motion. One solution to this problem is to include a folded-beam suspension.
To design the suspension without sideways motion, we resort to the use of continuous equilibrium as the criterion for static balancing. The use of continuous equilibrium is a consequence of the use of finite elements as the analysis method which provides results directly in terms of forces.

$$f(t) = 0 \qquad t_{\min} < t < t_{\max} \tag{6.39}$$

Here, $f(t)$ is the force function and t is the suspension deflection which defines the statically

balanced trajectory $\mathbf{r}(t)$. The force function is decomposed as the summation of two zero degree polynomials which are additive inverse, or in other words, the force is decomposed as the summation of two opposite constant force functions. In this case the constant force is not obtained from one structure, but it is created by further decomposition of the constant force function as the summation of two polynomials of first degree. These first degree polynomials are again additive inverse but in this case they are shifted, so they create a non-zero constant value.

$$f(t) = 0 = c + (-c) \tag{6.40}$$

$$c(t) = (b_1 t + c_1) + (-b_1 t + c_1) \tag{6.41}$$

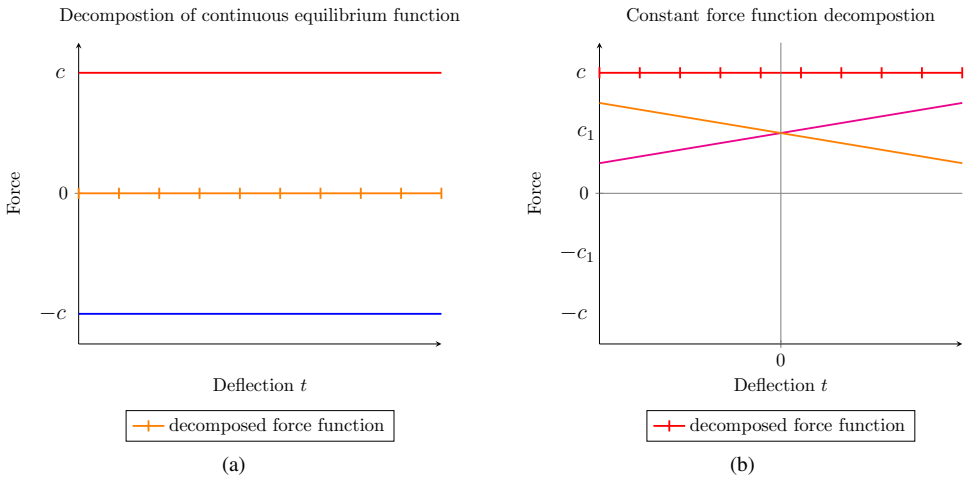

Figure 6.29: Decomposition of the continuous equilibrium function. (a) The equilibrium function as a zero degree polynomial is decomposed into two zero degree polynomials or constant values. (b) The function of a constant force is decomposed into two polynomials of first degree.

The design problem becomes a matter of finding two structures with linear force-deflection function, which when combined, create a constant force compliant mechanism. The statically balanced compliant suspension results from the combination of the constant force mechanism and its mirror structure.

A double-arch suspension is designed to provide the linear force-deflection function with negative slope (negative stiffness), while a folded-beam suspension is designed to provide the linear force-deflection function with the same slope but positive (positive stiffness) along the same range of motion.

The design of the double-arch suspension is done by using shape optimization. The design variables are the location of the moving control points of the Bezier's curve describing the arches'

geometry. The objective function is set as the linear correlation coefficient of the force function. The objective function is only computed along a section of the deflection path.

$$\begin{aligned} \min_{\mathbf{x}} \quad & r(\mathbf{x}) \\ s.t.: \quad & \mathbf{Ku} - \mathbf{f} = 0 \\ & \mathbf{x}_{\min} \leq \mathbf{x} \leq \mathbf{x}_{\max} \end{aligned} \tag{6.42}$$

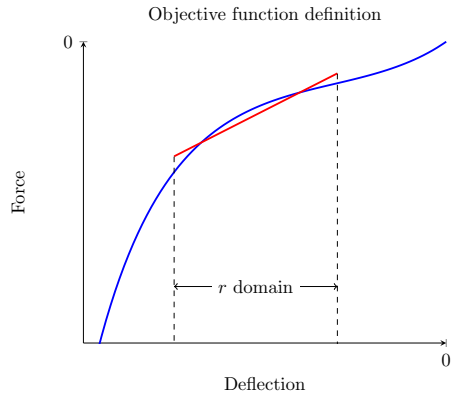

Figure 6.30: The objective function of the shape optimization is taken as linear correlation coefficient r of the force along an interval in the deflection path.

The optimization problem is solved using genetic algorithms. The objective function is computed from the deflection path obtained through the use of nonlinear finite elements. The structure is modeled by frame elements with large deflection and small strains.
Using the values presented in Tab. 6.7, the result of the shape optimization is the geometry depicted by Fig. 6.31a. The resultant structure exhibits the force-deflection function shown in Fig. 6.31b. The linear correlation coefficient for the function is 0.9987 along the interval [-20,-40]mm.

Table 6.7: Values used for the shape optimization of the SBC suspension - concept 2

Property	Value
Young's modulus E (N/mm^2)	2000
out-of-plane thickness t (mm)	5
Yield strength σ_y (N/mm^2)	75
Double-arch suspension span l (mm)	140

The folded-beam suspension is designed to provide the same linear force-deflection function but with positive stiffness for a deflection of 20mm. The stiffness of the suspension is adjusted by modifying only its height, while keeping the in-plane thickness constant. The value of the height is found by a bisectioning search within two limit values, this is bisecting the interval

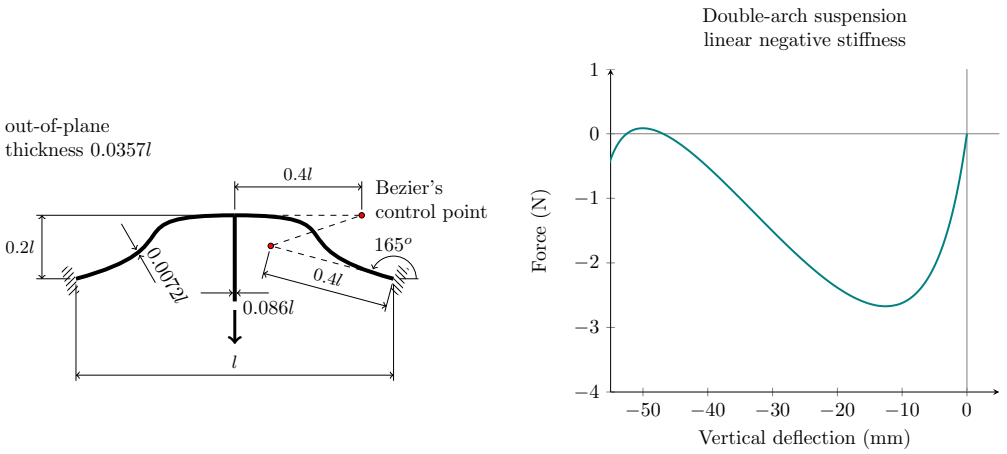

(a) (b)

Figure 6.31: The result of the shape optimization is a compliant mechanism with a nearly linear force ($r = 0.9987$) and negative stiffness along a deflection range of 14% of the suspension span. (a) Dimensions of the double-arch suspension after shape optimization. (b) Force-deflection behavior of the double-arch suspension after shape optimization

and selecting a subinterval repeatedly. The limit values are two suspension heights at which one stiffness is higher than required, while the other stiffness is lower.

The result is the folded-beam suspension with the dimensions shown in Fig. 6.32a. The folded-beam suspension can deflect in two opposite directions from its equilibrium configuration. Figure 6.32b shows the force-deflection function for the deflection in the negative direction.

Connecting the double-arch suspension to the folded-beam suspension creates a constant force compliant mechanism. The connection of the two suspensions is done through a rigid beam that avoids relative motion between the suspensions. The force-deflection function of the combined structure measured at any point along the connecting rigid beam is shown in Fig. 6.33.

Now we create the mirror structure of the combined suspension in order to obtain the additive inverse function to the constant force, see Fig. 6.34a. Notice that the folded-beam suspension in the mirror structure has been flipped. This modification has no influence on the force-deflection function but it helps to create a more compact design.

The combined suspension and its mirror structure exhibit opposite force-deflection functions, but they do not overlap along the same interval of deflection, so the forces do not cancel each other (see Fig. 6.34b).

In order to overlap the two force-deflection functions of the two combined structures, we need to apply a relative displacement between the ground ports of the structures (a_u, c_u, d_u, e_u, a_l, c_l, d_l, e_l) and the rigid beam connecting the two structures along points b_u and b_l, see Fig. 6.35a. Applying this relative displacement corresponds to the pre-stressing of the structure.

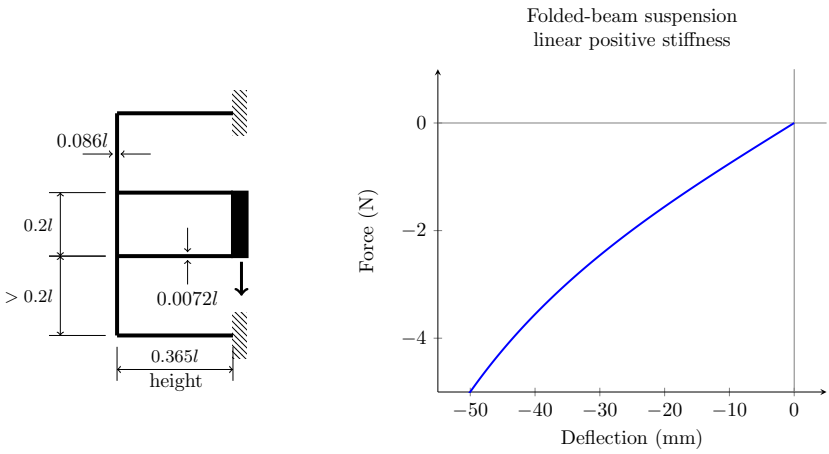

(a) (b)

Figure 6.32: The dimensions of the suspension that provide the required stiffness are found by bi-sectioning the suspension's height while keeping the in-plane and out-of-plane thickness constant. (a) Dimensions of the folded-beam suspension. (b) Force-deflection function of the folded-beam suspension. The linear correlation of the function for the deflection interval [0,-56]mm is $r = 0.9894$.

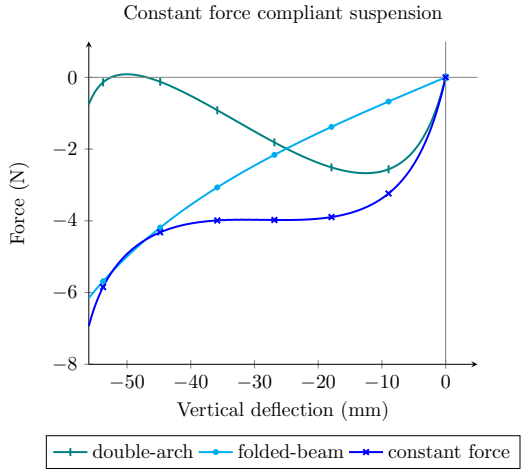

Figure 6.33: Combination of the double-arch suspension and the folded-beam suspension creates a constant force compliant mechanism.

The final result is a nearly statically balanced compliant suspension with high lateral stiffness. The stroke of the statically balanced deflection is around 20% of the double-arch suspension's span. The force-deflection function of the whole structure is shown in Fig. 6.36b. Figure 6.36a shows the force-deflection function of the four suspensions when the whole structure is actuated

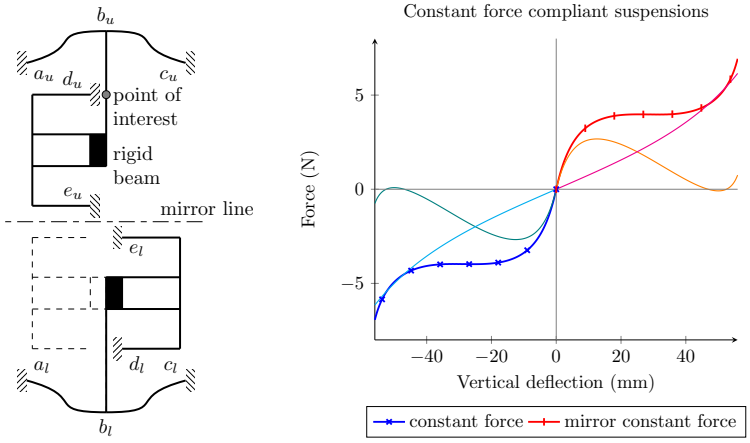

Figure 6.34: The statically balanced compliant suspension is the combination of two constant force mechanisms. (a). The combined structure and its mirror structure. (b) The two constant forces do not overlap along the same interval of deflection, hence they do not cancel each other.

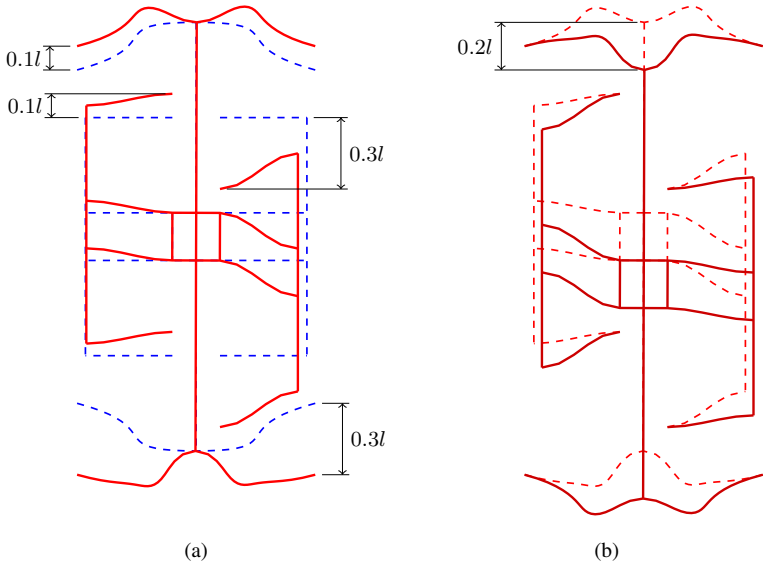

Figure 6.35: Prestressing and actuation of the compliant suspension. (a) The eight ground ports of the four suspensions are displaced in order to prestress the structure. (b) The prestressed structure is actuated in a state near to static balancing.

in a state of static balancing.

From the stress distribution it is possible to get an idea on how the strain energy builds up in

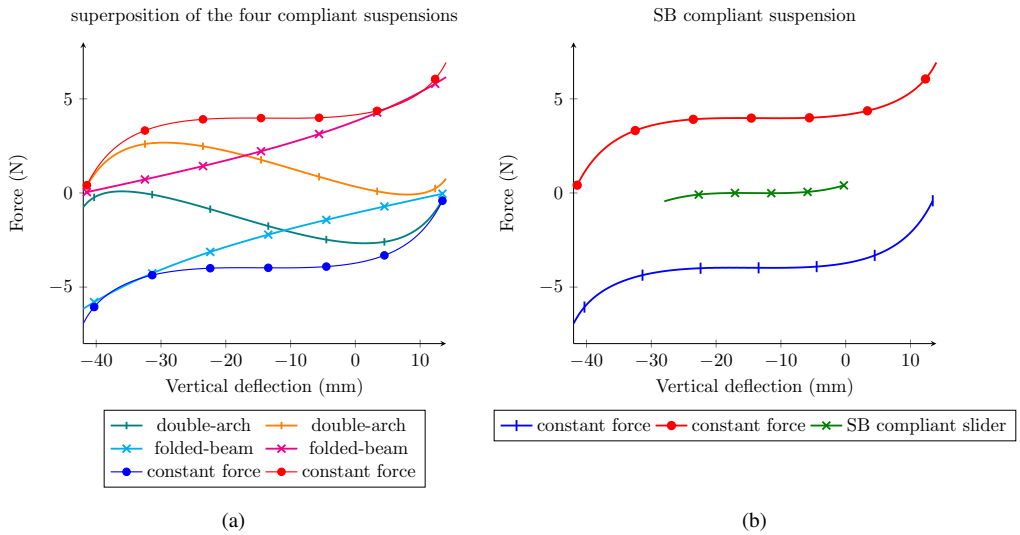

Figure 6.36: After pre-stressing the whole structure, the four force-deflection functions of the four suspensions do overlap. (a) The four suspensions are combined to create two opposite constant force functions. (b) The two constant force functions cancel each other to create a statically balanced compliant mechanism along a range of motion equal to 20% of the double-arch suspension's span.

the structure during the pre-stressing phase (Fig. 6.37a) to later flow across the structure during actuation, so throughout the stroke the strain energy remains nearly constant.

The statically balanced compliant suspension exhibits a force RMS value of 0.156N along 28mm of deflection. A comparison along the same 28mm of deflection between the statically balanced compliant suspension and one single folded-beam suspension shows a reduction of 91.39% in the energy required for the actuation and an 87.76% reduction in the force RMS value.

Design of statically balanced compliant suspension - concept 3

In the previous section, the design of a statically balanced compliant suspension with high lateral stiffness was shown. However this suspension is rather bulky and its embodiment does not lead to a slender design, so it is desirable to reduce the number of suspension modules that are used.

To design the statically balanced suspension, we use the static balancing criterion of continuous equilibrium in order to simplify the structural analysis by the use of finite elements. The continuous equilibrium expresses that force function $f(t)$ must be zero along the deflection t of the suspension. Here, the deflection t is also the parameter defining the statically balanced trajectory $\mathbf{r}(t)$.

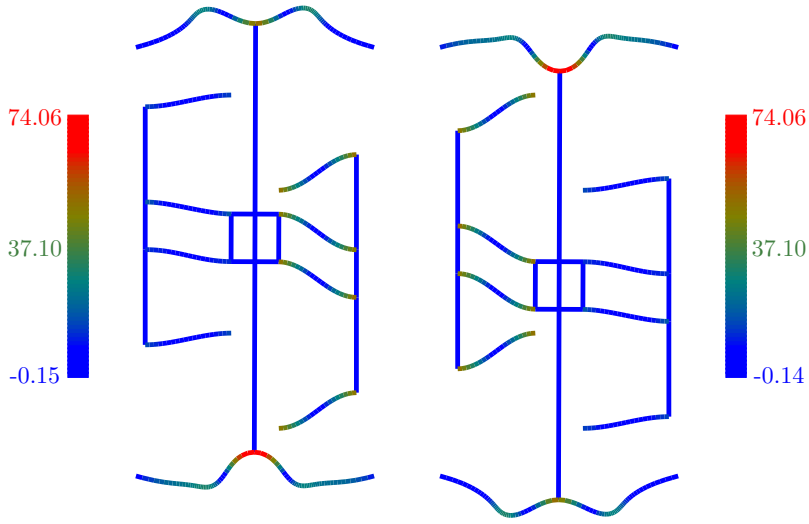

Figure 6.37: Maximum stress distribution of the compliant suspension (axial stress+maximum bending stress) in N/mm^2. (a) Stress distribution after pre-stressing and before actuation. (b) Stress distribution after actuation.

$$f(t) = 0 \qquad t_{\min} < t < t_{\max} \tag{6.43}$$

The force function is a zero degree polynomial which, in this case, is decomposed as the summation of two additive inverse first degree polynomials, as shown in Eq. 6.44 and Fig. 6.38a. The polynomials represent two opposite linear force functions, one with positive slope (positive stiffness) and the other with negative slope (negative stiffness).

Notice that the two linear functions are symmetric with respect to their x-intercept points. This kind of symmetry in a linear function has the advantage of allowing further decomposition into two linear functions with the same slope but shifted apart, as shown in Eq. 6.45 and Fig. 6.38b.

$$f(t) = 0 = a_1 t + (-a_1 t) \tag{6.44}$$

$$-a_1 t = \left(-\frac{a_1}{2}t - b_1\right) + \left(-\frac{a_1}{2}t + b_1\right) \tag{6.45}$$

To create the linear negative stiffness force function symmetrical with respect to its x-intercept, first we need to find a structure that provides a linear negative stiffness force function. Then a combination of such structure with its overlapped mirror structure will provide the desired symmetric linear force function.

To find a structure that exhibits a linear negative stiffness force function, we use shape optimiza-

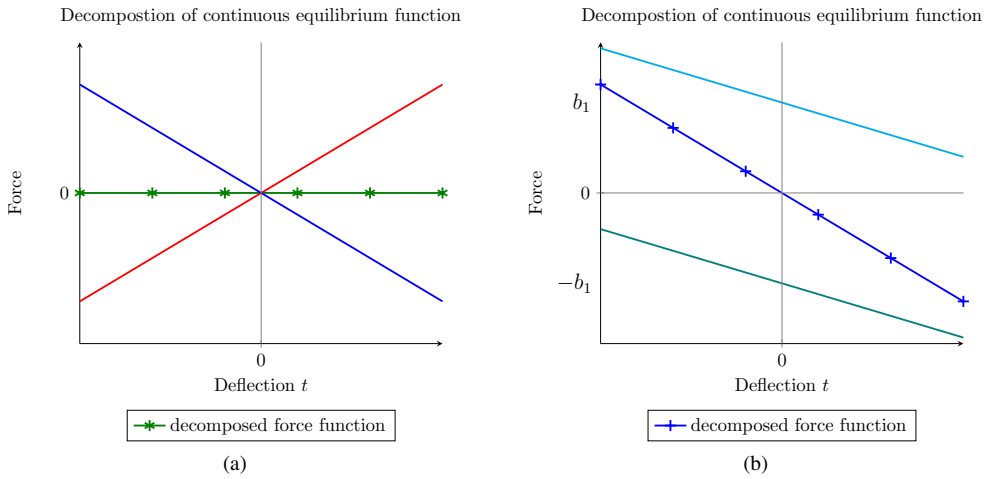

Figure 6.38: Decomposition of the continuous equilibrium function. (a) The equilibrium function as a zero degree polynomial is decomposed into two opposite first degree polynomials. (b) The force function with negative slope (negative stiffness) is decomposed into two polynomials of first degree with equal negative slope but shifted appart.

tion of a double-arch suspension. The optimization problem is solved using genetic algorithms. The design variables are defined as the location of the moving control points of the Bezier's curve describing the arches' geometry. The objective function is set as the linear correlation coefficient of the force function. The linear correlation is only computed along a section of the deflection path (see Fig. 6.30).

$$\begin{aligned} \min_{\mathbf{x}} \quad & r(\mathbf{x}) \\ s.t.: \quad & \mathbf{Ku} - \mathbf{f} = 0 \\ & \mathbf{x}_{\min} \leq \mathbf{x} \leq \mathbf{x}_{\max} \end{aligned} \tag{6.46}$$

The objective function is computed from the deflection path obtained from nonlinear finite elements analysis. The finite element problem is solved using displacement control while the structure is modeled by frame elements with large deflection and small strains.

Table 6.8 presents the values assumed in the optimization problem. Figure 6.39a shows the solution to the shape optimization problem.

To create the linear positive stiffness function symmetrical with respect to its x-intercept, we use a folded-beam suspension moving in both directions from its equilibrium point. The suspension is designed in such a way that its positive stiffness matches the negative stiffness of the combined double-arch suspensions. The stiffness of the folded-beam suspension is adjusted by modifying its height while keeping its in-plane and out-of-plane thickness constant. The value of the height is found by using a bi-sectioning search within a higher and lower limit value with respect to the

Table 6.8: Values used for the shape optimization of the SBC suspension - concept 3

Property	Value
Young's modulus E (N/mm^2)	2000
out-of-plane thickness t (mm)	5
Yield strength σ_y (N/mm^2)	75
Double-arch suspension span l (mm)	100

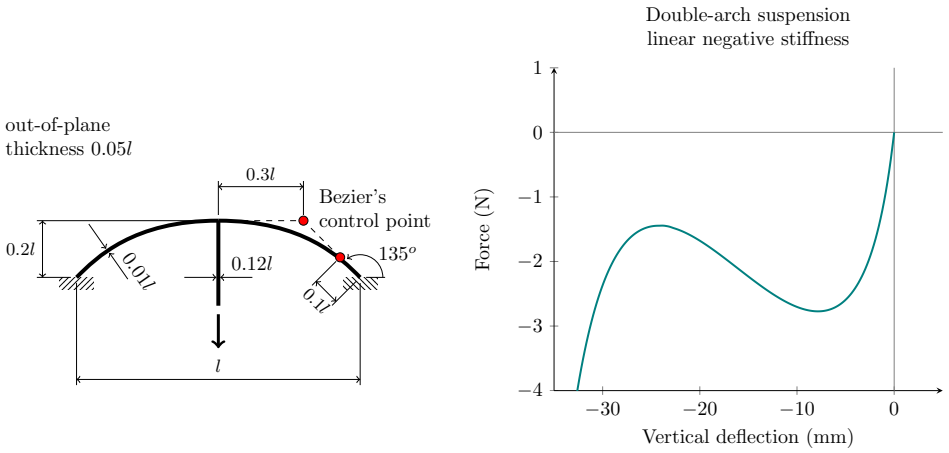

(a) (b)

Figure 6.39: The result of the shape optimization is a compliant mechanism with a nearly linear force ($r = 0.998$) and negative stiffness along a deflection range of 10% of the suspension span. (a) Dimensions of the double-arch suspension after shape optimization. (b) Force-deflection behavior of the double-arch suspension after shape optimization.

desired one.

We combine the folded-beam suspension with the double-arch suspension and its mirror structure by using a rigid beam element, as depicted in Fig. 6.41a. The rigid beam removes the relative motion with respect to the suspensions. The force-deflection function of the suspensions is measured with respect to any point along the rigid beam or point of interest. If the structure is not pre-stressed, the force functions of the three individual suspensions do not overlap along the same interval of deflection. Figure 6.41b shows the force-deflection functions of the three suspensions before pre-stressing.

If we apply a relative displacement between the ground points of the structure (points a_u, c_u, d_u, a_l, c_l, and d_l) and any point of interest, as shown in Fig. 6.42a, then the force-deflection functions of the suspensions overlap, canceling each other's forces along a range of motion of 5% of the double-arch suspension span. Figure 6.43a shows the force combination of the two double-arc suspensions, while Fig. 6.43b shows the result of combining the folded-beam suspension with

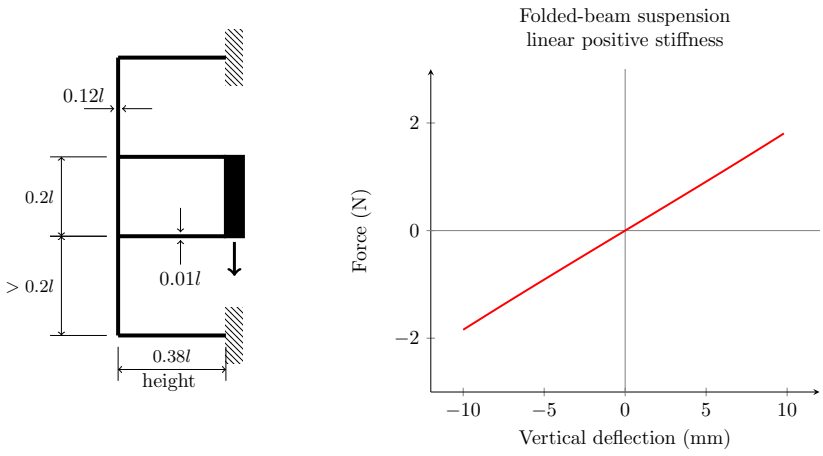

(a) (b)

Figure 6.40: The dimensions of the suspension that provided the required linear positive stiffness symmetrical with respect to its x-intercept. (a) Dimensions of the folded-beam suspension. (b) Force-deflection function of the folded-beam suspension.

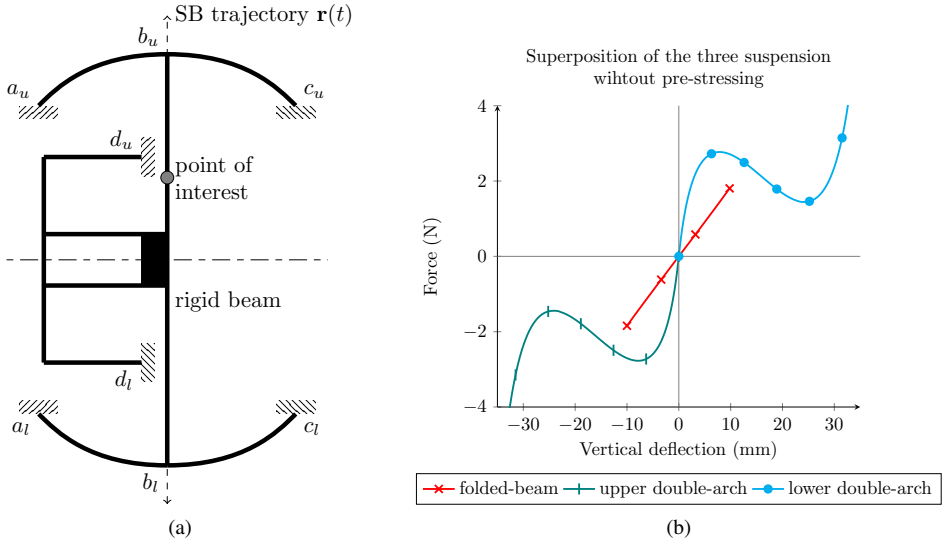

(a) (b)

Figure 6.41: Assembly of the three suspensions to create a statically balanced suspension. (a) The folded-beam suspension is connected with the double-arch suspension and its mirror structure through a rigid beam. (b) Without pre-stressing of the structure the three force-deflection functions of the suspensions do not overlap along the same interval of deflection, hence the forces do not cancel each other.

the net force of the two double-arch suspensions.

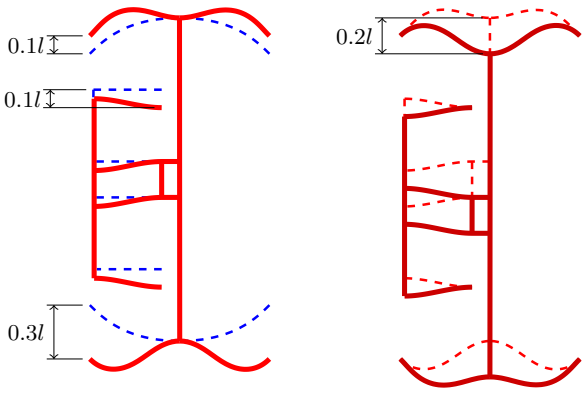

Figure 6.42: Prestressing and actuation of the compliant suspension. (a) The six ground ports of the whole suspension are displaced in order to prestress the structure. (b) The prestressed structure is actuated in a state near to static balancing.

The final result is a nearly statically balanced compliant suspension with high lateral stiffness. The suspension behaves statically balanced for about 10mm of its range of motion. Along this 10mm of deflection, the suspension exhibits a standard deviation of 0.048 with respect to zero. A comparison between the statically balanced compliant suspension and the folded-beam suspension shows a reduction of 93.86% in the energy required for the actuation and a 90.89% reduction in the force RMS value.

This suspension has a smaller number of ground points which simplifies the embodiment of the final design. The stroke of the statically balanced deflection is around 10% of the double-arch suspension's span which is shorter than the one in concepts 1 and 2. The stroke of the suspension may be increased by searching for better geometries of the double-arch suspension which provide a larger linear force-deflection function.

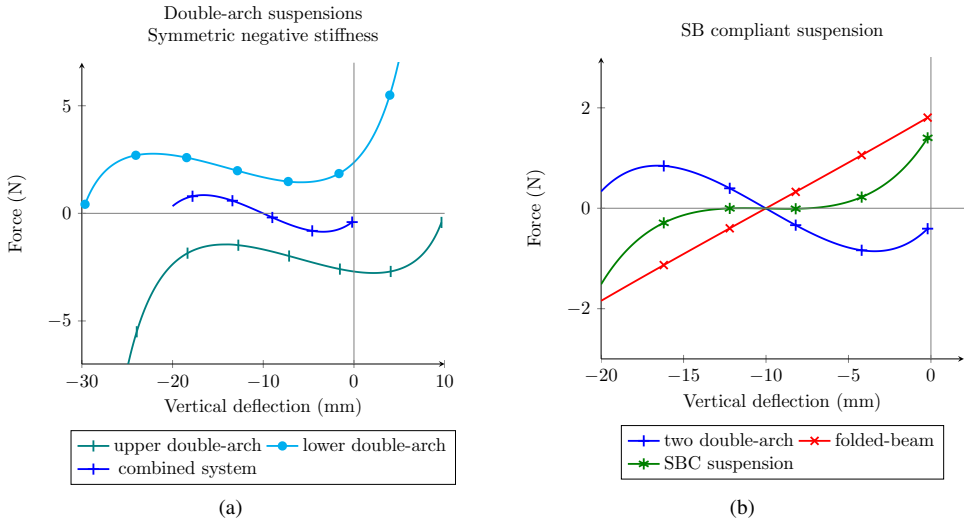

Figure 6.43: Pre-stressing of the statically balanced compliant suspension overlaps the force-deflection functions of the individual suspensions allowing for the cancellation of each other's forces. (a) Force-deflection function as a result of combining the two doble-arch suspensions after pre-stressing of the structure. (b) Force-deflection function of the pre-stressed SB compliant suspension.

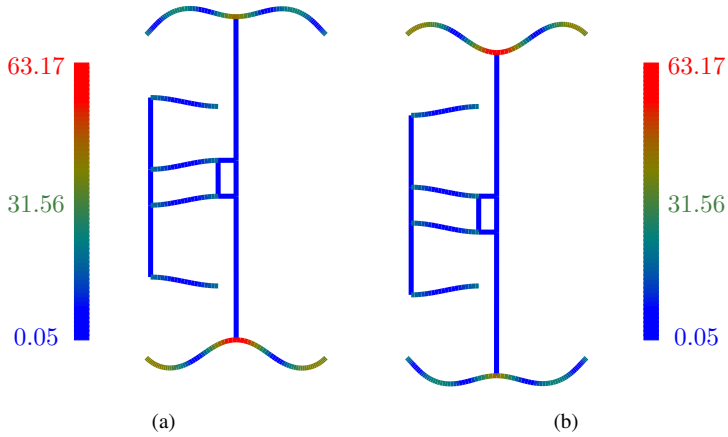

Figure 6.44: Maximum stress distribution of the compliant suspension (axial stress+maximum bending stress) in N/mm^2. (a) Stress distribution after pre-stressing and before actuation. (b) Stress distribution after actuation.

6.2.4 Modular design method for fully compliant mechanisms using SO-SO and buckling based on continuous force criterion

In this section we test a modular design method for fully compliant mechanisms that is entirely based on structural optimization (SO). Both the functional and balancing modules, are designed using structural optimization. The idea is to obtain a functional module with a given topology that is susceptible to buckling. Once this topology is found, the design is adjusted to attain a state of static balancing through observation of the continuous equilibrium criterion. Figure 6.45 depicts the design process at hand.

To know if a topology is susceptible to buckling we look for two conditions, (i) there must be straight beam elements in which their intended deflection is perpendicular with respect to their longitudinal axis and (ii) it should be possible to load these beam elements under compression without affecting the static equilibrium of the whole system. If these two conditions are met, then it may be possible to reduce the stiffness of the system and induce a state near to static balancing by either (i) buckling at critical load these beam elements or (ii) post-buckling these elements in order to induce negative stiffness that compensates for the remaining positive stiffness of the system.

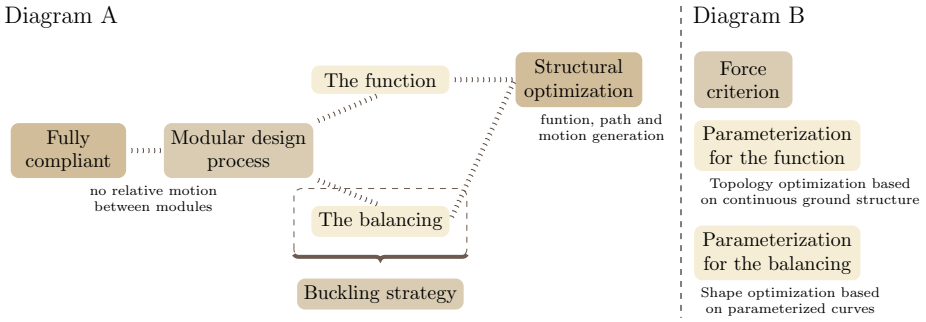

Figure 6.45: Diagram of a modular design method for fully compliant mechanisms using structural optimization and buckling based on continuous force criterion

To test this method we will use one of the benchmark examples in the design of compliant mechanisms, the inverter mechanism. The inverter takes a displacement in one direction at the input port and delivers a displacement in the opposite direction at the output port.

Figure 6.46 shows the problem setup for the inverter which is to be solved using topology optimization with a continuous ground structure parameterization. The optimization is set as the problem of maximizing the output displacement with respect to a unitary force applied at the input port. The maximization is subjected to static equilibrium of forces, a volume constraint and bounded design variables.

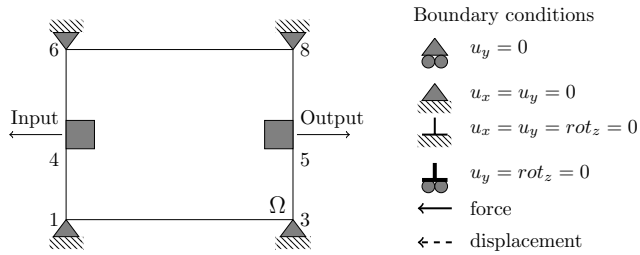

Figure 6.46: Setup of the functional design problem which is to be solved using topology optimization with a continuous ground structure.

$$\begin{aligned} \max_{\mathbf{x}} \quad & u_{out} \\ s.t.: \quad & \mathbf{Ku} - \mathbf{f} = 0 \\ & V \leq V_{\max} \\ & 0 \leq \mathbf{x} \leq 1 \end{aligned} \tag{6.47}$$

The topology optimization problem is solved using the 104 line code from Bendsoe [11]. The ground structure is taken as a mesh of 40x40 elements, with a maximum allowable volume of 30% of the total design domain. It is used a penalization factor of 3.0 with a sensitivity filtering based on radial averaging with a length of 1.2. The result of the topology optimization problem is shown in Fig. 6.47

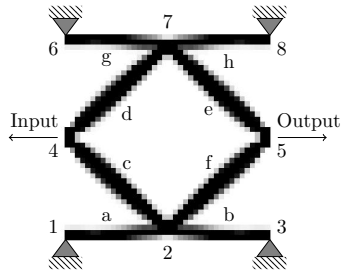

Figure 6.47: Initial design for the functional module (the inverter) using topology optimization.

This result shows that the horizontal beam elements a, b, g and h are in such configuration that it is possible to apply a compressive horizontal load to buckle these elements. The idea is to later, during actuation, use the strain energy stored in the buckled elements to help in the deflection of the rhombus formed by the elements c, d, e and f, so that the whole strain energy of the system is kept constant.

For this idea to work it must be guaranteed that during the pre-loading no energy (meaning no deflection) will be induced to the elements forming the rhombus, so the vertical deflection of

points 2 and 7 must be minimized during pre-loading. If this condition is not guaranteed, it would mean that during pre-loading the rhombus would already be deflected and later during actuation the flow of strain energy between the buckled elements and the rhombus would be inefficient or, even, no flow would be present at all.
This problem is posed as a shape optimization problem of the buckling beams a, b, g and h. The beams' shape is parameterized by the use of cubic Bezier curves (see Fig. 6.48) where the initial and final control points of each curve are fixed and the x and y position of the remaining two control points of each curve are used as the design variables.

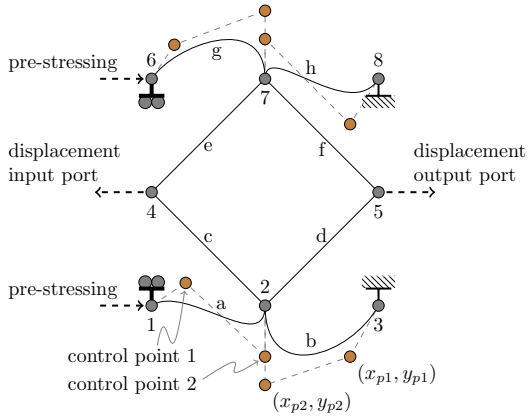

Figure 6.48: Parameterization for the optimization of elements a, b, g and h as cubic Bézier curves.

The objective function is set as the root mean square (RMS) value of the actuation force. Notice that for Eq. 5.7 in section 5.2.2, if the force vector $\mathbf{f}$ and the trajectory vector $d\mathbf{s}$ are parallel, then the equation can be set as a RMS function which attains its minimum value at zero.
The shape optimization problem is subjected to static equilibrium of forces and bounded design variables. The total deflection actuation at point 4 is 3mm while the pre-loading deflection at points 1 and 6 is 1.1mm.

$$\begin{aligned} \min_{\mathbf{x}} \quad & \mathbf{f}_{rms} \\ s.t.: \quad & \mathbf{Ku} - \mathbf{f} = 0 \\ & \mathbf{x}_{\min} \leq \mathbf{x} \leq \mathbf{x}_{\max} \end{aligned} \tag{6.48}$$

To guarantee minimum vertical deflection of points 2 and 7 during pre-loading, we look for a vertical slope of the Bézier curves at points 2 and 7 and keep points 1, 2, and 3 collinear as well as points 6, 7, and 8. The vertical slope is secured by setting the x coordinate of the moving control points next to points 2 and 7 to coincide with the x coordinate of points 2 and 7.
The optimization is solved using the genetic algorithm toolbox in Matlab with a maximum of

60 generations and a population of 20 individuals per generation. The rest of setup choices for crossover, mutation, genetic coding, initial population and elite count are set to their default values. In order to keep symmetry, the optimization algorithm is run with only three design variables corresponding to one Bézier curve (x_{p1}, y_{p1}, y_{p2}), the other nine variables from the remaining three curves are mirror values with respect to the vertical and horizontal symmetry axes 2-7 and 4-5, respectively.

The objective function of each individual in the genetic algorithm is computed from a finite element static analysis for large deflections and small strains. The solution is done through the use of displacement control in two load steps with 50 substeps each, where the first step is the pre-loading and the second step is the actuation. The structure is modeled using a co-rotational total lagrangian formulation for planar nonlinear frame elements (see Mankame [81]).

The result of the shape optimization is shown in Fig. 6.49. Without losing accuracy, the shape of the buckled beam is a curve that can be simplified into a half ellipse where the minor axis is $1/8$ times the major axis.

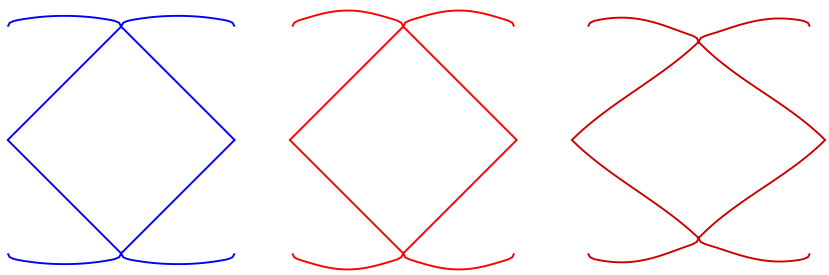

Figure 6.49: (a) Undeformed shape of the inverter without prestressing. (b) Deformed shape of the inverter after prestressing without actuation. (c) Deformed shape of the inverter during actuation in a state of quasi-static balancing.

The force-deflection path of the inverter's input port (point 4) is shown in Fig. 6.50a. A comparison of the force-deflection path for the inverter before and after pre-loading is shown in Fig. 6.50b. Comparison of the areas under the force-displacement curves in Fig. 6.50b shows a theoretical reduction of 94.28% in the actuation energy for the range of motion [0,-3]mm. If we only consider the range of motion [0,1.65]mm, then the reduction increases to 97.76%.

One problem found with the design is that due to its symmetry, the structure is likely to deflect during pre-loading into its first buckling mode which does not match the desired behavior. The first buckling mode corresponds to a vertical displacement of the rhombus at the center of the structure. The desired behavior corresponds to the second buckling mode, see Fig. 6.51. The linearized pre-buckling analysis shows that the vertical displacement of the rhombus during pre-loading is more likely to occur as compared to the desired behavior. The predicted buckling load

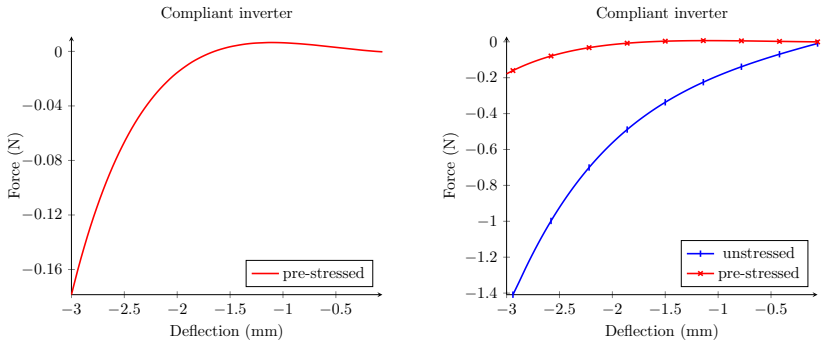

(a) (b)

Figure 6.50: Inverter's force vs displacement behavior at the input port. (a) Behavior of the inverter after pre-loading. (b) Comparative behavior of the inverter before and after pre-loading. The pre-loaded configuration exhibits a strain energy reduction in actuation of 94.28%.

of the first mode is 56% lower with respect to the buckling load of the second mode. To obtain the correct behavior it is necessary to constrain the respective downward and upward motion of points 2 and 7.

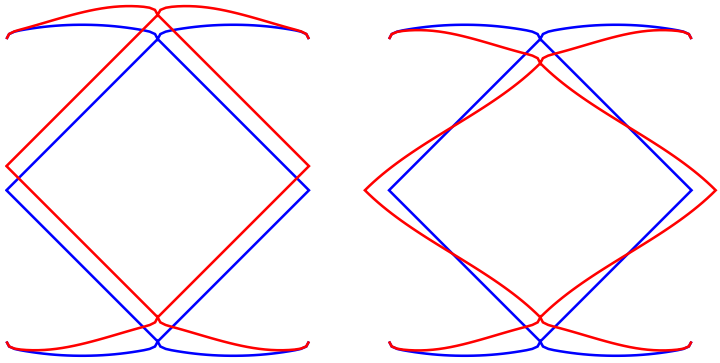

(a) (b)

Figure 6.51: Inverter's buckling modes predicted by linearized pre-buckling analysis of the inverter. (a) First buckling mode showing a vertical displacement of the rhombus. (b) Second buckling mode which is the desired behavior.

6.3 Summary

In this chapter we presented a design methodology from which is possible to derive design methods for statically balanced compliant mechanisms (Fig. 6.2). The design methodology is based on what is called as the seven *recurrent elements*:

- Compliancy type
- Classification of the functional requirements
- Modularity of the mechanism
- Static balancing strategy
- Modularity of the design process
- Design methods for compliant mechanisms
- Static balancing criteria

The proposed methodology is meant to be used in the design of planar structures where their statically balanced workspace corresponds to a line trajectory, although some of the derived design methods are not entirely limited to such dimensionality. For instance, the design methods based on rigid-body-replacement may provide SBC spatial mechanisms as long as the spatial rigid body mechanism can be converted into a compliant one.

The fact that the methodology is based on the recurrent elements helps the designer to consider a priori the available analysis tools and the basic requirements that most influence the design process and the final design. When the designer is able to consider all of these elements, then the selected design method allows to foresee the entire design process as well as the design space in which the solution lies.

Several examples were developed in detail in order to provide acquaintance with the design methodology. Each example tries to show in context how the design methods for compliant mechanisms are combined with some of the static balancing criteria and how the static balancing criteria can be implemented through the use of the static balancing strategies.

For instance in the example presented in section 6.2.2, one of the key ideas is to show the challenges that come from the application of the replacement methods. The example shows how the conversion of rigid body joints into compliant flexures is performed in a way that the resultant flexures, without overcoming the yield strength limit, provide the compliant mechanism with the proper kinematics and stiffness.

The examples presented in sections 6.2.4 and 6.2.3 show buckling and function decomposition, respectively, as the conceptual strategies for the static balancing of compliant mechanism.

The use of design examples also intends to show the non-linear nature of statically balanced compliant mechanisms and the high dependency of static balancing of, (i) the boundary conditions applied to the structures and (ii) the way the structures are pre-stressed using either forces or displacements.

7 Topology Optimization of Statically Balanced Compliant Mechanisms

A computer will do what you tell it to do, but that may be much different from what you had in mind.
Joseph Weizenbaum

In this chapter, we explore more deeply the possibilities of using topology optimization as a design method for planar statically balanced compliant mechanisms (SBCM's), limited to designs with functional requirements categorized as function generation. The optimization problems in this work are solved by the use of genetic algorithms and based on partial ground structure parameterization. To achieve static balancing characteristics, in this chapter we introduce two optimization formulations based on the ideas of (i) neutral stability, through the use of buckling modes resulting from linear pre-buckling analysis, and (ii) continuous equilibrium, through the use of static analysis for large deflections. The selection of these two statically balanced criteria is explained in section 7.3.

Topology optimization as a sub-class of design optimization is an iterative design method in which functional and non-functional requirements are set through the objective function, constraints and parameterization. The link between requirements and optimization is done through the conceptual framework of mechanisms as design objects introduced in chapter 2 (Fig. 2.10). In this framework it was said that compliant mechanisms must perform their main function —here some sort of function generation— while they meet the functional characteristic of *statically balanced* and the product characteristic of *monolithic*.

If we apply these three elements from the design framework of mechanisms —main function, statically balanced and monolithic— into optimization as an iterative design method we see that (i) the function generation problem (the main function) can be defined as the optimization's objective function, (ii) the static balancing characteristic can be set as constraints, and (iii) the product characteristic of monolithic can be reflected in the parameterization.

In the following sections we expand the ideas about these relations between the function generation problem and characteristics with the objective function, constraints and parameterization.

First, section 7.1 introduces the view and definitions assumed in this work about design optimization, structural optimization and topology optimization. Sections 7.2, 7.3 and 7.4 present of the objective function, the constraint functions and the parameterization. Subsequently section 7.5 presents the entire optimization setup and, finally, the results and discussion are presented.

7.1 Topology optimization, structural optimization and design optimization

Topology optimization and structural optimization are a form of design optimization. Design optimization is a design method that automates the search for the design that best fulfills the design requirements. The automated search is based on finding the minimum value of a cost function f, while keeping a set of constraints expressed as equalities $\mathbf{h}$, inequalities $\mathbf{g}$ and boundaries $\mathbf{lb}$ and $\mathbf{ub}$ of the design variables.

$$\begin{aligned} &\underset{\mathbf{x}\in\Omega}{minimize}\, f(\mathbf{x}) \\ &\textit{subject to} \\ &\quad \mathbf{h}(\mathbf{x}) = \mathbf{0} \\ &\quad \mathbf{g}(\mathbf{x}) \leq \mathbf{0} \\ &\quad \mathbf{lb} \leq \mathbf{x} \leq \mathbf{ub} \end{aligned} \tag{7.1}$$

The cost function or objective function is defined in a way that at its minimum, the function provides an optimum configuration of the design variables. The design variables are the domain of the objective function and constraint functions. When the design variables assume values, they model a candidate solution inside the design search space. The way these variables model and represent the design solution is called the parameterization.

By way of illustration, imagine that you want to find the trapezoid-like structure with the lowest weight, which can withstand a force while allowing for the minimum deflection in the elastic range, Fig.7.1. We could choose to remove the unnecessary material using a circular mask defined in terms of its position and radius. By doing so, we would be parameterizing the problem in terms of three variables, x_1, x_2 and x_3, representing the mask x and y position and its radius r, but we would also be limiting the design space to the solutions that the parameterization can express.

The view of design optimization as a design method can be contemplated when we consider the iterative design cycle, Fig. 7.2. In this view, setting the requirements corresponds to defining (i) the functional requirements which are expressed mathematically as the objective function, and (ii) the product characteristics and design constraints which are expressed mathematically as equalities, inequalities and boundaries of the design variables.

The synthesis step is performed when the optimization procedure assigns values to the design

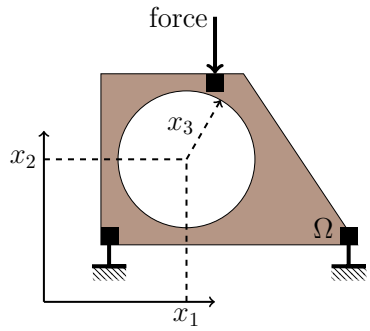

Figure 7.1: Example of a parameterization where the optimum design is described in terms of three design variables. The three variables determine the size and x and y location of the circular mask representing an internal material void.

variables without violating their boundaries. At this step, candidate solutions are proposed.

The analysis step is performed by evaluating the objective function, equalities and inequalities at the point given by the assumed values of the design variables in the synthesis step. The performance of the candidate solution is analized from the perspective of the requirements expressed as the objective function and constraints.

The evaluation step verifies if the objective function value from the analysis is, in fact, the minimum and if the equalities and inequalities have not been violated. If these verifications are found to be false, the design cycle is iterated. If they are found to be true, then the assumed values of the design variables at the last synthesis step define the design solution.

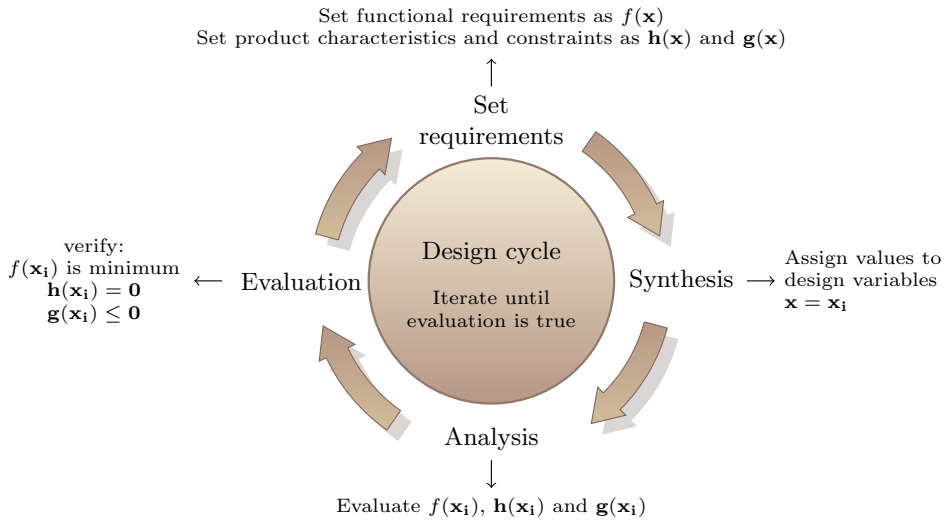

Figure 7.2: Design optimization as a cyclic design method.

In the case of structural optimization and topology optimization, the design object is a structure. By structure we mean an arrangement of bodies assembled in such a way that they perform a given function over a system of forces. By this definition, a rigid body mechanism and a compliant mechanism are structures with the function of transmitting and/or transforming forces, while a static structure has the function of supporting loads.

Generally speaking, structural optimization is a design method used to find optimal material distributions in a structure to ensure a desired behavior, while topology optimization is a design method used to find optimal connectivities among the constitutive elements of a structure in order to achieve a desired behavior.

To illustrate the difference between structural optimization and topology optimization, we observe that the behavior of a structure is determined by the material properties and the geometrical properties. Geometrical properties are defined in terms of sizes, shapes and topologies. This means that in structural optimization, finding the material distribution is to find the location and values of the material properties as well as the sizes, shapes and topologies.

On the other hand, in topology optimization we do not look directly for a material distribution but for the connectivity of the constitutive elements and, depending on how the constitutive elements are defined, their connectivity might or might not determine the location and values of the material properties as well as the shapes and sizes. The way the constitutive elements are defined and parameterized, delimits the material distribution problem in a topology optimization. Think for example of a problem where the constitutive elements are defined as bar elements with given shape and size, Fig.7.3a. It does not matter how you connect these elements, the diversity on shapes and sizes of the overall structure is limited. But if, in the same problem, the constitutive elements are defined as small square elements, Fig.7.3b, then it is possible to describe similar structures where the shapes and sizes can be modified to some extent.

Topology optimization methods search for the connectivities mainly as an existence/nonexistence problem of the constitutive elements inside a universal structure where all the possible and allowed connections are already defined. Here the design variables are normally defined as (i) a set of discrete variables defining the possible states of existence, typically binary variables 0 or 1, or (ii) as continuous variables defining some material or geometrical property like Young's modulus, density, width, thickness, etc [119][76]. In the case of continuous variables when their value is zero, they set the nonexistence state of the constitutive elements. This approach transforms the topology optimization problem to a size optimization problem.

A topology optimization can be used to perform a structural optimization, by properly defining the constitutive elements. However, topology optimization does not necessarily lead to a structural optimization, when the existence/nonexistence state of constitutive elements does not modify the shapes and sizes.

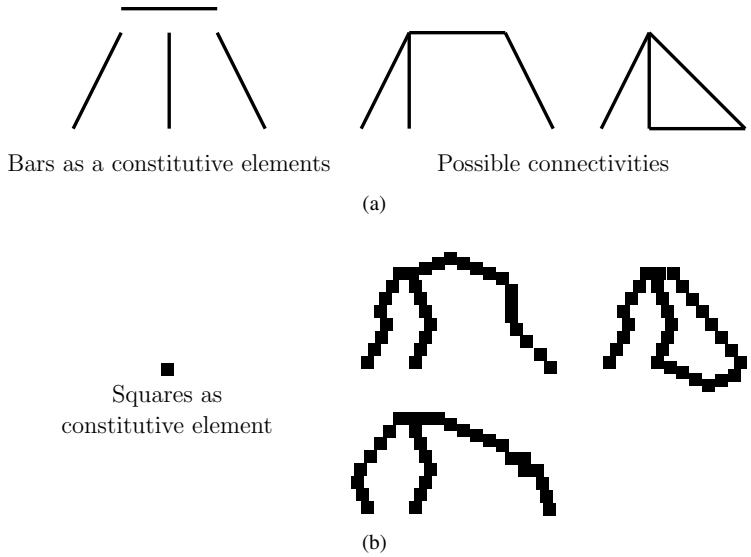

Figure 7.3: (a) Four bars as constitutive elements. This definition limits the structure diversity in shape and size. (b) 30 square elements as constitutive elements can define similar structures with some diversity in shapes.

7.2 The objective function

For the topology optimization problem we need to set the main function of the mechanism — some sort of function generation or relation between input and output— as the objective function for the optimization problem. We need to find a mathematical expression which, at its minimum or maximum, expresses that the mechanism accomplishes its intended purpose.

In chapter 3.4.2, it was shown that most of the objective functions for the design of compliant mechanisms attempt to adjust the conflicting requirements of stiffness and flexibility. Maximization of the force transmission between input and output, and maximization of the flexibility (maximum deflection with minimum force) are desired. Viewing compliant mechanisms as structures, stiffness ensures the ability to withstand the reaction forces, while flexibility ensures the motion of the structure.

Stiffness, in most of the cases, is achieved by the minimization of the strain energy (SE) [27] or by the inclusion of a spring at the output port simulating the stiffness of the workpiece [126]. The inclusion of the spring makes the mechanism to account for the reaction forces during the optimization process.

Flexibility is achieved through the maximization of the geometrical advantage (ratio between displacements at the output and the input).

$$GA = \frac{u_{output}}{u_{input}} \tag{7.2}$$

In some formulations, this geometrical advantage is expressed directly [126] while in some others it is expressed as the mutual potential energy (MPE) between the actuating force at the input and a dummy load at the output [27].

$$MPE = \Delta\mathbf{v}^T\mathbf{K}\Delta\mathbf{q} = \Delta\mathbf{v}^T\Delta\mathbf{f} = \Delta\mathbf{f}_d^T\Delta\mathbf{q} \tag{7.3}$$

Here, $\Delta\mathbf{q}$ is the displacement field caused by the actuating force $\Delta\mathbf{f}$ at the input, while $\Delta\mathbf{v}$ is the displacement field due to the dummy load $\Delta\mathbf{f_d}$ acting at the output. $\mathbf{K}$ is the stiffness matrix.
For the case of statically balanced compliant mechanisms, it is not possible to ensure the ability to withstand the reaction forces by minimizing the strain energy simply because it goes against definition 5.1, which states that a SBCM must exhibit constant strain energy along the statically balanced motion. Besides, in chapter 2.1, we stated precisely that static balancing is another way to address the strain energy storage problem without the need to minimize the strain energy.
The use of a spring at the output port will not be considered. The evaluation of the static balancing quality on the mechanism is done by observing the reaction forces at the input, which ideally must be zero. The inclusion of the spring at the output would add noise to this observation.
On the other hand, the use of the MPE to ensure flexibility is also excluded due to two problems, (i) Maximization of the MPE promotes flexibility when the deflection of the structure is induced by the application of forces. The change in force $\Delta\mathbf{f}$ or $\Delta\mathbf{f_d}$ is assumed constant, leaving no other option than to maximize the MPE by maximizing the deflection. However, in SBCM, we rather apply displacements than forces since the actuation forces are supposed to be zero. So, if the deflection of the structure is induced by nodal displacements, those displacements become constant, leading for the optimization to maximize the MPE by maximizing the input force, thus promoting rigidity rather than flexibility. (ii) The second problem comes from remembering proposition 5.3, where it was stated that a SBCM must exhibit a singular semi-positive definite matrix in which the displacement vectors belong to the null space of the stiffness matrix and they are spanned by the eigenvectors $\mathbf{u_{0_i}}$ with zero eigenvalues. So, if the stiffness matrix becomes singular semi-positive definite, the change in force would be zero meaning that the MPE would be zero no matter the change in deflection, therefore impeding the maximization of the MPE. In other words, if the state of static balancing is achieved, there is no way to know if the compliant mechanism is becoming more flexible or not.
To achieve flexibility, we are left only with the option of maximizing the geometrical advantage (GA) as expressed by Eq. 7.2. However, we need to remark that the displacement values to compute the GA can come from two different sources. In the first one, which is the conventional source, displacement values are given by the solution of a static analysis. These values are absolute displacements contained in the displacement field. In the second source, displacement

values are given as proportions between the displacements. This results when the displacement field is contained in the null space of the stiffness matrix.
For the cases when a specific value of geometrical advantage is required, it is proposed to set the objective function $f(\mathbf{x})$ as,

$$f(\mathbf{x}) = \sin(\alpha\theta) \tag{7.4}$$

where α is a correction factor and θ is the actual GA expressed as the orientation angle of a vector v. The components of such vector are the values of the displacement at the input and output port (see Fig. 7.4).

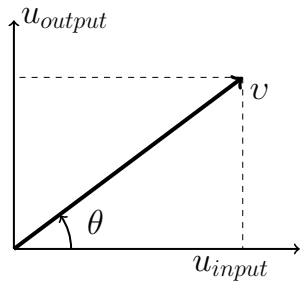

Figure 7.4: Displacements at the input and output port seen as components of a vector, which defines a fixed value of geometrical advantage.

The idea is as follows, by defining a desired GA we are defining the orientation angle θ_d of vector v.

$$\theta = \arctan\left(\frac{u_{output}}{u_{input}}\right) \tag{7.5}$$

Notice that Eq. 7.5 is used to compute both θ and θ_d. Once we know the desired orientation angle θ_d, we compute the correction factor α.

$$\alpha = \frac{\pi}{2\theta_d} \tag{7.6}$$

The correction factor α guarantees that the objective function in Eq. 7.4 has a maximum of 1 only when the actual GA expressed by θ is equal to the desired GA expressed by θ_d. Any other value of GA during the optimization will decrease the objective function.
For the case when the displacements are in relative proportions, i.e., displacements computed as eigenvectors, it is not possible to control the sign of the displacements by setting vector v in a specific quadrant of the Cartesian plane (for instance, input displacement positive while output negative). In this case, we define vector v only in the first quadrant and, by adding a (+) or (-) sign to Eq. 7.4 we control whether the displacements have the same orientation or are opposed

respectively. Be aware that if the maximization problem is posed as a minimization problem, this sign convention is inverted.
Here we have proposed the objective function expressed in Eq. 7.4, which allows for the design of compliant mechanisms with a desired geometrical advantage.

7.3 The static balancing constraint

It has been shown that static balancing is not a functional requirement but a functional characteristic that constrains the behavior of the system. We want to express the characteristic of *statically balanced* as a constraint in the optimization formulation. Mathematically this constraint can be expressed as constant potential energy, continuous equilibrium, neutral stability, zero natural frequency, constant speed or continuous zero virtual work, see chapter 5.
Assuming that during the optimization design cycle (Fig. 7.2), the analysis step is performed through the use of Finite Elements Analysis (FEA), the natural choice for the formulation of the static balancing constraint is related to the criterion of continuous equilibrium and/or neutral stability. The choice of the constraints comes by observing that the Finite Element Method (FEM) formulates the deflection problem of a structure in terms of the stiffness properties of the constitutive elements. The material and geometrical properties (topology, shapes and sizes) are collected into one global stiffness matrix which when combined with a set of known displacements, allows for the prediction of the forces or vice versa.
The use of one of these two static balancing constraints means that the optimization problem is approached from either of two perspectives, (i) to verify or (ii) to guarantee. After the analysis at the evaluation step, we could verify that the system is statically balanced, or during the analysis step prior to the evaluation, we could guarantee that FEA results provide with a statically balanced system. In the development of this work, we explore both perspectives, *to verify* and *to guarantee*. For a constraint based on neutral stability we explore the *to guarantee* perspective as a way to secure feasible solutions and get acquainted with the specifics of the approach, while for a constraint based on continuous equilibrium we explore the *to verify* perspective.

7.3.1 Neutral stability constraint

From proposition 5.3, we know that for a discretized system expressed in terms of a stiffness matrix, singular semi-positive definiteness is a necessary but not sufficient condition for neutral stability. Guaranteeing a state of neutral stability is not easy, so we trade certainty for the promise of neutral stability by guaranteeing the singular semi-positive definiteness of the stiffness matrix.
A way to ensure that the stiffness matrix is singular semi-positive definite is by solving the deflection problem as a generalized eigenvalue problem.

Assuming that the system is at the first equilibrium state, the stiffness matrix can be expressed as,

$$\mathbf{K} = \mathbf{K}_l + \mathbf{K}_\sigma \tag{7.7}$$

where $\mathbf{K}_l$ is the linear elastic stiffness matrix, which is independent of loads and deflections, and $\mathbf{K}_\sigma$ is the stress stiffness matrix at the first equilibrium state. Matrix $\mathbf{K}_\sigma$ is a function of the applied load and accounts for the stresses induced on the structure. The generalized eigenvalue problem is set as,

$$(\mathbf{K}_l - \lambda_f \mathbf{K}_\sigma)\,\mathbf{u} = \mathbf{0} \tag{7.8}$$

Equation 7.8 describes what is called eigenvalue buckling or linearized prebuckling analysis [20][154]. Here, the eigenvectors $\mathbf{u}$ are the buckling modes and the eigenvalues λ_f are the load factors. The i^{th} load factor λ_f defines the critical buckling load p_{cr} of the i^{th} buckling mode as a proportion of the applied load p used during the analysis.

$$p_{cr} = \lambda_f p \tag{7.9}$$

We are interested only in the lowest eigenvalue associated to the first buckling mode. Notice that if, during the analysis, the structure is deflected using a unitary load ($p = 1$), then the load factor is equal to the critical buckling load required to take the structure into a state of zero stiffness. The buckling mode $\mathbf{u}$ is precisely the eigenvector $\mathbf{u_0}$ that spans the null space of the stiffness matrix. This is observed if we redefine the stiffness matrix in Eq. 7.7 as,

$$\mathbf{K} = \mathbf{K}_l + \lambda_f \mathbf{K}_\sigma \tag{7.10}$$

then, substituting Eq. 7.10 into Eq. 7.8,

$$\mathbf{K}\mathbf{u} = \mathbf{0} \tag{7.11}$$

we see that the buckling mode $\mathbf{u}$ is in the null space of $\mathbf{K}$ and is also and eigenvector associated to a zero eigenvalue in the solution of the problem

$$\mathbf{K}\mathbf{u} = \lambda\mathbf{u} \tag{7.12}$$

The static balancing constraint is included in the analysis by performing a linearized prebuckling analysis rather than a static analysis. Here it is necessary to remark two implications on the constraint imposed in this way, (i) the analysis, while nonlinear in essence, is linear with respect to the deflections, and (ii) the condition leads to a zero stiffness solution but does not guarantee the equilibrium condition required in a neutrally stable state.

The aforementioned means that the optimization using the static balancing constraint imposed on the analysis could lead to either statically balanced systems or constant force systems, but, as mentioned in chapter 6, constant force mechanisms are building blocks in the design of statically balanced systems.

7.3.2 Continuous equilibrium constraint

In this section, we present the static balancing constraint based on continuous equilibrium. The constraint is used to verify the static balancing quality of the synthesized solution during the optimization.

Definition 5.2, which defines static balancing as a state of continuous equilibrium, is expressed mathematically by Eq. 5.9

$$0 = \int_s \left| f_i \frac{\partial \mathbf{r}}{\partial q_i} dq_i \right| \quad \text{where} \quad \int_s \frac{\partial \mathbf{r}}{\partial q_i} dq_i > 0 \tag{5.9}$$

where f_i are the force components tangent to the statically balanced trajectory $\mathbf{r}(\mathbf{q})$. If we define the trajectory $\mathbf{r}$ as the motion of a specific DOF q_a on a finite element mesh (for instance the x DOF of the input port), we get

$$\mathbf{r} = q_a \tag{7.13}$$

Now, applying Eq. 5.8 on Eq. 7.13, we find that,

$$\frac{\partial \mathbf{r}}{\partial q_a} dq_a = dq_a \tag{7.14}$$

where equation 5.9 becomes

$$0 = \int_{q_{a1}}^{q_{a2}} |f_a dq_a| \quad \text{where} \quad \Delta q_a > 0 \tag{7.15}$$

Equation 7.15 is the constraint equation to be used in order to verify the state of static balancing during the optimization process. This equation can be simplified for a discrete force function rising from the solution of a nonlinear finite element analysis as

$$0 = \sqrt{\sum (f_a)^2} \tag{7.16}$$

This is done by assuming equally spaced time steps in the solution and by replacing the absolute value function for the square root of a series of squares.

7.4 The parameterization

Parameterization as such, is the way in which a model is described in terms of a set of parameters. In design optimization, the model represents the set of solutions of the design search space. A given parameterization constrains the solution space to only the solutions that can be described in terms of the parameters. The parameterization bounds the domain of the objective function. In the following paragraphs, we define a parameterization which guarantees a mechanism design with the product characteristic of *monolithic*.

In structural optimization, an ideal parameterization gives the most with the fewest. It should provide with the most amount of possibilities to describe topologies, shapes and size by using the fewest amount of parameters. Normally, the parameters are the design variables on which the designer can exert control.

Here we use a partial ground structure of frame elements parameterized in terms of binary design variables (see Fig. 7.5). The design variables determine the existence state of a frame element by taking values of 0 or 1.

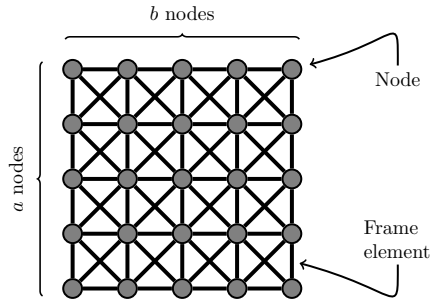

Figure 7.5: Partial ground structure composed of frame elements.

The number of design variables on a partial ground structure of $a \times b$ nodes is equal to the number of elements connecting the nodes, and is given by

$$4ab - 3a - 3b + 2 \tag{7.17}$$

The number of possible permutations described by a binary ground structure is

$$2^{(4ab-3a-3b+2)} \tag{7.18}$$

However, not all possible permutations represent valid structures. Therefore, during the synthesis step, it is necessary to guarantee that only valid structures are generated. A valid structure exhibits two characteristics, (i) the presence of only one connected component (no disconnected

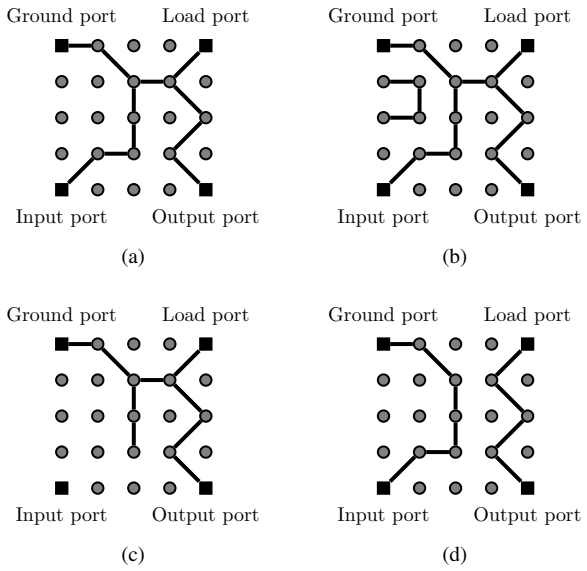

Figure 7.6: Validity of a structure seen as a graph. (a) Valid structure, one connected component and four ports connected. (b) Invalid structure, two connected components. (c) Invalid structure, disconnected port. (d) Invalid structure, two connected components and disconnected ports.

elements in the FE mesh), and (ii)inclusion of at least one walk in the component connecting the essential ports (input, output, load and ground port).

In graph theory, a component is a subgraph where an existing walk connects the vertices to each other. A walk is a sequence of vertices (the nodes) connected by edges (the elements) while a path is a walk along which vertices and edges are distinct [139].

We will verify the number of connected components in a graph and the connectivity of essential ports by using a modification of the Warshall's algorithm for undirected graphs. There are search algorithms such as Tarjan's or Depth-first search, which allow for the computation of the number of components as well as the nodes' associations to components [23]. While these search algorithms are efficient in the analysis of a directed graph, Warshall's algorithm is simpler to implement for a undirected graph and, as will be shown, we do not need to know the number of graph components and their structure.

Warshall's algorithm for undirected graphs computes the whole graph's connectivity by tracking the connections in the adjacency matrix and updating these connections into a connectivity matrix $\mathbf{P}$ in which the entry $p(i,j)$ is either 1 or 0, indicating the existence or not of a path between node i and node j, see appx. A.

The fact that Warshall's algorithm counts individual nodes as single components and that matrix $\mathbf{P}$ holds on each row i (and column j) the composition of the graph component to which vertex

i belongs, allows for the redefinition of a valid structure as the structure where only one graph component has multiple vertices and this component includes the essential ports.
We propose to validate the structures by multiplying the connectivity matrix $\mathbf{P}$ with a vector $\mathbf{s}$ filled with ones.

$$\mathbf{Ps} = \mathbf{t} \quad \text{where} \quad \mathbf{s} = [1 \ \ldots 1 \ ]^T \tag{7.19}$$

When matrix $\mathbf{P}$ represents the connectivity of a valid structure, the resultant vector $\mathbf{t}$ must be a vector filled with ones, except at n entries where their values must be n as well. Among these n entries there must be the indexes of the essential ports.
If vector $\mathbf{t}$ contains values different to 1 and n it means that there is more than one graph component with multiple vertices. If the vector contains only entries equal to 1 and n, but the number of entries with the value n is different of n, it means that there are two or more components connecting n vertices.
Validation using Warshall's algorithm removes the need to update the finite element mesh in order to remove disconnected nodes.

7.5 Setting the topology optimization problem

In this section we intend to design statically balanced compliant mechanisms by using topology optimization as a design method to obtain the connectivity of the constitutive elements while omitting the search for shapes and sizes. Because we will not be concerned with shapes and sizes and the number of the constitutive members is not defined, the connectivity problem is set as a binary existence/nonexistence problem on a universal structure or ground structure.
The design is constrained to the design of planar compliant mechanisms for function generation, i.e., designs with in-plane motion with a specific displacement relation between the input and the output.
The design search space is assumed as a rectangular contour with a minimum of four essential ports, (i) the input port, (ii) the output port, (iii) the ground port, and (iv) the preloading port. The preloading port is where the structure is prestressed in order to obtain a state of static balancing (proposition 5.1).
Two optimization formulations are set because of the existence of two different constraint functions. Formulation (1) uses the neutral stability constraint discussed in section 7.3.1 while formulation (2) uses the continuous equilibrium constraint discussed in section 7.3.2.
Both optimization formulations maximize an objective function, which promotes flexibility by securing a geometrical advantage equal to 1 (see section 7.2). A specific GA=1 means that the desired orientation angle is $\theta_d = \pi/4$ (Eq. 7.5), hence the factor α in the objective function is $\alpha = 2$ (Eq. 7.6).

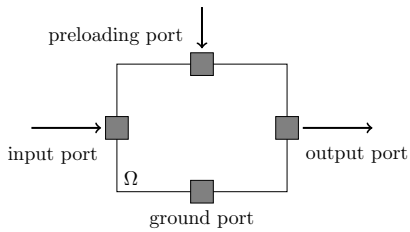

Figure 7.7: The design search space and the essential ports.

$$f(\mathbf{x}) = \sin(2\theta) \tag{7.4}$$

The parameterization is based on binary partial ground structures built out of frame elements. The deflection analysis of the structures is performed differently for each optimization formulation. Deflection analysis in formulation (1) is performed by using linearized prebuckling finite element analysis on 6DOF frame elements, while analysis in formulation (2) is based on two consecutive loading cases, using nonlinear finite element analysis solved through displacement control on 6DOF frame elements with co-rotational formulation for large deflections, small strains.

To solve the optimization problem we resort to heuristic algorithms. Finding the sensitivities of the objective function is not simple, they require to compute the derivatives of the displacements with respect to the design variables in a multi-step nonlinear finite element model solved through displacement control. It is possible to compute the sensitivities numerically, but the cost of doing so is comparable to the use of a heuristic approach, which has the benefit of increasing the probability to find the global optimum and, if the solutions are not optimum solutions, they are close to an optimum.

A genetic algorithm is set to run up to 100 generations. Wrong connectivities are penalized with a high value on their fitness value.

Both optimization formulations are used in the synthesis of two benchmark design examples, (i) the inverter, and (ii) the gripper. The inverter is a compliant mechanism where the displacement at the input induces a displacement with opposite direction at the output. The gripper, on the other hand, is a compliant mechanism where the displacement at the input induces an opening/closing deflection between two output ports. Typical configurations of these two problems are shown in Fig. 7.8.

Due to the symmetry of the design problem, the optimization is performed only on half of the design. The final topology optimization setting is composed of two optimization formulations applied to two design problems.

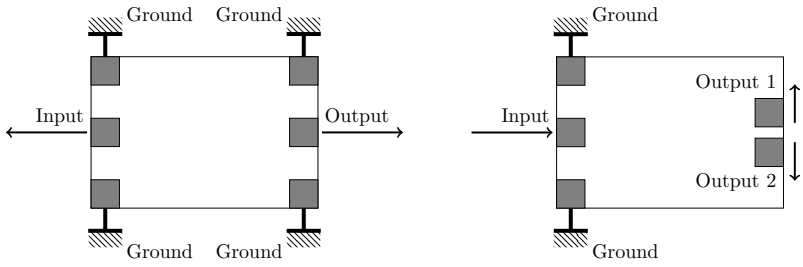

Figure 7.8: Configurations of the two design problems. (a) The inverter. (b) The gripper.

Table 7.1: Setup of the topology optimization.
Two formulations and two design problems.

Optimization formulation 1 Neutral stability	Optimization formulation 2 Continuous equilibrium
$\min_{\mathbf{x}} \quad \sin(2\theta)$ $s.t.: \quad (\mathbf{K}_l - \lambda \mathbf{K}_g)\,\mathbf{q} = \mathbf{0}$ $\mathbf{x} = [0,1]$	$\min_{\mathbf{x}} \quad \pm \sin(2\theta)$ $s.t.: \quad \int_{q_{in1}}^{q_{in2}} \lvert f_{in} dq_{in} \rvert = 0$ $\Delta q_{in} > 0$ $\mathbf{K}\mathbf{q} = \mathbf{f}$ $\mathbf{x} = [0,1]$
Design problem 1 The inverter	Design problem 2 The gripper
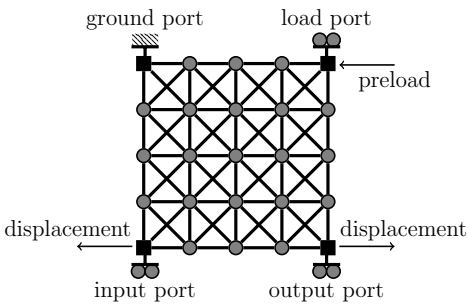	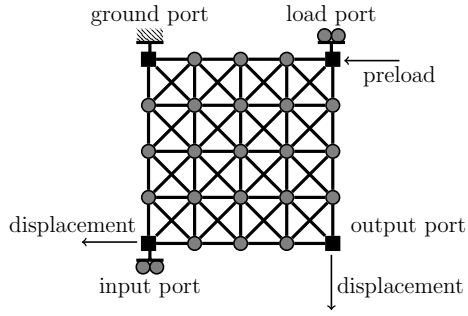

7.6 Results

The results of the optimization are presented in this section. Each optimization formulation applied to each design problem was solved several times in order to check the success of the

optimization procedure (see Tab. 7.2).

Table 7.2: Number of tryouts in the solution of each optimization formulation applied to each design problem.

Formulation	Design problem	Number of tryouts
neutral stability	inverter	30
	gripper	60
continuous equilibrium	inverter	30
	gripper closing	30
	gripper opening	30

The optimization formulation 2 (continuous equilibrium) applied to the design problem 2 (the gripper) was solved for two different variations, (i) the gripper closing, and (ii) the gripper opening, both using the same actuation.

7.6.1 Optimization formulation 1

Design problem 1 - The inverter

The optimization formulation 1 (neutral stability) applied to the design problem 1 (the inverter) was solved 30 times. From these 30 solutions, only three are considered as viable solutions for further development.

Table 7.3: Geometrical advantage and actuation energy reduction of the three viable solutions.

Solution	Geometrical advantage	Actuation energy reduction
A	0.84	50.09%
B	0.56	79.60%
C	0.91	77.56%

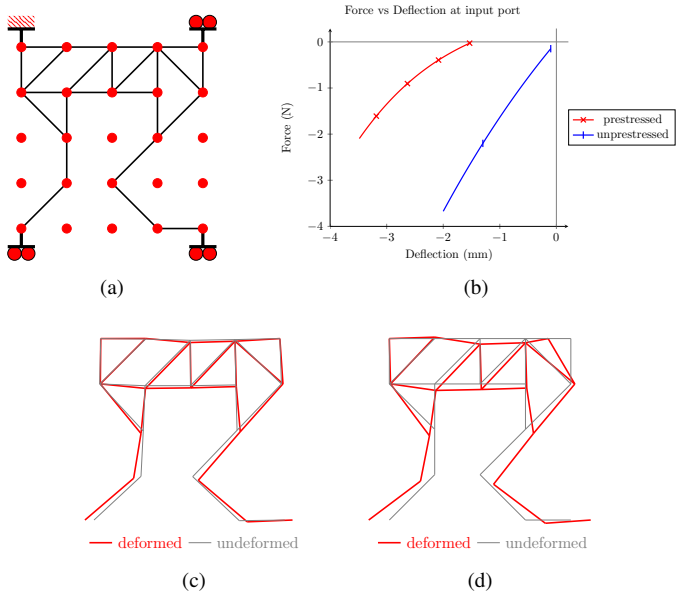

Figure 7.9: Compliant inverter. (a) Topology with a GA=0.84 and actuation energy reduction of 50.09%. (b) Force-deflection behavior at the input port. (c) Deflection configuration predicted by non-linear FEA. (d) Deflection configuration predicted by linearized pre-buckling analysis

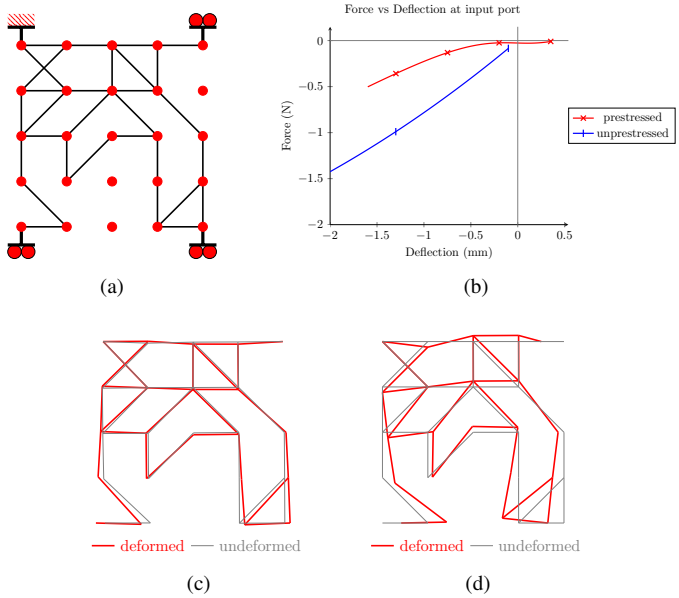

Figure 7.10: Compliant inverter. (a) Topology with a GA=0.56 and actuation energy reduction of 79.60%. (b) Force-deflection behavior at the input port. (c) Deflection configuration predicted by non-linear FEA. (d) Deflection configuration predicted by linearized pre-buckling analysis

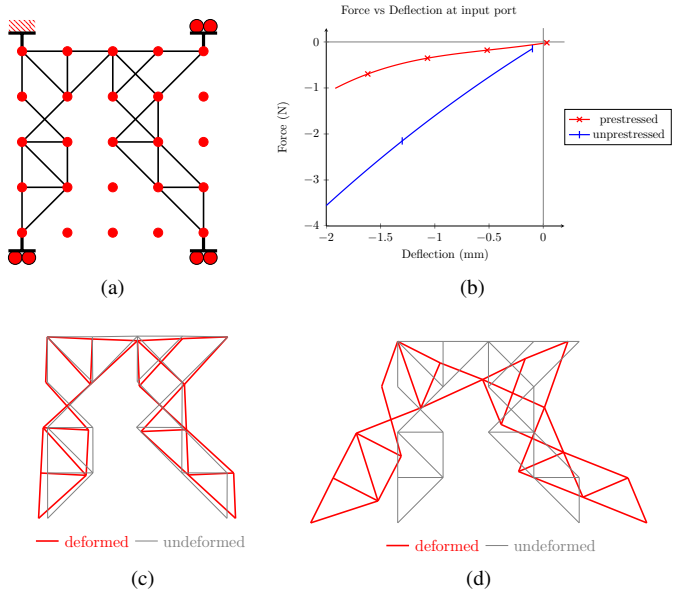

(a) (b) (c) (d)

Figure 7.11: Compliant inverter. (a) Topology with a GA=0.91 and actuation energy reduction of 77.56%. (b) Force-deflection behavior at the input port. (c) Deflection configuration predicted by non-linear FEA. (d) Deflection configuration predicted by linearized pre-buckling analysis

Design problem 2 - The gripper

The optimization formulation 1 (neutral stability) applied to the design problem 2 (the gripper) was solved 60 times. From these 60 solutions, only six are considered as viable solutions for further development.

Table 7.4: Geometrical advantage and actuation energy reduction of the six viable solutions.

Solution	Geometrical advantage	Actuation energy reduction
A	0.92	67.25%
B	0.92	63.43%
C	0.75	92.81%
D	0.97	73.56%
E	0.51	65.13%
F	1.03	56.52%

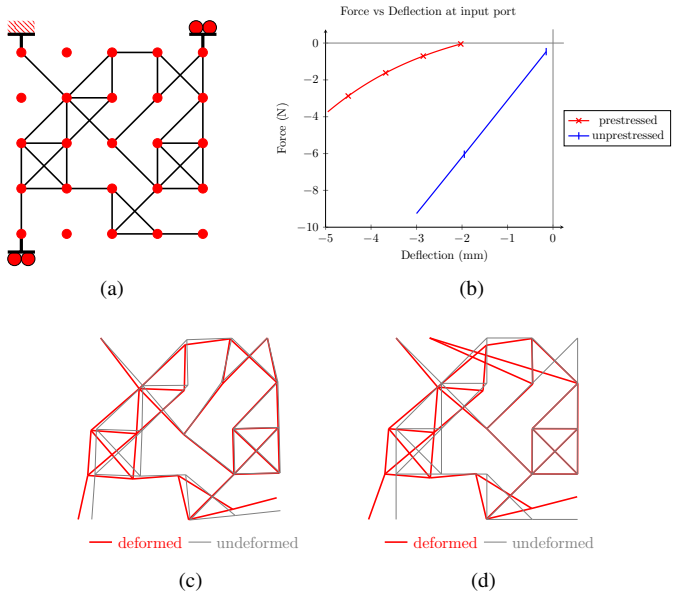

Figure 7.12: Compliant gripper. (a) Topology with a GA=0.92 and actuation energy reduction of 67.25%. (b) Force-deflection behavior at the input port. (c) Deflection configuration predicted by non-linear FEA. (d) Deflection configuration predicted by linearized pre-buckling analysis

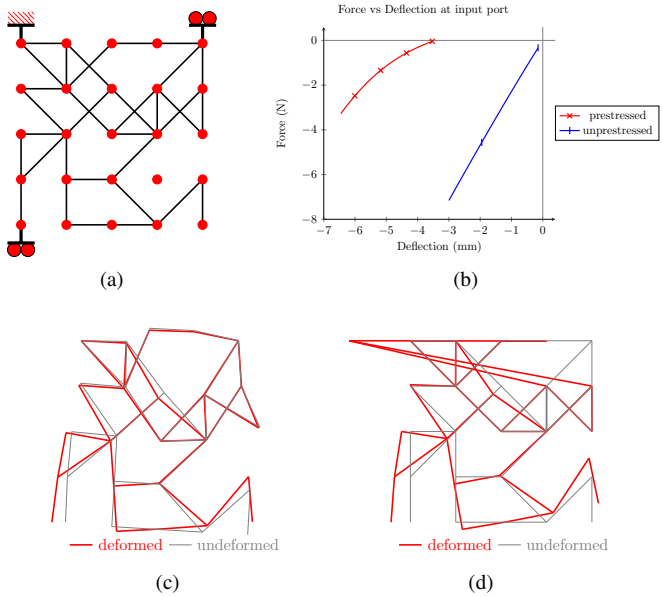

Figure 7.13: Compliant gripper. (a) Topology with a GA=0.92 and actuation energy reduction of 63.43%. (b) Force-deflection behavior at the input port. (c) Deflection configuration predicted by non-linear FEA. (d) Deflection configuration predicted by linearized pre-buckling analysis

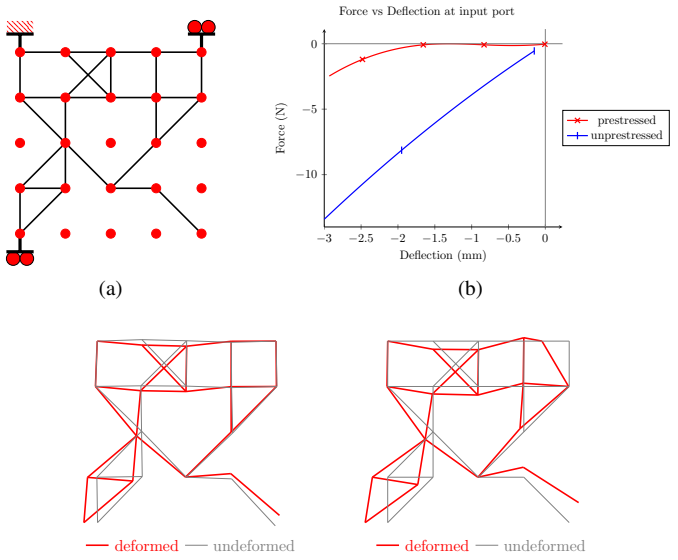

Figure 7.14: Compliant gripper. (a) Topology with a GA=0.75 and actuation energy reduction of 92.81%. (b) Force-deflection behavior at the input port. (c) Deflection configuration predicted by non-linear FEA. (d) Deflection configuration predicted by linearized pre-buckling analysis

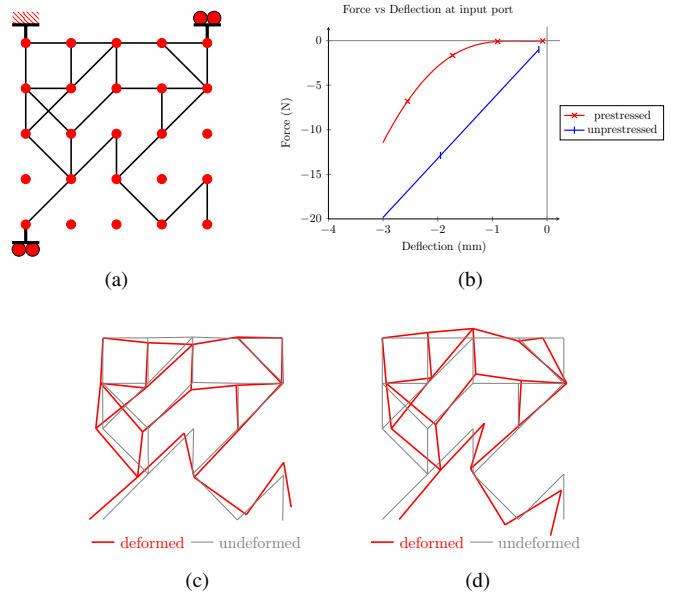

Figure 7.15: Compliant gripper. (a) Topology with a GA=0.97 and actuation energy reduction of 73.54%. (b) Force-deflection behavior at the input port. (c) Deflection configuration predicted by non-linear FEA. (d) Deflection configuration predicted by linearized pre-buckling analysis

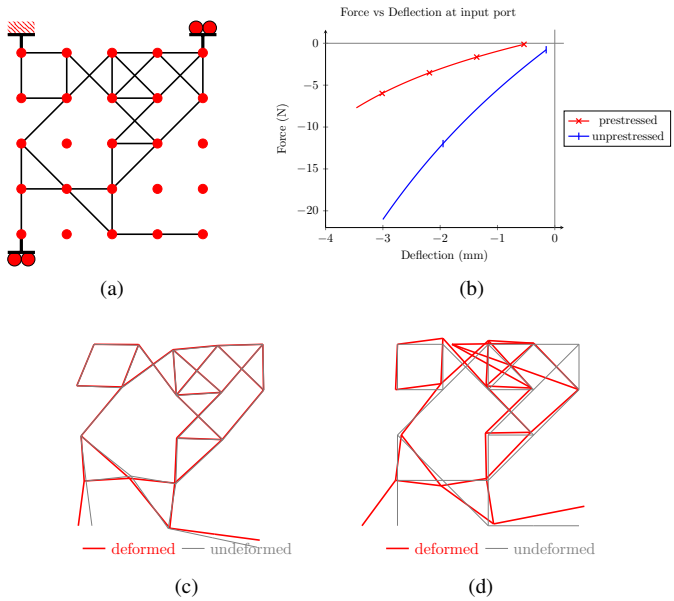

Figure 7.16: Compliant gripper. (a) Topology with a GA=0.51 and actuation energy reduction of 65.13%. (b) Force-deflection behavior at the input port. (c) Deflection configuration predicted by non-linear FEA. (d) Deflection configuration predicted by linearized pre-buckling analysis

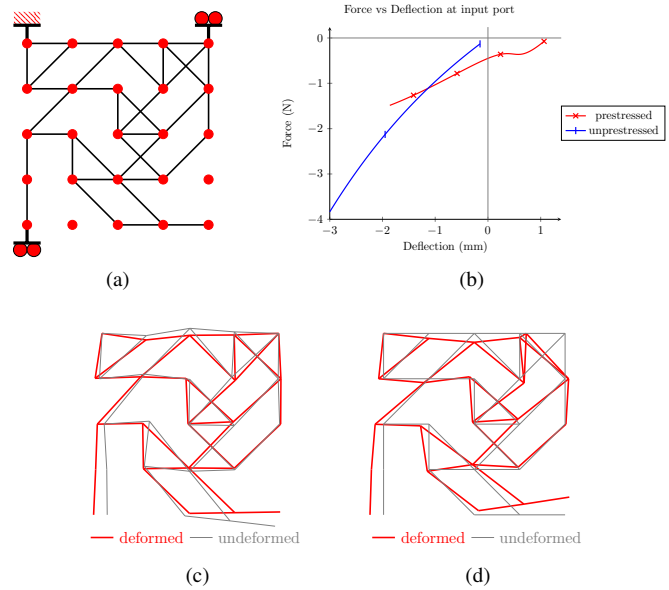

Figure 7.17: Compliant gripper. (a) Topology with a GA=1.03 and actuation energy reduction of 56.52%. (b) Force-deflection behavior at the input port. (c) Deflection configuration predicted by non-linear FEA. (d) Deflection configuration predicted by linearized pre-buckling analysis

7.6.2 Optimization formulation 2

Design problem 1 - The inverter

The optimization formulation 2 (continuous equilibrium) applied to the design problem 1 (the inverter) was solved 30 times. From these 30 solutions, only six are considered as viable solutions for further development.

Table 7.5: Geometrical advantage and actuation energy reduction of the six viable solutions.

Solution	Geometrical advantage	Actuation energy reduction
A	0.93	96.23%
B	0.83	88.12%
C	0.98	95.88%
D	0.66	84.20%
E	0.93	83.24%
F	0.66	95.48%

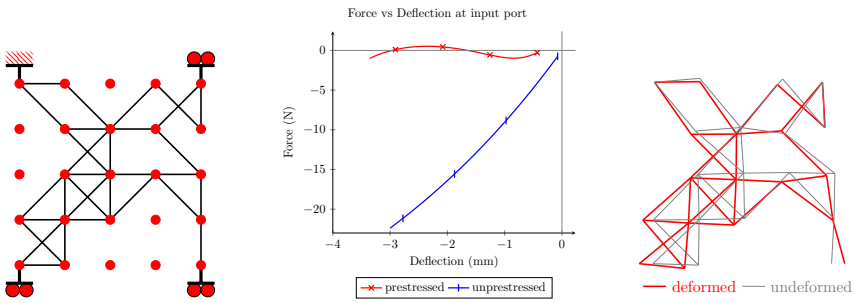

(a) (b) (c)

Figure 7.18: (a) Topology of a compliant inverter with a GA=0.93 and actuation energy reduction of 96.23%. (b) Force-deflection behavior at the input port. (c) Final deflection configuration of the compliant inverter

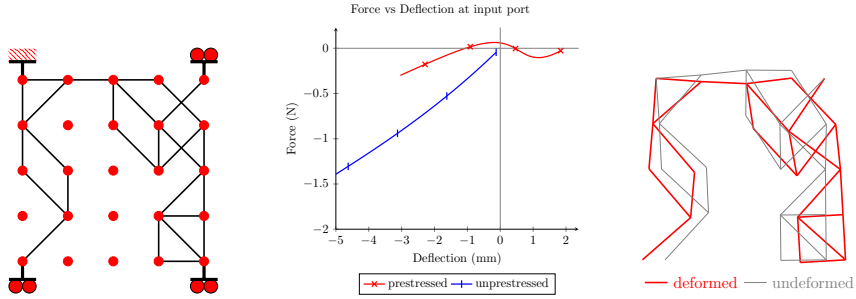

(a) (b) (c)

Figure 7.19: (a) Topology of a compliant inverter with a GA=0.83 and actuation energy reduction of 88.12%. (b) Force-deflection behavior at the input port. (c) Final deflection configuration of the compliant inverter

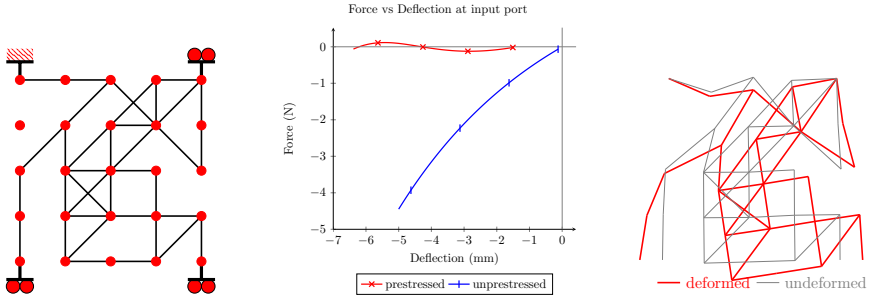

(a) (b) (c)

Figure 7.20: (a) Topology of a compliant inverter with a GA=0.98 and actuation energy reduction of 95.88%. (b) Force-deflection behavior at the input port. (c) Final deflection configuration of the compliant inverter

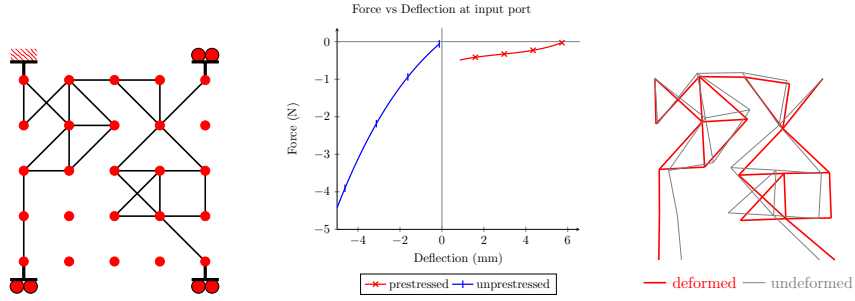

(a) (b) (c)

Figure 7.21: (a) Topology of a compliant inverter with a GA=0.66 and actuation energy reduction of 84.20%. (b) Force-deflection behavior at the input port. (c) Final deflection configuration of the compliant inverter

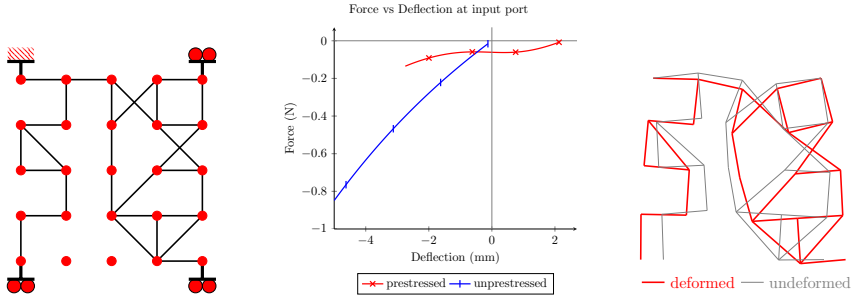

(a) (b) (c)

Figure 7.22: (a) Topology of a compliant inverter with a GA=0.93 and actuation energy reduction of 83.24%. (b) Force-deflection behavior at the input port. (c) Final deflection configuration of the compliant inverter

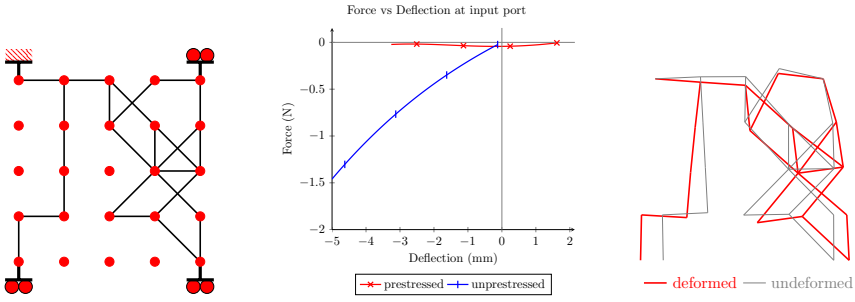

(a) (b) (c)

Figure 7.23: (a) Topology of a compliant inverter with a GA=0.66 and actuation energy reduction of 95.48%. (b) Force-deflection behavior at the input port. (c) Final deflection configuration of the compliant inverter

Design problem 2 - The gripper closing

The optimization formulation 2 (continuous equilibrium) applied to the design problem 2 with the gripper variation closing was solved 30 times. From these 30 solutions, only nine are considered as viable solutions for further development.

Table 7.6: Geometrical advantage and actuation energy reduction of the nine viable solutions.

Solution	Geometrical advantage	Actuation energy reduction
A	0.99	96.32%
B	0.97	90.29%
C	0.74	98.59%
D	1.11	95.13%
E	0.94	98.88%
F	1.03	99.26%
G	1.00	82.43%
H	1.01	73.04%
I	1.20	93.29%

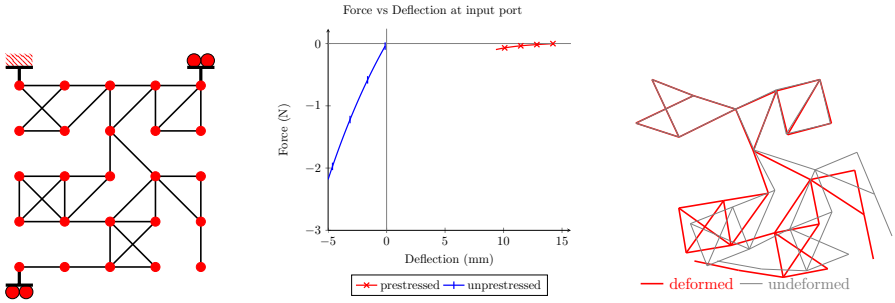

(a) (b) (c)

Figure 7.24: (a) Topology of a compliant gripper with a GA=0.99 and actuation energy reduction of 96.32%. (b) Force-deflection behavior at the input port. (c) Final deflection configuration of the compliant gripper

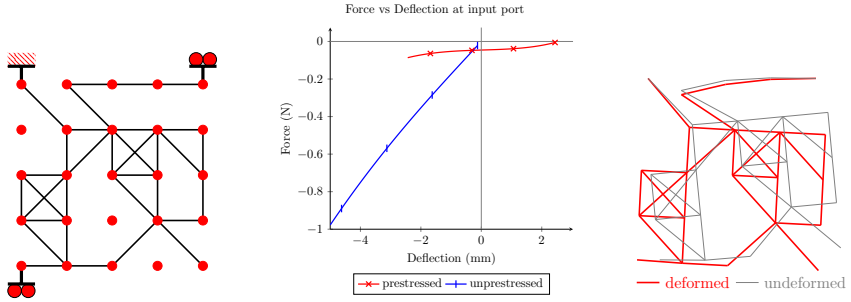

(a) (b) (c)

Figure 7.25: (a) Topology of a compliant gripper with a GA=0.97 and actuation energy reduction of 90.29%. (b) Force-deflection behavior at the input port. (c) Final deflection configuration of the compliant gripper

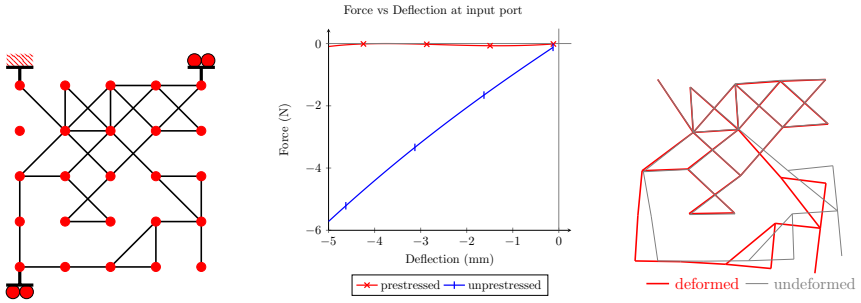

(a) (b) (c)

Figure 7.26: (a) Topology of a compliant gripper with a GA=0.74 and actuation energy reduction of 98.59%. (b) Force-deflection behavior at the input port. (c) Final deflection configuration of the compliant gripper

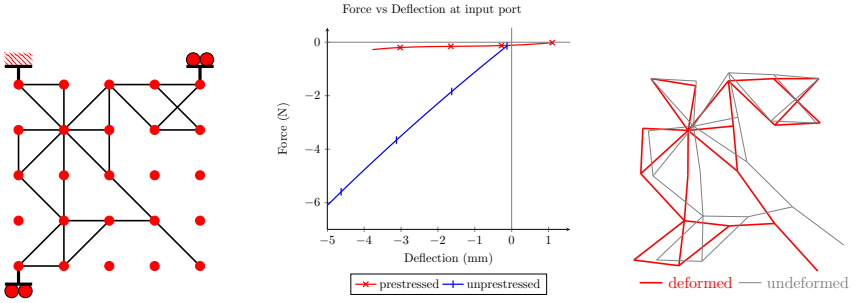

(a) (b) (c)

Figure 7.27: (a) Topology of a compliant gripper with a GA=1.11 and actuation energy reduction of 95.13%. (b) Force-deflection behavior at the input port. (c) Final deflection configuration of the compliant gripper

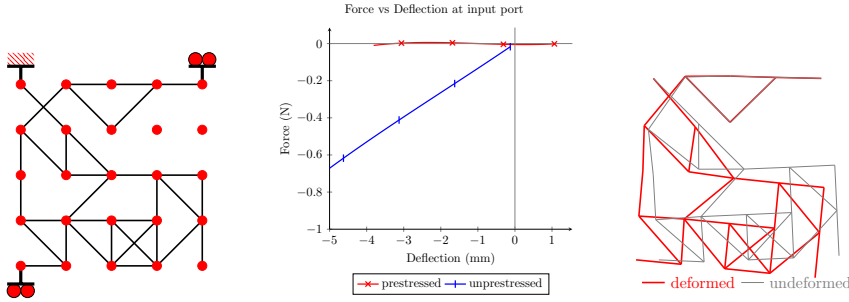

(a) (b) (c)

Figure 7.28: (a) Topology of a compliant gripper with a GA=0.94 and actuation energy reduction of 98.88%. (b) Force-deflection behavior at the input port. (c) Final deflection configuration of the compliant gripper

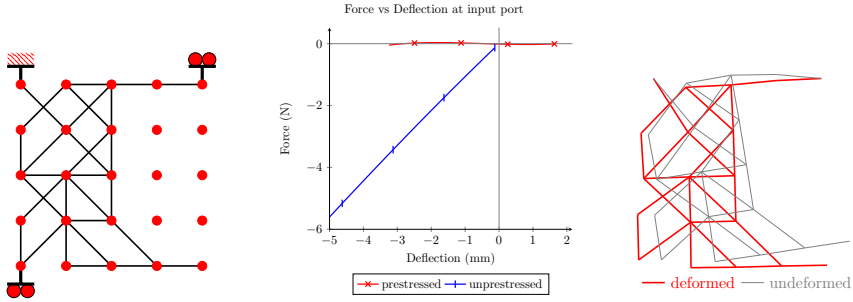

(a) (b) (c)

Figure 7.29: (a) Topology of a compliant gripper with a GA=1.03 and actuation energy reduction of 99.26%. (b) Force-deflection behavior at the input port. (c) Final deflection configuration of the compliant gripper

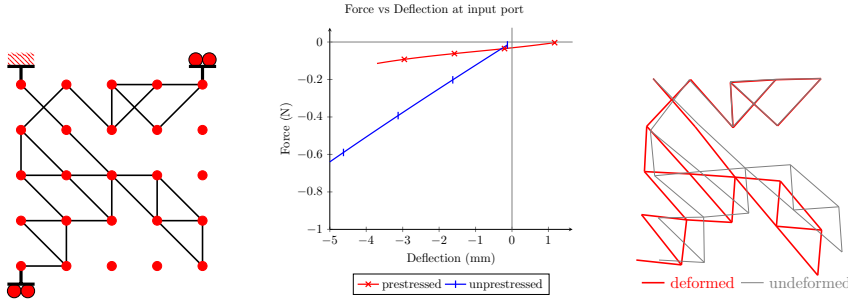

(a) (b) (c)

Figure 7.30: (a) Topology of a compliant gripper with a GA=1.00 and actuation energy reduction of 82.43%. (b) Force-deflection behavior at the input port. (c) Final deflection configuration of the compliant gripper

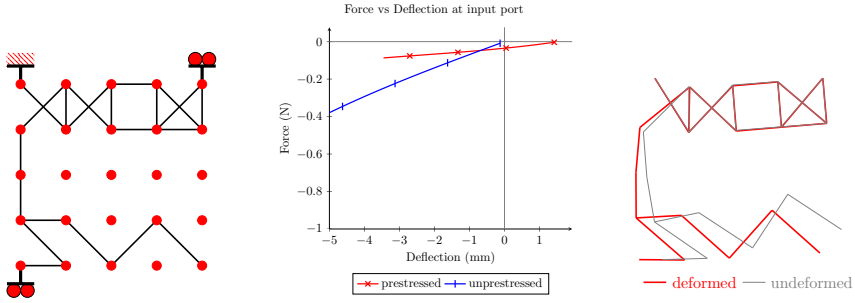

(a) (b) (c)

Figure 7.31: (a) Topology of a compliant gripper with a GA=1.01 and actuation energy reduction of 73.04%. (b) Force-deflection behavior at the input port. (c) Final deflection configuration of the compliant gripper

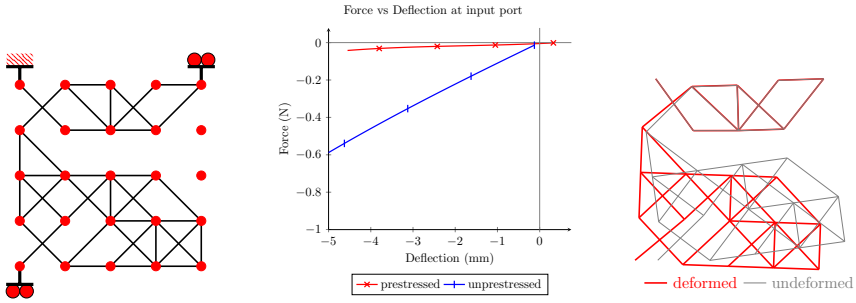

(a) (b) (c)

Figure 7.32: (a) Topology of a compliant gripper with a GA=1.20 and actuation energy reduction of 93.29%. (b) Force-deflection behavior at the input port. (c) Final deflection configuration of the compliant gripper

Design problem 2 - The gripper opening

The optimization formulation 2 (continuous equilibrium) applied to the design problem 2 with the gripper variation opening was solved 30 times. From these 30 solutions, only four are considered as viable solutions for further development.

Table 7.7: Geometrical advantage and actuation energy reduction of the four viable solutions.

Solution	Geometrical advantage	Actuation energy reduction
A	0.43	98.76%
B	0.52	84.12%
C	0.72	87.05%
D	0.70	95.70%

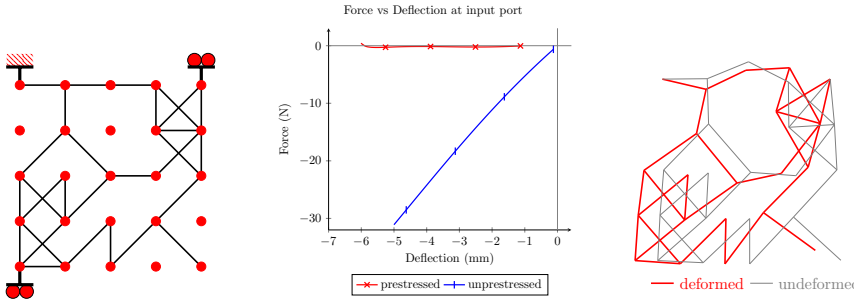

(a) (b) (c)

Figure 7.33: (a) Topology of a compliant gripper with a GA=0.43 and actuation energy reduction of 98.76%. (b) Force-deflection behavior at the input port. (c) Final deflection configuration of the compliant gripper

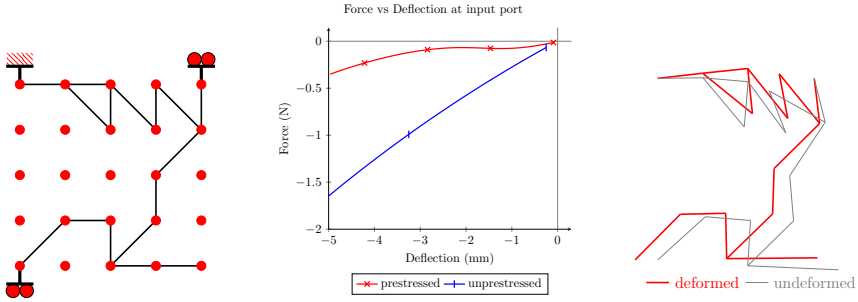

(a) (b) (c)

Figure 7.34: (a) Topology of a compliant gripper with a GA=0.52 and actuation energy reduction of 84.12%. (b) Force-deflection behavior at the input port. (c) Final deflection configuration of the compliant gripper

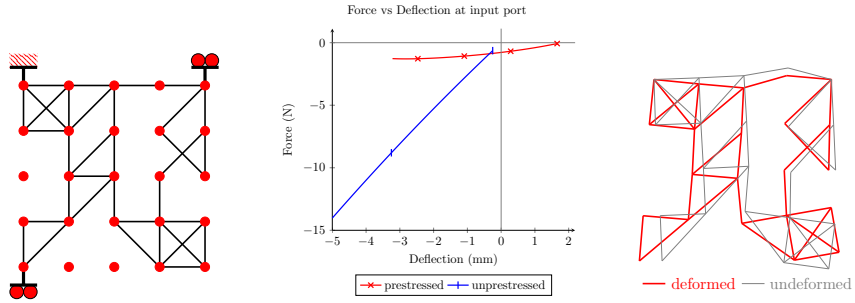

(a) (b) (c)

Figure 7.35: (a) Topology of a compliant gripper with a GA=0.72 and actuation energy reduction of 87.05%. (b) Force-deflection behavior at the input port. (c) Final deflection configuration of the compliant gripper

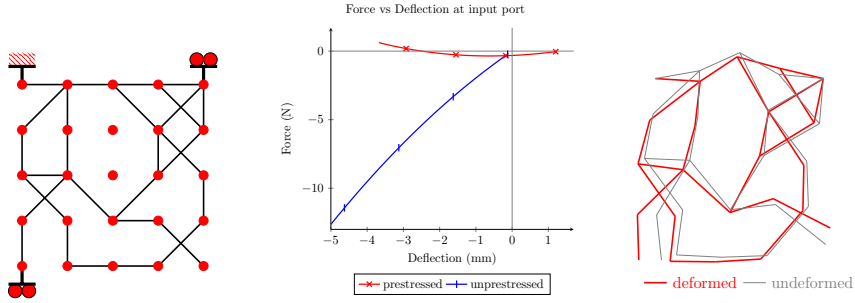

(a) (b) (c)

Figure 7.36: (a) Topology of a compliant gripper with a GA=0.70 and actuation energy reduction of 95.70%. (b) Force-deflection behavior at the input port. (c) Final deflection configuration of the compliant gripper

7.7 Discussion

The presented design procedure based on topology optimization using a partial ground structure with binary design variables is inefficient. The procedure presents a low average success rate of 15.6% for all the formulations and design problems used in this work. Table 7.8 consolidates the success rate for each design formulation and design problem, together with the average and standard deviation of the geometrical advantage and actuation energy reduction value (static balancing quality).

Table 7.8: Accomplishment of the topology optimization procedure. An ideal solution should exhibit a geometrical advantage and actuation energy reduction equal to 1.

Formulation	Design problem	Rate of success	Geometrical advantage		Actuation energy reduction	
			$\bar{\mu}$	σ	$\bar{\mu}$	σ
neutral stability	inverter	10.0%	0.77	0.15	0.69	0.13
	gripper	10.0%	0.85	0.17	0.70	0.11
continuous equilibrium	inverter	20.0%	0.83	0.13	0.91	0.06
	gripper closing	30.0%	1.00	0.12	0.92	0.08
	gripper opening	13.3%	0.59	0.12	0.91	0.06
Total		15.6%	0.85	0.19	0.84	0.14

Figure 7.37 shows the histogram of the geometrical advantage and actuation energy reduction values. These plots provide a graphical view of the average and standard deviation values presented in Tab. 7.8.

It is important to remark the difficulties of evaluating the static balancing quality. There is no clear metric that indicates how good a state of near static balancing is with respect to a state of perfect static balancing. We have evaluated the stiffness reduction of the mechanisms with respect to themselves in their prestressed and unprestressed configurations. A comparison of the actuation forces among designs in both configurations —unprestressed and prestressed— as well as the prestressing forces, shows that the values of these forces are in different scales of magnitude. This complicates an evaluation of the design since there is not a real problem to be solved constraining the solution.

The low success rate relates to a number of factors where the most relevant is the parameterization. In the following section, the relation between the low success rate and the parameterization is discussed.

7.7.1 The parameterization

One reason for the low success rate is that the dependency of the static balancing quality with respect to the structure's preloading is not considered during the optimization. As a consequence,

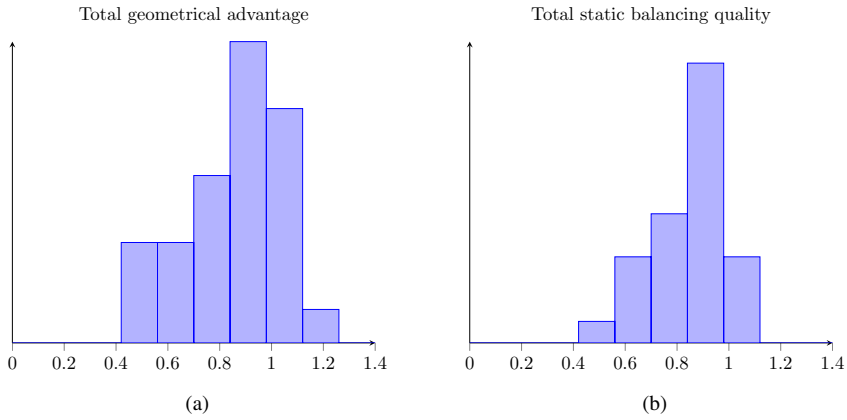

Figure 7.37: Histogram of the geometrical advantage and the static balancing quality for the 28 optimization results. The ideal value for the geometrical advantage and the static balancing quality is 1. (a) Histogram of the geometrical advantage value. (b) Histogram of the static balancing quality.

the solutions provided by the optimization do not exhibit the highest possible stiffness reduction. To get the best stiffness reduction, it is required to tune the value of the preloading displacement to the optimization solutions after the optimization has finished.

The fact that the solutions provided by the optimization do not exhibit the highest stiffness reduction is due to at least the following two particularities, (i) the preloading displacement applied to the structure is kept constant during the optimization in order to keep the design variables as a set of binary variables, and (ii) since a partial ground structure is composed of vertical, horizontal and diagonal frame elements, it is not possible to have a continuous set of values for any path-length between ports. These two conditions mean that compressive stresses responsible for the stiffness reduction can no longer be tuned during optimization, neither by modifying the preloading displacements at the load port nor by modifying the path-length between the load port and the ground port.

Another reason for the low success relates to the penalization of wrong connectivities. The optimization procedure is conceived to remove structures with either floating elements or disconnected ports. When individuals are removed from the population, their characteristics are not passed into the next generation, resulting in a reduction of the design search space.

Table 7.9 summarizes the average rate of individuals removed from the consolidated population along all the tryouts from the same formulation and design problem.

To understand this reduction of the design search space we need to note that genetic algorithms randomly create the first generation of individuals trying to distribute them evenly across the design search space. This even distribution of individuals increases diversity which, in turn,

Table 7.9: Average rate of exclusion of individuals due to wrong connectivities.

Formulation	Design problem	Average rate of individuals exclusion
neutral stability	inverter	4.53%
	gripper	3.52%
continuous equilibrium	inverter	7.42%
	gripper closing	5.18%
	gripper opening	5.08%
Total		4.67%

increases the chances of finding the global optimum. The idea is to find the optimum individual by pushing up the best individuals over the rest of the population in a wide design space. Figure 7.38 shows the average rate of exclusion for each formulation and design problem along 50 generations. Notice how, for each design problem at the first generation, the exclusion rate is about 45% and decreases to about 2% at generation 50. This behavior indicates that the final solution tends to be enclosed in a specific region of the design search space determined by the exclusion of individuals. The result is that the optimum comes from pushing up the best individual in a smaller design space.

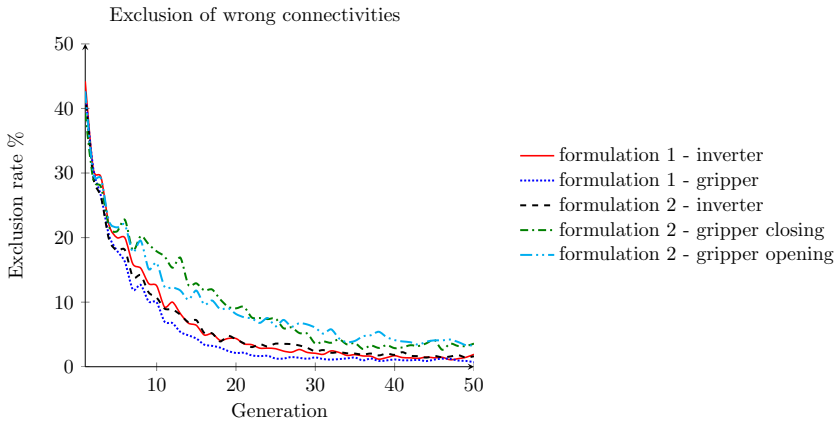

Figure 7.38: Average rate of excluded solutions along 50 generations due to wrong connectivities.

A parameterization based on partial ground structures can provide with a large number of different topologies. For instance, a partial ground structure holds 6561 valid topologies if we limit connectivities to just four frame elements between the four essential ports in a 5x5 nodes structure. It is clear that in the case of statically balanced compliant mechanisms topology diversity

is not enough. The dependency of the static balancing quality with respect to preloading — as a means to prestress the structure — suggests the need for parameterizations that also allow for the optimization of shapes and sizes.

7.8 Summary

The chapter introduces structural optimization as a design method under the view of the design framework presented in chapter 2. The relation between the objective function, constraints and parameterization with the function and characteristics resulting from the design requirements is explained.

The chapter presents the preliminary results of topology optimization as an integral design method for statically balanced fully compliant mechanisms. The design method is set as a binary topology optimization of a partial ground structure, where the problem is to maximize a function that guarantees a desired geometrical advantage between the input and output ports of the structure. The optimization problem is solved by using genetic algorithms and tested through the use of two design examples, (i) the inverter, and (ii) the gripper. The static balancing characteristic is included in the optimization as a constraint based on the continuous equilibrium and neutral stability criteria.

Topology optimization as a method for the design of statically balanced compliant mechanisms is proven to be able to provide feasible design solutions and interesting design configurations. The net result is 28 designs of nearly statically balanced fully compliant solutions. These solutions do not exhibit the ideal and intended geometrical advantage and static balancing characteristics. The average value of the objective function and the static balancing quality with respect to their ideal values is 85% and 84%, respectively.

The optimization procedure exhibits an average success rate of 10% for the formulation based on neutral stability and 21.1% for the formulation based on continuous equilibrium. The average success rate for the whole setup is 15.6%.

The chapter proposes a modification of Warshall's algorithm for the connectivity analysis of undirected graphs. The algorithm is used to remove structures with disconnected ports and floating elements generated during the solution process by the genetic algorithm.

8 Discussion

In this work a promising design methodology is proposed from which it is possible to derive several different methods for the design of nearly statically balanced compliant mechanisms. The design methodology is based on the interrelation of seven recurrent elements that influence the design outcome: compliancy type, classification of the functional requirements, modularity of the mechanism, static balancing strategy, modularity of the design process, design methods for compliant mechanisms, and static balancing criteria.

The recurrent elements on which the methodology is based are those elements constantly present in the answers to questions such as: what is a design method, how are compliant mechanisms designed, what conditions characterize a state of static balancing and how to include a state of static balancing in the design of compliant mechanisms.

The design methodology is able to provide with 16 different general design methods —if we do not count the variants resulting from considering the static balancing strategies, static balancing criteria, optimization parameterizations and compliancy type— or around 480 specific design methods.

The design methods derived from the methodology are structured methods that can provide conceptual and detailed solutions in terms of their topologies, shape and sizes. The fact that the design methodology is based on the recurrent elements forces the designer to initially consider the design requirements instead of going directly to the design task. As a consequence, the designer chooses the best design methods for the problem at hand, hence allowing the designer to foresee how the design process will take place and where in the design space the solution will lay.

In order to introduce the design methodology and its use, we derived four of the 16 general design methods as examples. The four design methods were selected in such a way that they demonstrated, in context, the use of synthesis methods such as the rigid-body-replacement and structural optimization in combination with static balancing strategies like buckling and function decomposition. These design methods were used in the design of 33 concepts of nearly statically balanced compliant mechanisms —4 suspensions, 10 inverters, 19 grippers— which show how the design methodology helps the designer to widen the solution space, increase design quality and structure the design process. We consider the design space widened since it is pos-

sible to obtain different concepts in terms of topologies, shape and sizes for the same problem. Take, for instance, the suspension design examples using either function decomposition 6.2.3 or Rigid-Body-Replacement 6.2.2 or the examples using topology optimization. The quality of the design is considered to be increased because it is possible to narrow the marginal values of the requirements' metrics and increase the number of design requirements as shown in the suspension design examples using function decomposition 6.2.3.

One drawback of the design methodology is the need for the designer to be familiar with the design methods for compliant mechanisms, since the recurrent elements which form the basis of the design methodology revolve around these design methods.

So far, the methodology has been tested with design problems comprising rather simple design requirements which do not allow for an evaluation of the methodology. A proper evaluation would require the methodology to be subjected to design problems with realistic, diverse and complex design requirements.

The whole idea behind the static balancing of compliant mechanisms is to get the good characteristics of compliant mechanisms while removing the energetic inefficiencies due to the strain energy storage. Designing a mechanism to be *compliant* implies that the design has the characteristics of being monolithic, predictable, precise, reliable, compact, noiseless, durable, energetically inefficient and motion limited. These characteristics can conflict or reinforce with the characteristics of being energetically efficient, prestressed, overconstrained, and enlarged that are associated with a mechanism that is *statically balanced.*

Static balancing improves the energy efficiency of compliant mechanisms since the characteristics of statically balanced mechanisms tend to dominate over the characteristics of compliant mechanisms —Energy efficiency dominates over energy inefficiency. The price to pay for the energy efficiency is that statically balanced compliant designs tend to be enlarged compared to their unbalanced versions —Enlargement dominates compactness. The enlargement comes from the addition of the balancing elements and the addition of mechanisms or actuators used for the prestressing of the statically balanced compliant mechanism.

The precision and predictability of compliant mechanisms could be compromised by the use of static balancing since static balancing based on the prestressing of elastic elements makes use of kinematic overconstraining. Overconstraining opposes to the principles of exact constraint design which are one of the cornerstones for design in precision engineering. However, overconstrained does not mean imprecise, it means that to achieve precision the design must rely on other principles such as elastic averaging (overconstraining of a system with a large number of compliant elements to achieve precision by averaging the error). Take for instance the work of Shu et al. [124][123] where precision at nanometer level is achieved through the use of an overconstrained design. As far as is known to the author, the relation between precision and overconstraining in statically balanced compliant mechanisms is still an open question.

This work constructs the conceptual and mathematical framework for static balancing as a state of

motion. The framework for static balancing is discussed with a view focused on systems modeled by discrete elements where the size, shape and topology properties are collected into the system's stiffness matrix. The framework included the three classical conditions characterizing a state of static balancing in terms of the potential energy, the forces, and the stability: (i) the potential energy is constant all across the statically balanced workspace, (ii) all the internal forces are in static equilibrium so the resultant forces are zero all across the workspace, hence no actuation forces are required besides those to overcome the inertial loads and non-conservative forces, (iii) due to continuous equilibrium, the stiffness is zero and the mechanism has no preferred configuration under a perturbation, therefore the mechanism is neutrally stable.

The framework for static balancing is expanded in this work from the three classical conditions to include new conditions based on the notions of virtual work, speed, natural frequency (large and small amplitudes), and buckling: (iv) the virtual work at any point of the workspace is always zero, (v) a statically balanced mechanism does not oscillate, so its natural frequency is zero as well as the harmonic natural frequency due to small displacements at any point of the workspace, (vi) in the absence of external disturbances, motion is driven by the inertia of the mechanism so the speed across the workspace is constant, and (vii) a statically balanced compliant mechanism is a pre-stressed structure, on which the pre-stressed areas induce a loss of structural stability, creating a state of elastic self-buckling at critical load across the workspace.

All the aforementioned conditions are necessary conditions for a state of static balancing but not all of them are sufficient. The necessary and sufficient conditions are: (i) the continuous constant potential energy, (ii) the continuous zero force, (iii) the continuous neutral stability, (iv) the continuous zero virtual work, (v) the constant speed, and (vi) self-buckling at critical load which applies only for compliant mechanisms. The necessary but not sufficient conditions are: (i) the continuous zero stiffness, (ii) the zero natural frequency, and (iii) the continuous zero harmonic natural frequency for small displacements. We need to keep in mind that the necessary but not sufficient conditions in static balancing are also necessary conditions to define a state of constant force. All the conditions defining a state of static balancing while they are different perspectives of the same state, different faces of the same dice, is their application as design criteria towards static balancing what make them different. The use of one condition or another can lead to different design results.

The construction of the framework also included the presentation of static balancing as a coordinate transformation problem, in which the system's workspace is a projection of a level set of the system's potential energy. Such a transformation problem allowed for the generalization of static balancing into the equation,

$$\mathbf{K}\left(\mathbf{t}\right) = 0 = \mathbf{J}^{T}\mathbf{K}\left(q_i\right)\mathbf{J} + \mathbf{f}(q_i)^{T}\frac{\partial \mathbf{J}}{\partial t_l} \tag{5.57}$$

The generalization shows that static balancing is a problem dependent of the system's deflec-

tion, its stiffness properties and the workspace on which the system moves. The generalization expresses that static balancing comes as a result of compensation by trajectory changes —constraining motion to move in a workspace with constant potential energy— and singularity with zero force —the system self-constrains its motion to a workspace with constant potential energy.

Static balancing in elastic systems with either constrained motion or self-constrained motion refers to a state of self-buckling at critical load in the elastic regime. This is loss of stability without collapsing. The traditional engineering view says that structures are designed to withstand forces with a minimum of deflection. This view contrast with the fact that compliant mechanisms are designed to deflect as much as possible with minimum force. So if we consider compliant mechanisms as failed structures under the action of a load, then statically balanced compliant mechanisms are failed structures that do not require any force to fail. Statically balanced compliant mechanisms are structures that load themselves to the critical buckling load, with a maximized range of motion where the self load is kept critical.

Buckling can be used as a simple design strategy towards static balancing. If a compliant mechanism has beam elements in which their longitudinal axis is perpendicular to the motion of their adjacent elements, then it is likely that the stiffness of the compliant mechanism can be reduced by simply buckling these beam elements. This strategy becomes relevant when we realize that many compliant mechanisms are compositions of straight beam elements.

Statically balanced mechanism are arrangements of elements, where not all the elements exhibit the same level of potential energy. Internally, some elements exhibit positive stiffness, while some other elements exhibit negative stiffness. During the motion, these elements with positive and negative stiffness exchange energy so the total potential energy is kept constant. Depending on how this exchange of energy takes place, some elements can switch their stiffness from positive to negative and vice versa, but the net overall stiffness of the mechanism is zero. In the case of statically balanced compliant mechanisms the elements with positive and negative stiffness are normally elastic elements that at their nearest equilibrium configurations, are stable and unstable, respectively.

From a design point of view, the whole idea of creating statically balanced compliant mechanisms relies greatly on the possibility to create elastic structures with negative stiffness. A structure that can be deformed from a mode with high density of strain energy per unit of deflection into a mode with lower density of strain energy per unit of deflection, is most likely to exhibit negative stiffness during the transition between modes. Negative stiffness is possible since the transition between modes releases an excess of strain energy that is translated into larger deformations in the low energy density mode. Under this view, when a SBCM is prestressed, some areas deform in high energy density modes developing negative stiffness, thus during the actuation the released excess of strain energy is absorbed by areas where the deformation follows an opposite transition between modes —from low energy density into high energy density.

For instance, negative stiffness in slender flexible elements can be achieved by a deformation sequence of axial compression and bending. For beams with constant rectangular or circular cross sections, the density of strain energy per unit of deflection in axial compression is greater than the density under pure bending by an approximate factor of α^2, where α is the ratio between the beam's length over the in-plane width or diameter (see appendix B).

Static balancing is a well defined and singular state that is quite difficult to reach. It can be compared to the idea of balancing a sharp pencil on its tip over a flat marble surface. In both cases, there is a theoretical point at which static equilibrium can be achieved in a passive way, but one thing is the theoretical existence of such point and another one is actually reaching this point. For instance, constructing a working version of the spring-to-spring zero stiffness balancer presented in chapter 4 is quite a challenge, although the balancer has closed-form expressions describing a state of perfect static balancing (see chapter 4), its design is defied by all sorts of irregularities in the constitutive elements. In the case of compliant mechanisms, while it is too venturous to say that perfect static balancing is impossible, it is better to say that it is unlikely to be achieved. When we refer to statically balanced compliant mechanisms we are, in reality, referring to compliant mechanisms with extremely low stiffness as an approximation to the perfect state.

Considering the design of statically balanced compliant mechanisms as an approximation to the perfect state raises the question of which amount of approximation is good enough, or in other words, how to define a state of nearly static balancing. For instance, if we evaluate static balancing by using the condition of zero continuous force, using as a metric the Root-Mean-Square (RMS) value of the force, then a state of perfect static balancing is a RMS value of zero, but which RMS value other than zero can be considered nearly static balancing?. Consider the cases where it is possible to compare an unbalanced mechanism with its statically balanced version, it is not clear which value of stiffness reduction can be considered as nearly static balancing, hence it is not possible to define the marginal values of the metrics to quantify the quality of such state. Consider the cases where the nearly statically balanced compliant mechanism does not have an unbalanced version for comparison, in which case it is only possible to compare the design with itself in the unprestressed configuration, then compromising the evaluation of the requirements (an example of the latter consideration are the designs resulting from topology optimization shown in chapter 7 where a comparison of the actuation forces among designs shows high variance). At the end the marginal values of the metrics used in the evaluation of a state of nearly static balancing will be dictated by the design requirements of the problem at hand.

Nearly static balancing means that a mechanism in such a state can exhibit a behavior with positive, negative or alternating stiffness along the workspace. Which behavior is desirable would depend on the design requirements. Now, all the static balancing conditions are some form of a constant value along the workspace hence making the standard deviation the natural choice for a metric. A state of perfect static balancing implies a standard deviation along the workspace

equal to zero, where the mean value is the target value of the condition —notice that a standard deviation with mean value equal to zero is a RMS value. The problem with the standard deviation is that it does not capture the changes in stiffness along the workspace. To evaluate nearly static balancing with stiffness changes along the workspace, the use of metrics based on the computation of error with respect to a prescribed behavior or metrics composed of several functions where each function captures an aspect of the desired behavior, is advised.

In addition to the problem of nearly static balancing evaluation, there is the problem of the sensitivity of static balancing quality with respect to (i) dimensional tolerances and (ii) prestressing. The relation between the type of compliancy and the dimensional accuracy of flexible elements and how this relation influences the static balancing quality is still an open question. A complete study of this relation must include the relation between type of compliancy with creep and fatigue and its effects on the static balancing quality. About prestressing, it is clear that the static balancing quality correlates with the amount of prestressing induced in the compliant mechanism. This correlation is function of the variables defining the way in which prestressing takes place. For instance, if prestressing is done by preloading, then static balancing quality is a function of the force magnitude or displacement of the preloading.

The relation between prestressing and static balancing quality is influenced by the chosen design method in the design methodology. For instance, the modular design method using function decomposition shown in section 6.2.3 led to designs in which the value of preloading was known exactly while design methods based on structural optimization where the prestressing variables were not included as design variables (chapter 7) led to designs in which prestressing had to be tuned. It is clear that during the design process of a statically balanced compliant mechanism a variable must be included to account for the prestressing of the structure. Now, if the prestressing value should be fixed at the beginning of the design process or searched along the process, is a designer's choice unless the design domain parameterization does not allow for a continuous prestressing with a fixed prestresssing value, in which case it is adviced to search for the correct prestressing value.

One problem that the designer could face in the design of statically balanced compliant mechanisms relates to the use of commercial finite element software. From the experience collected in realization of this work we have found two main problems, (i) convergency problems in the solvers when the solution is too close to perfect static balancing regardless of the use of arc length or displacement control methods, and (ii) resetting of nodal displacements in multiple load steps using displacement conditions. The resetting problem appears when after the first load step —prestressing— the input port displaces, then in the second load step —actuation— the location of the input port is reset to the initial location, just where it was before prestressing. The resetting of the input port introduces, in the middle of the force-deflection path, an unrealistic portion of behavior. These problems were avoided through a Matlab implementation of nonlinear finite elements using the displacement control algorithm described in appendix C and the nonlinear

formulation for frame elements presented in Mankame [81].

At the end of this work there are many open questions. The work introduced the general expression describing static balancing as a coordinates transformation problem, but its role in design —for instance, used as a design constraint— remains unexplored. There are novel techniques such as inverse finite elements and buckling under tensile load requiring research for their immediate application in the design of SBCM's. Topology optimization while tested as a viable design method, requires more fundamental work on parameterizations, objective functions and solution algorithms in order to develop an efficient design method towards static balancing of compliant mechanisms. Prestressing of the elastic elements based on thermal effects and the use of electric and magnetic fields in the static balancing of compliant mechanisms are open fields for research in design with application in MEMS.

Along this work we have presented design examples of statically balanced compliant mechanisms but the designs considered neither the effects of creep and stress relaxation due to the prestressing of the elastic elements, nor the effects of fatigue due to cyclic actuation. The design examples must be considered as the proof of concept of the design methods.

9 Conclusion

In this work we proposed a design methodology from which it is possible to derive several different methods for the design of nearly statically balanced compliant mechanisms. The design methodology is based on the interrelation of seven recurrent elements that influence the design outcome. The design methods derived from the methodology are structured methods that can provide conceptual and detailed solutions.

In the development of this work, the design methodology was used in derivation of four design methods out of 16 general design methods from which it was possible to create 33 concepts of statically balanced compliant mechanisms —4 suspensions, 10 inverters, 19 grippers. The concepts show how the methodology helps the designer to widen the design search space and increase the quality of the designs. The methodology while proven promising still has not been evaluated. Evaluation of the design methodology requires to test all the design methods that can be derived from the methodology under realistic, diverse and complex design requirements in a non-academic environment.

Using the elements of technical system representation, the relation between design requirements, main function and attributes in the design of statically balanced compliant mechanisms was explained for the first time. The procedure for the design of mechanisms was explained as the cyclic process of setting requirements, synthesis, analysis and evaluation, divided into conceptual and detailed design stages. It was explained how the attributes of *compliant* and *statically balanced* relate to design requirements that condition the main function and impose constraints and characteristics. A conceptual framework was proposed for the design of mechanisms from which it is possible to identify three recurrent elements —classification of the functional requirements, modularity of the mechanism, and modularity of the design process— and explain how these elements relate to the attributes of *compliant* and *statically balanced* and how they influence the conceptual and detailed design stages.

An extensive overview of the methods for the design and synthesis of compliant mechanisms was presented. The overview was pointed towards the basic ideas behind each method so the reader could get a conceptual image of the field. To facilitate the conceptualization, the overview was structured following a proposed classification of the field. The overview included a discussion about each method's simplicity, completeness and usefulness in the design of mechanisms for

motion, path or function generation, and their adequacy to cope with non-linearities, types of compliance, and designer's inexperience.

The construction of the conceptual and mathematical framework was presented for static balancing as a state of motion. The framework included the three main conditions characterizing a state of static balancing in terms of the potential energy, the forces, and the stability. The framework was expanded from the three classical conditions based on energy, force and stability, to include the new conditions based on the notions of virtual work, speed, natural frequency (large and small amplitudes), and buckling. The conditions characterizing a state of static balancing were discussed with a view focused on systems modeled by discrete elements where the size, shape and topology properties are collected into the system's stiffness matrix. The construction of the framework also included the presentation of static balancing as a coordinate transformation problem, in which the system's workspace is a projection of a level set of the system's potential energy. Such a transformation problem allowed the generalization of static balancing as a problem dependent on the system's deflection and its stiffness properties.

In the development of the design method based on topology optimization, a modification of the Warshall's algorithm was proposed for computing the connectivity matrix of an undirected graph. Since the graph represents the connectivity of a structure, the modification allows to validate the connectivity of the structure by simply observing the composition of a vector. The use of the algorithm during an optimization procedure using genetic algorithms removes the need to update the finite element mesh to remove disconnected nodes.

Appendix A Warshall's algorithm

The pseudo code for the Warshall's algorithm for computing the connectivity matrix $\mathbf{P}$ of an undirected graph is presented in the following paragraphs.
The algorithm is based on the fact that two vertices i and j adjacent to a vertex k are in fact connected to each other through vertex k. The algorithm starts by initially setting the connectivity matrix $\mathbf{P}$ as the same adjacency matrix $\mathbf{A}$. Then the algorithm extracts from the adjacency matrix all the indexes equal to 1 in row k (or column k, adjacency matrix is symmetric for undirected graphs) and add in the connectivity matrix a connection represented by a 1 at the entries (i, j) and (j, i). The Entries (i, j) and (j, i) are all the pairs constructed with the indexes extracted from row k. Once the connectivity matrix is updated, the process is repeated with the next row, and so on. Figure A.1 shows an example of this process.

Algorithm 1: Warshall's algorithm for graph connectivity

Data: $\mathbf{A}$ adjacency matrix.
Result: $\mathbf{P}$ connectivity matrix

```
P ⟵ A
n ⟵ size P
for k ← 1 to n do
    for i ← k to n do
        if P[i, k] = 1 then
            for j ← k to n do
                if P[k, j] = 1 then
                    P[i, j] = 1
```

If required, the number of components and the vertices' associations to components are found by observing that each row (or column) in the connectivity matrix $\mathbf{P}$ holds the indexes of an entire component. The algorithm simply clusters the vertices' indexes in a row as one component and then clusters indexes in the next row where its index has not been clustered in a previous component.

Algorithm 2: Extraction of the components and vertices' association from the connectivity matrix generated by the Warshall's algorithm

Data: $\mathbf{P}$ connectivity matrix.
Result: $ncomp$ number of components, $vrtxassc$ association of vertices to components.

$n \longleftarrow$ size P
$vrtxassc \longleftarrow \begin{bmatrix} 0 & 0 & \dots & 0 \end{bmatrix}_{n \times 1}$
$ncomp \longleftarrow 0$
$indexes \longleftarrow \begin{bmatrix} 1 & 2 & \dots & n \end{bmatrix}$
while *indexes not empty* **do**
  $ncomp \longleftarrow ncomp + 1$
  for $i \leftarrow 1$ **to** n **do**
    $j \longleftarrow indexes[1]$
    $indx \longleftarrow P[i, j]$
    $vrtxassc[indx] \longleftarrow ncomp$
    remove entry $indexes[indx]$

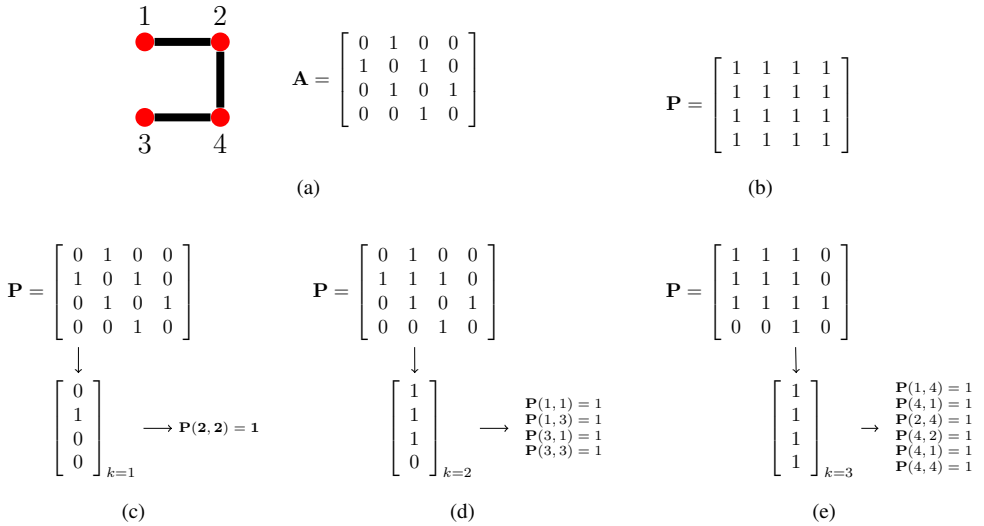

Figure A.1: (a) Graph and its adjacency matrix $\mathbf{A}$. (b) Connectivity matrix $\mathbf{P}$ shows that each vertex is connected to every other vertex, this matrix is obtained by following Fig. c, d and e. (c) Pivot on column 1, find vertices connected through vertex 1 and update matrix $\mathbf{P}$. (d) Pivot on column 2, find vertices connected through vertex 2 and update. (e) Pivot on column 3, find vertices connected through vertex 3.

Appendix B Strain energy in axial load and bending

In this section we compare the strain energy induced in a slender element under axial loading with respect to the strain energy on the same element subjected to bending. It is assumed that the slender element has constant cross section, where the ratio between the element's length l and its in-plane width w is defined by the term α

$$\alpha = \frac{l}{w} \tag{B.1}$$

B.1 Strain energy under axial load

Strain energy under axial load for an elastic slender element with constant cross section is given by the following expression,

$$U_a = \tfrac{1}{2} P \delta_a \tag{B.2}$$

where U_a is the strain energy, P is the axial load, and δ_a is the axial deflection. The relation between an axial load P and the axial deflection δ_a is,

$$P = \frac{AE}{l} \delta_a \tag{B.3}$$

where A is the cross section area, E is the material Young's modulus. By replacing Eq. B.3 into Eq. B.2 we get an expression for the strain energy as a function of the axial deflection,

$$U_a = \frac{AE\delta_a^2}{2l} \tag{B.4}$$

B.2 strain energy under bending

Strain energy under bending for an elastic slender element with constant cross section is given by the following expression,

$$U_b = \tfrac{1}{2} M\theta \tag{B.5}$$

where M is the applied moment, and θ is the angular deflection of the elastic element. The relation between the moment M and the angular deflection θ is,

$$M = \frac{EI}{l}\theta \tag{B.6}$$

where I is the cross section area second moment of inertia with respect to the bending axis. Replacing Eq. B.6 into Eq. B.5 yields an expression for the strain energy as a function of the angular deflection,

$$U_b = \frac{EI\theta^2}{2l} \tag{B.7}$$

In order to compare the strain energy between axial loading and bending we need to express Eq. B.7 in terms of a linear deflection instead of an angular deflection. To do so we assume that the elastic element under pure bending is a cantilever beam under the action of a moment, where the origin of coordinates is set at the free end tip. The horizontal and vertical deflection of the end tip is,

$$\delta_{bx} = l - \frac{l}{\theta}\sin\theta \tag{B.8}$$

$$\delta_{by} = \frac{l}{\theta}\left(1 - \cos\theta\right) \tag{B.9}$$

The total deflection of the free end tip is given by,

$$\delta_b^2 = \delta_{bx}^2 + \delta_{by}^2 \tag{B.10}$$

Replacing Eq. B.8 and B.9 into Eq. B.10 yields,

$$\delta_b^2 = l^2 + \frac{2l^2}{\theta^2} - \frac{2l^2}{\theta}\sin\theta - \frac{2l^2}{\theta^2}\cos\theta \tag{B.11}$$

Equation B.11 can be expressed as an infinite series in terms of the angular deflection θ as

$$\delta_b^2 = l^2\left(\sum_{n=1}^{\infty}(-1)^{n+1}\frac{2\theta^{2n}}{(2n+2)\,(2n)!}\right) \tag{B.12}$$

For angular deflections below $\pi/4$ the deflection δ_b^2 is approximated by the first term in the series,

$$\delta_b^2 = \frac{l^2\theta^2}{4} \tag{B.13}$$

Substituting Eq. B.13 into Eq. B.7, yields the expression for the strain energy as a function of the deflection of the end tip for angular deflections below $\pi/4$

$$U_b = \frac{2EI\delta_b^2}{l^3} \tag{B.14}$$

B.3 Comparison of strain energies under axial load and bending

In order to compare the stored strain energy in the slender element under the action of axial loading and bending, we assume that the axial deflection and deflection of the free end tip are the same deflection δ,

$$\delta^2 = \delta_a^2 = \delta_b^2 \tag{B.15}$$

now dividing Eq. B.4 by Eq. B.14 and replacing δ_a^2 and δ_b^2 by δ^2 yields,

$$\frac{U_a}{U_b} = \frac{Al^2}{4I} \tag{B.16}$$

This expression relates the strain energy under axial loading and bending assuming the same amount of deflection. If we assume for the slender element a rectangular constant cross section, we have that the cross section area and moment of inertia is,

$$A = wt \tag{B.17}$$

$$I = \frac{tw^3}{12} \tag{B.18}$$

then by replacing Eq. B.1, B.17, and B.18 into Eq. B.16 we get,

$$\frac{U_a}{U_b} = 3\alpha^2 \tag{B.19}$$

Now, if we assume that cross section of the slender element is circular,

$$A = \tfrac{1}{4}\pi d^2 \tag{B.20}$$

$$I = \tfrac{1}{16}\pi d^4 \tag{B.21}$$

then by replacing Eq. B.1, B.20, and B.21 into Eq. B.16 we get,

$$\frac{U_a}{U_b} = \alpha^2 \tag{B.22}$$

The result in Eq. B.19 and B.22 says that for a slender element with constant rectangular or circular cross section, the strain energy under axial loading is at least α^2 times greater than the strain energy under bending for the same deflection of the free end tip (for angular deflections below $\pi/4$). So if the length of the elastic element is 10 times the in-plane width, the density of strain energy per unit of deflection under axial loading is at least 100 times the density of strain energy per unit of deflection under bending.

Appendix C Displacement control pseudo-code

The notation used in this appendix is the following,

$$_{component}a^{iteration}_{index}$$

If the vector of nodal displacement $\mathbf{d}$ is divided between the components that can be moved freely ${}_f\mathbf{d}$ and the components that have a pre-assigned displacement value ${}_p\mathbf{d}$, then the system equation $\mathbf{K}_t(\mathbf{d})\,\mathbf{d} = \mathbf{f}_i$ can be written in terms of these free and pre-assigned displacements as

$$\begin{bmatrix} {}_{ff}\mathbf{K}(\mathbf{d}) & {}_{fp}\mathbf{K}(\mathbf{d}) \\ {}_{pf}\mathbf{K}(\mathbf{d}) & {}_{pp}\mathbf{K}(\mathbf{d}) \end{bmatrix} \begin{bmatrix} {}_f\mathbf{d} \\ {}_p\mathbf{d} \end{bmatrix} = \begin{bmatrix} {}_f\mathbf{f} \\ {}_p\mathbf{f} \end{bmatrix} \tag{C.1}$$

Equation C.1 can be decomposed into two sets of equations,

$${}_{ff}\mathbf{K}(\mathbf{d})\,{}_f\mathbf{d} + {}_{fp}\mathbf{K}(\mathbf{d})\,{}_p\mathbf{d} = {}_f\mathbf{f} \tag{C.2}$$

$${}_{pf}\mathbf{K}(\mathbf{d})\,{}_f\mathbf{d} + {}_{pp}\mathbf{K}(\mathbf{d})\,{}_p\mathbf{d} = {}_p\mathbf{f} \tag{C.3}$$

Displacement control must find the nodal displacement field $\mathbf{d}$ that makes $\mathbf{g} = \mathbf{0}$, where $\mathbf{g}$ is the difference vector between the internal forces $\mathbf{f}_i$ and external forces $\mathbf{f}_e$.

$$\mathbf{g} = \mathbf{f}_i(\mathbf{d}) - \mathbf{f}_e = \mathbf{0} \tag{C.4}$$

In the case of displacement control no external loads are applied except the reaction forces to the assigned displacements. Then, the vector of external forces $\mathbf{f}_e$ can be expressed as

$$\mathbf{f}_e = \begin{bmatrix} \mathbf{0} \\ {}_p\mathbf{r} \end{bmatrix} \tag{C.5}$$

where ${}_p\mathbf{r}$ are the reactions forces. To find the solution, first it is needed to calculate the first

estimation of the displacement field from Eq. C.2 , using the known incremental displacement ${}_p\mathbf{d}$ and solving for ${}_f\mathbf{d}$,

$$ {}_f\mathbf{d} = {}_{ff}\mathbf{K}(\mathbf{d})^{-1}\left({}_f\mathbf{f} - {}_{fp}\mathbf{K}\left(\mathbf{d}\right){}_p\mathbf{d}\right) \tag{C.6} $$

Now the iterative solution is found by expanding in Taylor series the components of the free displacements of $\mathbf{g}$,

$$ {}_f\mathbf{g} = {}_f\mathbf{g}_0 + \frac{\partial_f \mathbf{g}_0}{\partial_f \mathbf{d}}\Delta_f\mathbf{d} \tag{C.7} $$

but ${}_f\mathbf{g} = \mathbf{0}$, then solving Eq. C.7 for $\Delta_f\mathbf{d}$ and removing subscripts

$$ \Delta_f\mathbf{d} = -\left(\frac{\partial_f \mathbf{g}}{\partial_f \mathbf{d}}\right)^{-1}{}_f\mathbf{g} \tag{C.8} $$

Remembering that

$$ \frac{\partial_f \mathbf{g}}{\partial_f \mathbf{d}} = {}_{ff}\mathbf{K}_t \tag{C.9} $$

equation C.8 can be expressed as,

$$ \Delta_f\mathbf{d} = -{}_{ff}\mathbf{K}_t^{-1}{}_f\mathbf{g} \tag{C.10} $$

The final displacement field is found by updating the displacement field with the displacement increment given by Eq. C.10,

$$ \mathbf{d}^j = \mathbf{d}^{j-1} + \begin{bmatrix}\Delta_f\mathbf{d}^j \\ \mathbf{0}\end{bmatrix} \tag{C.11} $$

where superscript *j* indicates the iteration. Equation C.10 can be written in terms of the iteration index *j* as,

$$ \Delta_f\mathbf{d}^j = -\left[{}_{ff}\mathbf{K}_t\left(\mathbf{d}^{j-1}\right)\right]^{-1}\left({}_f\mathbf{f}_i\left(\mathbf{d}^{j-1}\right) - \mathbf{0}\right) \tag{C.12} $$

Now we can write the pseudo-code for the displacement control

Algorithm 3: Pseudo-code for a non-linear finite element solution using displacement control

initialization
$\mathbf{d} = \mathbf{0}$
$\mathbf{f}_i = \mathbf{0}$
$\Delta_p \mathbf{d}$

run iterative scheme

for *substep* $\leftarrow 1$ **to** *number of substeps* **do**
  ${}_p\mathbf{d} = {}_p\mathbf{d} + \Delta_p \mathbf{d}$
  function $[\mathbf{d}, \mathbf{f}_i] = solver\,(\mathbf{d}, \mathbf{f}_i, {}_p\mathbf{d})$
    $\mathbf{K}_t\,(\mathbf{d})$
    ${}_f\mathbf{d} = {}_{ff}\mathbf{K}(\mathbf{d})^{-1}\,({}_f\mathbf{f}_i - {}_{fp}\mathbf{K}\,(\mathbf{d})\,{}_p\mathbf{d})$
    $\mathbf{d} = \begin{bmatrix} {}_f\mathbf{d} \\ {}_p\mathbf{d} \end{bmatrix}$

    run Newton-Raphson scheme

    while *no convergency* **do**
      $\mathbf{K}_t\,(\mathbf{d})$
      ${}_f\mathbf{g} = {}_f\mathbf{f}_i - \mathbf{0} = ({}_{ff}\mathbf{K}\,(\mathbf{d})\,{}_f\mathbf{d} + {}_{fp}\mathbf{K}\,(\mathbf{d})\,{}_p\mathbf{d}) - \mathbf{0}$
      $\Delta_f \mathbf{d} = -{}_{ff}\mathbf{K}_t^{-1}\,{}_f\mathbf{g}$
      $\mathbf{d} = \begin{bmatrix} {}_f\mathbf{d} + \Delta_f\mathbf{d} \\ {}_p\mathbf{d} \end{bmatrix}$ or ${}_f\mathbf{d} = {}_f\mathbf{d} + \Delta_f\mathbf{d}$
    $\mathbf{f}_i(\mathbf{d})$

Bibliography

[1] S. Akhtar, K. Tai, and J. Prasad. Topology optimization of compliant mechanisms using evolutionary algorithm with design geometry encoded as a graph. In *Proceedings of the ASME Design Engineering Technical Conference*, Montreal, Canada, 2002. ASME.

[2] P. Alabuzhev, A. Gritchin, L. Kim, G. Migirenko, V. Chon, and P. Stepanov. *Vibration protecting with quasi-zero stiffness*. Taylor and Francis, 1989.

[3] G. K. Ananthasuresh. *A New Design Paradigm for Microelectromechanical Systems and Investigations on Compliant Mechanisms Synthesis*. PhD thesis, University of Michigan, 1994.

[4] G. K. Ananthasuresh, S. Kota, and N. Kikuchi. Strategies for systematic synthesis of compliant mems. In *American Society of Mechanical Engineers, Dynamic Systems and Control Division (Publication) DSC*, volume 55-2 of *Proceedings of the 1994 International Mechanical Engineering Congress and Exposition*, pages 677–686, Chicago, IL, USA, 1994. ASME.

[5] R. Ansola, E. Veguera, J. Canales, and J. A. Trragoa. A simple evolutionary topology optimization procedure for compliant mechanism design. *Finite Elements in Analysis and Design*, 44(1-2):53–62, 2007.

[6] D. R. Arango, D. A. Acosta, S. Durango, and O. E. Ruiz. Design of computer experiments applied to modeling compliant mechanisms. In *TMCE 2010*, Ancona, Italy, 2010.

[7] N. Bakhtiary, P. Allinger, M. Friedrich, F. Mulfinger, J. Sauter, O. Muller, and M. Puchinger. A new approach for sizing, shape and topology optimization, 26-29 February 1996 1996.

[8] A. Belendez, C. Pascual, D. Mendez, T. Belendez, and C. Neipp. Exact solution for the nonlinear pendulum. *Revista Brasileira de Ensino de Fisica*, 29(4):645–648, 2007.

[9] M. P. Bendsoe. *Optimization of structural topology, shape, and material*. Springer-Verlag, Berlin, 1995.

[10] M. P. Bendsoe and N. Kikuchi. Generating optimal topologies in structural design using a homogenization method. *Computer Methods in Applied Mechanics and Engineering*, 71(2):197–224, 1988.

[11] M. P. Bendsoe and O. Sigmund. *Topology Optimization - Theory, Methods, and Applications*. Springer Verlag, Berlin, second edition edition, 2003.

[12] M. D. Berglund, S. P. Magleby, and L. L. Howell. Design rules for selecting and designing compliant mechanisms for rigid-body replacement synthesis. In *Proceedings of the ASME Design Engineering Technical Conference*, Baltimore, Maryland, USA, 2000. ASME.

[13] P. Bernardoni, P. Bidaud, C. Bidard, and F. Gosselin. A new compliant mechanism design methodology based on flexible building blocks. In R. C. Smith, editor, *Proceedings of SPIE - The International Society for Optical Engineering*, volume 5383 of *Smart Structures and Materials 2004 - Modeling, Signal Processing, and Control*, pages 244–254, San Diego, CA, 2004.

[14] D. L. Blanding. *Exact constraint: Machine design using kinematic principles*. ASME Press, New York, 1999.

[15] S. Canfield and M. I. Frecker. Topology optimization of compliant mechanical amplifiers for piezoelectric actuators. *Structural and Multidisciplinary Optimization*, 20(4):269–279, 2000.

[16] J. R. Cannon and L. L. Howell. A compliant contact-aided revolute joint. *Mechanism and Machine Theory*, 40(11):1273–1293, 2005.

[17] J. R. Cannon, C. P. Lusk, and L. L. Howell. Compliant rolling-contact element mechanisms. In *Proceedings of the ASME Design Engineering Technical Conference*, Long Beach, California, USA, 2005. ASME.

[18] S. Chen and M. Y. Wang. Designing distributed compliant mechanisms with characteristic stiffness. In *Proceedings of the ASME Design Engineering Technical Conference*, Las Vegas, Nevada, USA, 2007. ASME.

[19] "compliance." Def. 3. Merriam-webster online dictionary. `http://www.merriam-webster.com/dictionary/compliance`, 2013.

[20] R. Cook, D. Malkus, M. Plesha, and R. Witt. *Concepts and Applications of Finite Element Analysis*. John Wiley and Sons, 4th edition edition, 2001.

[21] E. Dede and B. P. Trease. Statically-balanced compliant four-bar mechanism for gravity compensation. In *2004 ASME Student Mechanism Design Competition*, 2004.

[22] S. R. Deepak, M. Dinesh, and G. K. Ananthasuresh. A comparative study of the formulations for topology optimization of compliant mechanisms. In *Proceedings of the ASME Design Engineering Technical Conference*, Brooklyn, New York, USA, 2008.

[23] N. Deo. *Graph Theory with Applications to Engineering and Computer Science*. Prentice Hall, 1974.

[24] R. P. Dziedzic and M. I. Frecker. Design of multifunctional compliant mechanisms for minimally invasive surgery. In *Proceedings of the ASME Design Engineering Technical Conference*, Pittsburgh, Pennsylvania, USA, 2001. ASME.

[25] B. T. Edwards, B. D. Jensen, and L. L. Howell. A pseudo-rigid-body model for initially-curved pinned-pinned segments used in compliant mechanisms. *Journal of Mechanical Design*, 123(3):464–468, 2001.

[26] P. K. Freakley and A. R. Payne. *Theory and Practice of Engineering with Rubber*. Applied Science Publishers Ltd, London, 1978.

[27] M. I. Frecker, G. K. Ananthasuresh, S. Nishiwaki, N. Kikuchi, and S. Kota. Topological synthesis of compliant mechanism using multi-criteria optimization. *Journal of Mechanical Design*, 119(2):238–245, 1997.

[28] M. I. Frecker and S. Bharti. Toward the design of compliant actuators with a specified force and stroke. In *Proceedings of the ASME Design Engineering Technical Conference*, Pittsburgh, Pennsylvania, USA, 2001. ASME.

[29] M. I. Frecker and S. Canfield. Design of efficient compliant mechanisms from ground structure-based optimal topologies. In *Proceedings of the ASME Design Engineering Technical Conference*, Baltimore, Maryland, USA, 2000. ASME.

[30] M. I. Frecker, N. Kikuchi, and S. Kota. Topology optimization of compliant mechanisms with multiple outputs. *Structural Optimization*, 17(4):269–278, 1999.

[31] M. Grossard, C. R. Libersa, N. Chaillet, and Y. Perrot. Flexible building blocks method for the optimal design of compliant mechanisms using piezoelectric material. In *12th world congress in mechanism and machine science*, Besancon, France, 2007.

[32] J. L. Herder. Conception of balanced spring mechanisms. In *Proceedings of the ASME Design Engineering Technical Conference*, Atlanta,Georgia, USA, 1998. ASME.

[33] J. L. Herder. *Energy-free systems, Theory, conception and design of statically balanced spring mechanisms*. PhD thesis, Delft University of Technology, 2001.

[34] J. L. Herder and F. P. v. d. Berg. Statically balanced compliant mechanisms (sbcm's) an example and prospects. In *Proceedings of the ASME Design Engineering Technical Conference*, Baltimore, Maryland, USA, 2000. ASME.

[35] J. A. Hetrick and S. Kota. Topological and geometric synthesis of compliant mechanisms. In *Proceedings of the ASME Design Engineering Technical Conference*, Baltimore, Maryland, USA, 2000. ASME.

[36] K. Hoetmer, G. Woo, C. Kim, and J. Herder. Negative stiffness building blocks for statically balanced compliant mechanisms: Design and testing. *Journal of Mechanisms and Robotics*, 2(4):041007–7, 2010.

[37] J. B. Hopkins. *Design of Parallel Flexure Systems via Freedom and Constraint Topologies (FACT)*. PhD thesis, Massachusetts Institute of Technology, 2007.

[38] J. B. Hopkins and M. L. Culpepper. Synthesis of multi-degree of freedom, parallel flexure system concepts via freedom and constraint topology (fact) part i: Principles. *Precision Engineering*, 34(2):259–270, 2009.

[39] J. B. Hopkins and M. L. Culpepper. Synthesis of multi-degree of freedom, parallel flexure system concepts via freedom and constraint topology (fact). part ii: Practice. *Precision Engineering*, 34(2):271–278, 2009.

[40] L. L. Howell. *Compliant Mechanisms*. John Wley & Sons, Inc, New York, 2001.

[41] L. L. Howell and A. Midha. Evaluation of equivalent spring stiffness for use in a pseudo-rigid-body model of large-deflection compliant mechanisms. In *American Society of Mechanical Engineers, Design Engineering Division (Publication) DE*, volume 70 of *Proceedings of the 1994 ASME Design Technical Conferences. Part 1 (of 3)*, pages 405–412, Minneapolis, MN, USA, 1994. ASME.

[42] L. L. Howell and A. Midha. A method for the design of compliant mechanisms with small-length flexural pivots. *Journal of Mechanical Design*, 116(1):280–290, 1994.

[43] L. L. Howell and A. Midha. Parametric deflection approximations for end-loaded, large-deflection beams in compliant mechanisms. *Journal of Mechanical Design*, 117(1):156–165, 1995.

[44] L. L. Howell, A. Midha, and T. W. Norton. Evaluation of equivalent spring stiffness for use in a pseudo-rigid-body model of large-deflection compliant mechanisms. *Journal of Mechanical Design, Transactions of the ASME*, 118(1):126–131, 1996.

[45] P. V. Hull and S. L. Canfield. Optimal synthesis of compliant mechanisms using subdivision and commercial fea. In *Proceedings of the ASME Design Engineering Technical Conference*, Salt Lake City, Utah, USA, 2004. ASME.

[46] P. V. Hull and S. L. Canfield. Optimal synthesis of compliant mechanisms using subdivision and commercial fea. *Journal of Mechanical Design*, 128(2):337–348, 2006.

[47] D. J. Inman. *Engineering Vibration*. Prentice Hall, New Jersey, 2007.

[48] S. Jagirdar and C. P. Lusk. Preliminaries for a spherical compliant mechanism: pseudo-rigid-body model kinematics. In *Proceedings of the ASME Design Engineering Technical Conference*, Las Vegas, Nevada, USA, 2007. ASME.

[49] M. Jean and C. M. Gosselin. Static balancing of planar parallel manipulators. In *IEEE International Conference on Robotics and Automation*, volume 4, pages 3732–3737 vol.4, Minneapolis, Minnesota, USA, 1996.

[50] C. H. M. Jenkins. *Compliant Structures in Nature and Engineering*. WIT press, Southampton, UK, 2005.

[51] B. D. Jensen and L. L. Howell. The modeling of cross-axis flexural pivots. *Mechanism and Machine Theory*, 37(5):461–476, 2002.

[52] Y. Jingjun, Z. Guanghua, Y. Zhiwei, and B. Shusheng. A new family of large-displacement flexural pivots. In *Proceedings of the ASME Design Engineering Technical Conference*, Las Vegas, Nevada, USA, 2007. ASME.

[53] J. Joo and S. Kota. Topological synthesis of compliant mechanisms using nonlinear beam elements. *Mechanics Based Design of Structures and Machines*, 32(1):17–38, 2004.

[54] J. Joo, S. Kota, and N. Kikuchi. Topological synthesis of compliant mechanisms using linear beam elements. *Mechanics Based Design of Structures and Machines*, 28(4):245–280, 2000.

[55] D. Jung and H. C. Gea. Compliant mechanism design with non-linear materials using topology optimization. In *Proceedings of the ASME Design Engineering Technical Conference*, Montreal, Canada, 2002. ASME.

[56] C. V. Jutte and S. Kota. Design of planar nonlinear springs for prescribed load-displacement functions. In *Proceedings of the ASME Design Engineering Technical Conference*, Las Vegas, Nevada, USA, 2007. ASME.

[57] C. J. Kim. *A Conceptual Approach to the Computational Synthesis of Compliant Mechanisms*. PhD thesis, University of Michigan, 2005.

[58] C. J. Kim. Decomposition strategies for the synthesis of single input-single output and dual input-single output compliant mechanisms. In *Proceedings of the ASME Design Engineering Technical Conference*, Las Vegas, Nevada, USA, 2007. ASME.

[59] C. J. Kim, S. Kota, and Y.-M. Moon. An instant center approach to the conceptual design of compliant mechanisms. In *Proceedings of the ASME Design Engineering Technical Conference*, Salt Lake City, Utah, USA, 2004. ASME.

[60] C. J. Kim, S. Kota, and Y.-M. Moon. An instant center approach toward the conceptual design of compliant mechanisms. *Journal of Mechanical Design*, 128(3):542–550, 2006.

[61] C. J. Kim, Y.-M. Moon, and S. Kota. Conceptual synthesis of compliance at a single point. In *Proceedings of the ASME Design Engineering Technical Conference*, Philadelphia, Pennsylvania, USA, 2006. ASME.

[62] C. J. Kim, Y.-M. Moon, and S. Kota. A building block approach to the conceptual synthesis of compliant mechanisms utilizing compliance and stiffness ellipsoids. *Journal of Mechanical Design*, 130(2), 2008.

[63] C. Kimball and L.-W. Tsai. Modeling of flexural beams subjected to arbitrary end loads. *Journal of Mechanical Design*, 124(2):223–235, 2002.

[64] S. Kota, K.-J. Lu, Z. Kreiner, B. P. Trease, J. Arenas, and J. Geiger. Design and application of compliant mechanisms for surgical tools. *Journal of Biomechanical Engineering*, 127:981–989, 2005.

[65] C.-C. Lan and Y.-J. Cheng. Distributed shape optimization of compliant mechanisms using intrinsic functions. In *Proceedings of the ASME Design Engineering Technical Conference*, Las Vegas, Nevada, USA, 2007. ASME.

[66] D. J. B. A. d. Lange, M. Langelaar, and J. L. Herder. Design of a statically balanced compliant laparoscopic grasper using topology optimization. In *Proceedings of the ASME Design Engineering Technical Conference*, Brooklyn, New York, USA, 2008. ASME.

[67] U. D. Larsen, O. Sigmund, and S. Bouwstra. Design and fabrication of compliant micromechanisms and structures with negative poisson's ratio. *Journal of Microelectromechanical Systems*, 6(2):99–106, 1997.

[68] G. K. Lau, H. Du, and M. K. Lim. Use of functional specifications as objective functions in topological optimization of compliant mechanism. *Computer Methods in Applied Mechanics and Engineering*, 190(34):4421–4433, 2001.

[69] N. Lobontiu. *Compliant Mechanisms - Design of Flexure Hinges*. CRC Press, 2002.

[70] N. Lobontiu and E. Garcia. Static response of planar compliant devices with small-deformation flexure hinges. *Mechanics Based Design of Structures and Machines*, 32(4):459–490, 2004.

[71] N. Lobontiu, E. Garcia, M. Hardau, and N. Bal. Stiffness characterization of corner-filleted flexure hinges. *Review of Scientific Instruments*, 75(11):4355–5059, 2004.

[72] K.-J. Lu and S. Kota. Compliant mechanism synthesis for shape-change applications: Preliminary results. In V. S. Rao, editor, *Proceedings of SPIE - The International Society for Optical Engineering*, volume 4693 of *Smart Stuctures and Materials 2002: Modeling, Signal Processing and Control*, pages 161–172, San Diego, CA, 2002.

[73] K.-J. Lu and S. Kota. Design of compliant mechanisms for morphing structural shapes. *Journal of Intelligent Material Systems and Structures*, 14:379–391, 2003.

[74] K.-J. Lu and S. Kota. Parameterization strategy for optimization of shape morphing compliant mechanisms using load path representation. In *Proceedings of the ASME Design Engineering Technical Conference*, Chicago, Illinois, USA, 2003. ASME.

[75] K.-J. Lu and S. Kota. Synthesis of shape morphing compliant mechanisms using a load path representation method. In R. C. Smith, editor, *Proceedings of SPIE - The International Society for Optical Engineering*, volume 5049 of *PROCEEDINGS OF SPIE SPIE - The International Society for Optical Engineering: Smart Structures and Materials 2003 Modeling, Signal Processing, and Control*, pages 337–348, San Diego, CA, 2003.

[76] K.-J. Lu and S. Kota. An effective method of synthesizing compliant adaptive structures using load path representation. *Journal of Intelligent Material Systems and Structures*, 16(4):307–317, 2005.

[77] K.-J. Lu and S. Kota. Topology and dimensional synthesis of compliant mechanisms using discrete optimization. *Journal of Mechanical Design*, 128(5):1080–1091, 2006.

[78] Z. Luo and L. Tong. A level set method for shape and topology optimization of large-displacement compliant mechanisms. *International Journal for Numerical Methods in Engineering*, 76(6):862–892, 2008.

[79] Z. Luo, L. Tong, M. Y. Wang, and S. Wang. Shape and topology optimization of compliant mechanisms using a parameterization level set method. *Journal of Computational Physics*, 227(1):680–705, 2006.

[80] S. M. Lyon and L. L. Howell. A simplified pseudo-rigid-body model for fixed-fixed flexible segments. In *Proceedings of the ASME Design Engineering Technical Conference*, Montreal, Canada, 2002. ASME.

[81] N. D. Mankame. *Investigation on Contact-Aided Compliant Mechanisms*. PhD thesis, University of Pennsylvania, 2004.

[82] N. D. Mankame and G. K. Ananthasuresh. Topology synthesis of electrothermal compliant (etc) mechanisms using line elements. In *Proceedings of the ASME Design Engineering Technical Conference*, Pittsburgh, Pennsylvania, USA, 2001. ASME.

[83] N. D. Mankame and A. Saxena. Analysis of the hex cell discretization for topology synthesis of compliant mechanisms. In *Proceedings of the ASME Design Engineering Technical Conference*, Las Vegas, Nevada, USA, 2007. ASME.

[84] T. E. Mengesha and K.-J. Lu. Synthesis of planar compliant mechanisms. In *Proceedings of the ASME Design Engineering Technical Conference*, Las Vegas, Nevada, USA, 2007. ASME.

[85] J. Ming, Y. Jingjun, B. Shusheng, and X. Yicun. Analysis for stiffness of large-deformation flexure hinge and its application. In *Proceedings of the ASME Design Engineering Technical Conference*, Long Beach, California, USA, 2005. ASME.

[86] Y.-M. Moon and S. Kota. Design of compliant parallel kinematic machines. In *Proceedings of the ASME Design Engineering Technical Conference*, Montreal, Canada, 2002. ASME.

[87] Y.-M. Moon, B. P. Trease, and S. Kota. Design of large-displacement compliant joints. In *Proceedings of the ASME Design Engineering Technical Conference*, Montreal, Canada, 2002. ASME.

[88] F. M. Morsch and J. L. Herder. Design of a generic zero stiffness compliant joint. In *Proceedings of the ASME Design Engineering Technical Conference*, Montreal, Quebec, Canada, 2010. ASME.

[89] M. D. Murphy, A. Midha, and L. L. Howell. The topological synthesis of compliant mechanisms. *Mechanism and Machine Theory*, 31(2):185–199, 1996.

[90] R. H. Nathan. A constant force generation mechanism. *Journal of Mechanisms, Transmissions, and Automation in Design*, 107(12):508–512, 1985.

[91] J. P. J. Neto. Nonlinear pendulum: A simple generalization, 2010.

[92] S. Nishiwaki, M. I. Frecker, S. Min, and N. Kikuchi. Topology optimization of compliant mechanisms using the homogenization method. *International Journal for Numerical Methods in Engineering*, 42(3):535–559, 1998.

[93] R. L. Norton. *Design of machinery : an introduction to the synthesis and analysis of mechanisms and machines*. McGraw-Hill series in mechanical engineering. WCB/McGraw-Hill, Boston, 2nd edition, 1998.

[94] G. Pahl, W. Beitz, J. Feldhusen, and K. H. Grote. *Engineering design a systematic approach Online resource*. Springer, London, 3rd edition, 2007.

[95] S. T. Park and T. T. Luu. Techniques for optimizing parameters of negative stiffness. *Proceedings of the Institution of Mechanical Engineers, Part C: Journal of Mechanical Engineering Science*, 221(5):505–511, 2007.

[96] M. B. Parkinson, L. L. Howell, and J. J. Cox. A parametric approach to the optimization-based design of compliant mechanisms. In *Proceedings of the 23rd Design Automation Conference*, Sacramento, California, 1997. ASME.

[97] C. B. W. Pedersen, T. Buhl, and O. Sigmund. Topology synthesis of large-displacement compliant mechanisms. *International Journal for Numerical Methods in Engineering*, 50(12):2683–2705, 2001.

[98] D. L. Platus. Smoothing out bad vibes. *Machine Design*, pages 123–130, February 23, 1993 1993.

[99] D. L. Platus. Vibration isolation system, January 12, 1993 1993.

[100] K. M. Powell and M. I. Frecker. Method for optimization of a nonlinear static balance mechanism, with application to ophthalmic surgical forceps. In *International Design Engineering Technical Conferences and Computers and Information in Engineering Conference - DETC2005*, Long Beach, California, USA, 2005. ASME.

[101] P. Pracht, P. Minotti, and M. Dahan. Synthesis and balancing of cam-modulated linkages. In *ASME Design and Automation Conference*, volume 10, pages 221–226, 1987.

[102] G. Radaelli, J. A. Gallego, and J. L. Herder. An energy approach to static balancing of systems with torsion stiffness. *Journal of Mechanical Design*, 133(9), 2011.

[103] A. K. Rai, A. Saxena, and N. D. Mankame. Synthesis of path generating compliant mechanisms using initially curved frame elements. *Journal of Mechanical Design*, 129(10):1056–1063, 2007.

[104] A. K. Rai, A. Saxena, N. D. Mankame, and C. S. Upadhyay. On optimal design of compliant mechanisms for specified nonlinear path using curved frame elements and genetic algorithm. In *Proceedings of the ASME Design Engineering Technical Conference*, Philadelphia, Pennsylvania, USA, 2006. ASME.

[105] D. S. Ramrkahyani, M. I. Frecker, and G. A. Lesieutre. Hinged beam elements for the topology design of compliant mechanisms using the ground structure approach. In *Proceedings of the ASME Design Engineering Technical Conference*, Philadelphia, Pennsylvania, USA, 2006. ASME.

[106] N. O. Rasmussen, J. W. Wittwer, R. H. Todd, L. L. Howell, and S. P. Magleby. A 3d pseudo-rigid-body model for large spatial deflections of rectangular cantilever beams. In *International Design Engineering Technical Conferences & Computers and Information in Engineering Conference*, Philadelphia, Pennsylvania, USA, 2006. ASME.

[107] E. I. Rivin. *Stiffness and Damping in Mechanical Design*. Marcel Dekker, Inc., New York, 1999.

[108] E. I. Rivin. *Passive Vibration Isolation*. ASME Press, New York, 2003.

[109] A. Rodríguez. *Artefacto: Diseño Conceptual*. Fondo Editorial Universidad Eafit, Medellín, 2003.

[110] G. I. N. Rozvany. A critical review of established methods of structural topology optimization. *Structural and Multidisciplinary Optimization*, Not publish yet, 2008.

[111] M. J. D. Ruiter. *Topology Optimization using a Topology Description Function Approach*. PhD thesis, Delft University of Technology, 2005.

[112] M. J. D. Ruiter and F. v. Keulen. Topology optimization using a topology description function. *Structural and Multidisciplinary Optimization*, 26(6):406–416, 2004.

[113] F. A. Salustri and J. Parmar. Product design schematics: structured diagramming for requirements engineering. In *Proceedings of the 8th International Design Conference*, Dubrovnik, Croatia, 2004.

[114] A. Saxena. Synthesis of compliant mechanisms for path generation using genetic algorithm. *Journal of Mechanical Design*, 127(4):745–752, 2005.

[115] A. Saxena and G. K. Ananthasuresh. An optimality criteria approach for the topology synthesis of compliant mechanisms. In *Proceedings of the ASME Design Engineering Technical Conference*, Atlanta,Georgia, USA, 1998. ASME.

[116] A. Saxena and G. K. Ananthasuresh. On an optimal property of compliant topologies. *Structural and Multidisciplinary Optimization*, 19(1):36–49, 2000.

[117] A. Saxena and G. K. Ananthasuresh. Topology synthesis of compliant mechanisms for nonlinear force-deflection and curved path specifications. *Journal of Mechanical Design*, 123(1):33–42, 2001.

[118] A. Saxena and S. N. Kramer. A simple and accurate method for determining large deflection in compliant mechanisms subjected to end forces and moments. In *Proceedings of the ASME Design Engineering Technical Conference*, Atlanta,Georgia, USA, 1998. ASME.

[119] R. Saxena and A. Saxena. On honeycomb parameterization for topology optimization of compliant mechanisms. In *Proceedings of the ASME Design Engineering Technical Conference*, Chicago, Illinois, USA, 2003. ASME.

[120] J. A. Sethian. Tracking interfaces with level sets. *American Scientist*, 85(3):254–263, 1997.

[121] J. A. Sethian. Adaptive fast marching and level set methods for propagating interfaces. *Acta Mathematica Universitatis Comenianae*, 67(1):3–15, 1998.

[122] J. A. Sethian and A. Wiegmann. Structural boundary design via level set and immersed interface methods. *Journal of Computational Physics*, 163(2):489–528, 2000.

[123] D. Shu, W.-K. Lee, W. Liu, G. E. Ice, Y. Shvyd'ko, and K.-J. Kim. Development and applications of a two-dimensional tip-tilting stage system with nanoradian-level positioning resolution. *Nuclear Instruments and Methods in Physics Research Section A: Accelerators, Spectrometers, Detectors and Associated Equipment*, 649(1):114–117, 2011.

[124] D. Shu, T. S. Toellner, and E. E. Alp. Modular overconstrained weak-link mechanism for ultraprecision motion control. *Nuclear Instruments and Methods in Physics Research Section A: Accelerators, Spectrometers, Detectors and Associated Equipment*, 467468, Part 1(0):771–774, 2001.

[125] S. Shuib, M. Ridzwan, and A. H. Kadarman. Methodology of compliant mechanisms and its current developments in applications: A review. *American Journal of Applied Sciences*, 4(3):160–167, 2007.

[126] O. Sigmund. On the design of compliant mechanisms using topology optimization. *Mechanics Based Design of Structures and Machines*, 25(4):493–524, 1997.

[127] D. Simpson. The nonlinear pendulum, 2010.

[128] A. H. Slocum. *Precision machine design*. Prentice Hall, New Jersey, 1992.

[129] A. Stapel and J. L. Herder. Feasibility study of a fully compliant statically balanced laparoscopy grasper. In *Proceedings of the ASME Design Engineering Technical Conference*, Salt Lake City, Utah, USA, 2004. ASME.

[130] J. Stewart. *Calculus*. Brooks/Cole publishing company, 5th edition, 2003.

[131] D. A. Streit and E. Shin. Equilibrators for planar linkages. *Journal of Mechanical Design*, 115(3):604–611, 1993.

[132] H.-J. Su. A load independent pseudo-rigid-body 3r model for determining large deflection of beams in compliant mechanisms. In *Proceedings of the ASME Design Engineering Technical Conference*, Brooklyn, New York, USA, 2008.

[133] K. Tai and T. H. Chee. Design of structures and compliant mechanisms by evolutionary optimization of morphological representations of topology. *Journal of Mechanical Design*, 122(4):560–566, 2000.

[134] K. Tai, G. Y. Cui, and T. Ray. Design synthesis of path generating compliant mechanisms by evolutionary optimization of topology and shape. *Journal of Mechanical Design*, 124(3):492–500, 2002.

[135] S. P. Timoshenko and D. H. Young. *Theory of structures*. McGraw Hill, 2nd edition, 1965.

[136] N. Tolou, V. A. Henneken, and J. L. Herder. Statically balanced compliant micro mechanisms (sb-mems): Concepts and simulation. In *Proceedings of the ASME Design Engineering Technical Conference*, Montreal, Quebec, Canada, 2010. ASME.

[137] N. Tolou and J. L. Herder. Concept and modeling of a statically balanced compliant laparoscopic grasper. In *Proceedings of the ASME Design Engineering Technical Conference*, San Diego, California, USA, 2009.

[138] B. P. Trease, Y.-M. Moon, and S. Kota. Design of large-displacement compliant joints. *Journal of Mechanical Design*, 127:788–798, 2005.

[139] L.-W. Tsai. *Mechanism Design - Enumeration of Kinematic Structures According to Function*. CRC Press, 2000.

[140] V. van der Wijk. De acrobaat. `http://www.kineticart.nl/?page=acrobaat`, 2009.

[141] C. M. Vehar and S. Kota. Generalized synthesis of nonlinear springs for prescribed load-displacement functions. In *International Design Engineering Technical Conferences & Computers and Information in Engineering Conference*, Philadelphia, Pennsylvania, USA, 2006. ASME.

[142] H. V. Wang. *A Unit Cell Approach for Lightweight Structure and Compliant Mechanism*. PhD thesis, Georgia Institute of Technology, 2005.

[143] H. V. Wang and D. W. Rosen. An automated design synthesis method for compliant mechanisms with application to morphing wings. In *Proceedings of the ASME Design Engineering Technical Conference*, Philadelphia, Pennsylvania, USA, 2006. ASME.

[144] J. Wang and C. M. Gosselin. Static balancing of spatial three-degree-of-freedom parallel mechanisms. *Mechanism and Machine Theory*, 34(3):437–452, 1999.

[145] J. Wang and C. M. Gosselin. Static balancing of spatial four-degree-of-freedom parallel mechanisms. *Mechanism and Machine Theory*, 35(4):563–592, 2000.

[146] S. Wang and M. Y. Wang. Radial basis functions and level set method for structural topology optimization. *International Journal for Numerical Methods in Engineering*, 65(12):2060–2090, 2006.

[147] D. Xu and G. K. Ananthasuresh. Freeform skeletal shape optimization of compliant mechanisms. *Journal of Mechanical Design, Transactions of the ASME*, 125(2):253–261, 2003.

[148] P. Xu, Y. Jingjun, Z. Guanghua, and B. Shusheng. The modeling of leaf-type isosceles-trapezoidal flexural pivots. In *Proceedings of the ASME Design Engineering Technical Conference*, Las Vegas, Nevada, USA, 2007. ASME.

[149] Y. K. Yong, T.-F. Lua, and D. C. Handleya. Review of circular flexure hinge design equations and derivation of empirical formulations. *Precision Engineering*, 32(2):63–70, 2008.

[150] H. Zhou and K.-L. Ting. Spanning tree based topological optimization of compliant mechanisms. In *Proceedings of the ASME Design Engineering Technical Conference*, Long Beach, California, USA, 2005. ASME.

[151] H. Zhou and K.-L. Ting. Topological synthesis of compliant mechanisms using spanning tree theory. *Journal of Mechanical Design*, 127(4):753–759, 2005.

[152] H. Zhou and K.-L. Ting. Wide curve based geometric optimization of compliant mechanisms. In *Proceedings of the ASME Design Engineering Technical Conference*, Long Beach, California, USA, 2005. ASME.

[153] H. Zhou and K.-L. Ting. Shape and size synthesis of compliant mechanisms using wide curve theory. *Journal of Mechanical Design*, 128(3):551–558, 2006.

[154] R. D. Ziemian. *Guide to Stability Design Criteria for Metal Structures*. John Wiley and Sons, 6th edition edition, 2010.